

# **Material Management Framework utilizing Near Real-Time Monitoring of Construction Operations**

Farzaneh Golkhoo

A Thesis

In the Department

of

Building, Civil and Environmental Engineering

Presented in Partial Fulfillment of the Requirements

For the Degree of

Doctor of Philosophy (Building Engineering) at

Concordia University

Montreal, Quebec, Canada

August 2020

© Farzaneh Golkhoo, 2020

**CONCORDIA UNIVERSITY**  
**SCHOOL OF GRADUATE STUDIES**

This is to certify that the thesis prepared

By: **Farzaneh Golkhoo**

Entitled: **Material Management Framework utilizing Near Real-Time Monitoring of Construction Operations**

and submitted in partial fulfillment of the requirements for the degree of

**DOCTOR OF PHILOSOPHY (Building Engineering)**

complies with the regulations of the University and meets the accepted standards with respect to originality and quality.

Signed by the final examining committee:

\_\_\_\_\_Chair  
Dr. Anjali Awasthi

\_\_\_\_\_External Examiner  
Dr. Kasun Neranja Hewage

\_\_\_\_\_External to Program  
Dr. Amin Hammad

\_\_\_\_\_Examiner  
Dr. Fuzhan Nasiri

\_\_\_\_\_Examiner  
Dr. Sang Hyeok Han

\_\_\_\_\_Thesis Supervisor  
Dr. Osama Moselhi

Approved by

\_\_\_\_\_  
Dr. Michelle Nokken, Graduate Program Director

August 20, 2020

\_\_\_\_\_  
Dr. Mourad Debbabi, Dean  
Gina Cody School of Engineering and Computer Science

## ABSTRACT

### **Material Management Framework utilizing Near Real-Time Monitoring of Construction Operations**

**Farzaneh Golkhoo, Ph.D.**  
**Concordia University, 2020**

Materials management is a vital process in the delivery of construction facilities. Studies by the Construction Industry Institute (CII) have demonstrated that materials and installed equipment can constitute 40– 70% of the total construction hard cost and affect 80% of the project schedule. Despite its significance, most of the construction industry sectors are suffering from poor material management processes including inaccurate warehouse records, over-ordering and large surpluses of material at project completion, poor site storage practices, running out of materials, late deliveries, double-handling of components, out-of-specification material, and out of sequence deliveries which all result in low productivity, delay in construction and cost overruns. Inefficient material management can be attributed to the complex, unstructured, and dynamic nature of the construction industry, which has not been considered in a large number of studies available in this field.

The literature reveals that available computer-based materials management systems focus on (1) integration of the materials management functions, and (2) application of Automated Data Collection (ADC) technologies to collect materials localization and tracking data for their computerized materials management systems. Moreover in studies that focused on applying ADC technologies in construction materials management, positioning and tracking critical resources in construction sites, and identifying unique materials received at the job site are the main applications of their used technologies. Even though, various studies have improved materials management processes copiously in the construction industry, the benefits of considering the dynamic nature of construction (in terms of near real-time progress monitoring using state of the art technologies and techniques) and its integration with a dynamic materials management system have been left out. So, in contrast with other studies, this research presents a construction materials management framework capable of considering the dynamic nature of construction projects. It includes a vital component to monitor project progress in near real-time to estimate the installation and consumption of materials. This framework consists of three models: “preconstruction model,” “construction model,” and “data analysis and reporting model.” This framework enables (1) generation of optimized material delivery schedules based on Material Requirement Planning (MRP) and minimum total cost, (2) issuance of material Purchase Orders (POs) according to optimized delivery schedules, (3) tracking the status of POs (Expediting methods), (4) collection and assessment of material data as it arrives on site, (5) considering the inherent dynamics of construction operations by monitoring project progress to update project schedule and estimate near real-time consumption of materials and eventually (6) updating MRP and optimized delivery schedule frequently throughout the construction phase.

An optimized material delivery schedule and an optimized purchase schedule with the least cost are generated by the preconstruction model to avoid consequences of early/late purchasing and excess/inadequate purchasing. Accurate assessment of project progress and estimation of installed

or consumed materials are essential for an effective construction material management system. The construction model focuses on the collection of near real-time site data using ADC technologies. Project progress is visualized from two different perspectives, comparing as-built with as-planned and comparing various as-built status captured on consecutive points of time. Due to the recent improvements in digital photography and webcams, which made this technology more cost-effective and practical for monitoring project progress, digital imaging (including 360° images) is selected and applied for project progress monitoring in the construction (data acquisition) model. In the last model, which is the data analysis and reporting model, Deep Learning (DL) and image processing algorithms are proposed to visualize and detect actual progress in terms of built elements in near real-time. In contrast with the other studies in which conventional computer vision algorithms are often used to monitor projects progress, in this research, a deep Convolutional Auto-Encoder (CAE) and Mask Region-based Convolutional Neural Network (R-CNN) are utilized to facilitate vision-based indoor and outdoor progress monitoring of construction operations. The updated project schedule based on the actual progress is the output of this model, and it is used as the primary input for the developed material management framework to update MRP, optimized material delivery, and purchase schedules, respectively. Applicability of the models in the developed material management framework has been tested through laboratory and field experiments. The results demonstrated the accuracy and capabilities of the developed models in the framework.

## ACKNOWLEDGMENTS

My deepest acknowledgment is to God. I would like to express my deepest gratitude to my supervisor, Professor Osama Moselhi. This dissertation could not have been accomplished without his academic and personal advice. I believe without his support and encouragement, this research would have been more challenging. I am grateful to my examining committee members —Dr. Amin Hammad, Dr. Tarek Zayed, and Dr. Zhenhua Zhu—for their comments and feedback, which encouraged me to bring my work to a higher level. I also wish to thank Mitacs and Pomerleau for jointly funding and supporting this study in terms of an Accelerate Internship that enabled me to complete this research. It is worth mentioning that the opportunity did not come without Dr. Moselhi's support and guidance. I would also like to thank Mr. Fernando Valdivieso and the management team (Mr. Adel Kasaei, Mr. Jean-Francois Dupui, Ms. Carolyne Filion) at Pomerleau for their help and understanding during this process. I owe my deepest gratitude to my closest friend Dr. Saeed Moradi who has always stood by my side and helped me through the many stages of this research. I was fortunate enough to learn from his vast knowledge and experience. Last but not least, many thanks go to my parents and my brother for their infinite love and care throughout my life. I am ever grateful for my father's love and am sorry that he has not lived to see me graduate.

To my beloved mother, my kind father, and my brother

# TABLE OF CONTENTS

<b>LIST OF FIGURES .....</b>	<b>x</b>
<b>LIST OF TABLES .....</b>	<b>xvi</b>
<b>LIST OF ACRONYMS .....</b>	<b>xvii</b>
<b>CHAPTER 1: INTRODUCTION .....</b>	<b>1</b>
1.1 Problem Statement and Research Motivation.....	1
1.2 Research Objectives.....	3
1.3 Research Methodology .....	3
1.4 Organization of the Thesis .....	4
<b>CHAPTER 2: LITERATURE REVIEW .....</b>	<b>6</b>
2.1 Introduction.....	6
2.1.1 Construction Materials Management Overview .....	9
2.1.2 Major Problems and Needs of Materials Management and Control.....	15
2.2 Existing Studies .....	17
2.2.1 Construction Materials Management.....	17
2.2.2 Automated Construction Materials Management .....	21
2.3 Shortcomings and Limitations .....	42
2.4 Genetic Algorithm Optimization .....	43
2.5 Artificial Neural Network (ANN) and Multi-Layer Perceptron (MLP).....	44
2.6 Project Progress Monitoring .....	46
2.6.1 Comparison of Time-lapse Images with 4D BIM.....	47

2.6.2 Comparison of 3D As-Built Point Clouds with 4D BIM.....	48
2.6.3 Building Elements Detection .....	49
2.7 Deep Learning (DL) Algorithms .....	51
2.8 Deep Learning-Based Generic Object Detection.....	55
2.9 Summary.....	57
<b>CHAPTER 3: RESEARCH METHODOLOGY AND MODEL DEVELOPMENT.....</b>	<b>61</b>
3.1 Introduction.....	61
3.2 Preconstruction Model .....	64
3.2.1 Material Requirement Plan (MRP) .....	66
3.2.2 Optimized Material Delivery Schedule .....	69
3.2.3 Purchase Schedule .....	80
3.2.4 Purchase Order.....	82
3.2.5 Material Delivery.....	85
3.2.6 As-Planned 4D Simulation .....	86
3.2.7 Deep CAE .....	88
3.2.8 Reports and Warnings.....	92
3.3 Construction Model .....	92
3.4 Data Analysis and Reporting Model.....	100
3.4.1 CAE for Project Progress Visualization .....	101
3.4.2 Structural Similarity Index (SSIM) to Compare Images .....	103



3.4.3 Automated Detection of Building Components (Using Deep-Learning and Synthetic Images).....	104
<b>CHAPTER 4: TESTING AND VALIDATION.....</b>	<b>117</b>
4.1 GA-MLP Algorithm.....	117
4.2 Progress Visualization Methods .....	123
4.2.1 CAE.....	123
4.2.2 SSIM .....	136
4.3 Automated Detection of Building Components.....	139
<b>CHAPTER 5: RESEARCH CONTRIBUTION AND FUTURE WORKS.....</b>	<b>149</b>
5.1 Summary of Research.....	149
5.2 Expected Research Contributions.....	150
5.3 Limitations and Future Work.....	150
<b>BIBLIOGRAPHY .....</b>	<b>152</b>

## LIST OF FIGURES

Figure 1-1: Research Methodology .....	4
Figure 2-1: Structure of Chapter 2 (Literature Review) .....	8
Figure 2-2: Materials Management Functions (CII, 1999).....	12
Figure 2-3: Flow Chart of Construction Materials Management (Nasir, 2008) .....	13
Figure 2-4: Barcoding Hardware System Components (Nasir, 2008).....	26
Figure 2-5: Typical RFID System Components (Montaser, 2013).....	27
Figure 2-6: Different Types of RFID Readers (Atlas RFID Store) .....	28
Figure 2-7: RFID 3D Localization (a) Active Positioning Scheme (b) Passive Positioning Scheme (Wang et al., 2007).....	29
Figure 2-8: A Typical UWB Setup and Installation (Cheng et al., 2011) .....	32
Figure 2-9: ARMOR Hardware Architecture (Dong and Kamat, 2013) .....	34
Figure 2-10: Multi-Layer Perceptron Network (Shirvany et al., 2009).....	45
Figure 2-11: Significant Steps in the History of Neural Networks and Machine Learning Resulted in Deep Learning (Voulodimos et al., 2018) .....	52
Figure 2-12: The Architecture of a Simple Auto-Encoder (Géron, 2017).....	54
Figure 3-1: Developed CMM Framework .....	62
Figure 3-2: Main Components of the Developed CMM Framework .....	63
Figure 3-3: Application Steps of CMM .....	64
Figure 3-4: Preconstruction Model .....	66
Figure 3-5: MRP Development Algorithm (Golkhoo and Moselhi, 2019) .....	68
Figure 3-6: Material Requirement Vector for Material $j$ (Golkhoo and Moselhi, 2019) .....	69
Figure 3-7: Material Delivery Chromosome for Material $j$ (Golkhoo and Moselhi, 2019) .....	69
Figure 3-8: Vendors Selection and Material Costs (Golkhoo and Moselhi, 2019) .....	72

Figure 3-9: Calculated project Delay Algorithm (Golkhoo and Moselhi, 2019).....	74
Figure 3-10: GA-MLP Algorithm to Generate Optimized Material Delivery Schedule (Golkhoo and Moselhi, 2019) .....	77
Figure 3-11: User Interface for Optimized Material Delivery Schedule (GA-MLP) (Golkhoo and Moselhi, 2019) .....	79
Figure 3-12: User Interface for GA-MLP Constraints and Parameters (Golkhoo and Moselhi, 2019) .....	80
Figure 3-13: Calculated Issue Date of PO Algorithm.....	82
Figure 3-14: Final Material Purchase Order Issuance .....	84
Figure 3-15: Material Delivery Process .....	86
Figure 3-16: As-planned 4D Simulation and Generating Synthetic 2D Images.....	87
Figure 3-17: CAE Train and Test Using Synthetic 2D Images .....	89
Figure 3-18: CAE Architecture.....	90
Figure 3-19: ReLu Function vs. Leaky ReLU Function (Clevert et al., 2015).....	91
Figure 3-20: Captured Actual Job Site Images Fed into Trained CAE .....	93
Figure 3-21: Construction Model (First Perspective) .....	94
Figure 3-22: List of Viewpoints, Location, and Dates for Image Capturing.....	95
Figure 3-23: Example of 360-Degree Image in HoloBuilder Platform (©2020 HoloBuilder, Inc.) .....	96
Figure 3-24: Example of a 360-Degree Image and an Imported 3D Model to HoloBuilder Platform (©2020 HoloBuilder, Inc.).....	97
Figure 3-25: Creating Revit 360 Rendering Views .....	98
Figure 3-26: Importing 360° Views of 3D Model from Autodesk Revit into HoloBuilder .....	99

Figure 3-27: As-Built 360° Image vs. As-Planned 360° Image in HoloBuilder Platform (©2020 HoloBuilder, Inc.) .....	100
Figure 3-28: Ricoh Theta V Specifications (HoloBuilder, 2019).....	100
Figure 3-29: Progress Visualization Using Trained CAE.....	101
Figure 3-30: Trained CAE Fed with Job Site 2D Images for Progress Visualization .....	102
Figure 3-31: Progress Visualization using SSIM.....	104
Figure 3-32: Automated Detection of Building Components for Updating Project Schedule ...	106
Figure 3-33: Developed Framework of Automated Detection of Building Components.....	108
Figure 3-34: R-CNN Flow Diagram (Girshick et al., 2014).....	110
Figure 3-35: Fast R-CNN Flow Diagram (Girshick, 2015).....	110
Figure 3-36: Faster R-CNN Flow Diagram (Ren et al., 2017) .....	111
Figure 3-37: Mask R-CNN Framework (He et al., 2017).....	112
Figure 3-38: SSD Framework (Liu et al., 2016).....	112
Figure 3-39: YOLO Detection System (Redmon et al., 2016) .....	113
Figure 3-40: Evolution of Object Detection Performance on COCO from Early 2015 to Late 2017 (Liu et al., 2019).....	114
Figure 3-41: Detection Accuracy versus Detection Time of Different Algorithms (Huang et al., 2016) .....	114
Figure 3-42: Detection accuracy of different algorithms to detect objects with large, medium, and small sizes (Huang et al., 2016) .....	115
Figure 4-1: Material Requirement Plan (Golkhoo and Moselhi, 2019).....	118
Figure 4-2: Rebar Requirement Vector (ton/day) (Golkhoo and Moselhi, 2019) .....	118

Figure 4-3: Optimized Rebar Delivery Schedule and Rebar Stock Level (Golkhoo and Moselhi, 2019) .....	119
Figure 4-4: Rebar Delivery, Consumption and Stock Level (Golkhoo and Moselhi, 2019) .....	120
Figure 4-5: Convergence of Total Material Cost (Golkhoo and Moselhi, 2019) .....	121
Figure 4-6: Error in GA-MLP algorithm (Golkhoo and Moselhi, 2019).....	121
Figure 4-7: Comparison of the Convergence of Total Material Cost Using GA (Left) and GA-MLP algorithm (Right) (Golkhoo and Moselhi, 2019).....	122
Figure 4-8: Comparison of Error in GA-MLP (Left) and GA (Right) (Golkhoo and Moselhi, 2019) .....	122
Figure 4-9: Construction Process Simulation in Autodesk Navisworks: (a) Outdoor, and (b) Indoor Environment.....	125
Figure 4-10: Outdoor Test Images in Scenario #1: (a) at $T1$ , and (b) at $T2$ .....	127
Figure 4-11: CAE Output Images: (a) Reconstructed Image at $T1$ , (b) Reconstructed Image at $T2$ , and (c) Visualized SIP Wall.....	127
Figure 4-12: Test Images in scenario #2: (a) at $T1$ , (b) at $T2$ , and CAE Output: (c) Visualized Window Frames and Curtain Wall Mullions .....	127
Figure 4-13: Outdoor Test Images in Scenario #3: (a) at $T1$ , (b) at $T2$ , and CAE Output: (c) Visualized SIP Wall .....	128
Figure 4-14: Indoor Test Images in Scenario #4: (a) at $T1$ , (b) at $T2$ , and CAE Output: (c) Visualized Window Frames and Curtain Wall Mullions .....	129
Figure 4-15: Outdoor Test Images in Scenario #3: (a) at $T1$ (b) at $T2$ , and CAE Output: (c) Visualized SIP Wall and Interior Partition .....	130

Figure 4-16: Indoor Test Images in Scenario #4: (a) at $T1$ , (b) at $T2$ , and CAE Output: (c) Visualized Window Frames and SIP Wall.....	130
Figure 4-17: Outdoor Test Images in Scenario #5: (a) at $T1$ , (b) at $T2$ , and CAE Output: (c) Visualized SIP Wall.....	131
Figure 4-18: Indoor Test Images in Scenario #6: (a) at $T1$ , (b) at $T2$ , and CAE Output: (c) Visualized Window Frames and Curtain Wall Mullions.....	131
Figure 4-19: Construction Process Simulation.....	134
Figure 4-20: Outdoor Real Images in Field Experiment: (a) at $T1$ , (b) at $T2$ , and CAE Output: (c) Visualized the Constructed Façade of the Last Floor.....	135
Figure 4-21: Indoor Real Images in Field Experiment: (a) at $T1$ , (b) at $T2$ , and CAE Output: (c) Visualized the Installed HVAC Duct.....	136
Figure 4-22: As-Built 360° Image vs. As-Planned 360° Image in HoloBuilder Platform.....	137
Figure 4-23: Visualized Differences Using SSIM.....	138
Figure 4-24: Synthetic Image Examples Generated from 3D Models of Hospital and University Projects.....	139
Figure 4-25: Example Detections of HVAC Ducts Using Faster R-CNN.....	140
Figure 4-26: Mask R-CNN Architecture with Input and Output Images (He et al., 2017 & Liu et al., 2019).....	141
Figure 4-27: Samples of Real and Synthetic-Images Annotated by VIA.....	142
Figure 4-28: HVAC Duct Detection on Real-Images Using Mask R-CNN (a) Experiment #1, (b) Experiment #2, (c) Experiment #3, (d) Experiment #4, and (e) Experiment #5.....	145
Figure 4-29: HVAC Duct Detection on Synthetic-Images (Experiment #6).....	146

Figure 4-30: Performance Plot Indicating the Effect of Including Synthetic-Images in the Training Dataset..... 147

Figure 4-31: Updating Schedule, MRP and OMDS based on the Detected Building Elements (Perceived Progress) ..... 148

## LIST OF TABLES

Table 2-1: Capabilities and Limitations of ADC Technologies .....	39
Table 2-2: Studies Used Either Traditional Machine Learning or Deep Learning Algorithms to Detect, Recognize and Classify Various Objects of Interest in the Construction Industry .....	59
Table 4-1: Input Data for GA and GA-MLP (Golkhoo and Moselhi, 2019).....	117
Table 4-2: Laboratory Experiments Scenarios .....	124
Table 4-3: SSIM Index of Different Experiments .....	132
Table 4-4: Cross-Validation Errors of Different Designed CAE Architecture.....	133
Table 4-5: Performance Comparison for Different Experiments .....	144



## LIST OF ACRONYMS

ABC	Activity-Based Costing
ABM	Agent-Based Modeling
ADC	Automated Data Collection
AMCLOS	Automated Multi-objective Construction Logistics Optimization System
ANN	Artificial Neural Network
AR	Augmented Reality
ARMOR	Augmented Reality Mobile Operation
BIM	Building Information Modeling
BoM	Bill of Material
BRIEF	Binary Robust Independent Elementary Features
C2LP	Congested Construction Logistics Planning
CAE	Convolutional Auto-Encoder
CICE	Construction Industry Cost Effectiveness Committee
CII	Construction Industry Institute
CMM	Construction Materials Management
CMMS	Construction Materials Management Software
CNN	Convolutional Neural Network
COCO	Common Objects in Context
COME	Construction Materials Exchange
CPU	Central Processing Unit
CSCM	Construction Supply Chain Management
DAE	Deep Auto-Encoder
DBMs	Deep Boltzmann Machines
DBN	Deep Belief Network
DES	Discrete Event Simulation
DL	Deep Learning
ELU	Exponential Linear Unit
EPC	Engineering/Procurement/Construction
ERP	Enterprise Resources Planning
EVM	Earned Value Method
FCC	Federal Communications Commission
FCN	Fully Convolutional Network
FIATECH	Fully Integrated and Automated Technology
FIAPP	Fully Integrated and Automated Project Process
FM	Facility Management
FN	False Negative
FP	False Positive
FPN	Feature Pyramid Network
GA	Genetic Algorithm
GAN	Generative Adversarial Net
GIS	Geographic Information System
GPS	Global Positioning System
GPU	Graphics Processing Unit
GUI	Graphical User Interfaces

HMD	Head-mounted Display
HVAC	Heating, Ventilation, and Air Conditioning
<i>HD<sup>4</sup>AR</i>	Hybrid 4-Dimensional Augmented Reality
ICP	Iterative Closest Point
IFC	Industry Foundation Classes
ICT	Information and Communication Technologies
IOU	Intersection Over Union
IRP	Incentive Reward Program
IT	Information Technology
JIC	Just In Case
JIT	Just In Time
LADAR	Laser detection and Ranging
LIDAR	Light Detection And Ranging
(mAP)	mean Average Precision
ML	Machine Learning
MLP	Multi-Layer Perceptron
MMF	Material Management Framework
MMMS	Mobile Material Management System
MPS	Materials Planning System
MRP	Material Requirement Planning
MSE	Mean Squared Error
MTMIS	Materials Tracking Management Information System
MVS	Multi-View Stereovision
NFC	Near Field Communication
NIST	National Institute of Standards and Technology
NN	Neural networks
OMDS	Optimized Material Delivery schedule
OOM	Object-Oriented Methodology
PCC	Point Cloud Co-registration
PD	Path Difference
PO	Purchase Order
PPHT	Progressive Probabilistic Hough Transform
PPS	Precise Positioning Service
QR	Quick Response
RANSAC	Random Sample Consensus
RBM	Restricted Boltzmann Machines
R-CNN	Region-based Convolutional Neural Network
RFID	Radio Frequency Identification
RFP	Requests for Proposals
ReLU	Rectified Linear Unit
RTK	Real-time Kinematic
RoI	Region of Interest
RoIPool	Region of Interest Pooling
RPN	Region Proposal Network
SfM	Structure from Motion
SIFT	Scale-Invariant Feature Transform

SIP	Structural Insulated Panel
SMART	Scalable and Modular Augmented Reality Template
SPP	Spatial Pyramid Pooling
SPS	Standard Positioning Service
SSD	Single Shot multi-box Detector
SSIM	Structural Similarity Index
STL	Stereolithography
SURF	Speeded-Up Robust Features
SVM	Support Vector Machine
TLS	Terrestrial Laser Scanning
TP	True Positive
TQM	Total Quality Management
UAS	Unmanned Airborne Systems
UAV	Unmanned Aerial Vehicle
UWB	Ultra-WideBand
VAE	Variational Autoencoder
VCMR	Virtual Construction Material Router
VIA	VGG Image Annotator
VR	Virtual Reality
WAN	Wide Area Network
WORM	Write Once, Read Many
WSN	Wireless Sensor Networks
YOLO	You Only Look Once
$j$	Materials, $j = 1, 2, \dots, k$
$i$	Project activities, $i = 1, 2, \dots, n$
$T_C$	Current date, $T_C = 1, 2, \dots, D$
$ES_i$	Early Start dates of project activities
$EF_i$	Early Finish dates of project activities
$T_{sp}$	Pre-processed time required for the materials assembly before installation at the construction site
$q_{ij}$	Required amount of material $j$ assigned to activity $i$ at specific date
$N_p$	Total project duration in terms of the year
$L_N$	Number of material orders/deliveries made in year $N$
$Q_d$	Quantity of material for order $d$
$P_d$	Unit price of material for order $d$
$P_{average}$	Average unit price of material
$C_0$	Average administrative cost for making a single order
$SQ_{T_C}$	Stock quantity at time $T_C$
$C_s$	Storage cost for an individual unit quantity per unit time
$I$	Interest rate per unit time
$i$	Annual escalation rate
$SQ_{T_C-1}$	Stock quantity at time $T_C - 1$
$Q_{T_C}$	Material quantities which have to be ordered at time $T_C$
$q_{T_C}$	Required material quantities at time $T_C$
$C_d$	Cost resulted from project schedule delay due to material shortage

$D_p$	Project schedule overrun in terms of the number of days
$Q_{S_j}$	Max Storage Capacity for Material $j$
$Q_{MS_j}$	Minimum Shipping Quantity for Material $j$
$W_i$	weight vector generated by MLP
$\sigma_i$	Error value between two previous most fitted GA chromosomes
$\lambda_i$	Difference between two previous MLP network outputs
$\alpha$	Learning rate ( $0.1 < \alpha < 0.3$ )
$ET_{L_j}$	Expected Material Delivery Lead Time for material $j$
$T_{mp}$	Required pre-processed Time in the shop
$T_{A_j}$	Administrative Time to issue a PO for material $j$ to a vendor
$N_{PO}$	Number of issued POs
$n_j$	Number of input (fan-in) neurons
$n_{j+1}$	Number of output (fan-out) neurons
$\mu_x$	Mean pixel intensity at image $x$
$\sigma_x$	Standard deviations of pixel intensity at image $x$
$\sigma_{xy}$	Sample correlation coefficient between corresponding pixels in the patches centered at $x$ and $y$
$l(X, Y)$	Luminance similarity of two images $X$ and $Y$
$c(X, Y)$	Contrast similarity of two images $X$ and $Y$
$s(X, Y)$	Structural similarity of two images $X$ and $Y$
$S(X, Y)$	Similarity of two images $X$ and $Y$

# CHAPTER 1: INTRODUCTION

## 1.1 Problem Statement and Research Motivation

The significant role of materials management in the construction industry was first expressed in a report published by the Construction Industry Cost Effectiveness Committee (CICE) of Business Roundtable in 1982. After that, materials management as one of the vital functions of construction project management has been under the spotlight of study and development by the Construction Industry Institute (CII) and other researchers, which has resulted in the publication of various valuable handbooks and articles. For example, the procurement and materials management handbook was published as an implementation resource by CII in 1999 and was updated in 2011 to identify changes in materials management from 1999. Moreover, the Fully Integrated and Automated Technology (FIATECH) initiative presented a Material Management Framework (MMF) for the capital projects industry to integrate and automate procurement and supply management systems in 2011 as well. All these reputable works express the significance of materials management and its influence on the construction project. For instance, it has been stated that materials cost represents around either 50-60% of construction cost (Stukhart, 1995; CII, 1999; Nasir, 2008) or 40-70% of the total construction hard cost (Jaśkowski et al. 2018). It can control 80% of the project schedule as well (Kerridge, 1987; Stukhart, 1995). Dakhli and Lafhaj (2018) have stated that although materials cost forms a remarkable amount of construction costs, there is no systematic approach to manage them, and they are managed under improvised conditions. According to CII (1999) questionnaire survey, the benefits derived from the implementation of a properly structured materials management system were 40% reduction in bulk surplus, 24% improvement in supplier performance, 23% increase in cash flow savings, 21% reduction in site storage and handling, 16% improvement in craft labor productivity, 16% improvement in the project schedule, 15% reduction in management manpower, and 5% risk reduction. However, in contrast with the general industry in which 1% of the cost spent in production is invested in materials management and control, only 0.15% of the construction cost is assigned to materials management (Formoso and Revelo, 1999; Navon and Berkovich, 2006). In another study done by Rahman et al. (2013), it was shown that “late or irregular delivery or wrong types of material delivered during construction affect the utilization of other resources like manpower and machinery.” In other words, it can lead to low productivity, time delay, and also cost overrun. “Interruption to the work schedule, rework from having the wrong or out-of-order materials, double handling because of inadequate materials, material deterioration during extended storage periods, expenses associated with crews lacking proper materials, and lost items on or off-site” have been identified as the most common problems with materials in the small and medium-sized construction projects (Barry et al. 2014). The results achieved from the research done by Jung et al. (2018) showed that construction and material supply processes should be considered as one system while planning resource-constrained large-scale construction projects because of their interrelationships. They found that in high-rise building construction projects with many types of materials, the impact of changes in materials inventory levels for outdoor and indoor yard storage makes the entire construction process highly complex and unpredictable.

On the one hand, derived statistics of the influencing role of materials management in the construction projects and on the other hand, existing issues (such as inaccurate warehouse records, over-ordering, and large surpluses, poor site storage practices, running out of materials, late

deliveries, out of sequence deliveries, etc.) resulted in conducting a bunch of studies to prevent these issues. First, researchers focused on the concepts of materials management to improve it through the implementation of Just In Time (JIT) strategies, materials storage optimization, performance measurement, investigation of proper materials management practices, measurement and reduction of the influences of the most probable issues on project cost, schedule and productivity. Then they concluded that managing materials on-site through paper documents were not practical in complex and large scale construction projects, and if materials management processes were executed in a consistent manner, it would operate more efficiently. As a result, they developed computerized systems. Computerized construction materials management systems could be implemented more appropriately and lead to more benefits such as uniformity of documents generation, speed, and efficiency, automatic process implementation from inputting information to report generation in a matter of hours. In the next step, there was a question of the accuracy of input and output data obtained from their developed systems. In fact, a computerized system alone could not ensure the accuracy of the reports upon which corrective actions or various decisions were made, and the output information and reports were only as good as the input data created them. Since manual data collection was often slow, inaccurate, inefficient, and resulted in extensive amounts of paper-based reports, so Automated Data Collection (ADC) technologies were applied to reduce paper-based requirements and solve the issue (Golkhoo and Moselhi, 2017).

Furthermore, the report of the NIST Workshop (A workshop namely “Data Exchange Standards at the Construction Job Site” was sponsored by the National Institute of Standards and Technology (NIST), in cooperation with the Fully Integrated and Automated Technology (FIATECH) consortium in May 2003) expressed that “materials tracking remains a huge problem on the current construction job site” (Saidi et al. 2003). So a large number of researchers developed different methods to automate construction materials and equipment tracking and locating for improving productivity and cost-effectiveness. Despite the developed materials management systems and construction materials tracking and locating models, Caldas et al. in 2015 concluded that just around 26% of entire organizations (surveyed owner and contractor organizations) had IT systems to support synchronization across major supply chain tiers of project schedules. They also found that only 25% of them had materials management systems that allow engineering requirements to go directly to the materials management system as electronic data.

Studying the literature in depth resulted in identifying some issues and some points of view which have not been solved or addressed yet. The activities of construction projects are highly interdependent, and engineering, procurement, and construction phases overlap to a great extent (Yeo and Ning, 2002). It seems that the current state of research does not adequately consider the complex, unstructured, and dynamic nature of the construction projects in developing materials management systems. Even though various studies have improved the materials management process copiously in the construction industry using ADC technologies, most of them have applied these technologies only for positioning and tracking critical resources in construction sites and identifying unique materials received at the job site. In order to achieve an effective materials management framework especially in the construction phase not only the near real-time data related to the materials position, location and their arrival to the site should be acquired, but also the near real-time data of their consumption or installation on the construction site should be obtained.

It seems that the benefits of near real-time progress monitoring using state of the art technologies and techniques to estimate the quantities of installed or consumed materials in the job site and its integration with a materials management system have been left out. Such a dynamic framework resulting in taking more accurate and near real-time corrective actions, avoiding project schedule delays, and cost overruns has not been considered yet and hence is developed in this research.

## **1.2 Research Objectives**

The main objective of this research is to develop a Construction Materials Management (CMM) framework to optimize material delivery schedules considering the inherent dynamics of construction operations through monitoring project progress. CMM framework consists of three models entitled “preconstruction model”, “construction model” and “data analysis model”. In order to achieve the main objective, following sub-objectives are defined:

1. Developing a preconstruction model in which Material Requirement Planning (MRP) is generated, material delivery schedules are optimized, and materials management functions are integrated;
2. Evaluating and applying the most efficient near real-time site data acquisition technologies for project progress monitoring to estimate the quantities of installed materials in the construction model; and
3. Investigating and applying the most effective state-of-the-art image processing and computer vision algorithms to visualize and detect the actual progress in the data analysis model.

## **1.3 Research Methodology**

Figure 1-1 illustrates the methodology followed to achieve the objective of this research. The current study began with a problem statement and objectives definition. In the next step, a comprehensive review was performed in the following domains:

- Construction materials management
- Automated construction materials management
- Automated data acquisition technologies
- Vision-based project progress monitoring methods
- Deep Learning (DL) algorithms
- Object detection algorithms

After identifying gaps and limitations in the literature and in order to prevent the limitations and shortcomings, a framework was developed consisting of three models entitled “preconstruction model,” “construction model,” and “data analysis and reporting model.” Then to assess the feasibility of applying the developed models in the real world, laboratory and field experiments were conducted in the testing and validation stage. Eventually, findings, contributions, and limitations of this research, along with future works, are presented in conclusion.

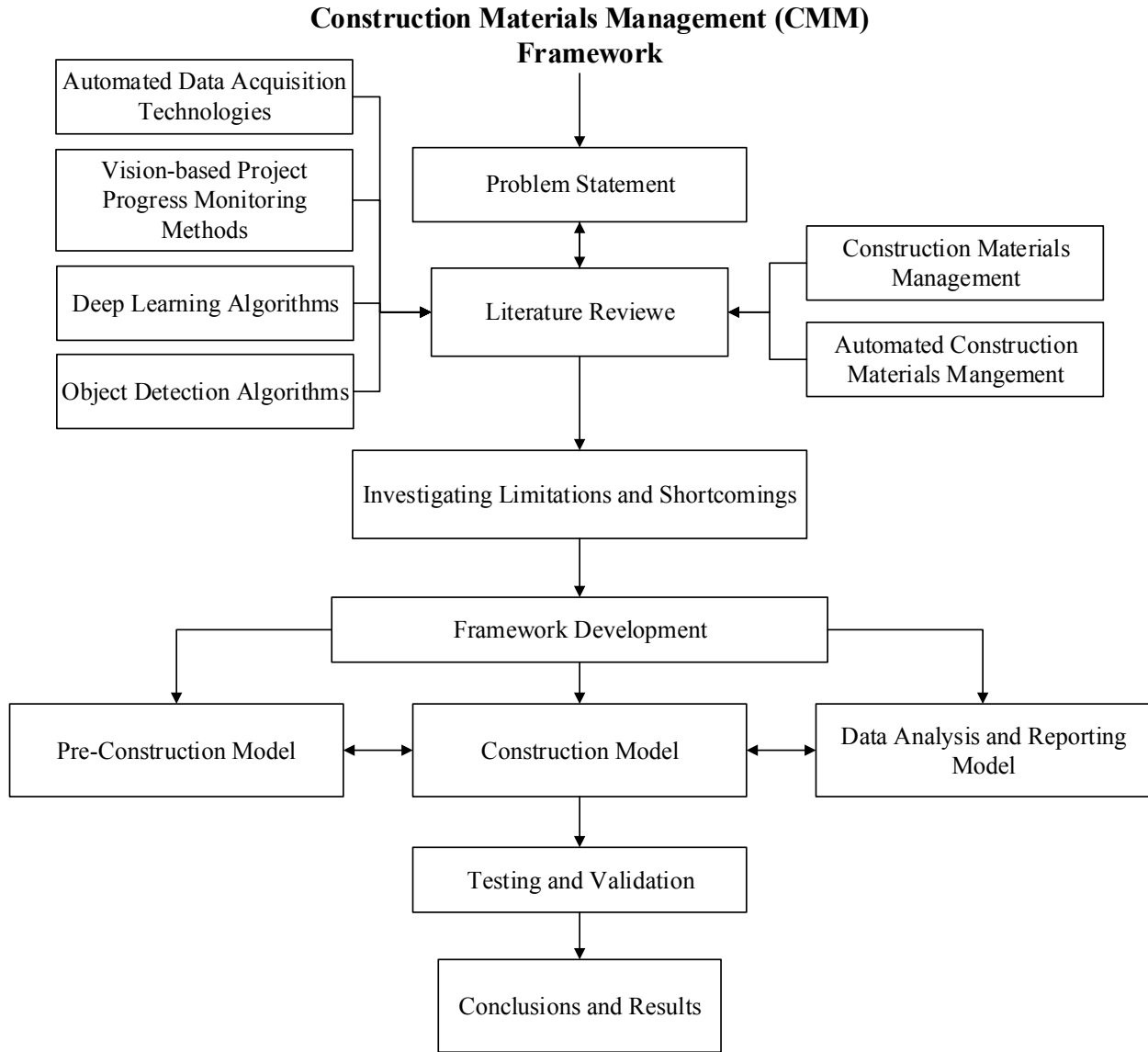


**Figure 1-1: Research Methodology**

### 1.4 Organization of the Thesis

This dissertation is comprised of five chapters. The summary of each chapter is presented as follows:

Chapter 2 reviews the previous works on the topics related to construction materials management, automated construction materials management, automated data acquisition technologies, vision-based project progress monitoring methods, DL algorithms, and object detection algorithms. This chapter proceeds with the presentation of findings from the literature, research gaps identification, and the investigation of techniques suitable for this research,

Chapter 3 presents the research methodology in detail. It is composed of three distinctive models, namely “preconstruction model,” “construction model,” and “data analysis and reporting model.”



Each model contains various sub-modules as well.

Chapter 4 investigates the verification and validation of the models and algorithms developed in Chapter 3 through laboratory and field experiments.

Finally, Chapter 5 highlights the expected contributions of the research and plans for future work.

## CHAPTER 2: LITERATURE REVIEW

### 2.1 Introduction

A report entitled "Modern Management Systems" was published in the year of 1982 by the Construction Industry Cost Effectiveness Committee (CICE) of Business Roundtable. In this report, two significant statements related to materials management in the construction industry resulted in conducting comprehensive research focusing on materials management by the Construction Industry Institute (CII) in 1984. Ignoring the significant contribution of materials management to the cost-effective execution of construction projects by senior construction managers and the hindrance of the construction industry against the manufacturing industry in applying the concepts of materials management were the construction industry problems mentioned in CICE report (Nasir, 2008). Research done by CII had two phases. The first phase investigated and defined the aspects of materials management systems being designed and executed properly. The second phase estimated and quantified both the benefits and costs of materials management systems. The second phase of this research indicated that improved craft labor productivity is the most significant benefit that can be derived from a proper materials management system. The improvement of craft labor productivity can be due to the fact that materials are more likely to be available when needed, and craft supervision can plan the work around material availability. Other benefits are reductions in bulk materials surplus, reductions in management manpower, purchasing improvements, cash flow savings, and reductions in required warehouse space (Bell and Stukhart, 1987). After the publication of the procurement and materials management handbook as an implementation resource by CII in 1999, another study was sponsored by CII to identify changes in materials management from 1999 and resulted in an updated handbook of materials management in 2011. This guide includes all materials management functions at both organizational and the project levels and recent practices and procedures of materials management. This reference guides material managers to handle material related issues from its production in manufacturing units to its installation on the construction site more properly by presenting and explaining a set of procedures, strategies, and necessary operations. Moreover, the Fully Integrated and Automated Technology (FIATECH) initiative presented a Material Management Framework (MMF) for the capital projects industry to integrate and automate procurement and supply management systems in 2011 as well.

This chapter presents the main concepts and the background of construction materials management in five main sections. It starts with an introduction to the preliminary researches in the field of materials management in the construction industry (section 2.1). It provides a holistic overview of construction materials management, including definitions, various types of construction materials, materials management functions, and the role of materials management in the construction industry in subsection 2.1.1. Significant problems and needs of materials management and control are explained in the next subsection (subsection 2.1.2). The second section (section 2.2) is dedicated to delving into currently available literature, which includes construction materials management (subsection 2.2.1) and automated construction materials management domains (subsection 2.2.2). In the second domain, not only the application of Automated Data Collection (ADC) technologies in the construction projects and materials management but also computer-based materials management systems have been investigated. Limitations and research gaps are identified and elaborated in section 2.3. Based on the identified limitations and requirements to develop a comprehensive construction materials management framework, genetic algorithm

optimization, Artificial Neural Network (ANN), and Multi-Layer Perceptron (MLP) are reviewed in sections 2.4 and 2.5 respectively. A review of project progress monitoring by focusing on the state of the art vision-based project progress monitoring methods has been elaborated in the next section (section 2.6). Three categories of vision-based methods are described in three subsections (subsections 2.6.1 to 2.6.3). Section 2.7 focuses on DL algorithms against conventional computer vision algorithms. Deep learning-based generic object detection is presented in section 2.8, and finally, identified limitations to be addressed are summarized in section 2.9. The structure of the chapter is illustrated in Figure 2-1.

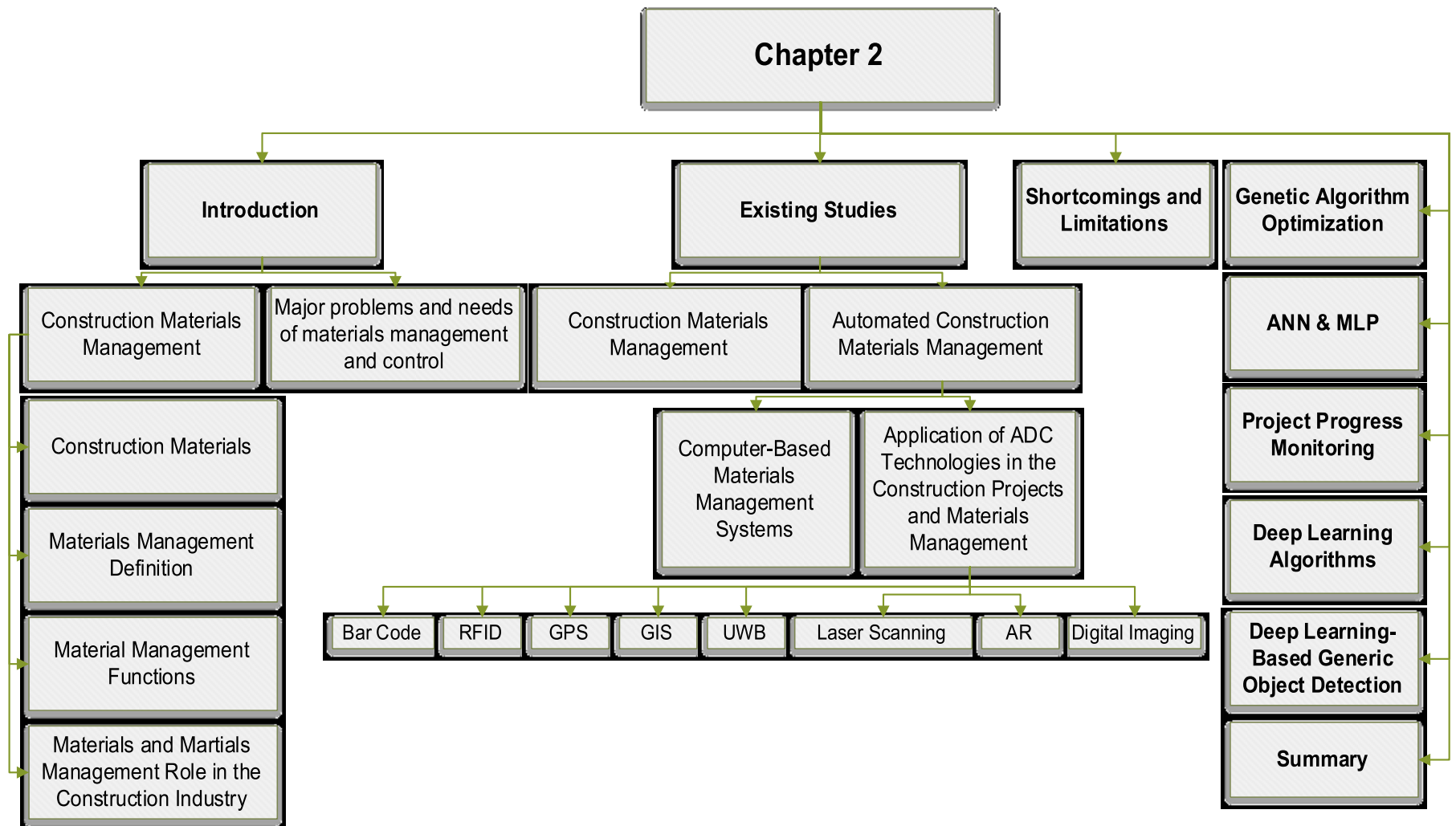


**Figure 2-1: Structure of Chapter 2 (Literature Review)**

### 2.1.1 Construction Materials Management Overview

In this section, a general overview of construction materials management, including various types of construction materials, materials management definition, materials management functions, and the role of materials management in the construction industry, is provided.

The term “materials” in the study done by Stukhart (1995) includes raw materials, components, finished products, consumables, packing and packaging, and equipment. Bailey and Farmer (1982) described construction materials as goods procured from sources out of the owner/contractor’s company and consumed to generate the construction project’s output. From the CII perspective of view, materials are categorized into three basic types: engineered (tagged) materials, bulk materials, and prefabricated materials (CII, 2011).

- Engineered materials: materials with a unique tag number which can be referred to and identified. They are subcategorized in major and minor materials/equipment.
- Bulk materials: materials manufactured to industry codes and standards and purchased in quantity.
- Prefabricated materials: materials engineered and fabricated according to the engineered specifications at a fabrication shop or outside the construction site.

Construction materials can be classified in the following groups as well (Chandler, Ian E., 1978; El-Qader Al Haddad, 2006):

- Bulk materials: this kind of material is delivered in mass. They are unloaded and deposited in containers, such as sand, gravel, cement, and concrete.
- Bagged materials: for easy usage and handling, this kind of material is delivered in bags, such as cement.
- Palletted materials: Bagged materials that are set on pallets for delivery are called palletted materials, such as cement and doors.
- Packaged materials: To avoid damage and deterioration during materials transportation and stock respectively, this kind of material is packaged together, such as tiles, pipes and electrical fittings
- Loose materials: this kind of material needs to be handled separately. They are partially fabricated, such as paving slabs, structural timbers, and pipes.

In another study by Stukhart (1995), materials used in construction projects are categorized as follows:

- Bulk materials: these kinds of materials, such as pipes, wiring, and cables, are produced meeting specific standards and are sold in quantity. Since their consumed amounts just can be measured at the end of the job, so their planning is much more difficult.
- Engineered materials: these kinds of materials are designed and manufactured uniquely by the engineering staff for a particular project. Their production and fabrication have a significant influence on the project schedule.
- Fabricated materials: these kinds of materials are manufactured based on a specific design for the project.

According to the study done by Halpin et al. (1987), materials for a construction project can be categorized into three groups: off-the-shelf, long-lead bulks, and engineered items.

Materials management has several definitions. Planning and controlling all the required processes to specify the right quality and quantity of materials and equipment appropriately in time, obtain the needed materials at a reasonable cost, and make them available when required is called materials management system (The Business Roundtable report, 1982). Materials takeoff, purchasing, expediting, receiving, warehousing, and distributing integrated with a process is defined as materials management (Bell and Stukhart, 1986). CII (1999) states that materials management is an integrated process of various functions, including traditional materials management tasks such as planning, material takeoff, and engineering interface, supplier inquiry, and evaluation, purchasing, expediting and logistics, field control, and warehousing. Ren et al. (2011) state that materials management includes the process of planning, inventory control, receiving and storing, material handling, physical distribution, and relevant information from the origin to consumption to conform with the customer requirements. According to the definition by Vrat (2014) in his book, materials management is concerned with the design, specification, procurement, transportation, inspection, storage, retrieval, use, disposal, and accounting of materials to maximize return on investment in materials. Caladas et al. (2015) describe it as a process in which materials and equipment are identified, acquired, and delivered to their intended points of use.

In addition to the definition of materials management, each study has defined various functions of the materials management process. In a holistic view, typical tasks associated with the materials management process are almost similar to each other, but each study has highlighted some functions more than the others based on its point of view. For instance, a study done by Chapman et al. (1990) has deliberated the results of the Science and Engineering Research Council's sponsored investigation. It has declared the following functions as materials management functions:

- Planning and communication
- Materials scheduling
- Supplier inquiry and evaluation
- Purchasing
- Expediting and shipping
- Receipt, storage, and distribution
- Materials control

According to the CII (1999) materials management process consists of the following functions:

- Planning
- Material take-off and design interface
- Supplier inquiry and evaluation
- Purchasing and subcontracts
- Quality assurance
- Expediting and transportation

- Warehousing and field control

These functions are illustrated in Figure 2-2.

Nasir (2008) illustrates the components of a materials management system in a flowchart (Figure 2-3), which is based on the research done by Stukhart (1995).

Georgy and Basily (2008) stated that the materials management process consists of the following functions and steps:

- Request for Quotation (RFQ)
- Bids and vendor selection
- Purchase Order (PO)
- Tracking and expediting
- Transport
- Receiving and inspection
- Inventory

Activities of Construction Material Management (CMM) process, which is described complex, integrated, and dynamic by Ren et al. (2011) are as follows:

- Material takeoff
- Material planning
- Ordering & purchasing
- Material inventory
- Site working
- Monitoring
- Control

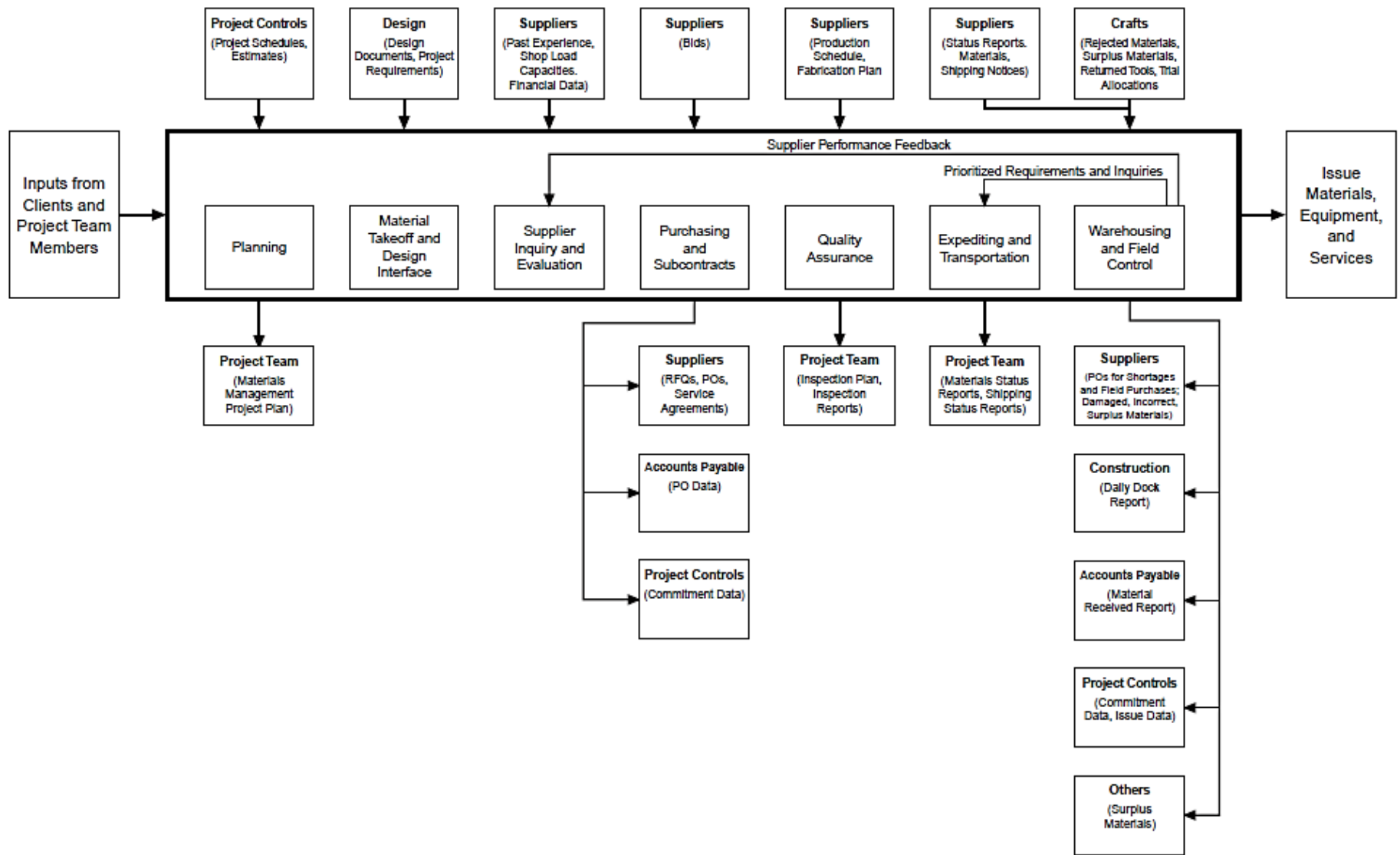
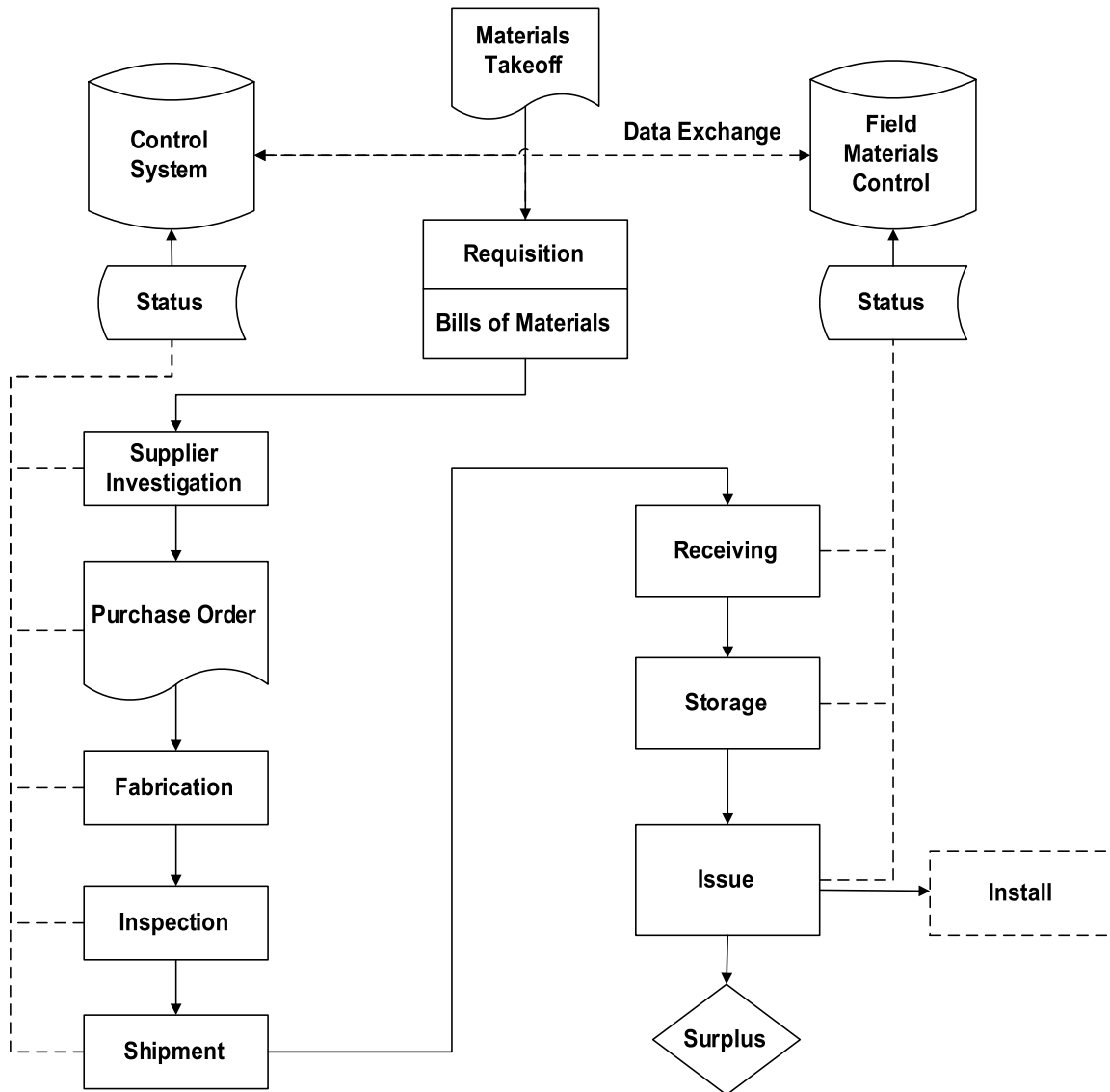


Figure 2-2: Materials Management Functions (CII, 1999)





**Figure 2-3: Flow Chart of Construction Materials Management (Nasir, 2008)**

Caldas et al. (2015) identified the following functions as the most significant materials management functions through the analysis of the results of the surveys and case studies and interviews with owners and contractors.

- Materials Requirements Planning (MRP): MRP consists of identifying, quantifying, and scheduling the required materials and equipment for the project.
- Project acquisition strategy: In this function, suppliers who can provide the required materials, equipment, and services are identified. So it needs knowledge related to industry, company procedures, required commodities, and the existing suppliers to qualify and certify the most proper suppliers.
- Purchasing: After requirement identification, goods, and services meeting the established delivery, quality requirements, and reliability standards have to be ordered at a competitive price in the purchasing function.

- Subcontracting: Subcontracting encompasses assessing the project and company requirements, development of subcontracting strategies and plans, subcontractors identification and validation, Requests for Proposals (RFP) issuance, receiving bids, commercial evaluations, negotiation, funds commitment for goods and services, and eventually contract administration.
- Expediting: In the expediting function, it should be guaranteed that the suppliers deliver materials, technical data, and equipment on time according to the purchase orders, the project's requirements, and schedules.
- Supplier quality management: The quality of construction materials, fabrication, and on-site services provided by suppliers have to be monitored in this function. The quality defects of materials and poor performance in the service and construction would increase the risk of future operational problems and, subsequently, the maintenance and operations cost.
- Transportation and logistics: The movement of materials to the job site has to be planned, controlled, and executed in this function, considering the engineering, procurement, and construction schedule requirements.
- Site materials management: Site materials management is a function in which the existence of the right materials and equipment with the right quantities and at the right time to the construction forces must be ensured.
- Materials management for operations and maintenance: This function consists of all aspects of running an asset. In this function, it should be ensured that the equipment is available as needed and is maintained for the startup. It is stated that the O&M materials requirements should be planned by the owner and the contractor jointly during the engineering and procurement phases of the project.

The significance of the materials and materials management role in the construction industry can be illustrated through the various statistics which are presented in this section. On the one hand, around 50-60% of the industrial construction projects cost is composed of identifiable cost of material in which the economic costs are not considered (Bernold, 1990b; Stukhart, 1995) and on the other hand, materials control 80% of the project schedule from the initial materials acquisition to the delivery of the last item (Kerridge, 1987; Stukhart, 1995). Fallahnejad (2013) has stated that on-time construction materials procurement is a key factor that can result in completing construction projects on time. Even though the significant portion of the total cost of a construction project belongs to its construction materials, only 0.15% of the construction cost is invested in materials management and control in contrast with the general industry that spends 1% of the production cost in materials management and control (Formoso and Revelo, 1999; Navon and Berkovich, 2006). In the Business Roundtable report (1982), it is stated that if materials and equipment had been available at the worksite when required, it could result in a 6% reduction of all construction labor costs (Bell and Stukhart, 1986).

The craft foremen reports had indicated that when there was not an effective materials management system, around 20% of their time was spent to hunt materials and about 10% to track purchase orders and expedite. It is illustrated that the timing and materials volume of the initial orders are two significant influencing factors on the materials surplus. It is estimated that fragmented materials management system and performing final takeoff function before final design drawings result in a 10% bulk materials surplus (Bell and Stukhart, 1987).

Similarly, Bell and Stukhart (1986) tried to converse about the aspects of materials management systems. It was indicated that improper material management functions would result in materials surpluses, shortages, costly labor delays, and problems in cash flow. Large stock of material or inventory buffer affects cash flow, loss and damage potential, storage and handling costs, and the flexibility for addressing design changes (Bell and Stukhart, 1987). In summary, inefficient materials management including late, improper or out of order materials delivery, large inventory, and lack of material can result in low productivity, cost overrun, schedule delay and poor quality in construction projects.

Some researchers investigate the mentioned causes and effects in their studies. For instance, Al-Momani (2000) examined 130 residential and small commercial projects, and it was concluded that the main cause of delays was late materials and equipment. Ahmed et al. (2002) also indicated that late fabricated materials were the third most common cause of construction projects delay in 380 building projects in the state of Florida. Perdomo and Thabet (2002) expressed that low labor productivity and project delay, which are the result of improper materials plan and control, lack of required materials, poor materials identification, re-handling, and insufficient storage, can lead to the project cost increase. Thomas et al. (2005) concluded that the documented frequent cause of disruptions in 125 studied projects was materials management problems. Considering lean construction researches, Kumar (2010) found that in the fast track projects, late delivery of drawings and materials force contractors to respond much more quickly, and it might result in lower quality performance. Another study done by Rahman et al. (2013) illustrated that contractors were often encountered with the late delivery of materials as the tenth most significant factor resulting in project cost overruns in Malaysia.

Furthermore, they stated that “late or irregular delivery or wrong types of material delivered during construction affect the utilization of other resources like manpower and machinery.” In other words, it can lead to low productivity, time delay and cost overrun as well. Barry et al. (2014) stated that in the small and medium-sized construction projects most common problems with materials are an interruption to the work schedule, rework from having the wrong or out-of-order materials, double handling because of insufficient materials, material deterioration during extended storage periods, expenses associated with crews lacking proper materials, and lost items on or off-site. Moreover, Gurmu (2018) has mentioned that advanced technology and change in management practices are the most important influencing factors on labor productivity in the construction industry. So the lack of proper materials management system can severely affect productivity, mainly when the required materials are purchased and imported from overseas in a construction project. Three most essential construction materials management practices to improve labor productivity are materials procurement plans, identification of long-lead materials, and materials delivery schedule

Considering studies’ outcomes and statistics mentioned before, it is easy to find out the significant role of materials management in construction projects and to see the negative impact that poor materials management can have on the cost and schedule of the construction projects.

### **2.1.2 Major Problems and Needs of Materials Management and Control**

Shortcomings and problems concerning construction materials management and the main objective of this research to address the main issues have been presented in this section. Materials management significant problems are as follows (The Business Roundtable, 1982; Bell and Stukhart, 1986; CII, 1999; Formoso and Revelob, 1999; Navon and Berkovich, 2006; Young et

al., 2011; Majrouhi Sardroud, 2012; Azarm, 2013; Barry et al., 2014; Ajayi et al., 2017; Dakhli and Lafhaj, 2018):

- Materials required but not ordered/purchased ;
- Materials purchased but not received;
- Materials arriving at the site at the inaccurate time;
- Materials arriving at the site in the incorrect quantity;
- Materials with different specifications compared with those in the purchase order;
- Lack of information associated with the status of the orders;
- Lack of comprehensive and up-to-date information related to the arrival of materials on the site;
- Lack of up-to-date information regarding site stocks;
- Extensive multiple-handling of materials inappropriately stocked while searching required pieces;
- Missing or surplus materials;
- Storage space shortage for materials on-site;
- Waste of man-hours to search and track materials;
- Materials that are issued to crafts and are then not used or installed (untargeted materials);
- Fragmented implementation of material management functions;
- Minimal communication and no clear responsibilities defined for the owner, engineer or contractor to perform materials management;
- The significant contribution of materials management to the cost-effectiveness of project operations is not recognized by the senior management;
- Materials management personnel with inadequate training;
- Damage of critical materials or equipment;
- Improperly sequenced deliveries;
- Incomplete, or erroneous definition of materials;
- Massive wastage of materials (deterioration, theft, lost);
- Inaccurate takeoff quantities;
- Unnecessary reordering of material;
- Materials ordered verbally or using short notice;
- Inability to determine material locations.

A couple of studies that have tried to obviate some of the mentioned shortcomings have been reviewed in the next section.

According to the research by Bell and Stukhart (1986) a desirable materials management system used by owners and contractors should consist of various attributes such as planning and communications, material takeoff and engineering interface, vendor inquiry and evaluation, purchasing, expediting and shipping, warehousing, receiving and material distribution, material control, computer systems. It was stated that on-line computer systems, personnel training, preconstruction materials planning, and the communications among owner, contractor, and engineer are the influencing factors to make materials management successful and hinder the before mentioned problems.

The activities of construction projects are highly interdependent, and engineering, procurement, and construction phases overlap to a great extent (Yeo and Ning, 2002). The current state of research does not adequately consider the complex, unstructured, and dynamic nature of the construction projects in developing the materials management systems. So, the present study has investigated the functions and processes which have to be integrated with the materials management framework to make it capable of considering the dynamic nature of construction projects and being updated frequently during the construction phase. It will result in taking more accurate and near real-time corrective actions and prevention of project schedule delay and cost overrun. Thus, a framework for the configuration of the whole construction materials management system is developed, and the efficient technologies and methods to implement the processes are proposed as well. To evaluate the developed framework, its various models are validated by laboratory and field experiments.

## **2.2 Existing Studies**

This section reviews the currently available literature classified into “construction materials management” and “automated construction materials management.”

### **2.2.1 Construction Materials Management**

In the study done by Thomas et al. (1989), the benefits of applying efficient material management practices on two commercial construction projects were quantified. The cumulative productivity was calculated in both projects. One project had effective informal material management practices, including organizing the storage area, expediting and sequencing material deliveries, and erecting the steel directly from the truck as it was delivered. In contrast, the other project did not have effective material management. On top of that, work-hour losses were calculated in one project based on the comparison between the productivity of the days with adverse material-related conditions and the expected productivity of the days with no adverse conditions. The results indicated an 18% work-hour overrun and about 19% time overrun. Accuracy, quality, quantity, cost, timeliness, and availability were six key measures used to evaluate the effectiveness of the materials management process for industrial construction projects by Plemmons and Bell in 1995. They used an industry-wide benchmarking procedure to simplify the application of the effectiveness measures. Thomas et al. (1999) studied three various structural steel erection projects in which the delivery methods of material (structural steel members) as a component of materials management were different. By quantification of labor productivity using the multiple regression techniques, the best delivery method of material (steel erection directly from the truck against two others including steel off-loading, sorting, and then erecting, and three bulk steel deliveries) was indicated. The study by Kini (1999) focused on the effective implementation of the materials management process as the key element to successful project management. In this study, seven stages of an engineering/procurement/construction (EPC) project: “planning, preliminary design, final design, procurement, vendor control, construction, and closeout” were explained by focusing on material management. In the small-sized building firms, Formosoa and Revelob (1999) used Total Quality Management (TQM) principles in their developed method to enhance the materials supply system. They applied simple quality techniques, including flowchart, brainstorming, checklist, and Pareto diagram, to identify, analyze, and solve the problem. The main investigated problems in this research consisted of design problems, unorganized materials transportation and delivery, verbal materials order, imperfect or inappropriate materials specification, unavailable estimation of the required amounts of materials, delayed price assessment, and surveys. Delayed

materials orders and delays in checking stocks. Thomas and Sandivo (2000) tried to illustrate the quantitative impact of the fabricator on construction labor efficiency through three case study projects. It was found that some materials management issues related to site storage conditions, delivery and erection methods, and contractor-fabricator coordination had a significant effect on labor performance. So the labor inefficiency percentage, as well as the percentage of schedule delay, were calculated for each case study, and it was indicated that labor inefficiencies resulted from inefficient materials management ranged from a low of 5.4% to a high of 56.8%. Moreover, considering the activities of case studies which took 50 to 130% more workdays than the required workdays, it was concluded that poor materials management practices would result in schedule delays as well. Perdomo and Thabet (2002) tried to survey current materials management practices for an electrical contractor to recognize and summarize problems and bottlenecks through interview visits. Thomas et al. (2005) stated that poor site materials management results in inefficient labor productivity practices in construction projects. So they divided a construction into three zones (semi-permanent storage, staging areas, and workface storage) and then developed site construction management principles for each zone to hinder poor practices. Wickramatillake et al. (2007) investigated a performance measurement methodology through a real case company. They concluded that there existed eight key areas of concern relating to supply chain performance measurement of a large-scale project and then proposed and recommended some solutions for each concern area. Polat et al. (2007) proposed a simulation-based decision support system to achieve an economic rebar management system. They defined three differences between the Just In Time (JIT) and Just In Case (JIC) materials management systems, including buffer size, scheduling strategy, and lot size. Then considering buffer size in terms of large, medium, and small, scheduling strategy in terms of optimistic, neutral, and pessimistic, and lot size in terms of large and small, contractors were faced with 18 alternative rebar management systems between the JIT and JIC management systems. By applying Discrete Event Simulation (DES), the most economical rebar management system with the least inventory cost at the planning phase of a project was selected. JIC was selected as the most economical rebar management system in their case study, with 4.8% savings of the total cost of inventory over JIT. Sacks et al. (2009) tried to use computer-aided visualization tools to support a set of lean construction management requirements for both planning and control. Lean construction requirements, including making the process transparent to all, JIT delivery of materials and respond flexibly to change, were difficult to achieve in construction projects than in manufacturing. So they investigated visual tools applications such as Building Information Modeling (BIM)-based visualization user interfaces to achieve a clear mental image of what was taking place and what could be expected in the near future, which supported lean construction requirements.

In research done by Azarm (2013), the shortcomings of the schedule performance index of Earned Value Method (EVM) were discussed. Then the material status index (MSI) was developed as a supplementary index to support the EVM. In this research, to improve the accuracy of duration forecasting and reporting on schedule performance of a project, it was stated that quantities of materials installed could represent schedule performance. So materials were considered as fuel to construction projects, and the physical progress of projects can be measured by defining the quantities of materials in place. Two automated data acquisition technologies (Radio Frequency Identification (RFID) and Light Detection And Ranging (LIDAR)) were only proposed to measure the current inventory. It was stated that the quantities of installed materials could be obtained by subtracting the current inventory and wasted materials (considered 10%-15% of the total amount installed) from replenished materials. All these steps are just proposed and have not been illustrated

and developed. Caladas et al. (2015) investigated 54 organizations through surveys, interviews, and case studies to identify current practices in terms of materials management techniques used in the capital projects industry. In fact, in their first survey, a preliminary snapshot of the current status of materials management functions in the construction industry was obtained and analyzed, in the second survey, trends and issues of materials management were predicted by leading industry practitioners. It was concluded that just around 26% of the entire organizations (surveyed owner and contractor organizations) had IT systems that supported synchronization across major supply chain tiers of project schedules and change to dates. Also, only 25% of them had materials management systems that allowed engineering requirements to go directly to the materials management system as electronic data.

In addition to transportation costs, which have to be considered while planning industrial megaprojects, Ahmadian et al. (2016) illustrated the significance of off-site material transport time as another crucial variable. They developed a framework to estimate the duration of off-site transportation considering various construction materials categories, transport mode, size, and weight of consignments. In one part of the study done by Gurmu (2019), a tool was proposed to score materials management practices for multistory construction building projects in Australia to predict construction productivity. It was shown that construction productivity could be increased by planning, monitoring, and evaluating materials management practices. Moreover, through in-depth interviews with experts, he found that procurement plans for materials, long-lead materials identification, and materials delivery schedule were the most significant practices to improve the productivity of building projects.

A group of researches has utilized simulation and optimization methods to enhance management processes, including material inventory optimization. Materials delivery and inventory were optimized by Georgy and Basily in 2008, utilizing Genetic Algorithm (GA). Project MRPs were used as input for GA to minimize the total material cost. Since the solution space for the optimization of delivery and inventory of materials is almost infinite, no specific number of orders is known in advance, material requisition schedule can be represented in a string form (consisting of material quantities delivered at a particular time) resembling the chromosomes used in GA as input and finally, a near-optimum solution minimizing material costs is obtained and is acceptable for all practical purposes, so they concluded that GA is a proper optimization engine for this purpose. Jang et al. (2007) optimized the floor-level construction material layout required for multiple-floor buildings in urban areas using GA and through removing unnecessary repositioning of construction materials. This optimized floor-level construction material layout determined how to appropriately position/place the construction materials to minimize the travel distance between work spots and construction materials. By implementing the proposed approach in a real case, it was found that inefficiencies in the positioning of construction materials at the floor-level could result in a 14% increase in the construction labor material handling distance. Fang and Ng (2011) used the Activity-Based Costing (ABC) approach to minimize logistics cost of construction materials (such as precast concrete units) between the supplier's factory and the construction site. Logistics cost consisted of procurement, stocking at the supplier's yard, transportation and loading and stocking on site. GA was used to find the optimal solution by defining activity start time and number of times for material delivery. In the research done by Said and El-Rayes (2011), a construction logistics planning model was developed in which the decisions of material supply and site layout were optimized simultaneously to minimize logistics costs (ordering cost, financing cost, stock-out cost, and layout costs). The model considered

interdependencies between material supply and layout decisions and was able to measure the impact of these decisions on project delays. They extended their research and developed a novel Congested Construction Logistics Planning (C2LP) model to optimize logistics plans. A multi-objective genetic algorithm was used to reach a trade-off between minimization of total logistics costs and schedule criticality. They considered different decision variables, including material procurement, material storage, facility layout, and scheduling of noncritical activities. Through shifting of noncritical activities, they tried to offer additional interior spaces for material storage and minimize the project logistics costs (Said and El-Rayes, 2013). One year later, they proposed a new Automated Multi-objective Construction Logistics Optimization System (AMCLOS) to optimize material supply and storage planning. Project spatial and temporal data are automatically retrieved from BIM and project schedule and integrated with contractor and suppliers' data to minimize total logistics costs (Said and El-Rayes, 2014). In all their researches, a fixed-ordering-period was selected in every construction stage. It means each material was considered to be delivered to the job site in fixed intervals. Inventory replenishment and allocation decisions were modeled by Lu et al. (2018) through integrating supply logistics and site logistics issues in a novel framework. By applying the GA-based simulation optimization method, they could find the optimal inventory level under various allocation policies (including schedule-based, cost-based, demand-based, schedule-cost-based, and schedule-demand-based policies.) It was concluded that the schedule-based policy was the best policy when the Path Difference (PD) value of a project network was small (or large).

According to the above literature review, it can be stated that research developments related to construction material management have been expanded in the following areas:

- Site layout planning for material storage or optimization of material storage on-site;
- Simulation and optimization of logistics plans, material delivery, and inventory to enhance management processes;
- Effectiveness and performance measurement of the materials management process;
- Efficient materials management practices and their applied approaches, materials management problems and their influences on project productivity, cost and schedule; and
- Lean construction or investigating the implementation of Just-In-Time (JIT) strategies in construction projects.

There are some studies as well which have focused on material waste management and quantification areas such as works done by Poon et al. (2001), Poon et al. (2004), Jalali (2007), Ajayi et al. (2017) and Mahmood Maad and Noori Sadeq (2019). In the research done by Ajayi et al. (2017), it is stated that to minimize construction waste, not only construction stages and the design impacts should be considered but also materials procurement process has to be observed and improved. They found that for waste mitigation, the five most critical procurement measures are: “commitment to take back scheme,” “procurement of waste efficient materials/technology,” “use of minimal packaging,” “use of Just in Time (JIT) delivery system,” and “prevention of over-ordering.”

The construction materials management concepts, efficient materials management practices, and their applied approaches, which have been discussed in this section, are considered in this research for the development of the materials management framework. For example, in the first (preconstruction) model of the developed framework, an optimized material delivery schedule



with the least cost is generated to avoid early/late purchasing and excess/inadequate purchasing because early purchasing and excess purchasing result in cash flow problems and wast or surplus, respectively.

### **2.2.2 Automated Construction Materials Management**

In the reviewed studies in the previous section, researchers tried to focus on the concepts of materials management and improve it through the implementation of JIT strategies, materials storage optimization, performance measurement, investigation of proper materials management practices, measurement and reduction of the influences of the most probable issues on project cost, schedule and productivity. But there were other points of view to improve construction materials management as well. It was concluded that managing materials on-site through paper documents was not practical in complex and large scale construction projects. Moreover, it was stated that when materials management processes were executed in a consistent manner, it operated more efficiently. So through a computerized system, construction materials management could be implemented more appropriately and lead to more benefits such as uniformity of documents generation, speed, and efficiency, automatic process implementation from inputting information to report generation in a matter of hours. But a computerized system alone could not ensure the accuracy of the reports upon which corrective actions or various decisions were made. The output information and reports were only as good as the input data created them. Therefore on top of the development of a computerized system, there was a question of the accuracy of input data. Since manual data collection was slow, inaccurate, and resulted in extensive amounts of paperwork and also paper-based reports were problematic, error-prone, and inefficient, so Automated Data Collection (ADC) technologies were applied to reduce paper-based requirements and solve the issue. The studies related to (1) computer-based materials management systems and (2) application of ADC technologies in the construction projects and materials management are reviewed and described below.

With respect to the first front (computer-based materials management systems), Elzarka and Bell (1995) developed materials management systems using an Object-Oriented Methodology (OOM) data structure. Its attributes included automated commodity code creation, automated takeoff, intelligent purchase order issuance, and integration of design and schedule. They believed that since many firms have applied the relational database model for their MMS, so they could not integrate it with external computer-based systems related to design, project scheduling, and cost accounting.

Wong and Norman (1997) presented a computer-aided Materials Planning System (MPS) in construction to increase cost savings. A study done by Chapman et al. (1990) brought up the result of the Science and Engineering Research Council's sponsored investigation into the impact and problems of automation in materials management on large construction projects. Through surveying five large construction firms in the U.K., the level of automation in materials management was assessed. In fact, in this research, automation refers to the degree to which the companies used computers. It was found that none of the companies had an integrated system for materials management, and the problems of using an automated materials management system were the attitude of the building firm, attitude of the firm's personnel, software, and hardware available. An e-commerce system named Construction Materials Exchange (COME) was developed by Kong et al. (2001) to hinder the limitations of the traditional construction materials procurement process and improve its effectiveness and efficiency. A software system entitled

“Virtual Construction Material Router (VCMR)” was designed and implemented by Nialidjoubi and Yang (2001) to behave as a decision-support system for materials movement in complex construction sites. Software systems such as computer-aided design, geographical information systems, and fuzzy logic were integrated to help site managers and planners to assess materials movement in the construction site and select the best available route. Subsomboon et al. (2003) proposed a three-dimensional (3D) and four-dimensional (4D) computer model, and a Fully Integrated and Automated Project Process (FIAPP-based) system for procurement and materials management. A material-status monitoring system was developed, which, along with the three-dimensional model, could record and retrieve construction material procurement status visually. So this status-monitoring system would “color-code” 3D objects in the computer model upon their procurement status (ordered, delivered, on-site, etc.). El-Qader Al Haddad (2006) developed a construction materials management software entitled "Construction Materials Management Software"(CMMS) using Microsoft Excel. His work was a solution to some issues, such as manually managing of construction materials in contracting companies, and shortage of user-friendly construction materials software packages. Navon and Berkovich (2006) developed an automated model for material management and control procedures, including materials purchasing, following up the status of PO, recording materials data when delivered at the site and their movement in the site, making recommendations, generating reports and issues warnings. They tried to replace manual materials management with an automated model to reduce materials surplus, delays, to remove the lack of timely information associated with the purchase orders (POs) status, the inventory levels, and the actual vs. planned materials consumption and to improve the productivity. Their study consisted of three major parts: literature was investigated in the first part to identify and analyze construction materials management problems and issues. An automated construction materials management was developed in the second part to prevent the identified issues, and the evaluation and application of the system under real condition was conducted in the third part. Lu et al. (2011) built a Materials Tracking Management Information System (MTMIS) for railway construction. Through establishing materials supplier files and recording key information from materials testing, receiving and allocation in the MTMIS, the supplier who has provided the materials and the place where those materials have been used, can be identified. In the case of material quality problems, other sites where the same batch of materials have been used can be traced. Tian et al. (2012) developed an electric materials management system/software in which two-dimensional barcode technologies were used for automated collection of material information and acceleration of inventory turnover. Ma et al. (2013) presented an integrated Mobile Material Management System (MMMS) in which Quick Response (QR) code and mobile terminals were applied with a special tagging method to improve material management on construction sites. It was integrated with an existing Enterprise Resources Planning (ERP) system through the Internet. Kasim (2008 and 2015) developed a real-time prototype system in which RFID-based materials tracking and resource modeling systems are integrated to improve tracking materials and inventory management processes. Kasim (2008) mostly focused on real-time identifying and tracking of materials using RFID on various locations, including construction site during materials delivery and materials installation and storage area. Jung et al. (2018) proposed a multi-method simulation model consisting of Discrete Event Simulation (DES) and Agent-Based Modeling (ABM) to model the interrelationships between construction and material supply processes and to analyze the complexity of supply chain process in high-rise building construction. Their simulation model includes off-site material supply process model, on-site material supply process model, and construction work process model.

This section of literature indicates that researchers concluded that on-line systems (which can control bills of materials, purchase orders, and material deliveries) were extremely cost-effective. So they tried to develop computer-based data systems for construction material management during the last four decades. But the existing computer-based material management systems focus on the following aspects:

- Integration of the materials management processes or integration of construction and materials management processes using various techniques, and
- Application of ADC technologies to collect materials localization and tracking data, and integration of these data with computer-based materials management systems.

As to the application of ADC technologies in the construction projects and materials management, it can be stated that, since the critical decisions have been taken based on erroneous or incomplete data, most of the project managers always encounter with project delays and cost overruns. So to collect more accurate data, ADC technologies that were used in the manufacturing and retail industries have been introduced and applied in the construction industry (Su and Liu, 2007). ADC technologies had been utilized for efficiency increase, reduction in data entry errors, which are always caused by human transcription, and reduction in labor costs (Nasir, 2008). Davidson and Skibniewski (1995) illustrated the performance, speed, and accuracy of ADC against traditional manual data collection systems. Their developed Automated Data Collection (ADAC) model was used to estimate the time, labor, and equipment which were required to scan the labels of equipment in an office building by ADC.

Moreover, the optimum configuration of ADC technology, labor, and label positioning was picked out through simulating various configurations. So, multiple researchers developed different approaches along with emerging various automated data acquisition technologies to automate the process of data collection required to perform identifying, location sensing, and tracking the movements of objects, control, and progress reporting in construction projects. These technologies include barcode technology, Radio Frequency Identification (RFID), Global Positioning Systems (GPS), Geographic Information Systems (GIS), Ultra-Wideband (UWB), laser scanning, Augmented Reality (AR), and digital imaging.

An overview of these automated data acquisition technologies, along with their applications in the construction industry, are presented.

It is stated that RFID systems and the Global Positioning System (GPS) are the foremost technologies for automated tracking and monitoring of construction resources and assets in recent decades (Soleimanifar, 2011; Jaselskis and El-Misalami 2003; Goodrum et al., 2006; Song et al., 2006b; Ergen et al., 2007; Lu et al., 2007; Wang, 2008; Behzadan et al., 2008; Chin et al., 2008; Khoury and Kamat 2009). Navon and Goldschmidt (2003) presented computerized algorithms in which labor inputs (productivity) were automatically measured by defining workers' locations at regular time intervals. They used Global Positioning Systems (GPS) and ground-based Radio Frequency (RF) to measure the position of workers performing outdoor and indoor activities, respectively. Sacks et al. (2003) developed a prototype labor control model in which the global positioning system (GPS) technology for the measurement of the workers' locations on-site was integrated with a computerized building project model (BPM) to monitor labor productivity. Su and Liu (2007) tried to obtain construction operational information through geometrical data analysis of resources. In their research, real-time positional data (x, y, z, time) of tracked resources

were collected using RFID or GPS and then translated to as-built productivity information such as a crew balance chart. In the mentioned researches, through defining the vicinity of a building element associated with activities and knowing the workers' locations, the activity a worker is involved in, and the time a worker spends doing an activity can be automatically determined.

Still, as their limitation, some situations cannot be taken in to account by the model. Situations in which workers are outside the vicinity of an element and still performing a value-adding task associated with the activity. Likewise, before mentioned studies, In the research done by Navon and Shpatnitsky (2005), productivity and progress were measured automatically by using GPS for monitoring and control of road construction projects. Navon et al. (2004) developed an automated model to control earthmoving operations. They translated measured locations obtained by GPS to real-time control data such as productivity and materials consumption to manage earthmoving operations. But applying GPS to identify and track all construction project resources is not logical because tagging hundreds of items with GPS receivers would be too expensive, so other technologies being less expensive would be required (Song et al., 2006b). Jang (2007) presented a new prototype framework and a localization algorithm for automated tracking and monitoring system of construction assets. Construction assets consist of equipment, materials, and labor. This tracking system is sensor-based, in which wireless sensor network technologies, including ultrasound and radio signals, are combined to provide full benefits in communication, labor usage, document, and resource management. Soleimanifar (2011) also focused on developing cost-effective resource tracking and positioning framework for indoor or partially covered site environments to improve safety and productivity. The developed positioning architecture entitled "IntelliSensorNet" is the integration of the environment of Wireless Sensor Networks (WSN) and Artificial Neural Networks (ANN) for positioning and tracking critical construction resources such as laborers and equipment. In the year 2014, Soleimanifar et al. investigated the positioning accuracy of two RSS-based location tracking techniques entitled "ranging-based method" and the "profiling-based method" in challenging and dynamic indoor construction applications. The profiling-based method resulted in the positioning error of less than 2.14 m with 95% likelihood, so they found it as an effective localization method to be used for real indoor construction applications.

Since the availability of required resources in a project is ensured by materials control systems, So Nasir (2008) stated that the improper materials control systems could be considered as the most common factor influencing the construction productivity resulting in productivity reduction of nearly 40%. The researchers concluded that effective materials tracking and control leads to the productivity increase, avoiding delays, reduction in the time needed for materials management, and reduction of materials cost due to a decrease in waste. Therefore they focused on tracking the location of materials and collecting the materials data in time, with ease and accuracy. The benefits of Information Technology (IT) to integrate Construction Supply Chain Management (CSCM) processes were investigated in the research done by Irizarry et al. (2013). They developed a BIM-GIS system to visualize not only the supply chain process but also the actual status of materials. In this system, BIM and GIS are used to provide a detailed material takeoff and geographical information required for the transportation and logistics of the CSCM, respectively. An optimal solution in which the logistics costs (cost of orders, warehousing, and transportation) are minimized is generated by the Python language module of ArcGIS.

Le (2017) tried to make materials real-time information (including the arrival of materials, the amount of materials received, the status of materials either in a storage area or in-production, and site stocks) accessible during the construction through developing an automated material inventory control and management system. GIS-based decision support system and a “hybrid” tracking system (Bluetooth scanner and Bluetooth tracker imbedded into a Near Field Communication (NFC) tag) were used to identify the need for materials, order, track, transport, store, and control the inventory, circulate on-site, and incorporate into production. Won et al. (2018) claimed that construction materials localization in complex or large-scale construction sites using GPS, Ultra-wide Band (UWB), and RFID were infeasible in terms of time and cost. They proposed a novel UAV-RFID integrated localization platform to address the limited recognition range and low accuracy of existing methods. They applied a machine learning algorithm (k-nearest neighbors), to increase the localization accuracy.

On top of the mentioned technologies, there are other technologies such as digital cameras, 3D range cameras, and laser scanners that have been applied for image-based modeling of the as-built status of buildings. These optical-based spatial data acquisition technologies have been used for defect and deviation detection, construction job site planning, on-site safety enhancement, and as-built documentation (Bhatla et al., 2012). But the As-built documentation, including a series of records, construction designs, specifications, and equipment location and as-built conditions of projects (Bhatla et al., 2012), is the main application of these technologies needed for construction progress monitoring purposes. For example in some studies (Bosché 2010; Bosché et al. 2009; Gordon et al. 2003; Huertas and Nevatia 2000) laser scanners and wireless embedded sensors have been used to achieve some goals including as-built dimension calculation and control, project 3D status visualization, performance control, early defect detection, and change detection. In fact, in these researches, as-built data are captured using laser scanners to create 3D as-built models. Then the 3D design model is comparing with 3D as-built models to achieve the goal. El-Omari (2008) investigated various automated data acquisition technologies and their capabilities and limitations to find and integrate the most suitable ones in one system to collect data from construction sites for tracking and progress measurement. In a holistic view, a cost/schedule control model was presented in which various automated data acquisition technologies (RFID, 3D laser scanning, photogrammetry, etc.), a software system for planning and scheduling, a relational database, and AutoCAD are integrated.

In the following, technologies which have got the potential to be used, particularly in materials identification, tracking, locating, detecting, and progress monitoring are discussed in detail. These ADC technologies are (1) Barcode (2) RFID (3) GPS (4) GIS (5) UWB (6) laser scanning (7) AR and (8) digital imaging.

In 1982, since the U.S. Department of Defense (DoD) asked its suppliers to ship their goods with attached barcode labels, barcode technology started to evolve and improve (Bernold, 1990a).

The application of barcoding was introduced to the construction industry in 1987 for materials management, plant and tool control (Bell and McCullouch, 1988; Bernold, 1990b; Stukhart, 1995; Chen et al., 2002, Nasir 2008). Due to the enormous potential of barcode technology to save cost, the Construction Industry Institute (CII) started a research project in 1987 to investigate the possible applications, and the achieved cost savings of applying barcodes in the construction industry (Bell and McCullouch 1988; Nasir, 2008). As Chen et al. (2002) states, the following functions can be provided through applying bar-coding technologies:

- Tracking real-time data of construction materials automatically on the site;
- Recording historical data of consumed construction materials automatically;
- Monitoring materials consumption of working groups automatically; and
- Transfer real-time data of materials automatically to head office via Intranet.

A typical barcoding system consists of three components: tags or labels, a reader or scanner, and a printer. Figure 2-4 indicates the barcoding system components (Nasir, 2008).

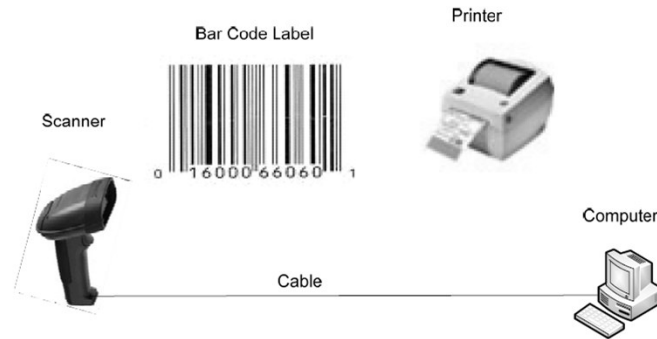


**Figure 2-4: Barcoding Hardware System Components (Nasir, 2008)**

There exist two different types of barcode tags. The first type is a one-dimensional barcode, which can be typically used as an identifier code on an object. In contrast, the second type is a two-dimensional barcode, which can contain a whole file of information about an object (Montaser, 2013). Another component of the barcoding system is a scanner that can read data coded on a barcode label. There are different types of scanners; however, the most useful are the laser scanners (Nasir, 2008). The third component of the barcoding system is the printer to produce high-quality barcode tags. One limitation of barcode labels is their need to have a line of sight to be read by the scanner, so the crew holding scanner has to physically go near the item having an attached barcode label to read the barcode and records the information. The recorded data by the scanner is downloaded into the office computer to update the related databases.

Various studies have focused on the application of barcodes in the construction industry for different purposes. For example, Vartiainen et al. (2008) experimented readability of the barcode and usability of a cellular phone camera for tracking goods in the construction industry. Lin et al. (2014) developed a novel 2D Barcode/RFID-based system for effective maintenance management in a construction lab. However barcodes are cheap, they have some limitations including the line of sight requirement, limited read range (inches or fraction of an inch), tags information cannot be modified, a limited amount of entered or stored data, identification of the product instead of the unique items, only one barcode can be read at a time, being affected by harsh environments (Nasir, 2008).

Another automated data collection (ADC) technology is RFID. The preliminary idea of what we now call RFID can be assigned to Mario Cardullo in 1969, but it was patented later in 1973. Although during the 1990s to 2000s, MIT automatic identification (Auto-ID) laboratory started to focus on the application of RFID in the context of logistics and supply chain (Hedgepeth, 2007), the application of RFID in the construction industry was introduced by Jaselskis et al. in 1995 (Nasir, 2008). As Jaselskis and El-Misalami (2003) state, RFID can be considered as a sister technology to barcode labels. Instead of light waves, radio waves are used to read a tag, and RFID

tags have transponders to communicate with readers through radio frequency waves. Nasir (2008) compared RFID with barcodes and stated that RFID does not require line of sight, it has longer read range (one inch to 100 feet), more data can be stored on RFID tags, it can identify both the product and item and even much more, there are read-write RFID tags, data from multiple tags (up to 1000 tags per second) can be read simultaneously, RFID tags are durable, they can perform in the harsh construction environment, but RFID tags are more expensive. According to the various researches, it can be stated that the RFID system consists of three main components, which are shown in Figure 2-5. (1) the tag, which is attached to the item expected to be tracked; (2) the reader, which identifies tags, reads tags' data, and transfers data to the host computer. The RFID reader has other responsibilities as well based on the type of used tags, including providing power and writing data, and (3) host computer as a data collector which receives data from the reader (Nasir, 2008).

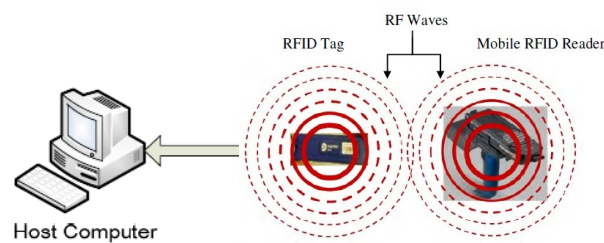


**Figure 2-5: Typical RFID System Components (Montaser, 2013)**

In an RFID system, a serial number or other required information is stored on RFID tags, which have been attached to the items. RFID tag transmits the captured information in forms of emitted radio waves to the RFID reader. Finally, the reader converts them into digital information to send to the computers for processing the data (Montaser, 2013). “The chip and the antenna together encapsulated in a protective shell are called an RFID transponder or an RFID tag.” (RFID Journal 2016). RFID tags are categorized from different points of view. The microchips in the RFID tag can be read-write, read-only, or “write once, read many (WORM).” The required information can be appended to the current information of the read-write tags while the tag is in the range of a reader. The needed information is stored in the read-only tags at the time of fabrication/production, which cannot be changed. This information can be read-only by the reader.

But regarding the WORM tags, after manufacturing, the user can write the required information only once over the current information of tag; after that, it can only be read (Nasir 2008). Moreover, RFID tags can be classified as active tags, passive tags, or semi-passive tags. Active RFID tags have their own power source (a battery) for running the microchip's circuit and also for sending a signal to a reader. Passive tags are activated by the electromagnetic energy emitted by the reader. Semi-passive tags have a battery just to run the microchip's circuit, but they use the reader's electromagnetic energy to communicate with the reader. Read and write ranges for passive tags are generally less than six feet, while active tags can be read or written to from approximately 5 to 100 feet. Active tags are usually more expensive than their passive counterparts and have a limited three to ten years life in contrast with the passive tags which have an unlimited lifetime (Jaselskis and El-Misalami, 2003).

The RFID reader can be fixed or mobile, as shown in Figure 2-6. Based on the model of RFID reader and also based on the types of tags, its read range varies. Typically, a reader can read thousands of tags per second. As Jaselskis et al. (1995) have stated, RFID readers can simultaneously communicate with different RFID tags. Therefore all the included information of an entire shipment as it is loaded into a warehouse or it is received to the construction site can be captured by RFID readers.



**Figure 2-6: Different Types of RFID Readers (Atlas RFID Store)**

The application of RFID in the construction industry to improve construction materials management have been surveyed in different studies.

Jaselskis and El-Misalami (2003) tried to illustrate RFID as a promising technology for improving construction operations, specifically in the materials receiving process. They indicated the potential applications of RFID technology in engineering/design, material management, maintenance, and field operations.

In the research by Song et al. (2006a), off-the-shelf RFID technology was used, and RFID tags were attached to all the materials. So the materials could be recognized and tracked automatically by field staff using an RFID reader and a GPS receiver. Then they investigated the technical feasibility of their proposed approach through developing a mathematical model. Their field experiments indicated that by using the proximity localization techniques, the proximate 2D locations of materials could be defined with acceptable cost. Song et al. (2006b) automated the tracking process of pipe spools in the long supply chain process, including design, fabrication, interim processing, delivery, storage, installation, and inspection of industrial projects by applying RFID technology. They concluded that if portal gates are equipped with four antennas and if pipe spools are driven at a speed less than two mph through portal gates, pipe spools are identified with 100% accuracy using current active RFID technology.

Moreover, they suggested that RFID technology should be extended through the construction stage for automated piping work progress tracking. The RFID gate sensor system, including passive RFID tags and wireless network technology, has been presented by Lee et al. (2008) for an intelligent logistics management system. Montaser (2013) developed an automated model in which project visualization-information aspects, automated site data acquisition, and earned value analysis were integrated to make data collection and project control automated. He applied short-range RFID for location estimation and material tracking in a cost-effective manner for indoor construction operations. RFID was utilized in the knowledge-based precast construction supply chain by Wang et al. (2017) to demonstrate that 62.0% of operational costs could be saved in 100



precast wall-panel construction compared with manual-, and barcode-enabled precast construction supply chain. As mentioned before, Won et al. (2018) developed a novel UAV-RFID for construction materials localization in complex or large-scale construction sites. Despite all the possible benefits of applying RFID for automated materials tracking, in a study done by Kasim et al. (2019), it is shown that manual materials tracking practices and very basic Information and Communication Technologies (ICT) are still used in construction projects in Malaysia.

In a holistic view, the reviewed researches demonstrate that RFID technology has been applied effectively in the construction industry for materials management and control, materials identification and tracking, tools tracking, tracking the work of workers on-site (using RFID card), identification of arrival dates of materials onsite (using RFID gates) as well as engineering/design, field operations, maintenance, and lay down yard management. But to have an effective materials management, it is required to know whether the planned amount of materials have been installed or consumed in the construction phase or not. Tracking materials and identifying their two-dimensional location  $(x, y)$  is not enough to investigate their consumption or installation, because the coordinate  $(x_{final}, y_{final})$  of a specific material which is in its final zone waiting to be consumed/installed is similar to the coordinate  $(x_{final}, y_{final})$  of another similar material that is consumed/installed. So, instead of 2D localization of construction materials, 3D localization is needed if their position and location are used to investigate their consumption/installation. In addition to the regular application of RFID for automatic identification, data collection, and assets/materials tracking and localization in 2-dimensional space, RFID can be used to locate an object in 3-dimensional space as well. In contrast with localization in 2-dimensional space applying RFID, localizing an object in a 3-dimensional space requires the deployment of a number of RFID tags and/or readers with known locations as reference nodes resulting in high hardware cost. Moreover, using a large number of RFID tags and readers in construction sites can sometimes be impossible. For instance, Wang et al. (2007) proposed two different 3D localization schemes, namely, the active scheme and passive scheme, to localize an object in a 3-dimensional space through using RFID. System set up for RFID 3D localization for both active scheme, and passive scheme is illustrated in Figure 2-7 (see Wang et al. (2007) for more details). It has been shown that a large number of tags and readers attached to the floor or ceiling is required.

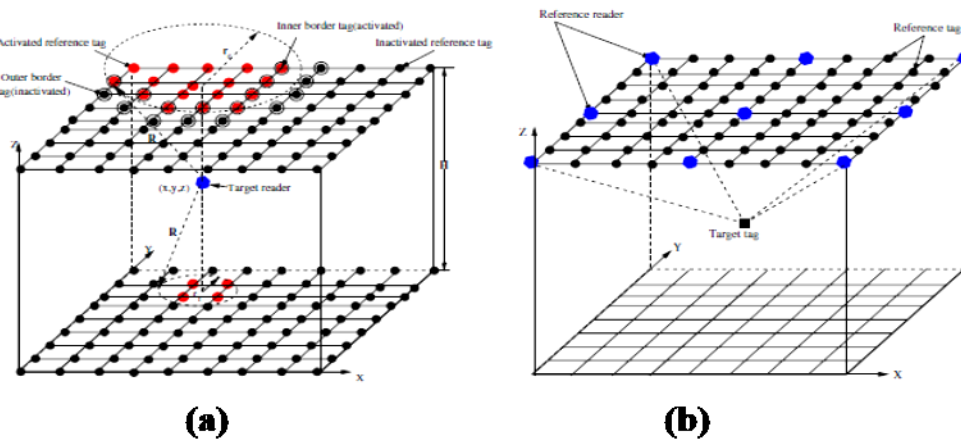


**Figure 2-7: RFID 3D Localization (a) Active Positioning Scheme (b) Passive Positioning Scheme (Wang et al., 2007)**

Regarding GPS, the U.S. Department of Defense positioned 24 satellites into the orbit to create GPS, which is a satellite-based navigation system for military applications. Civilian use of the GPS on land, at sea and in the air became permissible in the 1980s by the government. So to make GPS operational for civil and other users, two different GPS services were provided. The first service entitled “Precise Positioning Service (PPS)” assigned primarily to the military of the United States, but the second service called “Standard Positioning Service (SPS)” was designed to provide a less accurate positioning capability than PPS and assigned to civil and all other users throughout the world (Department of Defense - USA, 2008).

GPS technology also has been widely used to address the requirements of positioning data for the construction industry. The GPS consists of three segments: 1) space segment including a minimum of 24 satellites arranged in a way that radio signals from at least four of them will be received by a GPS receiver at any given time. These radio signals need line of sight, so they cannot pass through solid objects. 2) control segment, including five control ground stations located around the world. 3) user segments, including the users with their GPS receivers who want to know about their three-dimensional positions (latitude, longitude, altitude) (Nasir,2008). Triangulation is used for three-dimensional position determination at any given time. The final location and its accuracy can be affected by atmospheric conditions and satellites’ locations (Caldas et al., 2006).

In outdoor environments and on construction job sites, researchers applied GPS technology to automatically localize construction labor and equipment for various purposes including identification of the two-dimensional location of the objects, productivity and progress measurements, control of earthmoving operations, automated data collection for road construction control, increasing safety and quality control and (Peyret and Tasky 2002; Oloufa et al. 2003; Navon and Goldschmidt 2003; Sacks et al. 2003; Navon et al. 2004; Navon and Shpatnitsky, 2005; Song et al. 2006a; Su and Liu, 2007, and Moselhi and Alshibani 2007). Other benefits, including processes improvement, lost items reduction, improved construction performance, automation and standardization of localization processes, route sequences, and layout optimization, improved data entry, and direct savings of time by using the GPS technology, were reported (Caldas et al., 2006). GPS also has the following disadvantages:

- Low positioning accuracy of around 10 m in open areas (Lu et al. 2007)
- Lack of reliability for indoor areas due to the poor reception of satellite signals (Song et al., 2006b).
- High cost for automated tracking of individual material items using GPS (Song et al, 2006b).

Next technology which is GIS helps maps to be drawn from its database through integrating database management systems and computerized visual and geographic analysis in the form of maps. The GIS database includes various information such as geographic, environmental, political, and social information about objects and their relationship with each other (Bansal and Pal, 2009). So all the existing trends and relationships of data that have not been visible and clear enough can be visually seen and analyzed. It is worth noting that the maps would be automatically updated whenever their related database is updated. As Montaser (2013) indicated, GIS has been applied as a decision-making and problem-solving tool, and even it can be integrated with other automated data collection technologies and software to be more efficient.

The GIS has been utilized in various fields, including civil engineering, transportation, facilities management, urban planning, and waste management. GIS has got multiple applications in the construction projects, including monitoring project schedule and progress, materials procurement, construction waste reduction, automated data acquisition, earthmoving equipment control. For example, Cheng and Chen (2002) developed an automated schedule monitoring system entitled “ArcSched,” which was an integration of GIS and barcode technologies. Engineers could monitor and control the erection process of prefabricated structural components on a real-time basis with the help of this system. Li et al. (2005) combined the Incentive Reward Program (IRP)-based barcode system with GPS, GIS, and the Wide Area Network (WAN) technology to control and reduce construction wastes. Zhang et al. (2018) used Multi-View Stereovision (MVS), Point Cloud Co-registration (PCC), and Unmanned Airborne Systems (UAS) technologies to collect 3D construction site material information such as volumetric or area change of stockpiled construction material. A novel integrated framework was presented applying 4D BIM and a geographical information system (GIS) for supplier selection, determination of the number of material deliveries, and allocation of consolidation centers (Deng et al., 2019).

Ultra-Wideband (UWB) is another type of remote sensing technology that has been often applied in the construction projects for providing real-time data related to the locations of workers, materials, and equipment in outdoor and indoor environments.

The provenance of UWB technology dates back to the early 1960s. During this decade, researchers had focused on the time-domain of electromagnetic-wave propagation. Then in 1978, Bennett and Ross outlined the first applications of UWB. It is worthy to note that all the uses of UWB were under US government programs. But in 1994, non-governmental related researchers were allowed by the Federal Communications Commission (FCC), which resulted in the acceleration of developing UWB technology and its application for the precision localization (Teizer et al., 2007).

UWB is any signal that has a fractional bandwidth equal to or greater than 0.20 or has a UWB bandwidth equal to or greater than 500 MHz (Breed, 2005). A large amount of information can be transmitted over distances of up to 1,000 m using UWB technology. Commercially existing UWB systems consist of (1) processing computer and hub, including a graphical user interface (2) minimum of four UWB receivers at different height levels to record real-time three-dimensional signal data in a field of view of 90° (mid gain), 60° (high gain), and omnidirectional (3) CAT-5e shielded wires, and (4) Low- and high-powered UWB tags, including one reference tag (Teizer et al., 2008). Several lengths of shielded CAT-5e cables connect receivers and antennas to the hub either in-line or parallel to power the receiver(s). Tag identification and time readings are transmitted back to the hub via shielded CAT-5e cables as well. A reference tag is positioned ideally in the center of the space observed and in line of sight of the receivers. It is preferred to locate all the hardware components at the boundary of the observation area.

The three-dimensional position of receivers and reference tag is specified using a total station in advance of measuring tag locations. While tags are placed on any running resources and the receiver sends out pulses, each tag constantly fires out a packet burst of short UWB pulses, including the prerecorded identification number. The receivers receive these pulses through their sensitive antenna. The large bandwidth of UWB allows the receivers to measure the times of arrival of the signal with high accuracy. After the time-of-flight principle and through synchronizing the arrival signal, the location of each tag is calculated. Signals between receiver and tag can generate real-time two-dimensional positioning data if there exist only three receivers. The UWB tags exist

in a small badge ( $0.65 \times 0.34 \times 0.06$  m), asset cube ( $0.29 \times 0.29 \times 0.25$  m), or micro rectangular shape ( $0.13 \times 0.25 \times 0.06$  m) form. The weight for each tag is less than 12 g. The various application of UWB technology in the construction projects consist of facilitating on-site management, increasing resource usage and productivity, increase in the work zone safety, and schedule and cost reduction (Teizer et al., 2008). UWB has got unique advantages comparing other remote sensing technologies such as: providing accurate 3D location values in real-time, longer range, higher measurement rate, improved measurement accuracy, and immunity to interference from rain, fog, or clutter (Cheng et al., 2011; Teizer et al., 2007). The main limitation of UWB is a necessary measurement infrastructure (Teizer et al., 2007)

A typical UWB setup and installation with tags on construction assets, including workers, equipment, and materials, are shown in Figure 2-8.

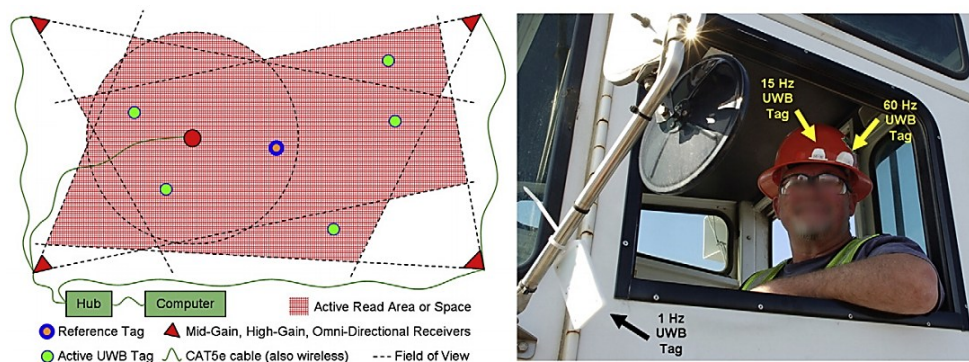


**Figure 2-8: A Typical UWB Setup and Installation (Cheng et al., 2011)**

Teizer et al. (2007) introduced UWB for real-time location sensing and resource tracking. They illustrated the applicability of UWB for construction and, in particular, to measure accuracies in field applications. Cheng et al. (2011) investigated the performance of a commercially-available UWB system for tracking mobile resources in the real-world and harsh construction environments. They used Robotic Total Station (RTS) to obtain ground truth for calculation of location error rates of UWB. Their research indicated the applicability of UWB for the design of construction management support tools. In the study done by Cheng and Teizer (2013), UWB has been applied for real-time (location) data collection and then is integrated with visualization technology in a novel framework for construction safety and monitoring applications. Macoir et al. (2019) proposed the use of autonomous indoor drones localized through a designed UWB for inventory management. UWB utilized infrastructure anchor nodes that did not require any wired backbone and could be battery powered. Despite the high accuracy of UWB in localizing objects and its ability to provide accurate 3D location values in real-time, its application has the following problems:

- The requirement of the dense and expensive network of fixed receivers (Soleimanifar, 2011; Khoury and Kamat, 2009);
- Difficulty in applying in a crowded construction environment (Soleimanifar, 2011); and
- Low performance due to harsh weather conditions such as high humidity (Soleimanifar, 2011).

The laser scanner is a kind of 3D imaging system. According to the ASTM 3D Imaging standards committee, a 3D imaging system has been defined as a “non-contact measurement instrument used to produce a 3D representation (e.g., a point cloud) of an object or a site (ASTM, 2009; Lytle, 2011).” Ground-based/Terrestrial Laser Scanning (TLS) as a kind of remote sensing technology has been applied as a new generation surveying technique. TLS measures the distance/range to each point of an object by analyzing a laser light return on an object’s surface. In this way, large amounts of 3D coordinates of objects’ surfaces in the form of a point cloud or three-dimensional digital model, with an unprecedented level of precision, are acquired. So a TLS makes it possible to remotely survey areas that are complex or inaccessible to traditional surveying techniques and analyze a real-world object or environment through collecting data on its shape or appearance (Soudarissanane, 2016). Three-dimensional laser scanning is a novel technology in the field of surveying and Architecture/Engineering/Construction (AEC) industries (Oliveira Filho et al., 2005). The scanning technology was created in the 60’s of the 20th century. Due to technological difficulties, the accurate scanning of objects was a very laborious process and took a significant amount of time and effort to scan objects accurately. Scanners that could use white light, lasers, and shadowing to scan a surface came to existence after 1985 (Artescan, 2016).

Laser scanners consist of three parts: (1) an emitted optical signal (2) a system to point the emitted signal, and (3) an optical receiver to detect and process the returned signal (Lytle, 2011). There are two common types of laser scanning technologies: phase-based scanners and time-of-flight (pulse-based) based scanners (Specht et al., 2016). In contrast with a pulse-based laser scanner which waits for the return signal before sending the next one signal, a phase-based laser scanner emits a continuous wave, which leads to much higher measurement rates. Moreover, using a phase-based laser scanner results in obtaining higher accuracy in the order of millimeters due to the modulation of such a continuous wave. It should be stated that the pulse scanners have a greater maximum scanning range than phase scanners. Therefore, compared with the phase-based approach, the time-of-flight approach is more suitable for long-range scans. “Various laser scanners are currently available with a range of speeds (typically 2,000–120,000 points per second), maximum resolutions (typically 1–100 mm at 50 m), and accuracies (typically 3–50 mm at 100 m) (Specht et al., 2016). The scanner must be stationary during scanning and requires minutes to tens of minutes to perform high-resolution scans of complex environments” (Olsen et al., 2010).

Gong and Caldas (2007) studied rapid local area modeling obtained from high-frequency laser scans for construction resource management applications. They explored the performance of various data processing algorithms in both indoor and outdoor environments. They could present an integrated range data processing module allowing for quickly experimenting with different combinations of data filtering, transformation, and segmentation approaches and could handle sensor noise and accurately process high-frequency local area laser scans. In the Ph.D. thesis done by Soudarissanane (2016), the significant factors influencing the quality of end product or point cloud of Terrestrial Laser Scanners are classified into four main categories: scanner mechanism, atmospheric conditions and environment, object properties, and scanning geometry. All the mentioned factors are out of the user’s control except the scanning geometry factor, because the user can determine the scan location and the view-point of a point cloud. So in his study, the influence of scanning geometry on the point cloud quality has been investigated. It was concluded that reducing the total error of the measurements was possible by placing the scanner at another position in the room, which was not necessarily a distinct position. Therefore, based on this result, a new method was developed based on terrestrial laser scanner capabilities to determine near-

optimal view-points in a scene. According to the reviewed literature, on top of the application of 3D laser scanning in other areas, including civil engineering, mechanical engineering, medical engineering, forensics, remote sensing, film and game industry, and archeology, it has been used for several purposes in the construction industry. Laser detection and Ranging (LADAR) is a 3D laser scanner that is used primarily for spatial measurement. Other applications of LADAR include “surveying, earthmoving operations, monitoring the progress of concrete casting, highway alignment, paving operations, and construction quality control” (Lytle, 2011).

As Golparvar-Fard et al. (2015) has stated, despite the extensive studies about the application of laser scanners in automated data collection, they have some shortcomings including limited spatial and temporal resolutions (Furukawa and Ponce 2006), need for frequent and manual registrations due to discontinuity of spatial information, the mixed-pixel phenomenon (Kiziltas et al. 2008), need for regular sensor calibrations, slow warm-up time, creation of noise resulted from moving objects, reduction of captured detail due to increase of distance between laser scanner and the building components and finally since they are not easily portable, so they are not proper for indoor environments.

AR is a visualization technique in which the real world and the virtual contents are blended in a 3D space to increase the user’s awareness of the real environment (Behzadan et al. 2015.) So through using advanced camera and sensor technology, AR adds a 3D model, which sometimes called cyber-information to the real world. To create AR visual simulations, both a software application and a hardware platform are required. As Dong and Kamat (2013) have stated, Scalable and Modular Augmented Reality Template (SMART) is a software application framework used for accurate registration and projection. Augmented Reality Mobile OpeRation platform (ARMOR) is a modular mobile hardware platform used for tracking user position and orientation and displaying the augmented view. As shown in Figure 2-9, ARMOR consists of orientation and position tracking devices such as electronic compass and Real-time Kinematic (RTK) GPS respectively, camera, Head-mounted Display (HMD), external power supply, Nintendo Wii Remote (Wiimote) which is a user command input and one load-bearing vest which compacts all the mentioned components.

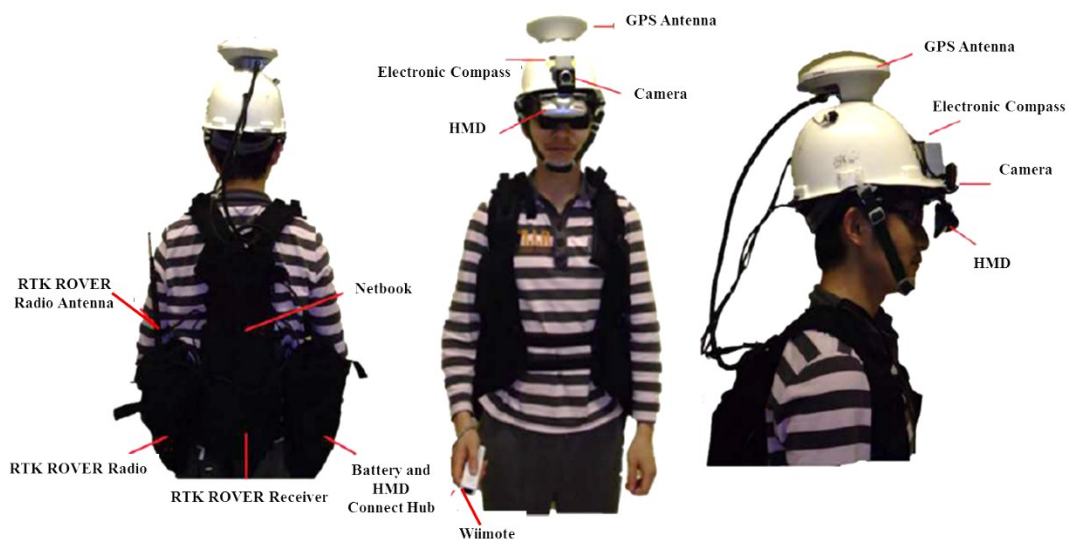


**Figure 2-9: ARMOR Hardware Architecture (Dong and Kamat, 2013)**

AR has been applied for different purposes including AR visual excavator-utility collision avoidance system (necessary for avoiding from the occurrence of accidental utility strikes through visualization of buried utilities), AR post-disaster reconnaissance (evaluation and quantification) of building structural damages occurred by earthquakes or blasts and tabletop collaborative AR visualization resulting in interactive visual simulations of engineering processes (Behzadan et al. 2015.)

AR works through some steps, including capturing real-world aerial images and generating 3D reconstruction, registration between digital data and physical world to make sure virtual objects are placed and aligned accurately to the real world, visualization, and displaying virtual pictures for the user.

However, in contrast with other industries such as manufacturing, medical operations, military, and gaming, application of AR technologies in Architecture, Engineering, Construction, and Facility Management (AEC/FM) industry is new (Behzadan et al. 2015), Rankohi and Waugh (2013) have expressed that AEC/FM industry can benefit from AR in visualization, information retrieval, and interaction. So they have classified the application of AR in the AEC/FM industry into the following areas:

- Visualization/simulation;
- Communication/collaboration;
- Information modeling;
- Information access;
- Progress monitoring;
- Education/training; and
- Safety/inspection.

Behzadan and Kamat (2013) utilized and integrated videotaping, AR, and UWB to develop a pedagogical tool. This tool generates live videos of remote construction job sites, and the students can interact with the objects from their classrooms using an intuitive interface. A novel vision-based mobile augmented reality system named “Hybrid 4-Dimensional Augmented Reality (*HD<sup>4</sup>AR*)” has been developed by Bae et al. (2013) in which the user’s location and orientation can be derived through comparing images (captured by a mobile device from the user’s location) to a 3D point cloud (generated from site images). Zollmann et al. (2014) developed a system to improve monitoring and documentation of construction site progress. This system includes three main components “an aerial client that captures aerial images for 3-D reconstruction on a regular basis”, “a reconstruction client that performs aerial reconstructions and remote localization,” and “an AR client that visualizes progress information spatially registered to the physical environment on site.” Wang et al. (2014), integrated BIM and AR prototypes to improve accessing the information and productivity in the concerned rationales. A novel system consisting of an Android application named “BIM-U” and a mobile augmented reality (AR) channel called “BIM-Phase” was proposed by Zaher et al. (2018) to improve monitoring construction progress using smartphones and to track time and cost on construction projects. Construction site activities are facilitated by using an augmented reality system developed by Kivrak and Arslan (2019). By using this system, information on training materials and construction methods are accessible for managers, engineers, and construction workers, and they can follow each step of the construction

activities assigned to them. So it can lead to a reduction of risks related to mistakes made in site activities and also the quality and productivity improvement of construction site activities.

Portable and mobile AR systems includes four different types of tracking technologies including “Radio-Frequency (RF) based tracking technologies such as GPS, WLAN, indoor GPS,” “infrastructure-dependent technologies such as fiducial markers,” “infrastructure-independent tracking technologies such as gyroscopes,” and “image-based tracking techniques” (Rankohi and Waugh, 2013). As Bae et al. (2013) have expressed, a high degree of dependency on pre-installed infrastructure is the major shortcoming of these RF-based location tracking technologies. Moreover, attaching markers to different surfaces is required while using fiducial markers and makes it infrastructure-dependent and challenging for large-scale implementations. Even if location tracking systems are used, which are infrastructure-independent, accumulated drift error will be inevitable, and also the error increases with the distance traveled by the users.

So despite the potential application of AR in the ACE/FM industry, there are still some limitations and issues in the employment of AR in the construction industry such as tracking and alignment problems, the visual illusion of virtual objects in the real world (i.e., occlusion), speed of 3D reconstruction/localization, mobility and ergonomics, power limitations, and adverse weather conditions (Bae et al. 2013; Rankohi and Waugh, 2013; Behzadan et al. 2015).

Digital Imaging is another technology that has been extensively used in construction projects. An image is considered as highly accurate information in the construction projects (Kim and Kano, 2008). Cameras have been applied widely to monitor and record various activities on a construction site, especially for construction control and inspection. Images produced by the cameras are processed using image processing techniques to help project participants better understand the project status (Wu and Kim, 2004). As Gonzalez et al. (2009) have stated “an image is specified as a two-dimensional function,  $f(x, y)$ , where  $x$  and  $y$  are spatial coordinates and the amplitude of  $f$  at any pair of coordinates  $(x, y)$  is called the intensity of the image at that point.” An image is a digital image when  $x$ ,  $y$ , and the amplitude values of  $f$  are all finite and discrete quantities. So a digital image is made up of a finite number of elements; each element has a specific location and value. These elements can be called picture elements or pixels. A digital image is represented as a matrix of intensity values, so processing and analysis of digital images consist of transformations, operations, and manipulations of such image matrixes. Fathi et al. (2015) classified imaging systems into active and passive sensing technologies to capture and model reality. Based on these technologies’ working principle, any kind of optical energy is not shoot up into the scene by passive sensors (such as RGB cameras) against active sensors (such as an RGB-D, LiDAR). Limited working range (1–3 m) of active sensors, large energy consumption, dependency on the resolution of the projector, inability to scan dark surfaces make their application improper in the construction and infrastructure sectors. Against RGB-D, RGB cameras are flexible for data capturing in the construction industry with lower cost and acceptable working range. In contrast with the imaging systems mentioned above in which just a snapshot of a scene is captured, and the images are static, there is another type of image called “360-degree image” which can visualize the real environment surrounding the point from which the image has been captured. So using cameras to take 360-degree images makes it possible to look around the scene to the left, right, up, and down. As Eiris Pereira and Gheisari (2018) have stated, 360-degree images can fully immerse the user in real-world spaces. So a realistic and detailed reflection of construction sites can be generated using this technology, and the user is in the shoes of a person who is capturing



the image and can turn around looking at surroundings. There are various 360° cameras (with either traditional or fish-eye lens) that can capture all of our surroundings and produce 360-degree images such as Ricoh Theta V, Garmin VIRB 360, Insta360 ONE X, and Samsung Gear 360. The application of 360-degree images in the construction domain is classified into three groups, including: “interactive learning, reality backdrop to augmented information, and visualize safe/unsafe situations.” Some off-the-shelf platforms are using 360-degree panoramic techniques in the construction field to make visualizing and traveling job sites remotely possible such as HoloBuilder®, in which as-built conditions are visualized through spatially linking the images to existing 2D plans. Progress motoring can be another application of using this platform if 360-degree images of the construction site are taken across time. Low image quality, the inflexibility of 360-degree images regarding visual rotation, and parallax issues when objects are near the focal point of the camera are the limitations of 360-degree images (Eiris Pereira and Gheisari, 2018).

It is expressed that there are no clear-cut boundaries between image processing and computer vision. The field of computer vision uses computers to emulate human vision, which includes learning and the ability to deduce and take actions based on visual inputs. So there are some definitions to illustrate these field boundaries. The best paradigm considers three types of computerized processes in this continuum: low-, mid-, and high-level processes. Low-level processes consist of primitive operations such as image preprocessing to reduce noise, contrast enhancement, and image sharpening. In this level, both inputs and outputs are images. Mid-level processes include “tasks such as segmentation (partitioning an image into regions or objects), description of those objects, and classification (recognition) of individual objects.” In mid-level processes, inputs and outputs are images and attributes extracted from the same images (e.g., edges, contours, and the identity of individual objects), respectively. Eventually, higher-level processing involves "making sense" of recognized objects, and performing the cognitive functions normally associated with human vision (Gonzales et al., 2009). So against computer vision in which the goal is to understand the image and mimic human vision, image processing alludes to the quantitative evaluation techniques, which can be used to images for the quality improvement for analysis purposes. These techniques have been introduced to and used in the civil engineering discipline not long ago and enable civil engineers to carry out many labor-intensive tasks automatically (Shehab-Eldeen, 2001). In general, image processing includes image normalization, image enhancement and image warping or registration. The first step is image normalization, in which the images are of the same size and focus. In the image registration process (including feature extraction, feature matching, determination of a transformation function, and image resampling and transformation), images taken from different viewpoints or by different cameras are aligned point-to-point correspondence. In the image enhancement process, the features in the images are more perceptible for visual pattern recognition algorithms (Guo, 2008).

On top of the common usage of digital imaging such as the decrease of theft and vandalism of site equipment and material, identification of the completion of building sections/components and required rework, reduction of inspection time, and quick identification of issues/problems during construction, there are other applications of this technology (Brilakis, 2007). Construction images taken from one point or various points of view have been used for reconstructing as-built BIM, detection, and recognition of different types of construction materials, volume estimation of bulk materials, recognizing diverse construction activities, and resources pose estimation. For example, Yang et al. (2016) reconstructed an as-built 3D building facade using images taken from various points of view. The materials of the building surface were recognized using machine learning

techniques then. In another research done by Luo et al. (2018), 22 classes of construction-related objects and 17 types of construction activities were automatically detected and recognized respectively using still site images and convolutional neural networks. Their developed method could result in spending managers' time to solving problems instead of manual data collection. Recent improvements in digital photography and webcams have made them more cost-effective and practical methods for project information gathering (Golparvar-Fard et al., 2009). It is stated that as-built data acquisition by images and videos has some benefits, including no need for specialized knowledge, portability, low cost, short time, and ease of collection (Kropp et al., 2018). Since image-based approaches have the advantage of low costs and a simple acquisition process, they have been used to record the actual status of the project visually to be compared with the expected project status and identify deviations. It can be stated that, instead of manually methods, image-based approaches have been widely applied to collect large amounts of spatial data in a rapid, accurate, and timely manner for monitoring projects progress. There are various researches improving project progress monitoring using digital images (Kim et al., 2013b; Golparvar-Fard et al., 2015, and Kropp et al., 2018)

Regarding 360-degree images, Gheisari et al. (2015) proposed 360-degree interactive panoramas (Augmented Panorama) to visualize the whole structure of a building to students. They tried to bring physical locations closer to online users and give them experiences similar to the physical presence at the job site. So standing in front of a building structure and interacting with various structural elements became possible for the students while sitting in their classes. 360-degree images were used in another study done by Gheisari et al. (2016) for a construction renovation project. They superimpose the BIM models on the captured 360-degree images to visualize and communicate the finished work to subcontractors and even to record and document the building processes in the job site. Eiris et al. (2017) used augmentations in the 360-degree images to generate virtual tour in the construction projects, locate and visualize different building elements, and document potential issues in the construction processes. 360-degree images were utilized for improving safety education by Pham et al. (2018). A learning platform was developed for the student in which students were allowed to look at a digital site and identify hazards. Table 2-1 presents a concise overview of the capabilities and limitations of ADC technologies.

**Table 2-1: Capabilities and Limitations of ADC Technologies**

Technology	Capabilities	Limitations	Refs.
Barcode	<ul style="list-style-type: none"> <li>• Reasonable price</li> <li>• uncomplicated usage with standard protocols for implementation</li> <li>• Speedy computer data entry</li> <li>• Portability</li> </ul>	<ul style="list-style-type: none"> <li>• limited reading range</li> <li>• Sensitivity to the harsh environment</li> <li>• Low capacity for data storage</li> <li>• line of sight requirement</li> <li>• only one barcode can be read at a time</li> </ul>	(Moselhi et al., 2020; Nasir, 2008)
Laser scanning	<ul style="list-style-type: none"> <li>• Point clouds generation with High accuracy</li> <li>• Well-defined and straightforward internal coordinate system</li> <li>• Homogeneous spatial distribution of range points</li> <li>• Capable of scanning in darkness and shaded areas</li> <li>• Capable of measuring textureless areas</li> <li>• Capable of scanning a large area</li> </ul>	<ul style="list-style-type: none"> <li>• Laser scanners are expensive</li> <li>• Time-consuming process</li> <li>• Requirement of clear line-of-sight</li> <li>• Limitations associated with modeling of edges and linear features</li> <li>• High storage capacity requirement</li> <li>• No information on material type, texture, and color</li> <li>• Eye-safety distance concerns</li> <li>• Need for frequent and manual registrations due to discontinuity of spatial information</li> <li>• Need for regular sensor calibrations</li> <li>• Slow warm-up time</li> <li>• Creation of noise resulted from moving objects</li> <li>• Reduction of captured detail due to the increase of distance between the laser scanner and the building components</li> <li>• Scanners are not easily portable</li> </ul>	(Moselhi et al., 2020; Golparvar-Fard et al., 2015)

Technology	Capabilities	Limitations	Refs.
RFID	<ul style="list-style-type: none"> <li>• Longer range compared with barcodes (up to 100 m for Ultra-high frequencies)</li> <li>• Non-line-of-sight</li> <li>• Providing cost-efficient location information</li> <li>• Light tags</li> <li>• RFID tags are durable in the harsh construction environments</li> <li>• Batch readability of tags for the more efficient identification process</li> <li>• RFID tags can be the read-write type</li> <li>• More data can be stored on RFID tags</li> </ul>	<ul style="list-style-type: none"> <li>• Lack of accuracy and complexities for 3D positioning</li> <li>• Calibration difficulties</li> <li>• Affected by the multipath effect</li> <li>• Problems of simultaneous recognition of many tags</li> <li>• Expensive active tags</li> <li>• The requirement of battery replacement in active tags</li> <li>• Influenced by metal and high humidity especially in high frequencies</li> </ul>	(Moselhi et al., 2020; Nasir, 2008)
UWB	<ul style="list-style-type: none"> <li>• Longer range (up to 1000 m), higher measurement rate, and more accurate real-time 3D positions (less than 1 m) compared with typical RFID systems</li> <li>• Suitable for both indoor and outdoor environment</li> <li>• Not affected easily by other RF systems</li> <li>• Relative resistance to multipath fading</li> <li>• Immunity to interference from rain, fog, or clutter</li> </ul>	<ul style="list-style-type: none"> <li>• The requirement of the dense and expensive network of fixed receivers</li> <li>• Violation of line-of-sight can lead to performance degradation especially in congested areas</li> <li>• Limited update rate</li> <li>• Multipath and radio noise effect in the case of metal occlusion</li> <li>• Some calibration difficulties</li> <li>• Tagging issues (e.g., battery replacement)</li> <li>• High cost</li> <li>• Excessive missing data</li> <li>• Degraded range measurement (in case of distance increase)</li> </ul>	(Moselhi et al., 2020; Cheng et al., 2011; Solenmanifar, 2011; Khoury and Kamat, 2009; Teizer et al., 2007)

Technology	Capabilities	Limitations	Refs.
GPS	<ul style="list-style-type: none"> <li>• Outdoor environment access</li> <li>• Flexible and quick reacting based on the construction site requirements</li> </ul>	<ul style="list-style-type: none"> <li>• Low positioning accuracy of around 10 m in open areas</li> <li>• Lack of reliability for indoor spaces due to the poor reception of satellite signals</li> <li>• High cost for automated tracking of individual material items using GPS</li> <li>• Multipath errors in the congested environment</li> </ul>	(Moselhi et al., 2020; Lu et al. 2007; Song et al., 2006b)
Digital Imaging and Photogrammetry	<ul style="list-style-type: none"> <li>• Straightforward configuration</li> <li>• Cost-effective field data collection</li> <li>• Portability</li> <li>• Captures material, texture, and color information of the target object</li> <li>• High update rate</li> <li>• Well known internal geometry</li> <li>• Good interpretability</li> <li>• no need for specific knowledge</li> <li>• Low cost</li> <li>• Collecting large amounts of spatial data in a rapid, accurate, and timely manner using image-based approaches</li> </ul>	<ul style="list-style-type: none"> <li>• Calibration difficulties</li> <li>• Mirror effect caused by reflective surfaces</li> <li>• Less accurate point clouds generating compared with laser scanners</li> <li>• Limitations of depth calculation in 3D modeling</li> <li>• Another technology (e.g., RTS) is required to provide the geo-referenced inputs for photo-based 3D modeling</li> </ul>	(Moselhi et al., 2020; Kropp et al., 2018; Golparvar-Fard et al., 2015; Kim et al., 2013b)

### 2.3 Shortcomings and Limitations

Reviewing the literature in detail indicates that the main subjects of available studies are: (1) optimization of material procurement and storage on-site frequently through GA optimization (2) integration of the materials management processes (3) integration of materials localization and tracking data with the computer-based materials management systems (4) positioning, tracking and monitoring critical resources (including material, labor, and equipment) using ADC technologies, and (5) investigating the application of ADC technologies for identifying unique materials received at the job site. Various ADC technologies, their applications, particularly in materials identification, tracking, locating, detecting, and progress monitoring along with their advantages and disadvantages, have been discussed in this chapter as well.

In the studies presenting quantitative methods to address construction materials inventory optimization problems, the total cost of inventory at the planning phase of projects has been optimized without considering introduced changes in the construction phase. Fixed-ordering-period was selected for construction materials in every construction stage by several researchers which can result in improper material management considering probable changes in the construction phase. Although defining the start date of project activities is dependent on various factors and the delivery date of materials is as important as the number of deliveries to the project cost, most of the researchers have focused on finding the optimal solution of delivery and inventory of materials by changing the activities start date and only the total number of material deliveries throughout the construction duration (for example 20 times delivery of precast concrete units in a project with construction duration equal to 42 days (units are always delivered every two days)). Moreover, most often GA as the optimization engine is used for procurement optimization without preventing the lack of enough diversification in the generated populations, which is the limitation of GA.

The activities of construction projects are highly interdependent, and engineering, procurement, and construction phases overlap to a great extent. The reviewed researches have improved the construction materials management process from various perspectives utilizing different methods and ADC technologies. However, it seems that the current state of study does not adequately consider the complex, unstructured, and dynamic nature of the construction projects in developing the materials management systems. Furthermore, one question has not been sufficiently answered in both planning and construction phases using an efficient method. The question is: Which material and how much of that material must be ordered and bought on which day to result in the least cost without material shortage or surplus?

In a nutshell, it was concluded that (1) efficient material management system requires trade-offs and optimized balance among elements of material cost including purchase cost, storage cost, opportunity cost, ordering cost and unavailability cost, (2) since the amount of both consumed bulk materials and installed tagged materials can be obtained more easily by monitoring the as-built status of the building elements under construction on each day, so utilization of ADC technologies just for 2D/3D localization and tracking project resources is not enough for an effective materials management system, (3) without considering the dynamic nature of construction projects in terms of updated project status or project progress and using proper methods, making materials purchase orders by contractors to procure the right quantity of materials with the right quality and the least cost without delay is impossible and (4) materials management

related functions must be integrated and updated repeatedly during the project lifecycle in order to consider schedule and design changes resulting from actual circumstances.

So the followings must be considered to achieve a practical materials management framework which can perceive the dynamic nature of construction projects:

- Near real-time progress monitoring using state of the art technologies and techniques is required to estimate the quantities of materials installed or consumed at the job site; and
- There is a critical need to develop an efficient inventory control and management method to support contractors in making decisions and taking actions on how much and when to order materials that result in inventory at an optimum level with the least cost.

Thus not only a balance among cost categories has to be achieved, but also the dynamic nature of construction projects has to be taken in to account. Such a dynamic framework can result in taking more accurate and near real-time corrective actions, avoiding project schedule delays, and cost overruns.

To develop an efficient inventory control and management method, a proper optimization engine is developed, which can follow up on the project progress throughout the construction phase. Furthermore, to detect installed materials or estimate the quantities of consumed materials at the job site, not only the most proper technology is selected to capture the as-built status of buildings in both outdoor and indoor environments easily, safely, and at low cost, but also a novel near real-time progress monitoring method and a framework for automated detection of building components are developed to visualize and detect the progress at different time intervals in near real-time with acceptable accuracy. However, the developed CMM framework is elaborated in detail in the next chapter; the following sections provide the basics and literature of the applied techniques and algorithms.

## **2.4 Genetic Algorithm Optimization**

AS Kirk (2010) stated, after the introduction of the field of Artificial Intelligence, the first Evolutionary Algorithms came to existence and were developed. In 1964, the first formal research on Evolutionary Algorithms was done by Lawrence J. Fogel. Then in 1973, Ingro Rechenberg focused on evolutionary strategies and could develop the foundation of EAs. Finally, John Holland published his book as the first literature on Genetic Algorithms (GAs) in 1975.

Genetic Algorithms (GAs) as the simulations of natural selection are the earliest, most famous, and most widely-used Evolutionary Algorithms (EAs) (Simon, 2013). A great diversity of constrained and unconstrained optimization problems can be solved by applying GA as a universal method (Holland, 1975). Genetic Algorithms as a type of optimization engine try to find the optimal solution(s) of a computational problem in terms of maximizing or minimizing a particular function. They are used in various applications, including automatic programming and machine learning. They are applied to model phenomena in economics, ecology, the human immune system, population genetics, and social systems (Carr, 2014). Genetic algorithms have been used in the construction industry as well to solve different issues such as construction site layout problems, resource allocation, scheduling problems, shape design of structures problems, and manpower scheduling problems. Fitness function for optimization, Initial population of chromosomes, and rules to create the next generations are the GA components. An initial

population is a group of possible solutions to the given problem. GA will modify the initial population in consecutive iteration to obtain a better solution. At each iteration, the GA selects chromosomes as parents from the current population randomly. Then, by using some rules, the GA generates their children as the next generation. This procedure is repeated for several generations, and the GA is trying to move to the best solution during these consecutive iterations. For creating the next generation from the current population, the GA applies three following main types of rules (Tahmasebi and Hezarkhani, 2012):

- Selection rules: by applying these rules, parent chromosomes are selected to generate the population at the next generation;
- Crossover rules: by applying these rules the parent chromosomes are combined to produce the children for the next generation;
- Mutation rules: by applying these rules, the values of chromosomes are changed and altered to generate new chromosomes for the next generation.

As Carr (2014) stated, the way of translating candidate solutions into chromosomes and defining fitness function are the main elements affecting the performance of a genetic algorithm. Other factors such as the probability of crossover, the probability of mutation, the size of the population, and the number of iterations can be modified regarding the algorithm's performance through a few trial runs.

As mentioned in section 2.2.1, among optimization methods, GA has been often selected and utilized to enhance management processes due to its advantages. But GA has a limitation, which is the lack of enough diversification in the generated populations. Similar to a greedy optimization algorithm, in each iteration, GA selects the fittest chromosomes. In other words, without any memory, GA makes a locally-optimal choice in each generation with the hope that these choices could lead to a globally optimal solution using various operators. So to avoid the major limitation of GA, which is getting stuck at local optimal values, MLP is combined with GA to create a memory of the fittest solutions previously found and improve the probability of identifying global optimal solutions. MLP, as a feed-forward neural network, has not been used in terms of a classifier, but it is integrated with GA only to generate memory for GA to follow the trend of data. Creating memory means that GA can memorize the properties of its previous generations. Since in pure GA, after applying crossover and mutation in the current population, everything else will be removed, MLP is integrated to retain the trend of data associated with the previous generation. The next section is a brief explanation of MLP as a kind of Artificial Neural Network (ANN).

## **2.5 Artificial Neural Network (ANN) and Multi-Layer Perceptron (MLP)**

Neural networks (NN) came to existence unexpectedly in the late 1980s and were fully matured in the following decades. Neural networks have been applied in various industries to solve a particular problem. Its application areas include but not limited to process control, manufacturing, quality control, product design, financial analysis, fraud detection, loan approval, voice and handwriting recognition, and data mining (Poulton, 2001). Artificial Neural Networks (ANNs) have been used in the construction industry as well to solve different issues such as investigation of the relationship between pre-project planning and project success, modeling construction labor productivity of construction crafts, predicting height mark deviation of main beams of cable-stayed bridges during construction, and construction controlling of cable-stayed bridges. The procedure of processing information in ANNs is similar to that of biological neural systems (Morgan et al.,



1991). Neural networks are made up of many artificial neurons. Neural networks in which the neurons in each layer feed the next layer as their output until the final output is obtained are called feed-forward networks. As Shirvany et al. (2009) have stated, due to structural flexibility, excellent representational capabilities, and availability of a large number of training algorithms of feed-forward networks, they are the most popular fully connected network architectures. Multi-Layer Perceptron (MLP) networks are also a kind of feed-forward neural network in which different transfer functions can be applied based on various conditions. It is also stated that the MLP network is a universal function approximator, and it can be considered as a powerful architecture of ANN for interpolation in multidimensional space.

MLP networks involve at least three layers entitled “input layer, hidden layer, and output layer.” The input layer is an information recipient, and various nonlinear transformer functions can be applied for transformation from input space to high dimensional hidden space. An output of a three-layer MLP network is defined by Equation 2-1, as shown in Figure 2-10 (Shirvany et al., 2009):

$$a_k^2 = f^2(\sum_{j=1}^{S^1} w_{jk}^2 f^1(\sum_{i=1}^R w_{ij}^1 p_i + b_j^1) + b_k^2), \quad k = 1 \text{ to } S^2 \quad \text{Equation 2-1}$$

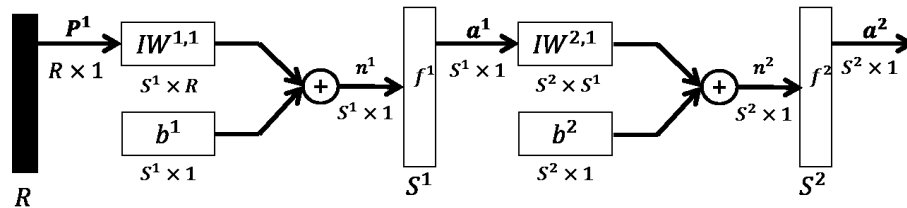


Figure 2-10: Multi-Layer Perceptron Network (Shirvany et al., 2009)

Where the hidden layer and output layer are indicated by superscript 1 and superscript 2, respectively. The numbers of the input unit are denoted by  $R$ , and the numbers of hidden and output units are demonstrated by  $S^1$  and  $S^2$  respectively. Also,  $f$  indicates activation function,  $W$  represents the synaptic weight parameter, and  $b$  illustrates bias. There are different activation functions as follows (Shirvany et al., 2009):

Linear:  $f(x) = x$  Equation 2-2

Log – sigmoid:  $f(x) = \frac{1}{1+e^{-x}}$  Equation 2-3

Tan – sigmoid:  $f(x) = \frac{2}{1+e^{-2x}} - 1$  Equation 2-4

Positive linear:  $f(x) = x \text{ if } x \geq 0, f(x) = 0 \text{ if } x < 0$  Equation 2-5

Supervised and unsupervised learning are learning strategies that indicate how the network is trained. In supervised learning, input and output pairs are required to be provided. The provided output patterns are compared with the output calculated by the network, and any difference between them has to be minimized through updating parameters in the network. In an unsupervised

learning strategy, only input patterns are provided, and the network finds common features in groups of those patterns.

While the application of ANN is expanding in different domains, some researches focus on the selection of the ANN architecture and its efficient training procedure. These researches are trying to combine ANN and GA to enhance the performance of their proposed networks (Seiffert 2001; Nasseri et al. 2008; Divya et al. 2014; Allahkarami et al. 2017). GA is used to train and optimize the networks to increase the accuracy and efficiency of classification and prediction done by ANN. The backpropagation training algorithm is frequently used in ANN to adjust the weights through comparison between the desired and actual network response, and as Allahkarami et al. (2017) have stated, it may trap ANN into the local minima and lead to converging slowly. So integrating GA with ANN can optimize the initial weights of ANN and improve its performance.

As mentioned earlier, MLP is integrated with GA in a novel algorithm to prevent the shortcoming (local minima and the lack of memory) of GA while generating the optimized material delivery schedule.

## **2.6 Project Progress Monitoring**

Accurate project progress measurement and periodic updating of the project schedule to track actual progress are an integral part of the project control plan. To deliver projects on time and within budget, progress monitoring is considered a critical success factor (Iyer and Jha, 2005). So effective, real-time, and accurate project progress monitoring continues to be one of the highest challenges for project managers (Saidi Kamel et al., 2003; Zhang et al., 2009) and has become a significant field of study in recent years.

In traditional construction progress monitoring, site data acquisition relied heavily on manual observation, which renders it subjective, time-consuming, error-prone, and labor-intensive. Percentage progress and subsequently, the project schedule had been updated manually based on the feedback and reports submitted by superintendents on construction job sites. So the lack of accuracy in tracking progress, delays in site data acquisition, time-consuming information extraction, and manual updates were reported to be the main hindering issues of efficient progress monitoring (Navon, 2007; Yang et al., 2015). Moreover, generating a 3D model of the as-built environment with the purpose of progress monitoring includes data acquisition, modeling, and analysis, which all are performed manually in current practice (Tang et al., 2010; Dimitrov and Golparvar-Fard, 2014). It is shown that due to the improper illustration of discrepancies between the as-planned and as-built models, only 12% and 11% of the meetings time are spent on evaluative and predictive tasks, respectively. The remained time is assigned to descriptive (35%) and explanative tasks (42%) for making project current status understandable (Golparvar-Fard, 2006).

The advancements made in Information and Communication Technology (ICT), and in sensing technologies made it possible for the development of automated site data acquisition and automated project progress tracking methods. Proper automated project progress monitoring leads to timely identification of deficiencies and supports timely decisions for corrective actions (Maalek and Sadehpour, 2012). Progress made on this front using automation technologies, including 3D imaging, GPS, RFID, UWB, hand-held computers, voice recognition, wireless sensor networks, and various combinations of such technologies. In view of the speed and accuracy of 3D data collection by 3D Imaging-based technologies (Turkan et al., 2012), multiple researchers have used

Laser Distance and Ranging (LADAR), Terrestrial Laser Scanning (TLS) and digital photogrammetry to collect 3D geometrical data pertinent to as-built 3D modeling to track project progress. Recent improvements in digital photography and webcams have made vision-based construction performance monitoring methods more cost-effective and practical (Golparvar-Fard et al., 2009). It is recognized that the use of images and videos for as-built data acquisition is easy, does not need specialized knowledge, is not costly, and not time-consuming (Kropp et al., 2018). So this research has focused on RGB cameras as passive sensors for project progress monitoring due to the mentioned benefits and the superiority of RGB cameras over RGB-D, as explained before. Furthermore, easily captured images and videos being commonly used on construction job sites have brought attention to developing and applying computer vision techniques for estimating project progress (Yang et al., 2015).

Vision-based methods for effective project progress monitoring have attracted the attention of researchers in recent years. Vision-based construction monitoring methods have been classified into two main groups and then are reviewed and elaborated in the research done by Yang et al. (2015). Methods in the first group focus on visual monitoring of civil infrastructure and building elements in the project level by comparing the as-built status against the as-planned model and methods in the second group have been applied for visual monitoring of construction equipment and workers in the operational level through detecting, location tracking, and analyzing their activities. The focus of this paper is on the first group in which there are three different research series to estimate project progress applying vision-based methods. “comparison of time-lapse images with 4D Building Information Modeling (BIM)”, “comparison of 3D as-built point clouds with 4D BIM”, and “detection of building elements” are the research series in the first group.

### **2.6.1 Comparison of Time-lapse Images with 4D BIM**

In the first research series captured time-lapse images from fixed camera viewpoints have been compared with one another (Abeid et al., 2003; Ibrahim et al., 2009) or with 4D Building Information Modeling (BIM) (Zhang et al., 2009; Golparvar-Fard et al., 2009; Rebolj et al., 2008; Kim and Kano, 2008). For instance, in (Golparvar-Fard et al., 2009), through the superimposition of 4D BIM on the as-built time-lapse photo and assigning traffic light colors to the 3D components, project progress deviations are identified and visualized, respectively. To perform superimposition, some steps, including geometric camera calibration, feature selection, and feature matching between the photograph and the 3D model, are required. In this research, the superimposed 4D as-planned model and the photographs are visually compared, and the discrepancies are identified and analyzed manually. In (Ibrahim et al., 2009), a framework for automatic generation of work packages is developed, and computer vision algorithms are applied to measure the progress of these work packages. Converting to greyscale, partitioning, normalizing, using a spatial-temporal derivative filter, and segmentation masks are the steps that have to be done for each captured image to calculate the mean change in a particular region of interest determined for each component of work packages. In another study done by Pour Rahimian et al. (2020), a framework consisting of the Convolutional Neural Network (CNN) algorithm as a machine learning (ML) algorithm, image processing, BIM and Virtual Reality was proposed for an on-demand automated simulation of construction projects. Computer vision and ML techniques have been used to process and compose as-built images (site photographs) with the as-planned BIM models by the aid of Virtual Reality (VR) game engines, such as the Unity engine. Building elements and unwanted objects were recognized and removed, respectively, using ML and image processing. Then the extracted building elements were overlaid on the corresponding

as-planned BIM components to effectively compare as-built construction with as-planned BIM model for the purpose of deficiency detection.

### **2.6.2 Comparison of 3D As-Built Point Clouds with 4D BIM**

Researchers in the second series have focused on generating 3D as-built point clouds or 3D reconstruction by applying Structure from Motion (SfM) techniques and comparing it with 4D BIM (Golparvar-Fard et al., 2011; Pučko et al., 2018). SfM is a general method to obtain information about the geometry of 3D scenes from 2D images using corresponding image points in multiple views and estimation of camera pose. So given an image in two or more views, a 3D point can be reconstructed by triangulation. The method is summarized as follows (Sakurada, K., 2015):

- 1) Feature points are extracted and matched for two consecutive images using the descriptors of feature points.
- 2) Essential matrices are calculated, and mismatches of feature points are rejected using the Random Sample Consensus (RANSAC).
- 3) Camera poses and positions of feature points are calculated using those essential matrices.
- 4) Camera poses and positions of 3D points are optimized to minimize re-projection errors of feature points.

In the study done by Golparvar-Fard et al. (2011), after capturing unordered daily site photographs to reconstruct 4D as-built point-cloud, progress monitoring and revising work schedule can be achieved in two different ways. First, by having as-built visualization system, project managers or superintendents can virtually walk on the construction site to perceive the progress easily and second through semiautomatic superimposing 4D as-built point cloud over 4D BIMs, progress deviations are visualized and interpreted manually. One of the main challenges of their proposed method is the high computation time of implementing the algorithm due to the pairwise matching step. SfM consists of pairwise feature matching and bundle adjustment, which are the most time-consuming steps of their process. Moreover, SfM requires images with an overlap, which leads to photograph with poor texture creating difficulties for searching corresponding feature points in consecutive images (Lei et al., 2019). So Lei et al. (2019) proposed data-driven CNN to improve the registration accuracy of multi-scanned point clouds and then to automatically detect spatial changes by comparing various point clouds. In another study done by Golparvar-Fard et al. (2015), in addition to the automated reconstruction of as-built point clouds and manual registration of the BIM and point cloud models using a set of initial control points, occlusions are taken into account using voxel coloring algorithm. The monitoring of physical progress is also automated by comparing progress measurements with dynamic thresholds learned through a Support Vector Machine (SVM) classifier. It is stated that computing progress using their approach takes a few hours whenever any observation is received. Bognot et al. (2018) generated and georeferenced as-planned 3D model by the digitization of CAD models in the ArcScene environment and establishing ground control points from the GNSS field survey, respectively. Generating as-built 3D point cloud by capturing videos of the building with a camera-equipped Unmanned Aerial System (UAS) is the next step. Then a sparse point cloud and a densified point cloud are reconstructed by Visual SfM and multi-view reconstruction (CMPMVS) software, respectively. In the fourth step, the textured meshes are georeferenced using MeshLab. Then construction progress is monitored and visualized using Geographic Information System (GIS). Point clouds from the as-built 3D model are extracted after aligning the georeferenced as-built and as-planned 3D models

using ArcGIS, and then building elements are labeled “built” or “not built” through calculation point cloud density, the difference in centroid and threshold. In their study, only four types of building elements (beams, columns, slabs, and walls) are considered. Moreover, the interior building elements were labeled as “not built” because they cannot be seen or captured by the video due to occlusions by other objects or missing illumination.

It is worth mentioning that another way for monitoring project progress is comparing actual performance with planned performance through updating BIM in real-time. General contractors and also subcontractors are reluctant to change their paper workflows and generate ‘As Built’ BIM. So when construction begins, a BIM which has been developed to detailed design is not anymore up-dated. In order to address this issue, BIM 360 as a centralized cloud-based information platform during construction can be used. The effectiveness of this platform is due to the fact that it allows collected job site information (such as ‘As-Built’ schedule) to be synchronized with the current BIM and generates ‘As Built’ BIM in real-time. But the most important limitation with BIM 360 as cloud-based BIM is related to the real-time site data collection and retrieving information from the collected data. In fact a site engineer is responsible to visually select objects in the BIM, subjectively estimate their relevant % complete at specific points of time and finally input these data into the BIM 360™ Field application using an iPad (Matthews et al., 2015). So there is not any algorithm, method or any application embedded in BIM 360 to automatically analyze the collected and synchronized data for construction progress monitoring.

Another possible approach is providing images along with a 3D reconstruction of the scene using RGBD devices such as Microsoft HoloLens. For example, Kopsida and Brilakis (2020) proposed a real-time automated progress-monitoring system in which as-built spatial data is captured using Microsoft HoloLens (by inspector wearing the wearable device) and then is compared with the 4D as-planned BIM. Identification of the visible objects from the camera and comparison as-built captured data with 3D as-planned objects are the main two steps of their system. If an object meets the following requirements, it is considered as visible: being in camera’s frustum, having a distance to the camera less than 4 m, and not being occluded by an object known to be completed. They applied their developed system by having two assumptions, including “planned 3D objects do not extend into more than one room” and “the 3D as-planned model is always correctly registered to the as-built scene.” It is worth mentioning that the applications of RGBD devices like Microsoft HoloLens are limited to interior implementations.

### **2.6.3 Building Elements Detection**

Third research series has concentrated on building elements detection for project progress monitoring (Bosché and Haas, 2008; Bosché et al., 2009; Wu et al., 2010; Son and Kim, 2010; Turkan et al., 2012; Kim et al., 2013a, Kim et al., 2013b, Turkan et al., 2013; Bosché et al., 2014). As an example, in (Bosché et al., 2009), they developed an automated approach to recognize three-dimensional (3D) CAD objects from 3D site laser scans for progress tracking. First, they generated the Stereolithography (STL) format and a point cloud representation of the available 3D CAD model. Then the STL-formatted project 3D model was registered in the scanner’s spherical coordinate frame. In the third and fourth steps, they calculated and recognized the as-planned range point cloud, respectively. Finally, CAD objects and their current status were identified based on the object’s recognized surface (by calculating and comparing the number of actual recognized points covering the surface of any particular object with a pre-established threshold, respectively). Hamledari et al. (2017) have focused on the application of computer vision techniques for

automated detection of components of indoor under construction partitions. They have developed a computer vision-based algorithm consisting of four integrated shape and color-based modules to automatically detect the interior partition components and identify their current state. The input and output of the developed algorithm are 2D digital images of indoor construction sites taken by a mobile camera (quadcopter or smartphone) and classified images into one of the five possible states (framing, insulation, installed drywall, plastered drywall, and painted partition) respectively. Instead of feature-based detection techniques, the object-based approach, including various vision-based algorithms, has been applied to detect the mentioned building elements in terms of multiple modules. For instance, to detect studs, the captured image is first smoothed through applying a bilateral filter and then is converted to LAB color space. In the next step, Otsu cluster-based image thresholding and L channel are used to differentiate the studs from their closest vicinity. After thresholding, the L channel, morphological transformation for noise removing, and Progressive Probabilistic Hough Transform (PPHT) for extracting the vertical stud lines are applied. A novel automated method for indoor project progress monitoring is proposed in (Kropp et al., 2018). As-built video data, as-planned BIM data, and computer vision algorithms are used in their method, which includes two steps. In the first step, named “registration,” the pose of each image is defined based on the coordinate system of the building model. In the second step, entitled “recognition,” the activity state is determined through search space reduction, image rectification, object recognition, and material recognition.

On top of the mentioned research series, another group of researchers has tried to automatically detect and classify construction materials from captured site images to monitor project progress. They believe that generating point clouds which illustrate 3D geometrical information of building elements do not include semantic information of the scene. For instance, Dimitrov and Golparvar-Fard (2014) have proposed a vision-based method to classify materials using images captured under unknown viewpoints and site illumination conditions. Their method uses joint probability distribution of responses from a filter bank and principal Hue-Saturation-Value color values and kernel Support Vector Machine classifier.

Against a clear majority of researchers who have addressed the progress monitoring of outdoor sites, some studies have focused on the indoor environment (Lin and Fang, 2013; Klein et al., 2012; Hamledari et al., 2017; Kropp et al., 2018). However, the lack of image-based modeling for interior construction progress monitoring can be seen in the existing researches (Rankohi and Waugh, 2014). The majority of the existing image-based 3D reconstruction solutions augmented reality-based methods, and appearance-based techniques have not been advanced enough to be applied for indoor construction site progress monitoring. Approaches using fixed cameras are inflexible to record all changing structures in construction job sites for project progress monitoring (Hamledari et al., 2017). In the majority of the existing progress monitoring approaches, registration of either captured images to 4D BIM models or as-planned 3D model formatted as stereolithography to laser scan derived point clouds have been done manually.

Moreover, developed automated registration approaches heavily rely on Iterative Closest Point (ICP) algorithm, which needs a good initial guess to converge (Kropp et al., 2018). Also, most of the mentioned researches analyze and visualize the progress manually or semi-automatically through automatically generating as-built 3D reconstruction and comparing it with as-planned information. Despite all the irrefutable improvements made in construction progress measurement during recent decades, there are still significant issues and limitations for construction progress

monitoring and control (including progress measurement of limited types of building elements and project activities, inflexibility of fixed cameras, changing viewpoints, cluttered scenes, occlusions and diverse illumination conditions and complexity and high computational cost of proposed computer vision algorithms such as conventional feature matching algorithms, color/texture-based or shape-based object detection, object recognition algorithms and material classifiers), which have to be appropriately addressed as much as possible using novel concepts and methods.

To wrap up, according to the findings in the reviewed works and as Pučko et al. (2018) have stated, none of the observed methods is yet able to provide reliable monitoring of construction, which would cover the whole building (outdoor and indoor) through the entire construction process. Therefore the development of an efficient near real-time progress monitoring and visualization method to be applied by the industry is of vital importance. Recently, Deep Learning methods including Deep Auto-Encoders (DAEs), Deep Belief Networks (DBNs), Convolutional Neural Networks (CNNs), Restricted Boltzmann Machines (RBMs), and Generative Adversarial Nets (GANs) are widely used in the field of computer vision and have put it on the map in the industry. Several challenging tasks, including image classification, object detection and recognition, image retrieval, scene parsing, speech recognition, and speech content retrieval, natural language processing, human pose recovery and estimation, face alignment, and facial feature tracking, have been addressed successfully applying developed DL algorithms. Due to success and effectiveness of DL methods in a variety of visual applications, in this research, near real-time progress monitoring for both indoor and outdoor environment under different conditions and automated detection of building elements are addressed by applying DL algorithms named deep Convolutional Auto-Encoder (CAE) and Mask Region-based CNN (Mask R-CNN) respectively.

## **2.7 Deep Learning (DL) Algorithms**

As Voulodimos et al. (2018) have stated, simulating the human brain was the initial motivation for the development of neural networks. McCulloch and Pitts (1943) defined interconnected basic cells entitled “neurons” to simulate how the brain could create complex patterns that resulted in the inception of artificial neural networks. Figure 2-11 indicates the significant milestones in the development of neural networks and machine learning, giving rise to DL in the last decade.

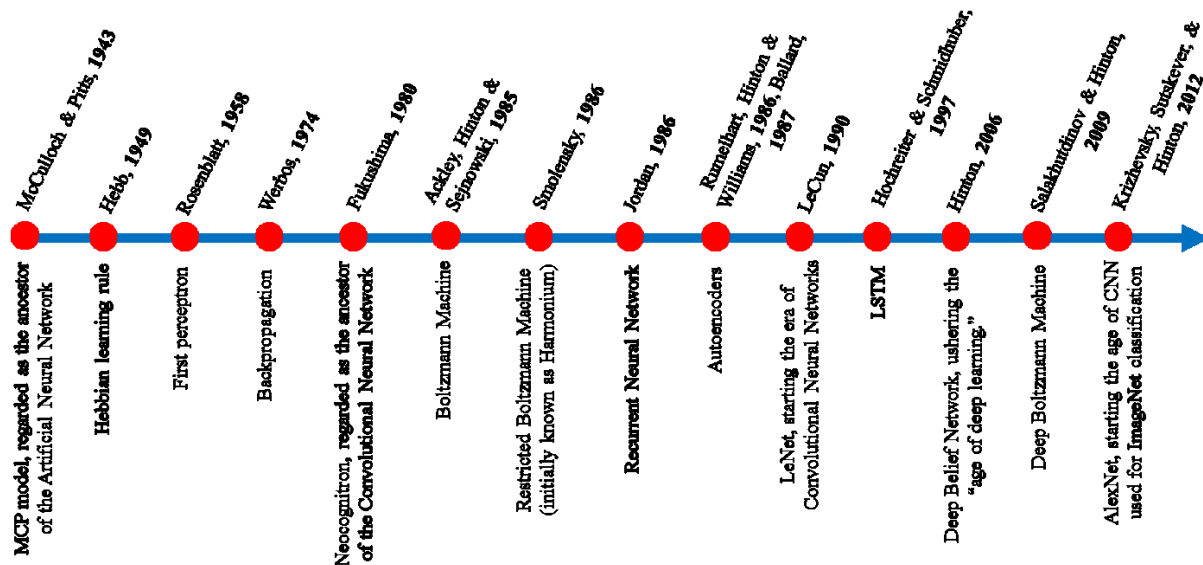


**Figure 2-11: Significant Steps in the History of Neural Networks and Machine Learning Resulted in Deep Learning (Voulodimos et al., 2018)**

To compare DL with traditional machine learning algorithms, Paine (2017) has focused on humans as an example object. Besides different genotype characteristics of each human, his/her limbs can have too many configurations while being photographed from various viewpoints, and illumination. So instead of manually defining a fixed set of rules to consider all these variations done by traditional algorithms, in DL algorithms, machines are asked to learn a denser and denser representation of input data (exhibiting variability) that can deal with all those variabilities and configurations. As a result, during the last decade, DL algorithms have surpassed the existing state-of-the-art machine learning techniques in computer vision as a field of machine learning (Voulodimos et al., 2018).

Conventional computer vision and image processing feature-learning algorithms such as feature descriptor algorithms (SIFT, Speeded-Up Robust Features (SURF), and Binary Robust Independent Elementary Features (BRIF)), classification algorithms (SVM, K-Nearest Neighbors), color/texture-based or shape-based object detection algorithms, image segmentation, edge detection algorithms, Hough transform, and SfM, learn human-engineered features (edges, corners, color) from images to interpret these images (Lee, 2016). The drawback of this feature extraction is manual specifying the proper feature vector in each given image, which is exacerbated in the presence of considerable visual variation in complex images. Choosing many features results in a plethora of parameters that have to be fine-tuned (Zdziarski, 2018). Deep learning brings a revolution in computer vision because it has introduced the concept of end-to-end learning where the machine is guided to learn the most descriptive and salient features of an image and discover the underlying patterns in each given image. Learning a denser and denser representation of given information (training images), which can mimic the human brain function to perceive and analyze information, is the central concept of the deep architecture of deep neural networks (Zdziarski, 2018). It has been revealed that due to the universal approximation ability of deep hierarchy models, they can capture high-level abstract features (borders, components, and the combination



of several components) in addition to low-level characteristics (intermediate features non-meaningful to the human visual system which neural nets are sensitive to them) (Leng et al. 2015).

DL is not task-specific, and it is a universal learning method because it has been used in almost all domains to address different problems. DL can represent a hierarchy of features or concepts in which high-level and low-level concepts are defined from each other. There is no need to design features while applying DL. Features and subsequently, the robustness to natural variations in the data are automatically learned. Furthermore, through transfer learning, applied DL algorithms to solve specific problems can be used for other applications with different data types. This is very beneficial to address some problems without adequate data. DL, which is a data-driven technique can handle the volume, velocity, variety, and veracity of the big data problems. So advantages such as being a universal learning approach, robustness, generalization, and scalability of the DL approach indicate its superiority over other techniques (Alom, 2018). It is worth noting that, on top of the advantages of DL approach, other factors such as the advent of large, high-quality, publicly available labeled datasets, empowerment of parallel GPU, the appearance of proper activation functions, new regularization techniques, and powerful frameworks like TensorFlow have affected the considerable boost of DL during recent years (Voulodimos et al., 2018).

Similar to machine learning, DL algorithms are classified in supervised (learning techniques that use labeled data), semisupervised (learning techniques that are based on partially labeled datasets), and unsupervised (learning techniques that try to find unknown patterns, relationships or structure in terms of internal representation or important features without any teacher or labeled datasets) categories (Alom, 2018). Convolutional Neural Networks (CNNs), Deep Boltzmann Machines (DBMs), Deep Belief Networks (DBNs), and Autoencoders are among the most significant DL schemes which are often used in computer vision problems.

As mentioned earlier, the success and effectiveness of DL methods in a variety of visual applications are due to the fact that they can represent images through automatically learning the features with the superior discriminatory power rather than using hand-crafted image descriptors. So in this research, near real-time progress monitoring for both indoor and outdoor environments under different conditions is addressed by applying a DL algorithm. In this study, a deep Convolutional Auto-Encoder (CAE) algorithm instead of conventional computer vision algorithms is utilized to facilitate indoor and outdoor progress monitoring under various illumination conditions.

Dealing with the problem of backpropagation by using input data instead of labeled datasets as a teacher resulted in the introduction of Autoencoders by Hinton and the PDP group (Rumelhart et al., 1986). So AE is able to extract valuable features from unlabeled data in an unsupervised manner, and it has been broadly applied in various applications, including network pre-training, feature extraction, dimensionality reduction, and clustering. Autoencoders are classified in classic AEs (only one hidden layer), and deep AEs (with many hidden layers in the encoder and decoder parts). AEs consist of two parts. The first part is an encoder or a recognition network that maps the inputs to an internal representation (a set of feature spaces). The second part is a decoder or a generative network that maps the internal representation to the outputs by reconstructing the original data shown in Figure 2-12 (Géron, 2017).

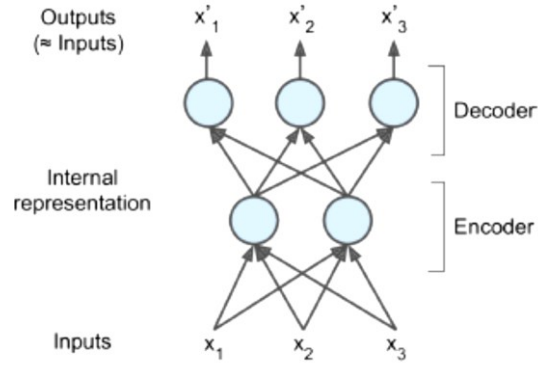


**Figure 2-12: The Architecture of a Simple Auto-Encoder (Géron, 2017)**

Hierarchical features extracted by the hidden layers of a deep AE leads to considerable quality improvement in solving any specific task. If the fully-connected layers are replaced by convolutional and deconvolution layers in the encoder and decoder parts respectively, a deep Convolutional Auto-Encoder (CAE) is generated, which is more proper to address image processing problems. This is due to the fact that AE is exploiting CNNs properties to deal with noisy, shifted, and corrupted image data more properly within an unsupervised learning paradigm (Turchenko et al., 2017). Unsupervised CAE is trained through minimizing the differences between original and reconstructed data with distance metrics (Alqahtani et al., 2018).

In CAE, the latent representation of the  $k$ -th feature map for a mono-channel input  $X$  is (Masci et al., 2011):

$$h^k = \sigma(X * W^k + b^k) \quad \text{Equation 2-6}$$

Where the bias ( $b^k$ ) is broadcasted to the whole map,  $\sigma$  is an activation function, and  $*$  indicates the 2D convolution. A single bias per latent map is used, as we want each filter to specialize in features of the whole input. The reconstruction is calculated using (Masci et al., 2011):

$$y = \sigma(\sum_{k \in H} h^k * \tilde{W}^k + c) \quad \text{Equation 2-7}$$

Where there is one bias ( $c$ ) per input channel, the group of latent feature maps is denoted by  $H$ , and  $\tilde{W}$  indicates the flip operation over both dimensions of the weights. The cost function to minimize is the Mean Squared Error (MSE) (Masci et al., 2011):

$$E(\theta) = \frac{1}{2n} \sum_{i=1}^n (x_i - y_i)^2 \quad \text{Equation 2-8}$$

The backpropagation algorithm is applied to update the weights by computing the gradient of the error function with respect to the parameters using the following Equation (Masci et al., 2011):

$$\frac{\partial E(\theta)}{\partial W^k} = x * \delta h^k + \tilde{h}^k * \delta y \quad \text{Equation 2-9}$$

Where  $\delta h$  is the deltas of hidden states, and  $\delta y$  is the deltas of the reconstruction.

Modifications and variations can be considered in CAE network architecture to improve the network's ability for image interpretation. A further superiority of DL methods over conventional computer vision has been shown in the field of computer vision (Voulodimos et al., 2018). But on the other hand, to learn a good representation of images with large visual variation and fill the gap among training examples, a large amount of data is required (Zhang et al. 2014). However large datasets are necessary for proper training of deep learning algorithms, and generating these huge datasets of actual images for different tasks in computer vision usually encounters various issues such as oversampling, variability, scarcity, and unavailability, rendering synthetic images has been very attractive to generate needed large datasets in recent years. The rich 3D repositories and photo-realistic rendering have been used for training deep learning algorithms such as Convolutional Neural Networks (CNNs) because of their high value for visual learning. Combining synthetic and real images, or purely synthetic images have been used for training and validating deep learning algorithms for various computer vision tasks such as object viewpoint estimation, object recognition, indoor scene understanding, and tracking applications (Su et al. 2015; Papon, and Schoeler, 2015; Ros et al., 2016; Movshovitz-attias et al., 2016; Hinterstoisser et al., 2017).

## **2.8 Deep Learning-Based Generic Object Detection**

The capability of acquiring and analyzing the information of project status at any particular point of time is critical for measuring and monitoring project progress and a set of project-related issues such as productivity, safety monitoring, and updating as-built information on a regular basis. Construction projects are complex and dynamic, making the assessment of project status difficult and time-consuming (Wu et al. 2010).

Recent significant improvements in digital photography have made it cost-effective and practical to record project information through easily captured images and videos on construction job sites. This acquired data often become unprofitable due to the adversities associated with grasping their contents and analyzing the extracted information (Alavi and Gandomi 2017; Han and Golparvar-Fard 2017; Hou et al. 2019). So there is a need for an effective method for extracting and processing the information included in the captured images. Recent decades witnessed substantial efforts to visualize accurate project status using digital images. Advances in big data analytics, Graphical Processing Units (GPUs), and deep learning methods resulted in the rapid development of computer vision applications (Hou et al. 2019). Object detection based on deep neural networks as one of the most fundamental and challenging fields in computer vision has been extensively used for intelligent video surveillance, robotics, security, autonomous driving, pedestrian detection, anomaly detection, and face detection. Thus applying object detection algorithms for automated identification of specific objects of interest in the images captured from construction job sites can be a suitable replacement of time-consuming manual information retrieval.

Despite the efforts being made in object detection using digital data mining and computer vision methods, there is no off the shelf open dataset of building structural component images in the construction industry (Hou et al. 2020). To the authors' best knowledge, not only building structural component images but also images visualizing other building components have not been captured and collected in a ready-made dataset in the construction industry.

Researchers applied different computer vision techniques for detection of structural components (Zhu and Brilakis 2010; Koch et al. 2014; Hou et al. 2020), safety monitoring (Yang et al. 2010;

Han et al. 2012; Ding et al. 2018; Mneymneh et al. 2018), detection and tracking of construction workers, materials, and equipment (Chi and Caldas 2011; Memarzadeh et al. 2013; Park and Brilakis 2016; Ren et al. 2017; Eirini and Ioannis 2018; Kim et al. 2018), defects detection (Butcher et al. 2014; Cha and Choi 2017; Kong and Li 2018), and progress monitoring (Golparvar-Fard and Peña-Mora 2007; Son and Kim 2010; Omar and Nehdi 2016; Kropp et al. 2018). Detecting objects of interest as one of the challenging problems in the computer vision field has often played an essential role in these applications. Object detection methods can be categorized into feature-based and deep learning-based algorithms (Hou et al., 2020). In other words, both traditional machine learning and deep learning algorithms can be applied to detect objects of interest. Using traditional machine learning algorithms needs the selection and extraction of hand-crafted features, which best represent the image contents in a specific dataset. This leads to a lack of generalization ability of algorithms developed in this manner. Deep learning algorithms eliminate manual feature extraction and learn features directly from the input images (self-learn features), which leads to significantly better results (Nath and Behzadan 2019). Substantial improvement in object detection performance (mean Average Precision (mAP)) has been attributed to the inception of deep learning methods in 2012 (Liu et al. 2019). It is worth mentioning that large amounts of labeled data are required to make deep learning algorithms applicable and practical for robust object detection. To be more precise, deep learning-based object detection methods owe their success to their deep networks (consisting of millions of parameters), available large datasets (such as ImageNet and MS COCO) for training and substantial computational capability of GPUs (Liu et al. 2019). Table 2-1 depicts studies in the construction industry in which either traditional machine learning or deep learning algorithms have been used to detect objects of interest. According to the source of images and also the type of used datasets (including real or synthetic-images) in each study (the last three columns of Table 2-2), it can be stated that real images have been regularly captured and used for object detection. Just in the study done by Hou et al. (2020), a dataset of synthetic-images was generated to train their developed model for the detection of structural components such as columns and beams. Their study, however, did not intend to benefit from synthetically generated datasets. They had to train and test the developed model on the synthetic-image datasets due to the lack of a ready-made, and open dataset of structural component real images available in the construction industry. As a result, they evaluated the performance of their model using synthetic-images as well, which means the performance was not based on real images. As mentioned before, to make deep learning-based algorithms effective for the detection of building components, large training datasets of images are required. However, there are no ready-made image datasets of building components in the construction industry. Aside from the required large datasets, annotating and labeling these datasets are also required, adding non-trivial and resource-intensive operations (Nath and Behzadan 2019).

Surveying the literature shows that different researches have been carried out to investigate the benefits of photo-realistic rendering for visual learning. Synthetic-images have been used to train deep learning methods (specifically CNNs) for diverse applications such as object viewpoint estimation (Movshovitz-Attias et al. 2014; Su et al. 2015; Movshovitz-Attias et al. 2016; Rad et al. 2018), and object detection (Vazquez et al. 2014; Sun and Saenko 2014; Hattori et al. 2015; Hinterstoisser et al. 2017; Tremblay et al. 2018). Beneficial results have been achieved from each of these studies. For example, Tremblay et al. (2018) concluded that non-artistically synthetic-images could be used to train deep neural networks with a convincing performance. Benefiting from datasets of less photorealistic synthetic images results in decreasing the necessity for

collecting large amounts of real-images and extensive effort for the generation of photorealistic synthetic-images. Rajpura et al. (2017) deduced that generating synthetic-images with a high level of photorealism was not fundamental for high detection performance of CNNs, specifically when real-image training data is limited or unavailable. A study done by Movshovitz-Attias et al. (2016) indicates the superiority of the deep learning-based networks trained on a combination of synthetic and real images over those trained on real images only. Others like Ros et al. (2016) and Jalal et al. (2019) generated and made publicly available datasets of synthetic-images entitled “SYNTIA” and “SIDOD,” respectively. SYNTIA includes more than 213,400 diverse urban images used for autonomous driving, and SIDOD consists of 144k stereo image pairs of 10 objects from 18 camera viewpoints used for object detection, pose estimation, and tracking applications. It was concluded that these datasets were good enough for deep learning-based networks to produce robust instance segmentations of test datasets of real-images. In research done by Braun and Borrmann (2019), 4D BIM and inverse photogrammetry have been integrated to label construction images used as training data for object detection algorithms. Automated labeling can be done through projecting building elements of the BIM into images captured from the site for point cloud reconstruction along with the utilization of semantic information of the type of the elements available in the BIM model related to the respective regions. In the construction industry, benefiting from datasets of synthetic-images using deep learning-based algorithms to detect building component is in the preliminary stage.

## 2.9 Summary

In summary, the identified limitations and research gaps are as follows:

1. Optimization of the inventory cost at the planning phase of projects without considering introduced changes in the construction phase;
2. Fixed-ordering-period for construction materials;
3. Finding the optimal solution of delivery and inventory of materials by changing the activities start date and only by changing the total number of material deliveries throughout the construction duration;
4. Using GA without preventing the lack of enough diversification in the generated populations;
5. Lack of considering the complex, unstructured and dynamic nature of the constructions projects in developing the materials management systems;
6. Limitations of construction progress monitoring methods due to changing viewpoints, cluttered scenes, occlusions, diverse illumination conditions, various types of building elements/project activities, complexity and high computational cost of applied conventional computer vision algorithms;
7. However, using deep learning-based object detection algorithms are an effective method for extracting and processing the information included in the images captured from construction job sites, large amounts of labeled data are required to make these algorithms applicable and practical for robust object detection. As mentioned before, there is no off the shelf open dataset of building component images in the construction industry and benefiting from datasets of synthetic-images to detect building component is in the preliminary stage In the construction industry; and

8. Lack of proper answer in both planning and construction phases to this question “which material and how much of that material must be ordered and bought on which day to result in the least cost without material shortage or surplus?”

Among mentioned gaps, this study addresses limitations number 2, 4, 5, 7 and 8. So, to achieve an effective materials management framework being capable of considering the dynamic nature of construction projects, a proper optimization engine (GA-MLP method) was developed, which can consider the project progress throughout the construction phase. Furthermore, to detect installed materials or estimate the quantities of consumed materials at the job site, not only a technology (digital imaging) was selected to capture the as-built status of buildings, both in outdoor and indoor environments easily, safely, and at low cost but also a novel near real-time progress monitoring method (deep CAE) and an object detection framework were developed to visualize and detect the progress at different time intervals in near real-time with acceptable accuracy. The developed CMM framework and its models are elaborated in detail in the next chapter.

**Table 2-2: Studies Used Either Traditional Machine Learning or Deep Learning Algorithms to Detect, Recognize and Classify Various Objects of Interest in the Construction Industry**

Traditional Machine Learning Algorithms					
#	Author/s	Method	Objects of interest	Source of images	Dataset (Synthetic/Real)
1	Lu et al. (2018)	Neuro-fuzzy based system	Walls, Columns, Beams, Windows, Doors	600 images taken with a digital camera and downloaded from the Internet	Real
2	Hamledari et al. (2017)	Four integrated shape and color-based algorithms	Drywall, Insulation, Studs, Electrical Outlets	900 images captured by UAV, 450 images captured by smartphone, 210 images from publically	Real
3	Zou and Kim (2007)	HSV color space, simple thresholding methods in conjunction with calculation of object centroid coordinates	Excavators	1080 images from the construction of the Natural Resources Engineering Facility (NREF) of the University of Alberta in Edmonton, Canada	Real
4	Brilakis and Soibelman (2008)	Flooding-based clustering algorithm along with the computing the Maximum Cluster Dimension (MCD) and the maximum dimension along the Perpendicular axis of MCD (PMCD)	Linear (beam and column) and nonlinear (wall, slab) construction objects	103 images	Real
5	Chi and Caldas (2011)	Morphological image processing, Normal Bayes (NB) and Neural Network (NN) classifiers	Backhoes, Loaders, Workers	750 images	Real

#	Author/s	Method	Objects of interest	Source of images	Dataset (Synthetic/Real)	
6	Han and Golparvar-Fard (2015)	Support Vector Machine (SVM)	Twenty types of construction materials	3740 image patches of various types of material from construction material library (publicly available) containing	Real	
<b>Deep Learning Algorithms</b>						
#	Author/s	Method	Objects of interest	Source of images	Training dataset	Test dataset
1	Ying and Lee (2019)	Mask R-CNN	Walls, Doors, Lifts	430 images from interiors of four multifunctional buildings in the University of Hong Kong	Real	Real
2	Nath and Behzadan (2019)	You-Only-Look-Once (YOLO) and Mask R- CNN	Buildings, Equipment, Workers	1000 images from the internet via web mining and 1000 images from crowdsourcing (construction projects in China)	Real	Real
3	Hou et al. (2020)	Deeply Supervised Object Detector (DSOD)	Structural components (columns and beams)	4,378 images derived from a 1:20 building entity scale model	Synthetic	Synthetic
4	Siddula et al. (2016)	CNN integrated with the Gaussian Mixture Model (GMM)	Roof objects	300 images taken from the cluttered real construction site	Real	Real
5	Ding et al. (2018)	CNN coupled with the Long Short-Term Memory (LSTM)	Unsafe behaviors of construction workers	200 video recordings (each is 8 s in length) of a person climbing and dismounting from a ladder in a laboratory environment	Real	Real



## **CHAPTER 3: RESEARCH METHODOLOGY AND MODEL DEVELOPMENT**

### **3.1 Introduction**

This study contains the development of a framework consisting of three models to address the main objective of the research explained in the first chapter.

Extensive literature review in the previous section has led to the fact that to develop a Construction Materials Management (CMM) Framework being able to address the sub-objectives of the research; the following items are considered and included in the framework:

- Integration of the materials management functions to facilitate intelligent construction materials management procedure;
- Integration CMM with design and project schedule to consider all changes and updates of schedule and design data automatically during the project lifecycle (So by using the last updated project schedule the developed CMM framework can fully consider design changes and change orders);
- Developing a preliminary material delivery schedule which leads to the least total material cost based on the MRP of the project through obtaining a trade-off and optimized balance among elements of material cost including purchase cost, storage cost, opportunity cost, ordering cost and unavailability cost. This schedule helps materials management professionals through defining the optimized dates and amounts of materials which have to be bought for the construction phase. The material delivery schedule is developed based on the initial estimation of materials consumption and planned project progress in the preconstruction phase. After construction initiation and occurrence of changes, this schedule and consequently purchase orders have to be updated and optimized frequently according to the actual progress;
- Application of a proper and efficient ADC technology for near real-time site data acquisition on a daily/weekly basis by site personnel during the construction phase;
- Analysis of the acquired near real-time data in the construction site and reporting them to monitor project progress and update the estimation of materials consumption/installation and materials demand dates.

Without taking into account the above-mentioned items, developing a CMM framework that can prevent low labor productivity, reduce materials surplus, optimize cash flow, reduce inventory and finally decrease project delays and cost overruns would not be possible. It is worth mentioning that even by developing CMM framework, the human expertise should not be ignored or underestimated. In other words the developed CMM framework is a complementary to project managers working alongside one another to perform a successful material management and optimize delivered materials at the job site on specific dates.

To consider and cover the mentioned items, the developed CMM framework consists of three main models entitled “Preconstruction Model, Construction Model, and Data Analysis and Reporting Model” and four databases, including Materials Database, Vendors Database, Inventory Database, and Tablet Database as shown in Figure 3-1. It is assumed that the developed system uses required data stored in all mentioned databases, and these data are always updated in case of any changes

in schedule, design, or any change orders. Figures 3-2 and 3-3 indicate more details related to the elements of each model and their application steps, respectively. The preconstruction model is executed in the planning phase for the first time, and two other models are implemented in the construction phase.

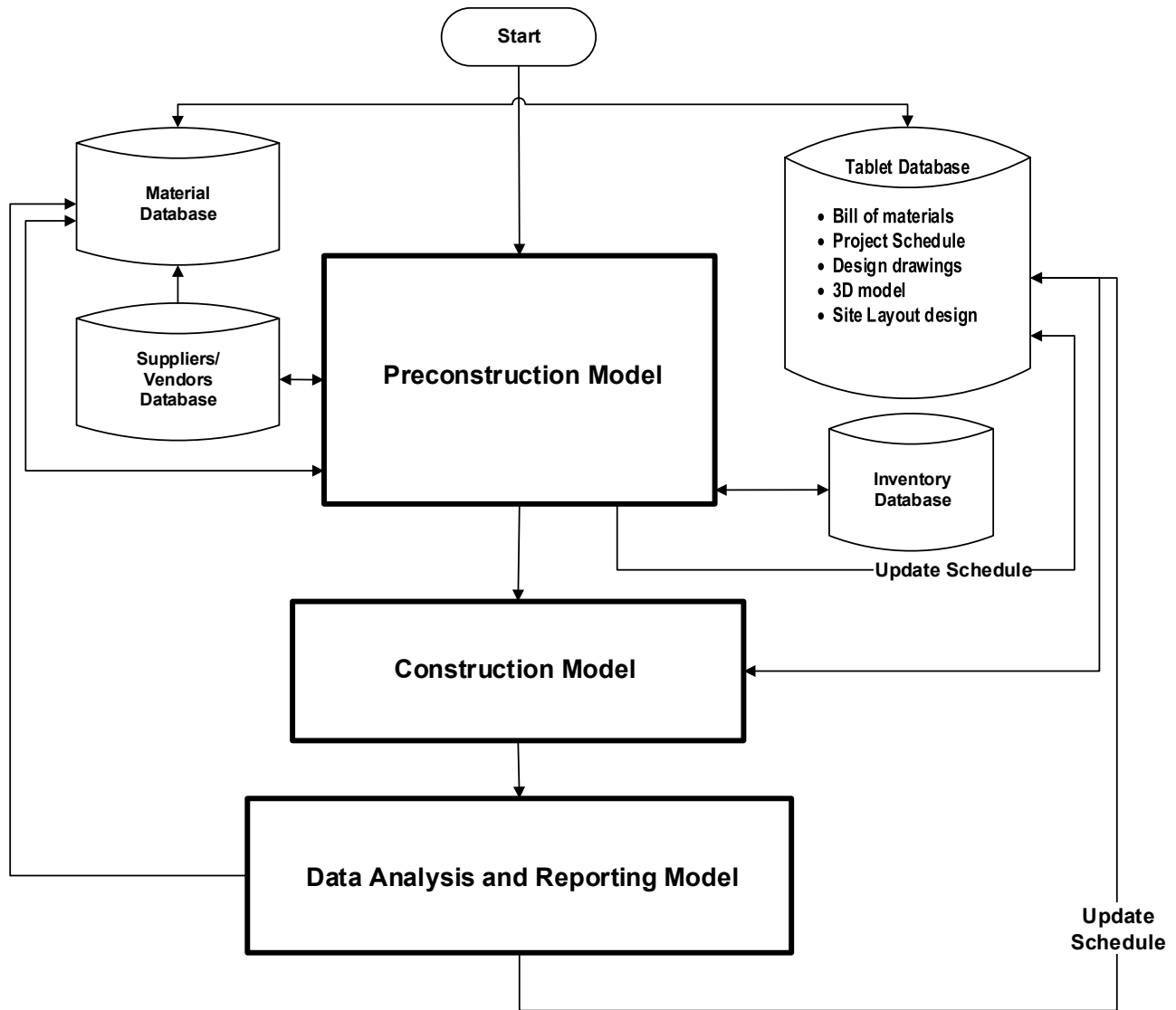


**Figure 3-1: Developed CMM Framework**

The objective of the preconstruction model is to obtain a preliminary optimized material delivery schedule based on MRP and consequently generate an optimized purchase schedule and purchase orders. Furthermore, training, validating, and testing the deep CAE algorithm proposed for monitoring project progress is another objective of this model in the planning phase. Thus, before construction initiation, on the one hand, the first model defines which material, how much of that material must be ordered and bought on which day considering the planned schedule and MRP. It assures that material procurement is done with the least cost, without any material shortcomings or surplus.

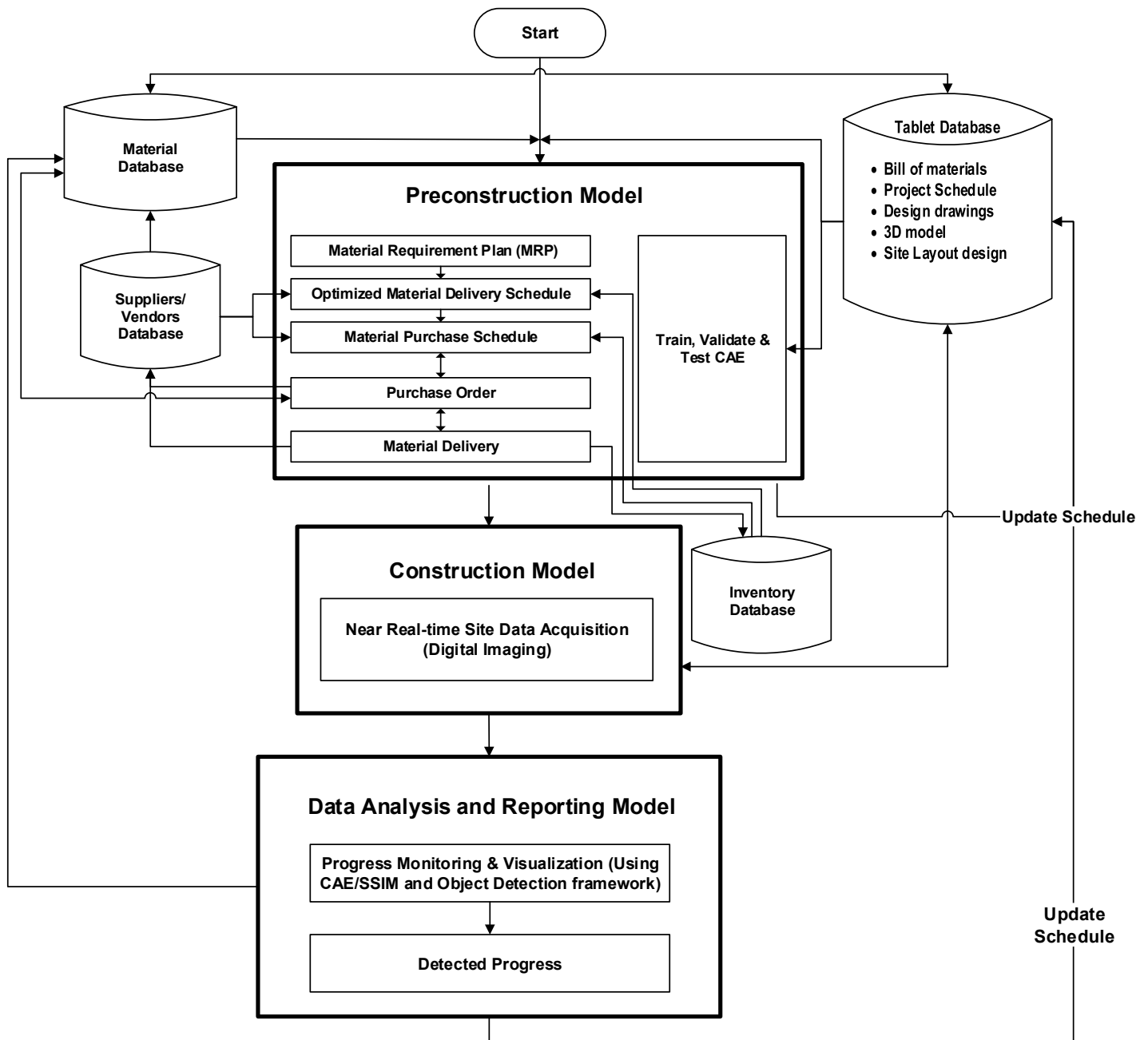


**Figure 3-2: Main Components of the Developed CMM Framework**

On the other hand, proposed CAE is trained, validated, and tested using 2D synthetic images (extracted from the as-planned 4D model) in the first model to be applied in the construction phase for visualizing actual progress using real 2D images from the actual job site. As soon as construction begins, changes might take place. To have efficient materials management, it is required to consider, measure, and exert the occurred changes in the previous plans and update them.

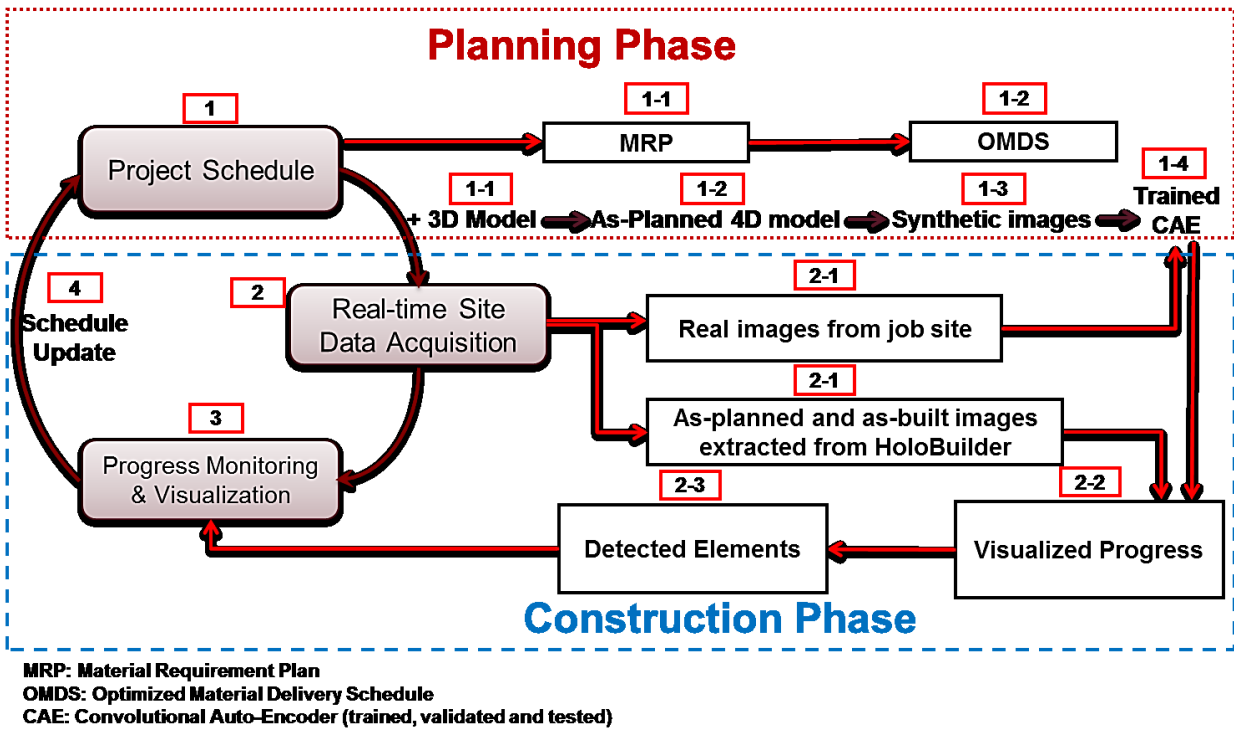


**Figure 3-3: Application Steps of CMM**

Therefore, the construction model focuses on the collection of near real-time project data through ADC technologies. In this research digital imaging, (RGB images and 360-degree images using RGB cameras as passive sensors and Ricoh Theta V respectively) is proposed for monitoring the progress due to its benefits mentioned in Chapter 2. In the third and last model, the collected data (real 2D images, as-planned and as-built images) has to be analyzed using the proposed algorithms (CAE, SSIM, and object detection framework) to visualize and detect progress for updating the schedule and estimating actual materials consumption. So the project schedule and MRP would be updated based on the actual project progress, and all the previous steps would be repeated automatically to achieve optimized material delivery and purchase schedule on a regular basis. So the steps of the preconstruction model will not be just implemented before the construction, but after starting the construction, they will be frequently implemented using the updated schedule and MRP to update optimized material delivery and purchase schedule. Each model, their steps, and proposed algorithms are explained in detail in the following subsections.

It is worth noting that the current developed materials management framework can be used and customized by materials management professionals in the corporate home office organization who are responsible for materials management systems of construction projects. Groups of materials management personnel in the home office and the field project organization are the next groups who are responsible for implementing the processes, and day-to-day functions of the developed and customized materials management framework as CII has recommended.

### 3.2 Preconstruction Model

During design development, a preliminary design is developed with more detail, and key design decisions, and all details of major design components of the project are defined and agreed upon.

Thus in the preconstruction phase of a project, all the construction elements (columns, curtain panels, doors, walls, etc.) are designed and have their properties, size, materials, and definite ID in the design drawings and 3D model. In this phase, the Bill of Material (BoM) resulted from materials takeoff function defines the amount and specifications of materials that are required for each construction element and also in total. Then, the project schedule defines all the activities which have to be performed in the construction phase. Each activity in the project schedule has a specific ID and illustrates the construction of a set of particular elements. It includes start date, duration, finish date, required materials and resources, and prerequisite activities. In this stage, there is a need to have a plan for efficient materials management. As shown in Figure 3-2, preliminary MRP, Optimized Material Delivery Schedule, Optimized Purchase Schedule, and Purchase Orders are generated in the preconstruction model based on the input data (from databases). Finally, in the last step of this model, materials would be delivered to the site according to the issued purchase orders. It should be mentioned that all the processes included in this model would be repeated during the project construction considering all the occurred changes and therefore mentioned documents can be generated on a regular basis. As illustrated in Figure 3-4, the first step is developing the MRP. Project schedule and materials information stored in databases are used as inputs to automatically calculate daily required quantities of each material throughout the construction phase following some steps. The output of each process is utilized as an input for the following process automatically. So by knowing the amount of each material required on each day, an optimized delivery schedule for each material can be generated using a novel developed optimization engine (GA-MLP) in the second step. Then, the purchase schedule is generated based on the optimized material delivery schedule obtained from the previous step, and the materials information such as materials lead-time, required pre-processed time and administrative time from the material database. Lead time for each material is the time between the placement of an order and the delivery of that material, which can be calculated by a probabilistic approach. Pre-processed time is the amount of time required in the shop to make fabricated materials ready for transportation, and administrative time demonstrates the time needed to issue a purchase order to a vendor. The purchase schedule defines the exact dates for issuing purchase orders for all the materials, and finally, purchase orders are issued on the dates predefined in the purchase schedule. In the last step, required materials have to be delivered, received, and checked at the job site on the specific date.

All the differences between planned and actual material delivery and all other changes during the construction phase are reflected in the project schedule. They are used afterward as an input to generate “MRP” and “Optimized Material Delivery Schedule.” Moreover, in the preconstruction model, the proposed deep CAE is trained, validated, and tested using synthetic images. As-planned 4D simulation is generated by integrating project schedule, and 3D model in the first step, and then 2D synthetic images are extracted from 4D simulation illustrating the project progress to train deep CAE. Detail descriptions of each step are demonstrated in the subsequent sections. Section 3.2.1 and Section 3.2.2 are marginally modified versions of “Optimized material management in construction using multi-layer perceptron” published in Canadian Journal of Civil Engineering (Golkhoo and Moselhi, 2019) and has been reproduced in these sections.

In a nutshell, all the steps of this model in the developed CMM framework help materials professionals to prevent early, excess, or late purchasing of materials. This model also guides material professionals on how to procure materials with the least cost and on time.

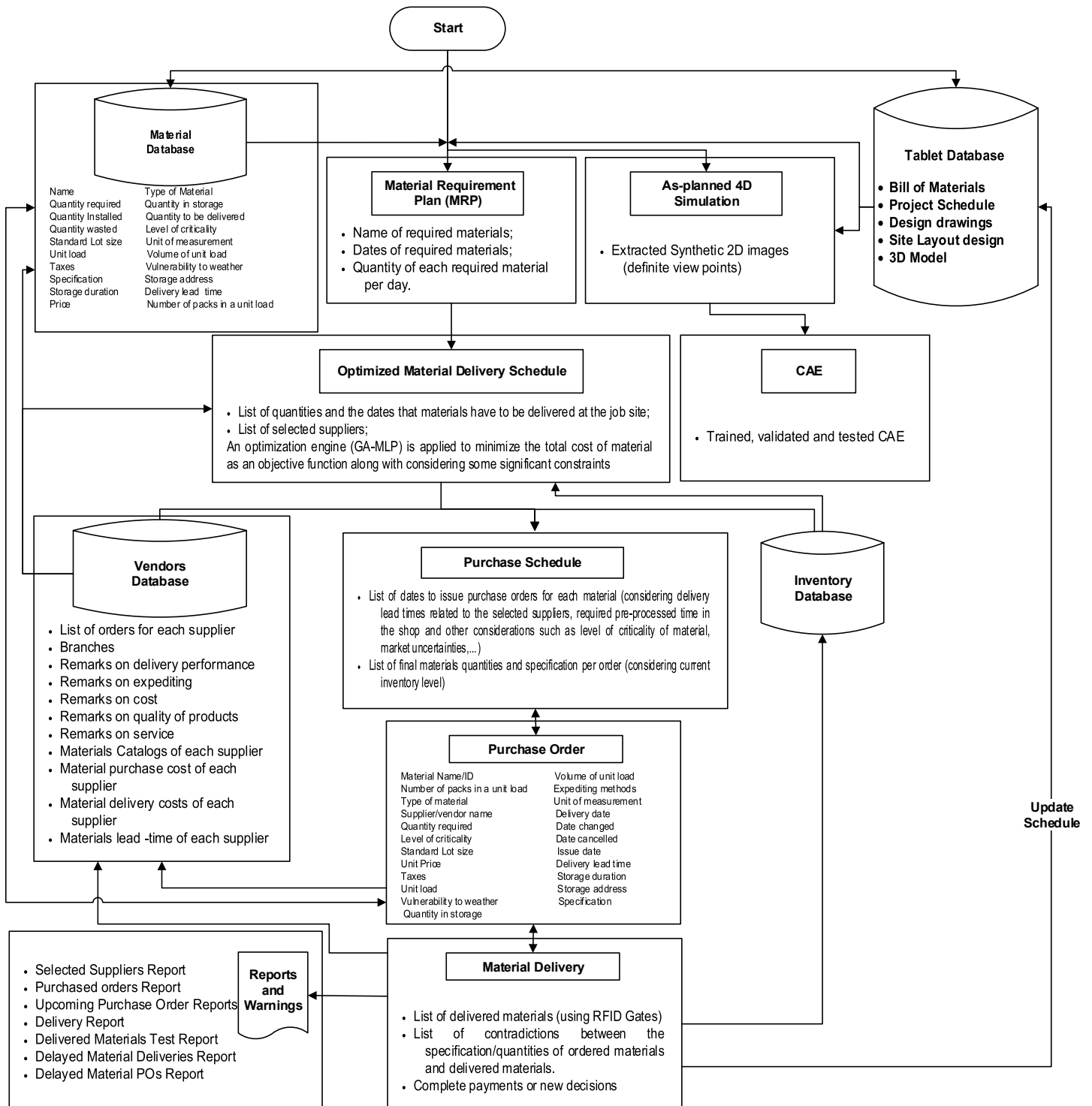


**Figure 3-4: Preconstruction Model**

### 3.2.1 Material Requirement Plan (MRP)

The required steps of the MRP development process are demonstrated in Figure 3-5. Following information are used as inputs to this process:

- The project schedule, which is integrated with construction elements, and all the required materials are assigned to the activities on a daily basis.
- Construction materials data and their specifications. For instance, job site pre-processed time for materials requiring assembly before installation at the construction job site.

In this developed model, there are various variables as follows:

- Project duration is shown by  $D$  (time unit is day).
- Materials have been shown by  $j$ , and it is assumed that there are  $k$  materials in a project, so  $j = 1, 2, \dots, k$ .
- Activities have been shown by  $i$ , and it is assumed that there are  $n$  activities in a project, so  $i = 1, 2, \dots, n$ .
- Since the developed algorithm has to consider each day of the project, so it needs to know the current date, which shows that the project is on which day of its duration. The current date in the system is demonstrated by  $T_C$ . It is evident that the first day of the project schedule has a particular date, but it can be shown by  $T_C = 1$ . So  $T_C = 1, 2, \dots, D$ .
- Early Start and Early Finish dates of all the activities are used in this system to avoid uncertainties, and they are shown by  $ES_i$  and  $EF_i$  for activity  $i$ , respectively.
- The pre-processed time for the materials requiring assembly before installation at the construction site is shown by  $T_{sp}$ . It can be obtained from the construction materials specifications input data.
- The required amount of material  $j$  assigned to each activity  $i$  on specific days is shown by  $q_{ij}$ .

The output of this step is MRP. As Caldas stated, MRP consists of identifying, quantifying, and scheduling the acquisition of project materials and equipment (Caldas et al., 2015). As shown in Figure 3-5, having input data, the algorithm selects a specific material and considers it as  $j = 1$ , and then it starts to calculate the total required amount of material  $j = 1$  on each day of the project. So the first day of the project is selected ( $T_C = 1$ ), and the algorithm compares the Early Start and Early Finish dates of all the activities (from  $i = 1$  to  $i = n$ ) with  $T_C = 1$  ( $ES_i \leq T_C$  &  $EF_i \geq T_C$ ), to identify the ongoing activities which use material  $j = 1$  on the first day.

Afterward the required amount of material  $j = 1$  relevant to the identified activities ( $q_{ij}$ ) are found and summed up ( $\sum_{i=1}^n q_{ij}$ ). The calculated value  $\sum_{i=1}^n q_{ij}$  must be assigned to  $T_C = 1$ , but if material  $j = 1$  needs pre-processed ( $T_{sp}$ ) time at the job site, the calculated value  $\sum_{i=1}^n q_{ij}$  has to be assigned to  $T_C - T_{sp}$ . It indicates that the material  $j = 1$  is required on the day  $T_C - T_{sp}$  with the amount of  $\sum_{i=1}^n q_{ij}$ .

All these steps are repeated for material  $j = 1$  from the first day of the project ( $T_C = 1$ ) to the last day ( $T_C = D$ ). The output of this process can be represented in the form of a vector with  $D$  columns for material  $j = 1$ , as shown in Figure 3-6. The columns demonstrate the days of the project duration, and the non-zero elements of this vector indicate the required amount of material  $j = 1$  on those special days. All the mentioned processes would be implemented for all the materials from  $j = 1$  to  $j = k$ . Finally, there would be  $k$  vectors for  $k$  materials.

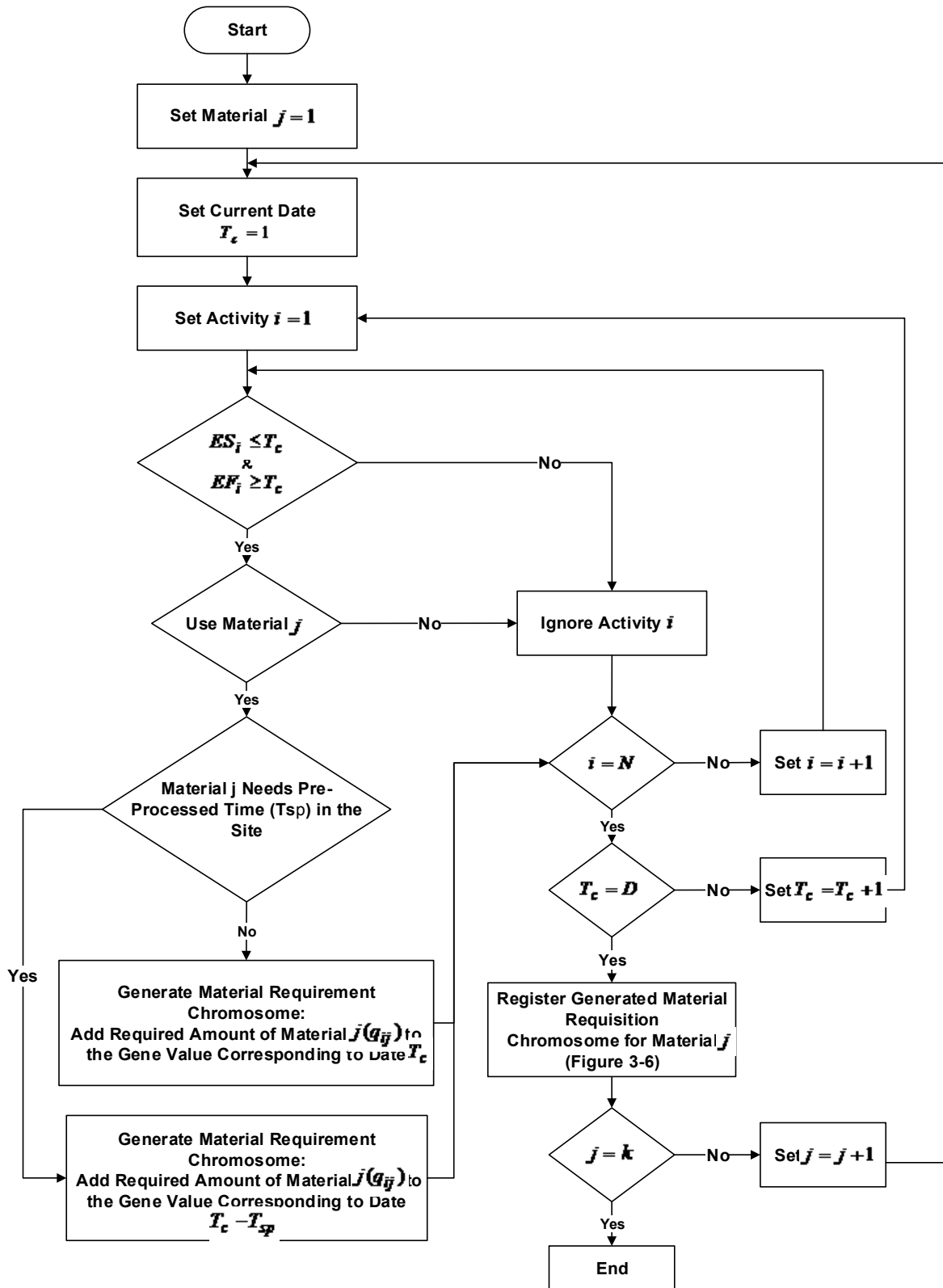


Figure 3-5: MRP Development Algorithm (Golkhoo and Moselhi, 2019)



$T_c = 1$	$T_c = 2$	$T_c = 3$	...	$T_c = D - 2$	$T_c = D - 1$	$T_c = D$
$q_{T_c} = \sum_{i=1}^n q_{ij}$	$q_{T_c} = \sum_{i=1}^n q_{ij}$	$q_{T_c} = \sum_{i=1}^n q_{ij}$	...	$q_{T_c} = \sum_{i=1}^n q_{ij}$	$q_{T_c} = \sum_{i=1}^n q_{ij}$	$q_{T_c} = \sum_{i=1}^n q_{ij}$

**Figure 3-6: Material Requirement Vector for Material  $j$  (Golkhoo and Moselhi, 2019)**

### 3.2.2 Optimized Material Delivery Schedule

Efficient materials management requires trade-offs and optimized balance among elements of material cost, including purchase cost, storage cost, opportunity cost, ordering cost, and unavailability cost. Thus, there is a need to develop an automated method for optimizing the delivery and inventory of construction materials not only in the planning phase but also in the construction phase to account for introduced changes. As explained in the section “shortcomings and limitations,” pure GA is used in the existing researches to solve the problem without obtaining enough diversification in the generated populations to escape from getting stuck to local minima. Moreover, materials unavailability cost is not considered in the GA objective function to enable the proposed method to consider various scenarios. In this step, a novel GA-MLP method is developed to generate an optimized material delivery schedule to answer this question: “how construction materials can be bought, delivered and stored (considering minimum order quantity (minimum shipping), and storage space) in such a way that it leads to the least cost?” This newly automated method optimizes the material delivery schedule based on MRP and the least total material cost. The developed method utilized GA and MLP. It follows up the progress as reflected in the last up-to-date schedule to update MRP and delivery schedules repetitively throughout the construction phase, as shown in Figure 3-2 and 3-3. MLP is utilized to improve GA by generating memory to overcome local minima encountered in applying GA for optimization. This automated method supports contractors to buy construction materials with the least cost and without leading to material shortage or surplus.

To perform encoding of each candidate solution of purchasing a specific construction material during the construction phase into chromosomes, chromosomes are employed to indicate the various possible amount of material  $j = 1$  which can be bought on different days of project duration from  $T_c = 1$  to  $T_c = D$ , as shown in Figure 3-7. The number of genes represents the total number of time units of project duration, and gene values indicate the amount of material that has to be ordered and bought at that particular time. Gene values can be zero, which means that there is no order or material delivery on that special day of the project.

$T_c = 1$	$T_c = 2$	$T_c = 3$	...	$T_c = D - 2$	$T_c = D - 1$	$T_c = D$	
$Q_1$	...	$Q_3$	...	...	$Q_{D-2}$	$Q_{D-1}$	$Q_D$

**Figure 3-7: Material Delivery Chromosome for Material  $j$  (Golkhoo and Moselhi, 2019)**

The objective function of the GA algorithm is minimizing the total material cost. So it is required to calculate the total cost of material  $j$  which would be delivered based on each material delivery chromosome. Each chromosome that leads to the lower cost can be selected as a better solution. If

terminating condition is not met, obtained better solutions will be recombined using genetic operators to breed new, better solutions among generations. To calculate the total material cost using the objective function, two scenarios have been taken into consideration: (1) the shortage of material is prohibited and (2) the shortage of material is not forbidden in the second scenario:

In the first scenario, the encounter with the material shortage is not acceptable even if the cost of buying and storing materials in advance results in a higher total material cost comparing the total material cost, including material unavailability cost. So in this scenario, the objective function is considered as Equation 3-1. According to the study done by Georgy and Basily (2008), total material cost includes four major cost categories including purchase cost of material (unit purchase price from a vendor including transportation and freight expenses), order cost (the administrative expense related to issuing a PO to a vendor), opportunity costs (the losses resulted from tied-up funds in the inventory and cannot be invested for other beneficial purposes) and finally storage cost (the cost related to the warehousing, handling, store workers, and equipment inside the warehouse). So through the following Equations, the total material cost can be calculated by considering the time value of money (escalation rate can take zero value for materials with short delivery period):

Minimize Total Material Cost = Minimize (Purchasing Cost + Ordering Cost + Opportunity Cost + Storage Cost) Equation 3-1

$$\text{Purchasing Cost} = \sum_{N=1}^{N_p} \sum_{d=1}^{L_N} (Q_d \times P_d)(1 + i)^{N-1} \quad \text{Equation 3-2}$$

$$\text{Ordering Cost} = \sum_{N=1}^{N_p} (L_N \times C_o)(1 + i)^{N-1} \quad \text{Equation 3-3}$$

$$\text{Opportunity Cost} = \sum_{N=1}^{N_p} \sum_{T_C=365(N-1)+1}^{365N} (SQ_{T_C} \times I \times P_{average})(1 + i)^{N-1} \quad \text{Equation 3-4}$$

$$P_{average} = \text{Purchasing Cost} / \sum_{N=1}^{N_p} \sum_{d=1}^{L_N} Q_d \quad \text{Equation 3-5}$$

$$\text{Storage Cost} = \sum_{N=1}^{N_p} \sum_{T_C=365(N-1)+1}^{365N} (SQ_{T_C} \times C_s)(1 + i)^{N-1} \quad \text{Equation 3-6}$$

Where,

$N_p$  is the total project duration in terms of the year;

$L_N$  is the number of material orders/deliveries made in year  $N$ ;

$Q_d$  is the quantity of material for order  $d$ ;

$P_d$  is the unit price of material for order  $d$ ;

$P_{average}$  is the average unit price of material;

$C_o$  is the average administrative cost for making a single order;

$SQ_{T_C}$  is the stock quantity at time  $T_C$  ;

$C_s$  is the storage cost for an individual unit quantity per unit time;

$I$  is the interest rate per unit time;

$i$  is the annual escalation rate;

Some input data, such as purchase cost and delivery cost of materials related to various vendors, are available in databases of the whole developed framework. Since each vendor has its own price and discounts for bulk purchases, so there is a need to select proper potential vendors to be able to calculate the total material cost for each generated chromosome in the objective function. The

associated process of the potential vendors' selection for the materials is shown in Figure 3-8. First, the algorithm selects a particular material and consider it as  $j = 1$ . By considering vendors selection criteria (such as the level of criticality of material, required quality and specification, various uncertainties, required delivery date, and the abilities and disabilities of vendors based on their background information), vendors would be evaluated, and some of them are selected and asked for quotations. After evaluation and comparison of received quotes, final potential vendors for material  $j$  would be chosen. Thus, at the end of this process, material purchase cost, material delivery cost, and material delivery lead time of each final selected potential vendor for Material  $j$  can be obtained using databases. All these steps must be repeated for all the materials from  $j = 1$  to  $j = k$ . There might be a yearly contract for some types of material with a particular supplier, so in this case, the supplier, the price, and other required data are clear for the algorithm from the beginning. The main user of this developed construction materials management framework is contractor, so a contractor or the employed materials professionals after successfully winning the job can use it to perform the materials management processes. This developed framework does not include the bidding process in which the contractor selects a vendor or supplier of a specific material through bidding processes.

Computing the stock quantity at time  $T_C$  ( $SQ_{T_C}$ ) is a prerequisite of storage cost and capital cost calculation for each generated material delivery chromosome at time  $T_C$ . Therefore Equation 3-7 is used to calculate  $SQ_{T_C}$ :

$$\text{Stock quantity at time } T_C (SQ_{T_C}) = SQ_{T_C-1} + Q_{T_C} - q_{T_C} \quad \text{Equation 3-7}$$

Where,

$SQ_{T_C-1}$  is the stock quantity at time  $T_C - 1$ ,

$Q_{T_C}$  is the material quantities which have to be ordered at time  $T_C$  which equals to  $Q_d$  when order  $d$  is taken place at time  $T_C$ ,

$q_{T_C}$  is the required material quantities at time  $T_C$  (These values can be obtained from the Material Requirement Vector for each material (Figure 3-6)).

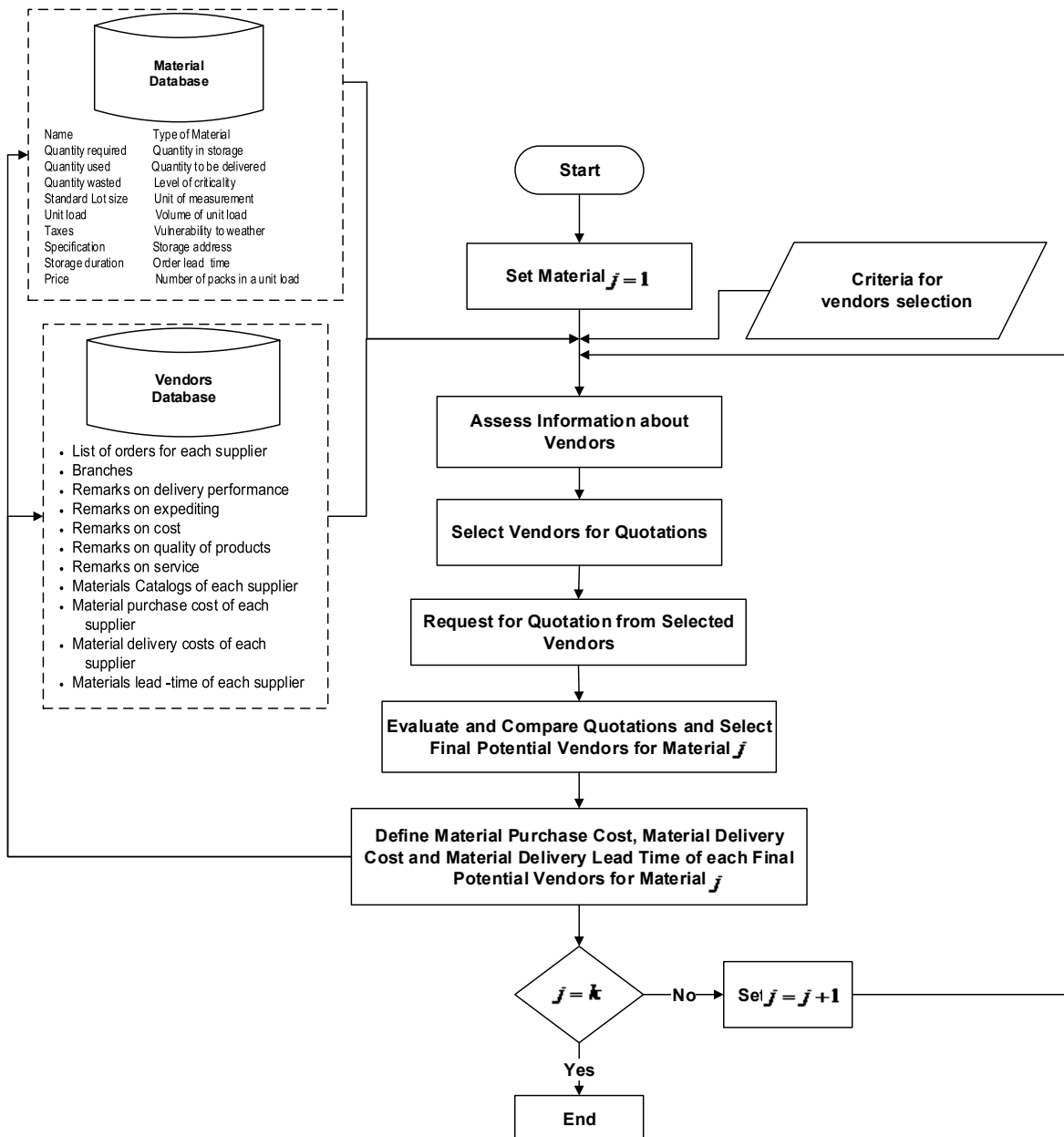


**Figure 3-8: Vendors Selection and Material Costs (Golkhoo and Moselhi, 2019)**

Contrary to the first scenario, in the second scenario, the material shortage can be acceptable at different time points of construction phase if the total material cost, including the cost of material unavailability, is less than the total material cost without material shortage. So in this scenario, the objective function is considered as Equation 3-8.

$$\text{Minimize Total Material Cost} = \text{Minimize (Purchasing Cost} + \text{Ordering Cost} + \text{Opportunity Cost} + \text{Storage Cost} + \text{Unavailability Cost)} \quad \text{Equation 3-8}$$

As Said and El-Rayes (2011) have stated, to calculate material unavailability cost, the first step is to estimate materials-related project delay. The algorithm to calculate project delay due to material

shortage is presented in Figure 3-9. When there is delayed delivery of a particular material at a specific time point of the construction phase, two factors have to be defined to calculate the project delay. The first factor is identifying the ongoing activities at that specific time point, consuming that particular material with their total floats. The second factor is defining the activities which cannot be completed due to material shortage after assigning the ordered quantity of that specific material to the activities with the minimum total float. Since the delay of each activity and consequently the project delay is calculated based on the material consumption rate, so after identifying and updating the affected ongoing activities by material shortage at different time points (from  $T_c = 1$  to  $T_c = D$  of each chromosome as a candidate solution), the project schedule can be updated and the amount of project schedule delay ( $D_p$  in Figure 3-9) can be calculated by subtracting the planned project duration from the last updated project duration.

As illustrated in Figure 3-9, since there are  $k$  materials in a project, so the mentioned process is performed for each material from  $j = 1$  to  $j = k$  to calculate the total material cost for chromosomes as candidate solutions of buying construction materials during the construction phase while the material shortage is allowed.

So, according to the study done by Said and El-Rayes (2011), unavailability cost is calculated according to Equation 3-9 considering the time value of money:

$$\text{Unavailability Cost} = (D_p \times C_d)(1 + i)^{N_p} \quad \text{Equation 3-9}$$

Where,

$C_d$  is the cost resulted from project schedule delay due to material shortage. It includes project liquidated damage per day and time-dependent indirect cost per day;

$D_p$  is the project schedule overrun in terms of the number of days.

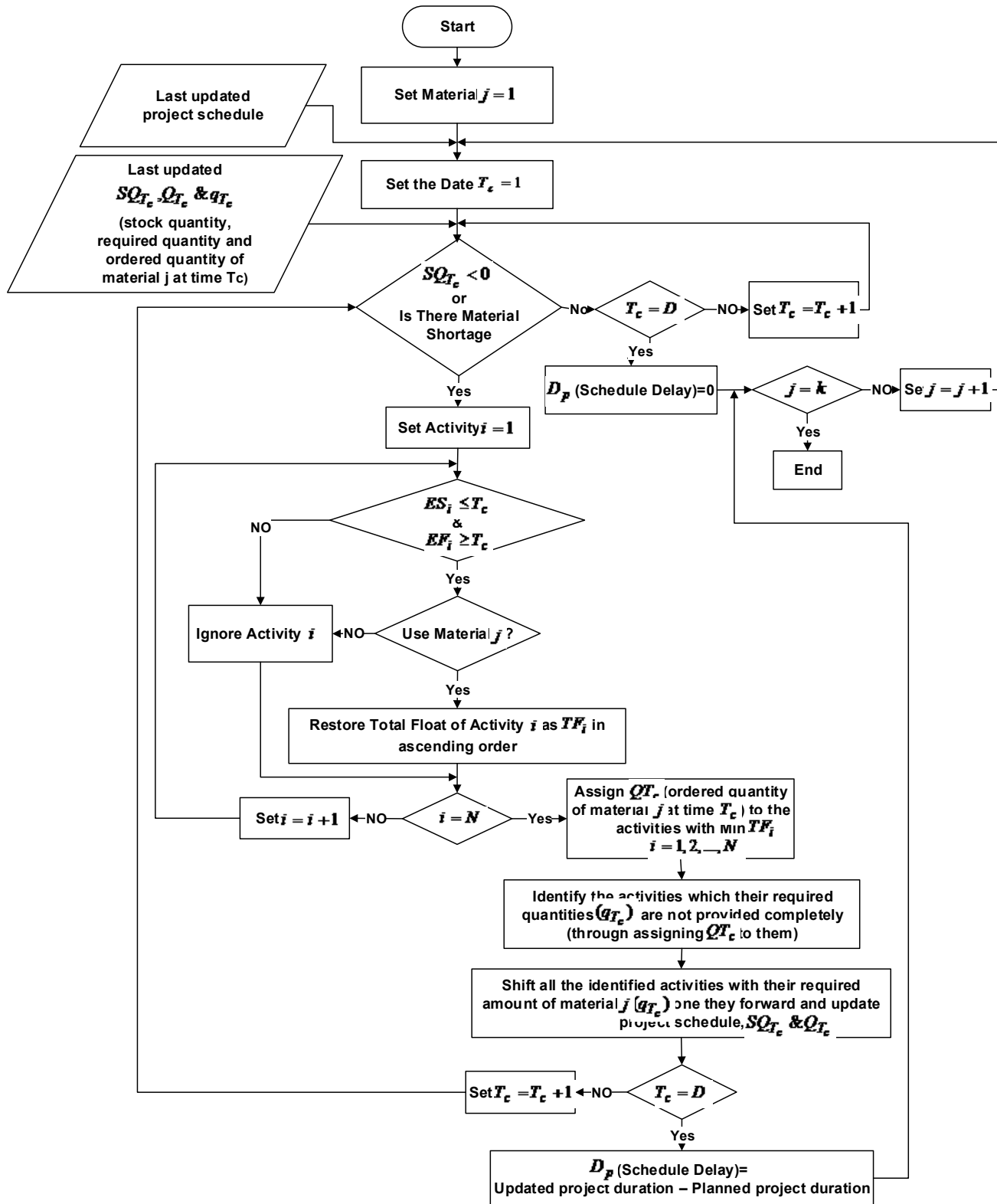


Figure 3-9: Calculated project Delay Algorithm (Golkhoo and Moselhi, 2019)

It should be noted that some constraints satisfaction has to be performed during the GA optimization to check the feasibility of each generated chromosome. The following constraints are considered:

- $0 \leq SQ_{T_C}$  (Stock Quantity at time  $T_C$ )  $\leq Q_{S_j}$  (Max Storage Capacity for Material  $j$ ). This means there should not be any shortage of material during the construction phase, and the storage space has to be considered as a limitation while ordering materials. This constraint is applied in the first scenario.
- $SQ_{T_C}$  (Stock Quantity at time  $T_C$ )  $\leq Q_{S_j}$  (Max Storage Capacity for Material  $j$ ). This constraint is applied to the second scenario because the material shortage is not prohibited in the second scenario, but the storage space should be considered as a limitation.
- $Q_{T_C}$  (Material Quantities Ordered at  $T_C$ )  $\geq Q_{MS_j}$  (Minimum Shipping Quantity for Material  $j$ ) in which  $Q_{MS_j}$  is an integer number showing the minimum quantity of material  $j$  which can be shipped to the construction site. This constraint is applied in both scenarios.
- The last constraint shows that at the end of the project, the total quantity of purchased materials must be equal to the total amount of required materials. There should not be a surplus quantity of material at the end of the project. So this constraint is applied for both scenarios and is shown by  $\sum_{T_C=1}^D Q_{T_C} - \sum_{T_C=1}^D q_{T_C} = 0$ .

As Golkhoo and Moselhi (2019) have stated, similar to a greedy optimization algorithm, GA selects the fittest chromosomes in each iteration. In other words, without any memory, GA makes a locally-optimal choice in each generation with the hope that these choices could lead to a global optimal solution using various operators. So, to avoid the major limitation of GA, which is getting stuck at local optimal values, MLP is combined with GA to create a memory of the fittest solutions previously found and improve the probability of identifying global optimal solutions. MLP, as a feed-forward neural network, has not been used in terms of a classifier, but it is integrated with GA only to generate memory for GA to follow the trend of data. Creating memory means that GA can memorize the properties of its previous generations. Since in pure GA, after applying crossover and mutation in the current population, everything else will be removed, MLP is integrated to retain the trend of data associated with the previous generation.

The architecture of the proposed MLP includes four hidden layers, followed by the Sigmoid activation function. Hidden layers are not subjected to any up or down-sampling. Based on several experiments, densifying this simple architecture not only does not improve the performance of the final model but also is costly in runtime and may lead to delay in the training process. Moreover, very simple architecture (i.e., with 1, 2, or three hidden layers) will not result in reliable weight vectors. As mentioned earlier, MLP has not been applied as a classifier; it is integrated with GA only to generate memory for GA to follow the trend of data. MLP is integrated with GA in a novel algorithm to prevent the shortcoming (local minima and the lack of memory) of GA while generating the optimized material delivery schedule. Each material should be considered separately from the beginning, so after selecting a particular material as material  $j$ , the developed GA-MLP algorithm illustrated in Figure 3-10 is performed.

In the first iteration ( $i = 1$ ), an initial population presenting different possible solutions of buying a specific construction material during the construction phase is generated randomly. There is no official reasoning around initializing the proper values in GA. But based on our experiment, using

material requirement vector can help the performance of the developed algorithm in terms of convergence, then the MLP network is initialized with random weights ( $W_i$ ), and it is fed with the initial population from GA to generate a modified population (Multiplying the initial population with the weight vector). In fact the value of each gene of a chromosome is multiplied by the corresponding element of generated weight vector and this is applied for all chromosomes in the GA population. In other words, MLP functionality is finding a regression between the current population and the previous generation. The reason for multiplying MLP weight vector to the GA population is biasing the current chromosomes to the proper direction. Since MLP weight vectors are being updated by Gradient Descent Scheme and the better MLP training procedure is done, the better generation is expected to be produced. The sigmoid function is selected as the activation function in MLP to generate the output.



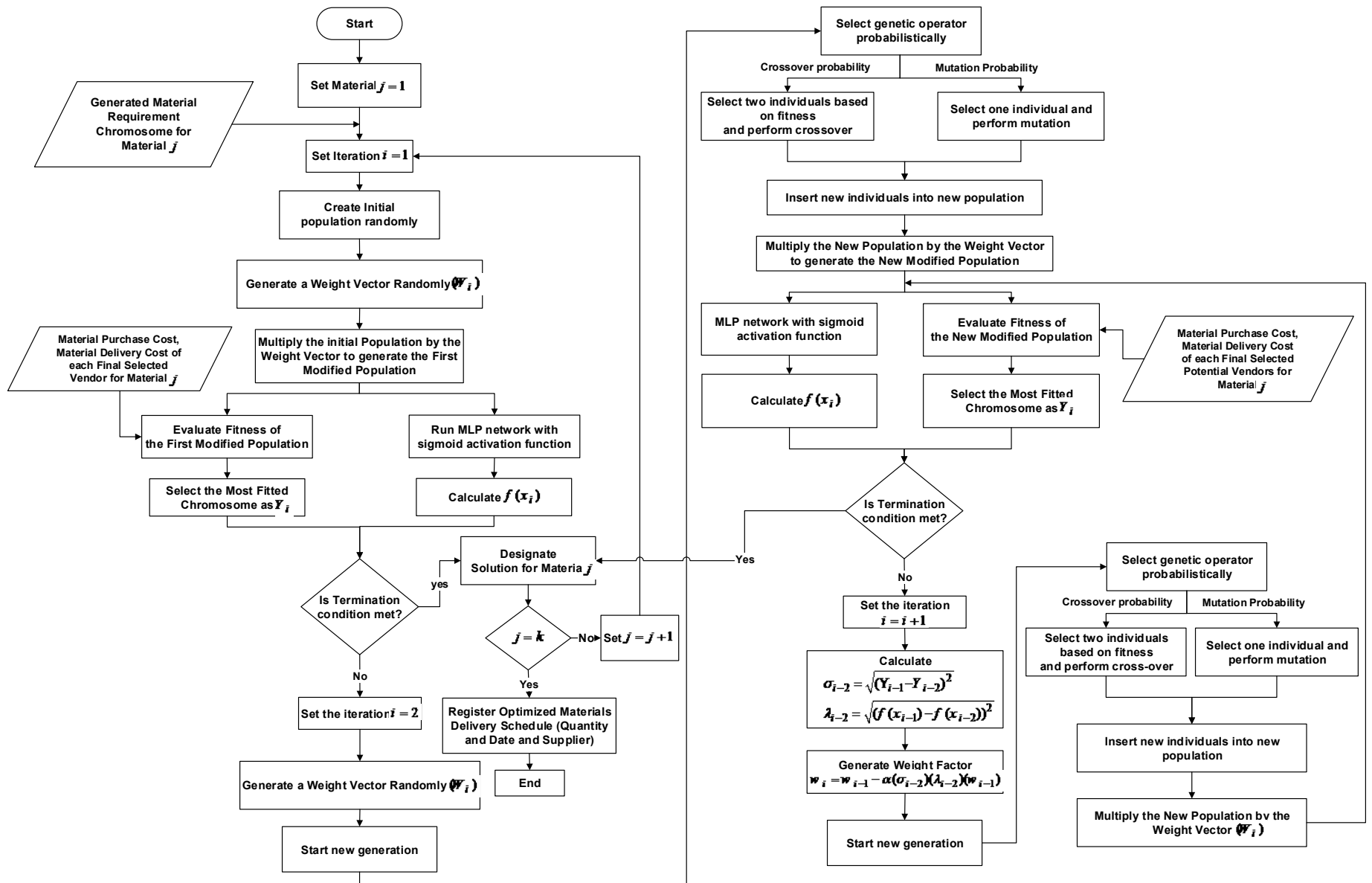


Figure 3-10: GA-MLP Algorithm to Generate Optimized Material Delivery Schedule (Golkhoo and Moselhi, 2019)

Thus, on the one hand, the modified population (which is the output of the hidden layer) is used as an input for sigmoid activation function to generate  $f(x_i)$  as the output of the MLP network, and on the other hand, the modified population has to be evaluated against the objective function, which is minimizing the total material cost. The most fitted chromosome (which leads to the lower cost) is selected as  $Y_i$  and if stopping criterion is not met, the next iteration is performed. In the next iteration ( $i = 2$ ), the better individuals of the former population are selected and recombined by applying crossover and mutation operators probabilistically to breed better solutions as a new population. Generated offspring's gene values should be checked against the constraints to remove infeasible solutions. As GA passes through the second iteration, MLP will get ready to start its second epoch. Though based on the MLP concepts, epochs should be a static value to control overfitting, in the developed algorithm, the number of epochs is set to be equal to GA's iteration as a dynamic hyper-parameter. The second weight factor is generated by MLP randomly ( $W_i$ ) and MLP is fed with the newly generated population from GA to form the second modified population (multiplying the new population with the second weight vector). Similar to the previous iteration, on the one hand, the second modified population is used as an input for sigmoid activation function to generate  $f(x_i)$  as the output of the MLP network and on the other hand, the modified population is evaluated against GA objective function and the most fitted chromosome is selected again as  $Y_i$ . If the population is not converged towards a single solution (stopping criteria is not met), the next iteration is performed.

According to Golkhoo and Moselhi (2019), after first and second iteration or epoch as illustrated in Figure 3-10, the weights vectors should be updated for the next iteration with respect to a specific policy as the following:

$$W_i = W_{i-1} - (\sigma_i \times \lambda_i \times \alpha \times W_{i-1}) \quad \text{Equation 3-10}$$

$$\sigma_i = \sqrt{(Y_{i-1} - Y_{i-2})^2} \quad \text{Equation 3-11}$$

$$\lambda_i = \sqrt{(f(x_{i-1}) - f(x_{i-2}))^2} \quad \text{Equation 3-12}$$

Where  $W_i$  is the new weight vector,  $W_{i-1}$  is the previously obtained weight vector,  $\sigma_i$  is called error value which is the difference between two previous most fitted chromosomes ( $Y_{i-1}$  &  $Y_{i-2}$ ). The policy for computing the error is calculating the L2-norm between the fitted chromosomes of the current and previous generation in GA.  $\lambda_i$  is the difference between two previous MLP network outputs ( $f(x_{i-1})$  &  $f(x_{i-2})$ ), and  $\alpha$  is the learning rate ( $0.1 < \alpha < 0.3$ ). After calculating the new weight vector for each iteration, all the following steps are performed as a loop in consecutive iterations till an individual chromosome reaches certain fitness which is obtaining a new better solution as a new population using crossover and mutation operators, and removing infeasible solutions from the new population by checking offspring's gene values using constraints. In the next step, MLP is fed with this newly generated population to form a new modified population (multiplying the new population with the new weight vector).  $f(x_i)$  is calculated using sigmoid activation function as the output of the MLP network as well as  $Y_i$  as the most fitted chromosome through evaluating the modified population against GA objective function. If the error value is less than its predefined threshold, then the termination condition is met, and the fitted chromosome is selected as the optimized material delivery schedule. Since there is  $K$  material in a construction project, all the steps of the developed algorithm must be repeated for each material ( $j = 1$  to  $k$ ).

It is worth noting that in this study, the selected and applied methods for the genetic operators of selection, crossover, and mutation are roulette-wheel, stochastic method, and random negate method, respectively. Different stopping criteria could be defined, including a specific number of iterations, a predetermined threshold of error value, and a predetermined threshold for the improvement value in the objective function over many consecutive generations. In this study, the algorithm comes to the point of convergence when the error value is less than a specified threshold. Finally, there would be  $k$  optimized delivery schedule chromosomes for  $k$  materials in which a zero value indicates that no delivery takes place at that particular day, and non-zero values show that there are deliveries at those specific days. If materials are delivered based on these schedules, the total materials procurement cost will stand at the minimum level.

The developed GA-MLP algorithm is coded in a user-friendly computational platform using MATLAB (2017a). It can be used as a stand-alone application or can be integrated with the other algorithms in the CMM framework. The developed software is a tool for generating an optimized material delivery schedule. Graphical User Interfaces (GUI) in MATLAB (Figure 3-11 and 3-12) is also developed to simplify data entry and reporting.

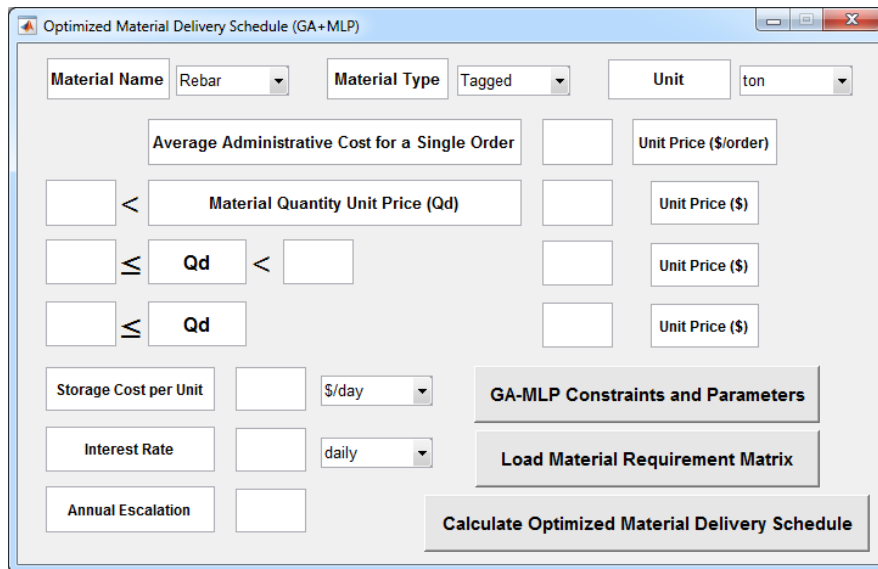


**Figure 3-11: User Interface for Optimized Material Delivery Schedule (GA-MLP) (Golkhoo and Moselhi, 2019)**

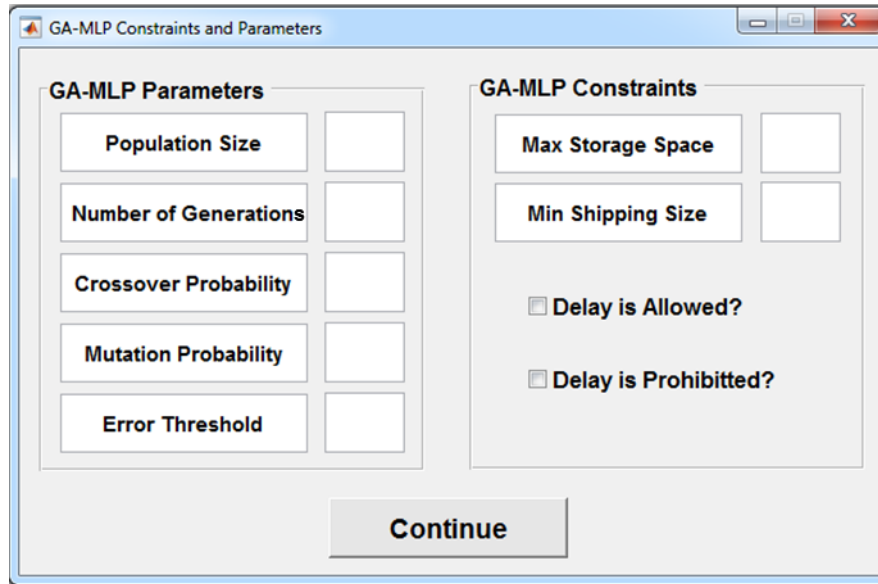


**Figure 3-12: User Interface for GA-MLP Constraints and Parameters (Golkhoo and Moselhi, 2019)**

### 3.2.3 Purchase Schedule

According to Figure 3-13, generating a purchase schedule is the third step of the preconstruction model. Up to this step, MRP and optimized material delivery schedule for each material have been generated. At this stage, there is a need to know on which dates POs must be issued based on the optimized delivery material schedules. Purchasing function in the materials management span the identification of a requirement and ordering of goods and services (Caldas et al., 2015). In a complex project consisting of hundreds of activities and materials, forgetting to order and start the purchasing process for some materials during the construction is a common issue, so automatic announcement and generation of POs subsequently can help material professionals to manage materials more effectively. The required steps for calculation of issue dates of POs are shown in Figure 3-13. As usual, the algorithm selects a particular material and considers it as  $j = 1$ . The optimized delivery schedule of material  $j = 1$  is available in which non-zero values show that there are deliveries at specific dates. The first delivery is considered  $d_j = 1$  and it would take place on a particular date called  $T_{Q_d}$ . In the next step, it should be checked whether material  $j$  is a fabricated material and needs some Pre-processed Time ( $T_{mp}$ ) in the shop to be ready for transportation or not. If material  $j$  is a fabricated material, the PO issue date of this delivery is calculated through the following equations:

$$\text{Issue date of PO} = \text{Optimized Delivery Date} - \text{Expected Material Delivery Lead Time} - \text{Preprocessed Time} - \text{Administrative Time} \quad \text{Equation 3-13}$$

$$\rightarrow T_{PO_j} = T_{Q_d} - ET_{L_j} - T_{mp} - T_{A_j} \quad \text{Equation 3-14}$$

Where  $ET_{L_j}$  is Expected Material Delivery Lead Time for material  $j$ , and  $T_{A_j}$  is Administrative Time to issue a PO for material  $j$  to a vendor.

If material  $j$  is not a fabricated material, the PO issue date of this delivery is calculated as follows:

Issue date of PO = *Optimized Delivery Date* – *Expected Material Delivery Lead Time* – *Administrative Time* Equation 3-15

$$\rightarrow T_{POj} = T_{Qd} - ET_{Lj} - T_{Aj} \quad \text{Equation 3-16}$$

As before mentioned,  $L_N$  is the number of material orders/deliveries made in year  $N$ , (from  $N = 1$  to  $N = N_p$ ) for each optimized delivery chromosome of each material, therefore all these steps are repeated for each delivery from  $d_j = 1$  to  $d_j = L_{N_p}$ . As usual, by changing materials from  $j = 1$  to  $j = k$ , the process will be run repeatedly and provides a purchase schedule for each material. It should be mentioned that the number of issued POs ( $N_{PO}$ ) for each material is equal to the number of material deliveries in each optimized delivery chromosome.

It is worth noting that the Expected Material Delivery Lead Time for material  $j$  can be calculated as the following:

$$ET_{Lj} = \sum_{t=a}^b t[p(t)] \quad \text{Equation 3-17}$$

$a, b$  are the lower and upper bounds of possible Lead time for material  $j$ ;

$p(t)$  is the probability that material  $j$  will be delivered after  $t$  days; and

$t$  is the various number of days for material  $j$  Lead time.

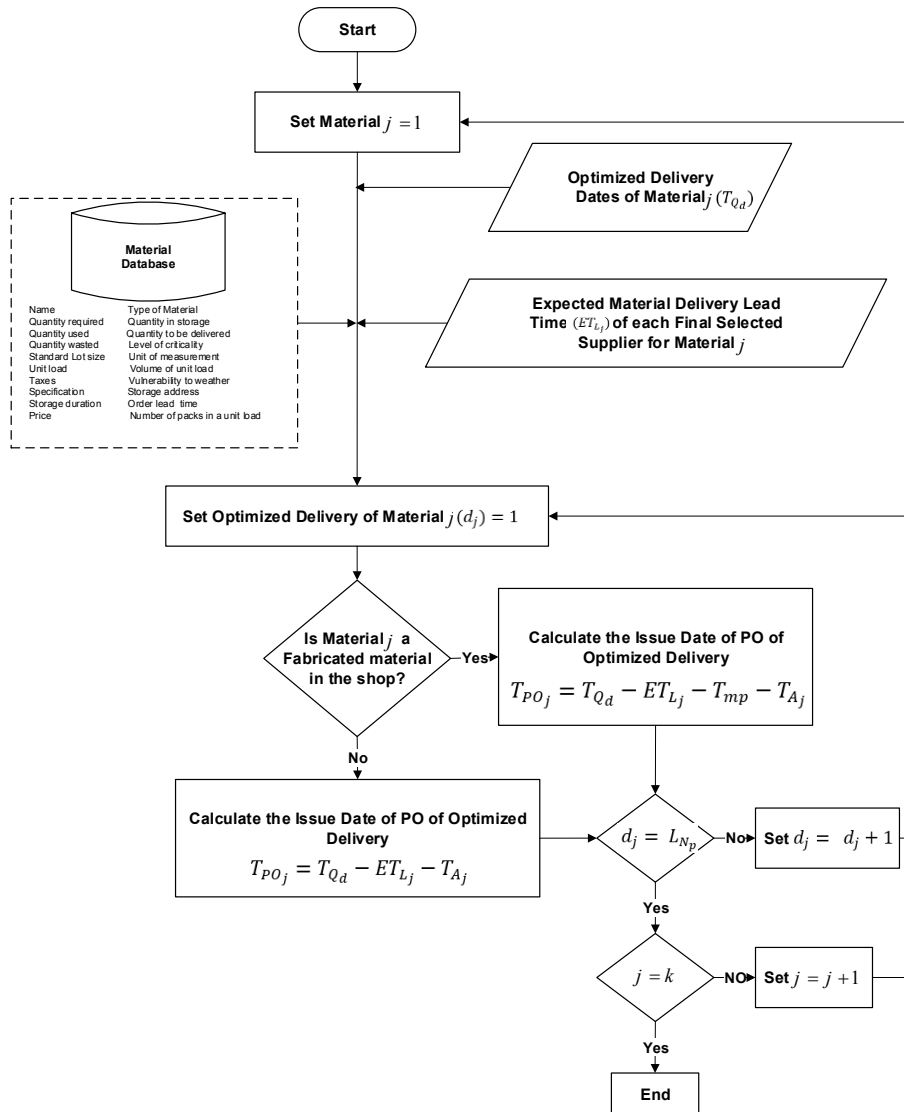


**Figure 3-13: Calculated Issue Date of PO Algorithm**

### 3.2.4 Purchase Order

The previous step provided a purchase schedule determining the issue date of POs of each material. This step “Purchase Order” as the fourth step of the preconstruction model is done by comparing the current date with issue dates of POs of each material retrieved from the purchase schedule. This step defines the POs whose issue dates are reached and must be issued and sent to the vendors. This is done automatically through some steps demonstrated in Figure 3-14.

While running the algorithm on each day of the project, the current date is defined. For instance, the first day of the project is selected  $T_c = 1$ , then a specific material ( $j = 1$ ) is selected. For material  $j$ , the number of POs throughout the project duration is  $L_{N_p}$ . So, in the next step the corresponding date ( $T_{PO_j}$ ) to the first PO of material  $j$  is compared to  $T_c = 1$ . If they are not equal, the algorithm ignores that PO, otherwise it means that the date of the first PO of material  $j$  is reached, and it must be issued. In this case, the required optimized amount and stock quantity of material  $j$  are needed to calculate the order quantity for material  $j$ . Required optimized amount

$(Q_d)$  is available in the optimized material delivery schedule and stock quantity at time  $T_c$  ( $SQ_{T_c}$ ) is always updated and available in the inventory databases. By subtracting the stock quantity/inventory level from the required amount, and by adding a percentage ( $A\%$ ) of required optimized amount ( $Q_d$ ) as materials wastage, the final quantity which must be ordered is determined (Equation 3-18).

$$\text{Order Quantity of Material } j \text{ at Time } T_c \text{ or } T_{PO} = Q_d - SQ_{T_c} + (A\%)Q_d \quad \text{Equation 3-18}$$

Finally, the PO is sent to the selected suppliers along with the method of payment and expediting dates list for confirmation. If the vendors or suppliers confirm the PO, the final purchase order will be issued and sent. The supplier sends an invoice for each PO and receives a partial payment. Expediting activities (dates of contacts, shipping details, and corrective actions) is the next step, which should be done by material professionals until material delivery.

All the above steps are iterated for all the POs for material  $j$  (from  $N_{PO} = 1$  to  $N_{PO} = L_{N_p}$ ), and for all the materials from  $j = 1$  to  $j = k$  for the current date. This process is a repetitive process for all the days of the project from  $T_c = 1$  to  $T_c = D$ .

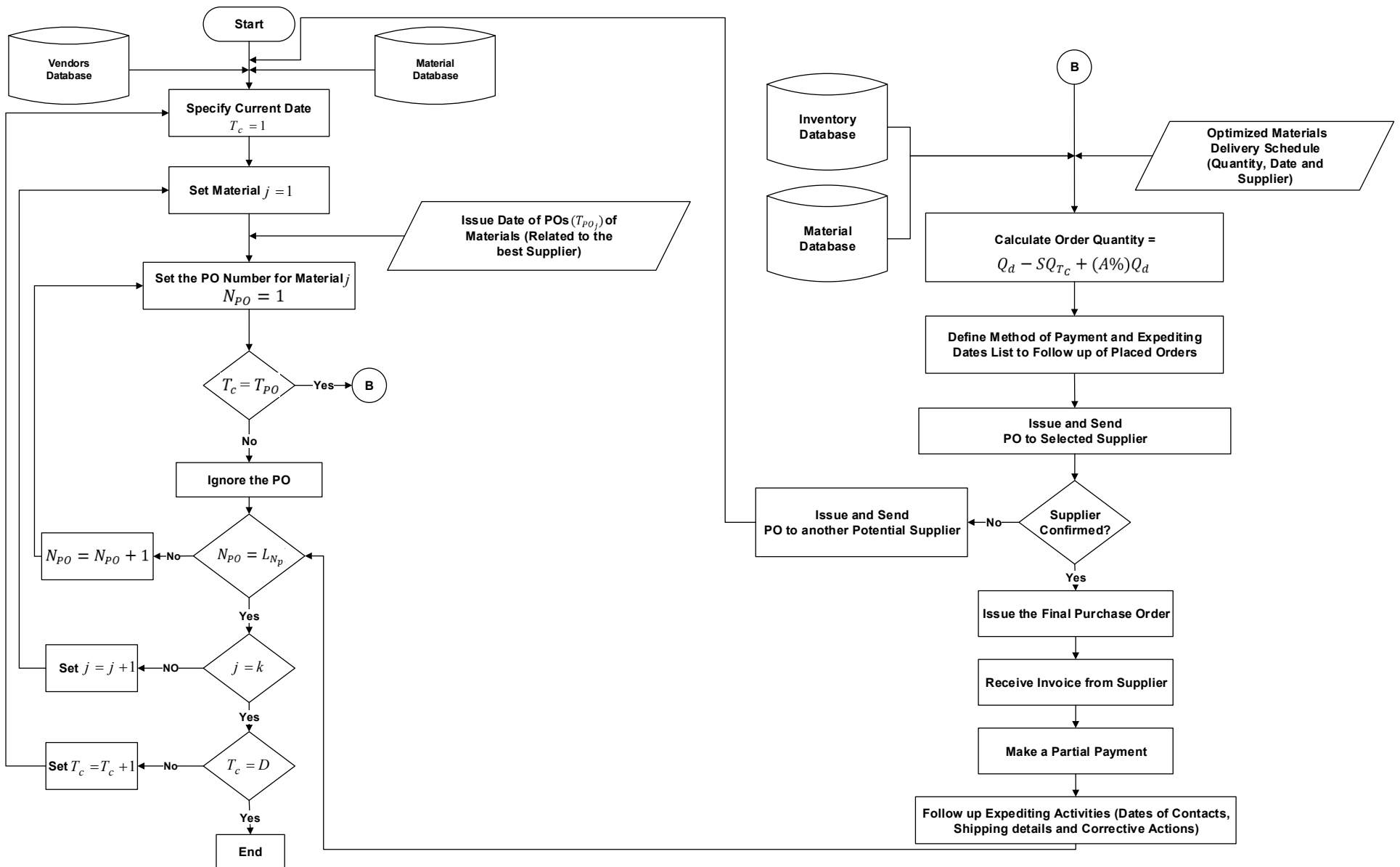


Figure 3-14: Final Material Purchase Order Issuance



### 3.2.5 Material Delivery

After issuing the final purchase orders and suppliers' confirmation, the required materials have to be delivered in the construction site by suppliers according to the optimized material delivery schedule. So the developed framework follows a specific process to identify which material is to be delivered on each day and then registers its acceptance or rejection and also updates the current information of databases if necessary. The material delivery process is illustrated in Figure 3-15. To define whether material  $j$  is to be delivered on any particular day of the project, the corresponding date to that specific day must be identified in the optimized delivery schedule of material  $j$ , in which non-zero values show that there must be a delivery and vice versa. So for each material (from  $j = 1$  to  $j = k$ ) the dates of the first day ( $T_c = 1$ ) to the last day ( $T_c = D$ ) of the project are compared with the dates of various deliveries ( $T_{Q_d} | Q_d \in \{Q_1, Q_2, \dots, Q_{L_{N_p}}\}$ ) of that material derived from the optimized material delivery schedule. If the dates are the same, it means that there must be a delivery on that date. For example, we are on the first day of the project ( $T_c = 1$ ), and the first delivery of material  $j$  ( $d_j = 1$ ) would take place on a particular date shown by  $T_{Q_{d_j}}$  or  $T_{Q_1}$ . So if  $T_{Q_1} = T_c$ , it indicates that the optimized amount  $Q_1$  of material  $j$  must be delivered on the first day. Material delivery depends on the supplier's commitment to the schedule, whether material  $j$  has been transported to the site and is ready to be delivered or not. If yes, it is suggested to use ADC technologies to collect data of incoming materials instead of manual data collection, which is labor-intensive and error-prone. So RFID gate can be used along with the algorithm developed by Jaselskis and El-Misalami (2003). Then, collected data, including delivery date, delivered quantity, and specifications of material  $j$  are compared with the data included in the final purchase order of material  $j$ . In case of conformity, the delivery of material  $j$  will be accepted, and the payment to the supplier will be made complete. Otherwise, the materials professional decides on material acceptance or rejection. In the next step, corrective actions for discrepancies must be taken, or new orders for material shortages are made, not only in case of rejection of the material but also in case of acceptance. It should be mentioned that even in the case of lack of supplier's commitment, which results in non-delivery of the material  $j$  based on the optimized delivery schedule, corrective actions should be taken as well. Finally, the last step is updating inventory and supplier databases or the schedule if necessary.

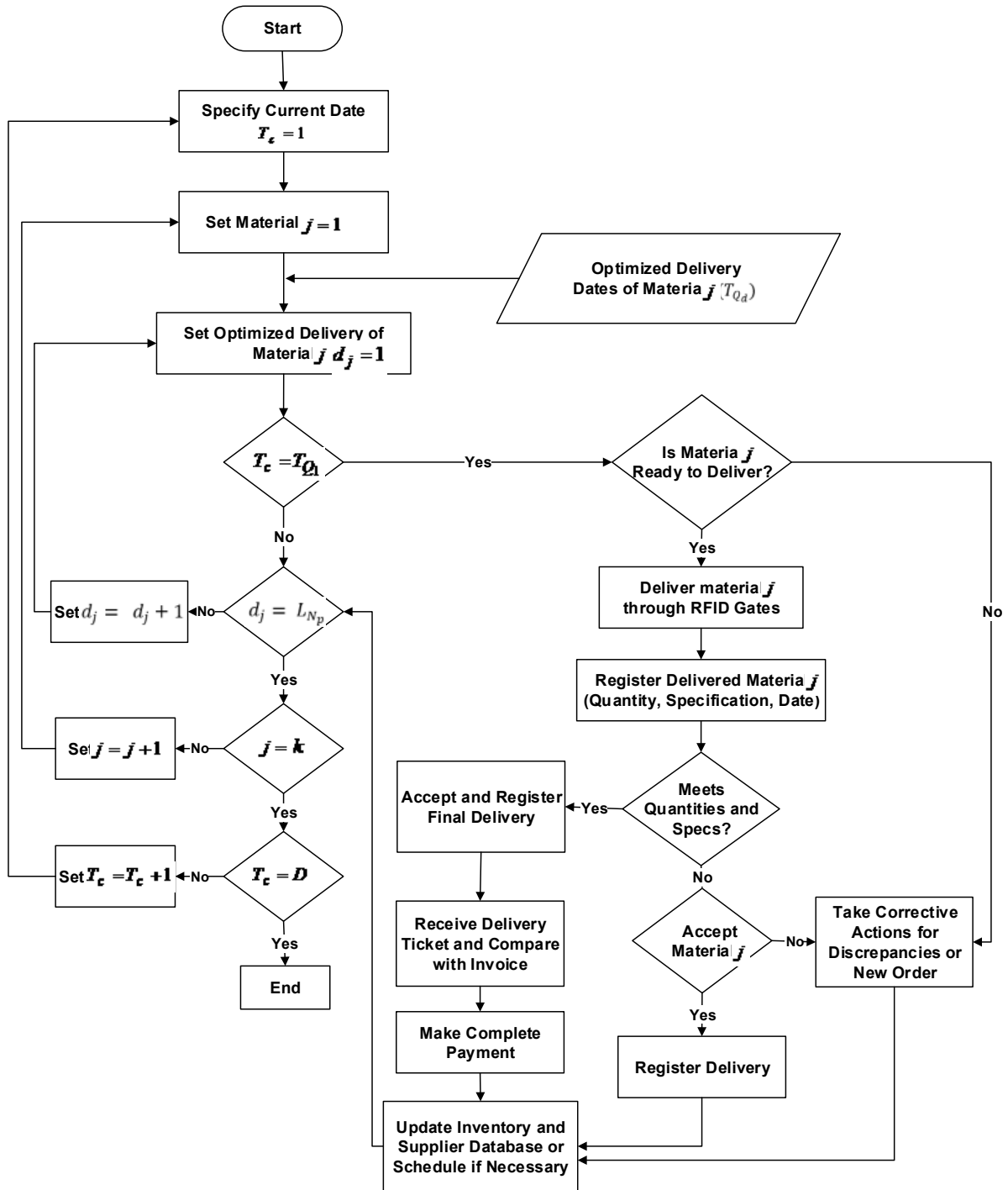


Figure 3-15: Material Delivery Process

### 3.2.6 As-Planned 4D Simulation

It should be mentioned that monitoring the project progress in this research consists of two steps. In the first step the progress (in terms of changes in the images taken at consecutive points of time) are just visualized and in the second step, the information from the

visualized changes are retrieved to define the building elements which have been installed or constructed during the time. So Deep CAE is applied for visualizing the changes in the images captured on different specific dates and a novel object detection framework is developed and applied for identifying constructed or installed building elements from changes visualized in the previous step. As mentioned in section 3.1, training, validating, and testing the deep CAE algorithm proposed for monitoring project progress is another objective of the preconstruction model. To achieve this objective, two steps, including “As-Planned 4D Simulation” and “Deep CAE,” are designed. Synthetic images are generated and used to train, validate, and test CAE in the planning phase in which real images of building under construction are not available.

As shown in Figure 3-16, the 3D BIM model and the schedule of the project are integrated to generate the as-planned 4D BIM model to simulate the construction operations in the first step. In the next step, several frames (images) having identical viewpoint and direction are extracted from the simulated construction operations in Virtual Reality (VR) space and used to train and test CAE in the planning phase.

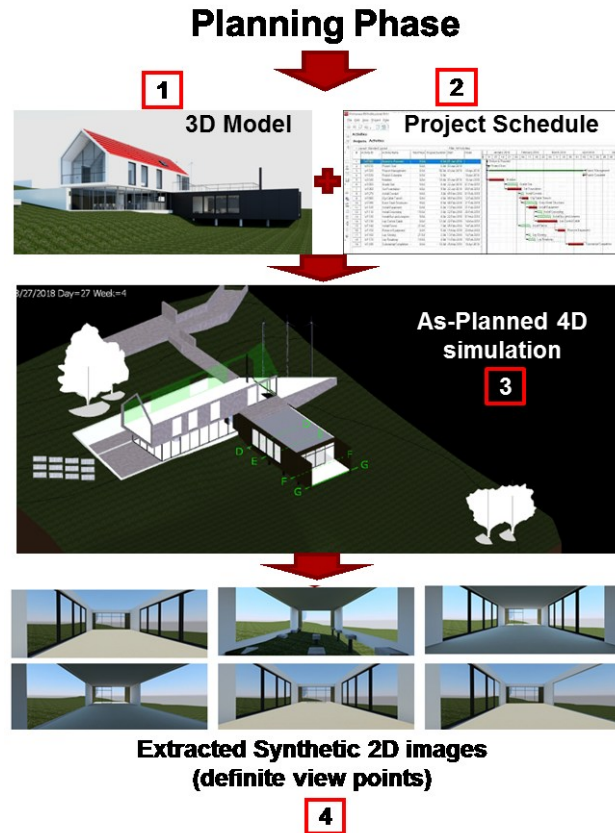


**Figure 3-16: As-planned 4D Simulation and Generating Synthetic 2D Images**

The 3D model of the building is exported from Autodesk Revit as an NWC file to be integrated with its corresponding schedule in Autodesk Navisworks Manage. The generated as-planned 4D model (saved as NWD file) is used to simulate the construction process. To train the proposed CAE algorithm for both indoor and outdoor progress

monitoring, various viewpoints (indoor and outdoor) are created and saved in Navisworks. Multiple viewpoints can be set and saved using options to control the camera projection, position, and orientation in Autodesk Navisworks. So the world coordinates of the camera can be predefined in the project 3D model to be used in the construction phase (construction model) for capturing real images from the construction job site.

On the one hand, when a viewpoint is set and saved in Autodesk Navisworks, the camera position (local coordinate  $(x, y, z)$ ) and the distance between camera location and any specific points are known. On the other hand, since there is always a site survey drawing for any construction projects which has been imported into Autodesk Revit, so the world coordinate of project origin point, base point, and all other specific points of the 3D model are known. As a result, the world coordinate of the camera can be achieved and saved easily for future use knowing the world coordinate of any specific points and the distance between the camera location and that particular point. It is worth mentioning that during creating viewpoints, there might be some overlap in viewpoints. It does not lead to any problem, because as mentioned at the beginning of this section, in the first step, progress is visualized by feeding CAE with input images with the same viewpoint and in the second step, installed or constructed building elements are detected from each point of view. So existing some overlap in viewpoints can only result in detecting one specific elements more than one time which will be modified during updating BIM or project schedule (using IFC data format).

Furthermore, as discussed in advance, to train CAE properly and to make it independent from small visual changes, both indoor and outdoor viewpoints with slight rotation are saved as new viewpoints in Navisworks. Having generated as-planned simulation model with definite indoor and outdoor viewpoints (with and without rotation), frames (image) are extracted from the simulation through rendering in the cloud and are saved in datasets. It is worth noting that, while extracting frames (images) from 4D model simulated in Autodesk Navisworks, factors affecting illumination such as sun, exposure, time zone, latitude and longitude, north direction, date and time of image capturing can be simulated according to the real project condition as well.

### **3.2.7 Deep CAE**

Most of the proposed conventional computer vision algorithms for project progress monitoring cannot be easily implemented in the construction industry. So, a novel near real-time method for project progress monitoring and visualization is developed in which CAE as a deep learning scheme is applied to facilitate vision-based indoor and outdoor progress monitoring of construction operations. The method is designed to visualize actual progress in terms of built elements in near real-time. As explained in section 2.7, CAE is an unsupervised feature-learning algorithm in which its training set is unlabeled, and the internal layer is a generic feature extractor of inner image representations.

Before describing the computational steps of the developed method in detail, it is worth noting that CAE behaves like a chess player in the method. It is proved that pattern matching results in storing information efficiently. For example, due to noticing chess patterns, chess players can memorize the positions of all pieces on the board by looking at them for just 5 seconds (Chase and Simon, 1973). So similar to chess players, CAEs look at the inputs, converts them to an efficient internal representation, and then generates something very similar to the inputs. CAEs can make the desired reconstruction of all or

part of their input. Autoencoders are the same as Convolutional Neural Network (CNN) with one difference, which is producing uniform samples from the given input. This could be interpreted as forcing CNN to learn the mapping from a given source image (“S”) to another target image (“T”) in which “S=T” is also allowed. In a case where “S” is an incomplete image, the learned CNN model can map it to complete the image “T.” This is known as image completion for autoencoders. So we have used CAE to learn a compact representation of 2D images of a building under construction from a definite viewpoint taken on consecutive days while retaining the most critical information. The developed CAE is trained to map an incomplete image to a complete image. The developed method can visualize the progress of any type of construction element regardless of its material or texture of its surface.

In this step, CAE is trained and tested by images generated from the as-planned 4D model simulated in a VR space, as shown in Figure 3-17.

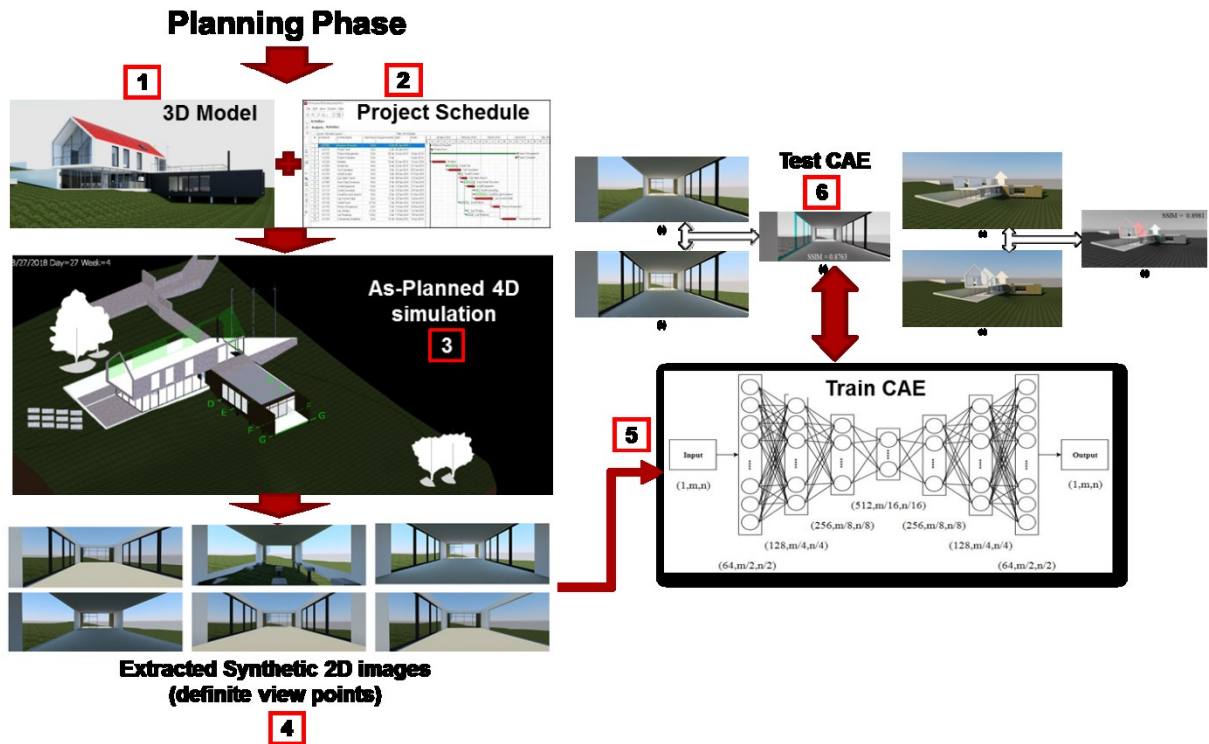
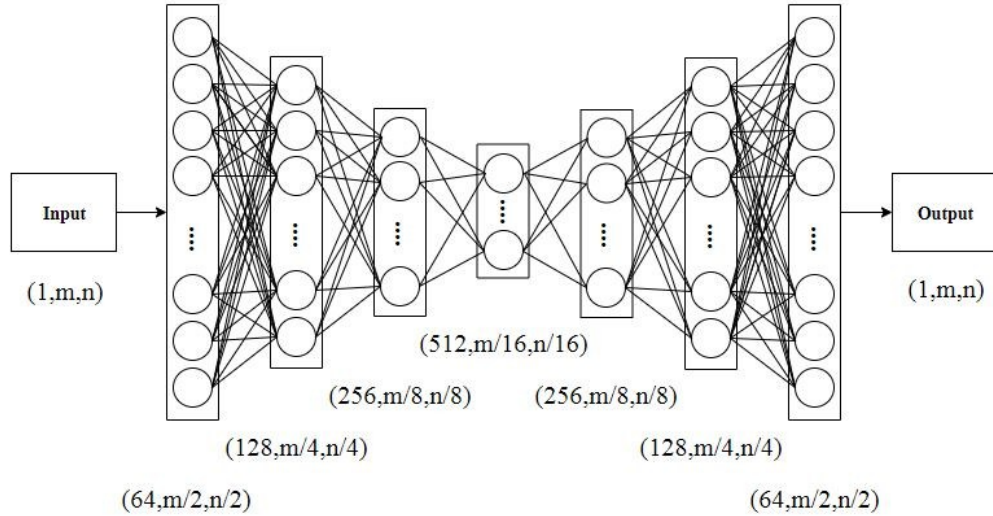


Figure 3-17: CAE Train and Test Using Synthetic 2D Images

The proposed architecture of deep CAE is depicted in Figure 3-18.



**Figure 3-18: CAE Architecture**

Where  $m$  and  $n$  denote width and height of the input image, respectively, and the first field of the parenthesis is the number of filters. Each hidden layer follows by a downsampling (max pooling operations) layer with a ratio of two. So the size of each hidden layer is reduced to half. The stride size is set to one for the receptive fields of the size  $3 \times 3$ . The activation function is the Rectified Linear Unit (ReLU), and there is no residual connection in the proposed CAE architecture.

Considering the input image as  $I_{m,n}$ , then each hidden layer will be represented as Equation 3-19, where  $x$  is randomly sampled from the given image. The Python and MATLAB bindings have efficiently implemented this random sampling.

$$p(x) \sim I_{m,n} \quad \text{Equation 3-19}$$

Glorot initialization technique (also known as Xavier), which is an improved version of the normal initialization, is used for initializing weight matrices. To investigate why deep multilayer neural networks were not successfully trained, Glorot and Bengio (2010) focused on the initialization and training mechanisms. They found that proper weight initialization can prevent the layer outputs and loss gradients from exploding or vanishing in the forward and backward pass, respectively, and result in faster convergence. Their new proposed initialization scheme is called “normalized initialization” or “Glorot initialization” in which a layer’s weights are selected from a random uniform distribution having the following lower and upper bounds:

$$\pm \frac{\sqrt{6}}{\sqrt{n_j + n_{j+1}}} \quad \text{Equation 3-20}$$

Where  $n_j$  and  $n_{j+1}$  indicate the number of input (fan-in) and output (fan-out) neurons. Hidden layers are convolution networks. The size of the convolution field is static of  $3 \times 3$ . We also apply weight normalization in each convolution layer. The reason for this operation is balancing the achieved weights because it is common to obtain very large and

very small weights. For reducing the effect of unbalanced weights, we use the approach proposed by Salimans and Kingma (2016).

The fourth layer in the proposed CAE architecture, known as the bottleneck, has the gist of the fed images to it, which is represented as several filters. Five hundred twelve (512) filters in the bottleneck are the posterior probability of the original images and generated outputs in the first three hidden layers. There are widely used activation functions in deep neural networks, including ReLU, Leaky Rectified Linear Unit (LeakyReLU), Softplus, and Exponential Linear Unit (ELU). ReLU (the definition of this function is  $\max(0, x)$ ), was first used in Restricted Boltzmann Machines (Nair and Hinton, 2010) and then was applied in neural networks as well (Glorot et al., 2011). It can be stated it is the most common activation function. The activation function for the bottleneck is no longer ReLU but Leaky ReLU, which has a small negative slope when  $x < 0$ . Leaky ReLU can prevent learning block in the negative region of feature information. Thus the reason is to avoid both gradient vanishing and dying ReLU problems. Figure 3-19 plots these two activation functions.

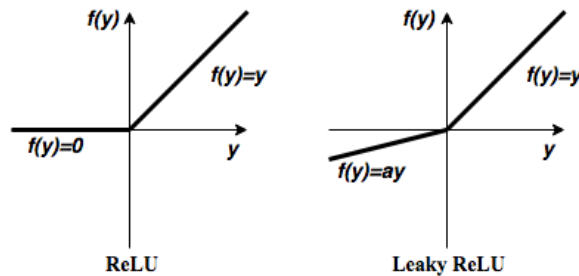


**Figure 3-19: ReLU Function vs. Leaky ReLU Function (Clevert et al., 2015)**

The architectures of the convolution layers from the fifth layer to the seventh layer are similar to the first layer to the third layer, respectively, see Figure 3-18. Finally, the output of the CAE will be very similar to the input image. If this fact is not realized, then its straightforward interpretation should be continued to more epochs (the number of times which we feed the entire sample to CAE) in the training process. Having trained CAE, progress is visualized in terms of constructed building elements between two consecutive time points using test images.

The main advantage of the autoencoders is that we can use it as a data augmentation module to increase both the quality of and quantity of input samples, especially when the given training dataset is poor. Another advantage of this algorithm is its schematic prediction of images. In other words, autoencoders can predict the appearance of a given input in the near future or even estimate and visualize the difference of two given images distributed over time. Moreover, conventional algorithms cannot predict the visual appearance of images with respect to the given input. So CAE can help project managers to visualize projects progress in near real-time.

For the performance evaluation purpose, the output image visualizing progress is compared with the ground truth image using the Structural Similarity (SSIM) index, which can measure the similarity between two images.

As shown in the research done by Snell et al. (2017), reconstructed outputs with higher quality can be obtained if deep networks for image synthesis such as autoencoders are trained with loss functions, which are calibrated to human perceptual judgments of image quality like SSIM. So SSIM, which can assess the changes in luminance, contrast, and structure between the output and the ground truth image, is selected in this study.

By using SSIM, corresponding pixels and their neighborhoods in two images ( $x$  &  $y$ ) are compared through the following comparison functions (Snell et al., 2017):

$$I(x, y) = \frac{2\mu_x\mu_y+c_1}{\mu_x^2\mu_y^2+c_1} \quad C(x, y) = \frac{2\sigma_x\sigma_y+c_2}{\sigma_x^2+\sigma_y^2+c_2} \quad S(x, y) = \frac{\sigma_{xy}+c_3}{\sigma_x\sigma_y+c_3} \quad \text{Equation 3-21}$$

“Where  $\mu_x$ ,  $\mu_y$ ,  $\sigma_x$  and  $\sigma_y$  denote mean pixel intensity and the standard deviations of pixel intensity in a local image patch centered at either image  $x$  or  $y$ .  $\sigma_{xy}$  denotes the sample correlation coefficient between corresponding pixels in the patches centered at  $x$  and  $y$  and for the numerical stability small values are added and shown by  $C_1$ ,  $C_2$  and  $C_3$ .” SSIM is calculated by combining the three comparison functions as follows (Snell et al., 2017):

$$SSIM(x, y) = I(x, y)^\alpha C(x, y)^\beta S(x, y)^\gamma \quad \text{Equation 3-22}$$

### 3.2.8 Reports and Warnings

However, reporting and warning is the last step of the preconstruction model (Figure 3-4); it does not mean that reports and warnings by the developed framework are just dedicated to the planning phase. The significance of this step is much more related to the construction phase in which material professionals can manage materials based on the reports and warnings generated by the developed framework. So the developed framework can generate MRP, optimized delivery schedule, the list of issue dates of purchase orders, the list of POs to be issued and sent to the suppliers on each day of the project, and the list of deliveries of materials on each day of the project. On top of the mentioned main reports, the developed framework can give warnings to the materials professionals about the various due dates to prevent material shortages and, consequently, schedule delay. The developed construction material management framework can be a web-based system providing multiple reports according to the role and level of responsibility of the users. So they can input the required data and have access to different reports to make decisions based on the reports.

### 3.3 Construction Model

In the planning phase, the preconstruction model helps material professionals to order and purchase a particular quantity of various materials on specific days, which results in the least total material cost. But as soon as the construction phase begins, the reality would be undoubtedly different from the first estimations. One of these differences relates to actual project progress, which directly affects the management of required materials. So to have an effective and acceptable materials management, not only the actual project progress must be monitored, but also the first estimations must be updated considering the changes. Consequently, preconstruction steps are performed repeatedly using near real-time acquired data to result in more realistic outputs for future decisions. Therefore construction



model has been developed to focus on the collection of near real-time actual data through ADC technologies.

As mentioned in the abstract, project progress is visualized from two different perspectives: (1) comparing various as-built status captured on consecutive points of time and (2) comparing as-built status with as-planned 3D model. So in the first perspective, during the construction phase, near real-time job site data in terms of daily photographs are collected using RGB cameras. Job site daily images are captured from the same 3D coordinate of viewpoint and direction as the corresponding images in VR space. Taking daily images before or after working hours, illustrating the progress is highly recommended. But small changes (around 5 degrees) in the viewpoint of real job site images do not affect the output. As shown in Figure 3-20, trained CAE (obtained from preconstruction model) is fed with images of job site taken on each day/week to visualize the progress in terms of building elements in the next model (data analysis and reporting model).

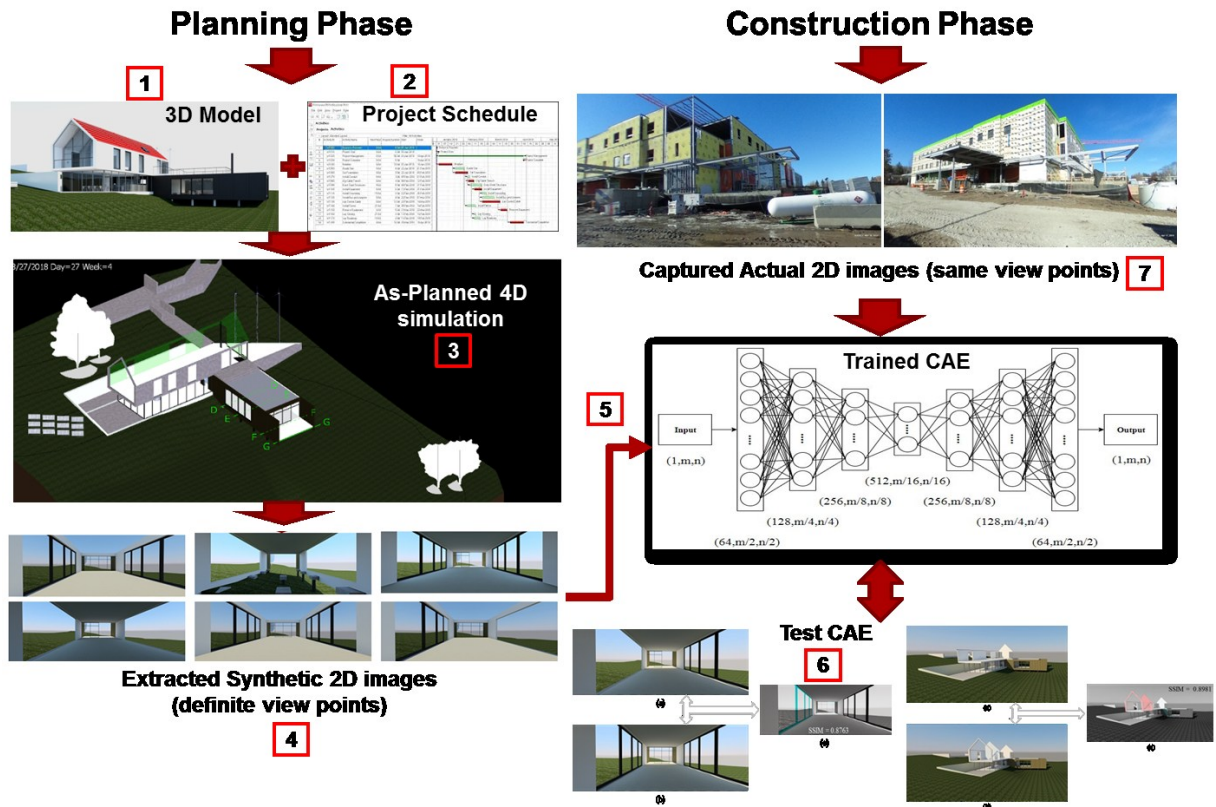
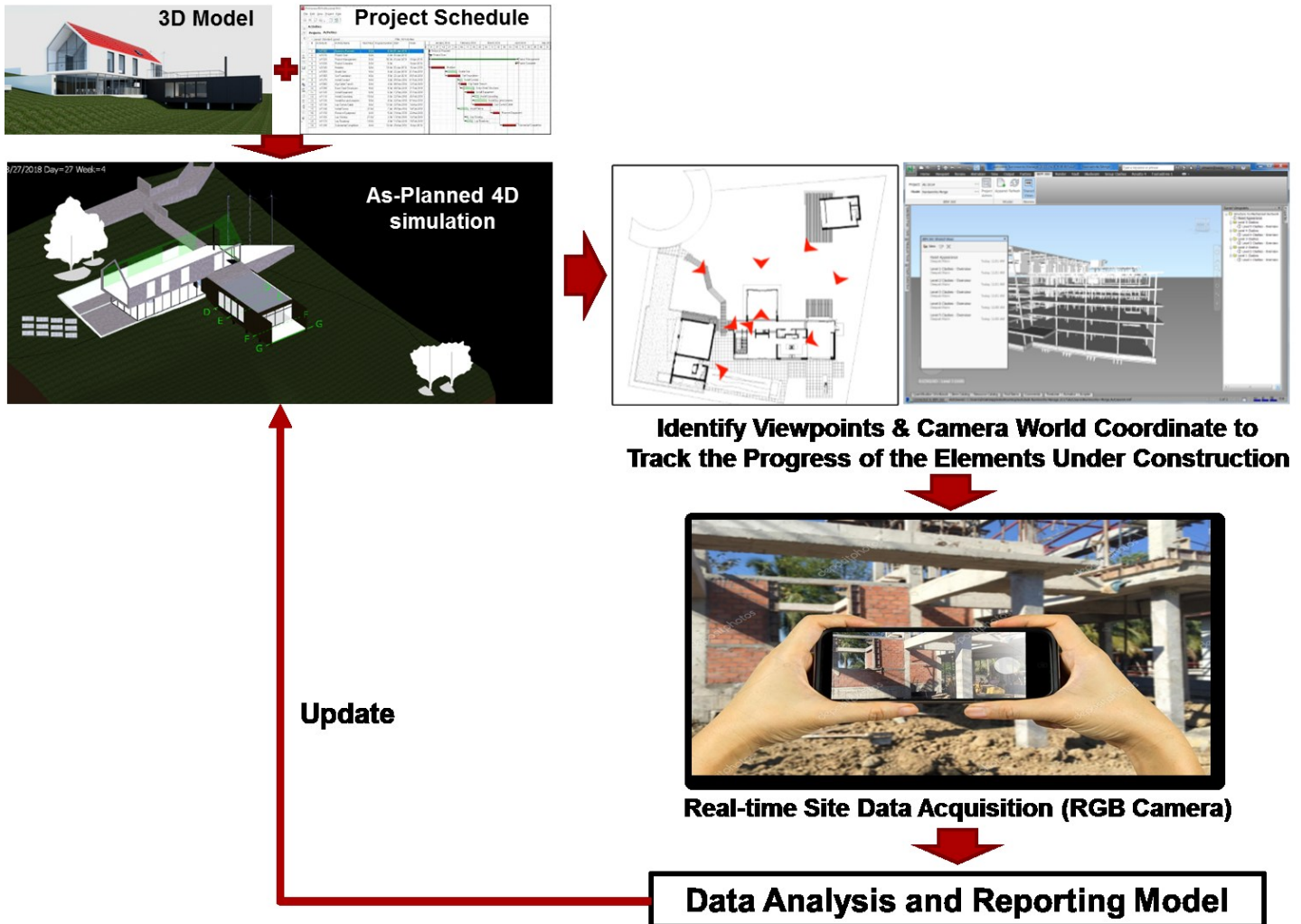


Figure 3-20: Captured Actual Job Site Images Fed into Trained CAE

As indicated in Figure 3-21, to collect real-time site data through capturing images, it is required to know which elements are under construction on each day. Running as-planned 4D simulation leads to the identification of the building elements under construction on each day from various viewpoints (from  $V = 1$  to  $V = M$ ) and, consequently, the world coordinate of the camera. Then by knowing the building elements and the camera coordinates, real images are frequently captured from the same coordinate to track the progress.



**Figure 3-21: Construction Model (First Perspective)**

Captured images on a daily/weekly basis will be sent and analyzed in the next model. Finally, by estimating the actual progress using developed algorithms in the data analysis and reporting model, the schedule is updated to be used as an input for the preconstruction model.

Figure 3-22 indicates the required steps to generate a list of viewpoints and their related camera coordinates to track the progress of building elements under construction on each day. It shows which activities are being carried out on each day of the construction phase and must be tracked. As-planned 4D simulation, including specific viewpoints and their related camera coordinates, are used as inputs. The first viewpoint is set  $V = 1$ , and 4D simulation is run on the current date shown as  $T_c = 1$ . If there is any new building element in this viewpoint on  $T_c = 1$ , this viewpoint is registered in the list along with its camera coordinate and the date. But if there is not any new building element, this viewpoint is checked for the next days (from  $T_c = 1$  to  $T_c = D$ ) to define whether there is any new building element or not. All the mentioned steps will be performed for all the viewpoints saved in as-planned 4D simulation (from  $V = 1$  to  $V = M$ ).

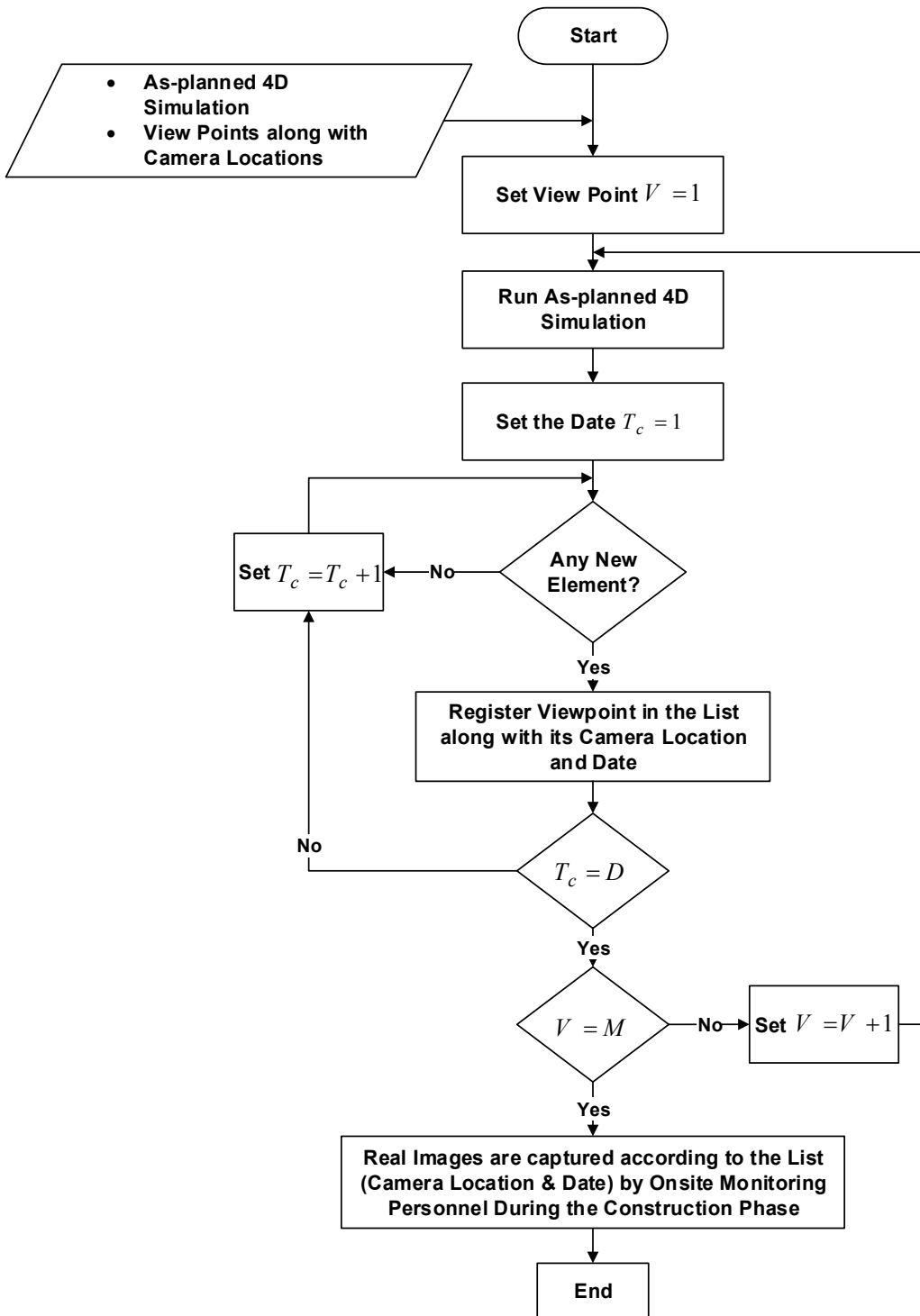


**Figure 3-22: List of Viewpoints, Location, and Dates for Image Capturing**

Thus a list of building elements/activities to be tracked/photographed at the job site on each day along with the location of the camera enables onsite monitoring personnel to capture real images during the construction phase.

In the second perspective in which progress is visualized through comparing as-built status with as-planned 3D model, 360-degree images, and the HoloBuilder platform are used. As mentioned in Chapter 2, by using the HoloBuilder platform, as-built conditions are visualized through spatially linking the 360-degree images to the existing 2D plans. Figure 3-23 illustrates an example of using the HoloBuilder platform for a project in which a 360-degree image is captured and linked to the project 2D plan. In the top left corner, the 2D floor plan of the project can be seen. The yellow circles indicate the different locations of the 360° camera that has been used to take required 360-degree images in this floor. By clicking on each yellow circle, a black point will appear in its center, and a new 360-degree image visualizing the real scene surrounding the 360° camera (from which the image has been captured) will be displayed.



**Figure 3-23: Example of 360-Degree Image in HoloBuilder Platform (©2020 HoloBuilder, Inc.)**

So, the as-built condition of the project can be capture and visualized using the HoloBuilder platform. But, to visualize the progress, the as-built status of the building must be compared with the as-planned 3D model. As shown in Figure 3-24, the 3D model can be imported and displayed side by side with the 360-degree image (as-built status) by enabling the Split-Screen feature of the HoloBuilder platform (yellow icon under the 2D plan). On top of the ability to rotate each scene (360-degree image or 3D as-planned model) independently in the HoloBuilder web player, it is possible to rotate both scenes simultaneously by adjusting the viewpoints and using “Lock View” button at the bottom of the screen. In this case, by dragging the 360-degree image, the 3D model will be rotated in the same way. It is worth mentioning that after rotating the scenes either independently or simultaneously to focus on different aspects of the building, various 2D images can be extracted and saved for future comparison.

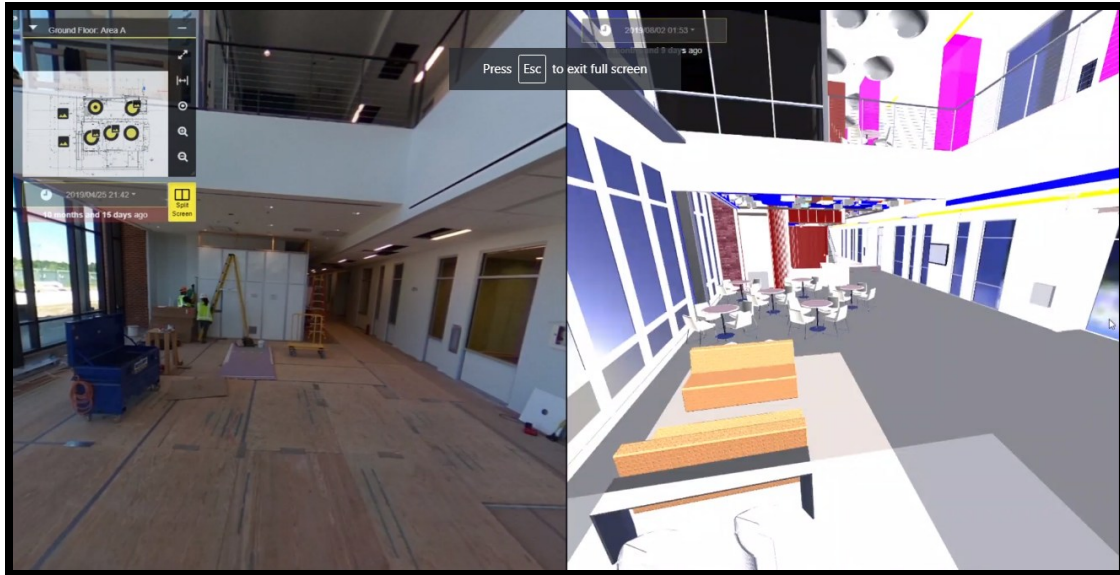


**Figure 3-24: Example of a 360-Degree Image and an Imported 3D Model to HoloBuilder Platform (©2020 HoloBuilder, Inc.)**

So keeping the same focus and point of view for both scenes (as-built status and 3D as-planned model) is required for comparison and visualizing the progress using the HoloBuilder web player. To achieve the same viewpoint in both as-built 360-degree image and as-planned 3D model, the following main steps are required to be done during the construction model (Marktscheffel, 2020, HoloBuilder Website):

- Creating Revit 360 rendering views and defining the world coordinate of 360° camera;
- Importing a 360° rendering view of the 3D model from Autodesk Revit into HoloBuilder;
- Capturing 360-degree images from actual job site using pre-defined world coordinate of 360° camera.

To implement the first step, HoloBuilder Add-In for Autodesk Revit must be installed appropriately. As shown in Figure 3-25, the sheet view (e.g., Floor Plan/Level 1) is selected to place the 360 views. Then, on this selected sheet, we have to define the locations where the 360-degree images in the 3D model must be captured. As explained in section 3.2.6, there is always a site survey drawing for any construction projects which has been imported into Autodesk Revit and the world coordinate of project origin point, base point, and all other specific points of the 3D model are known. So the locations of 360 renderings in terms of world coordinate and through using the “Place HoloBuilder View” button on the Add-In tab are defined and saved.

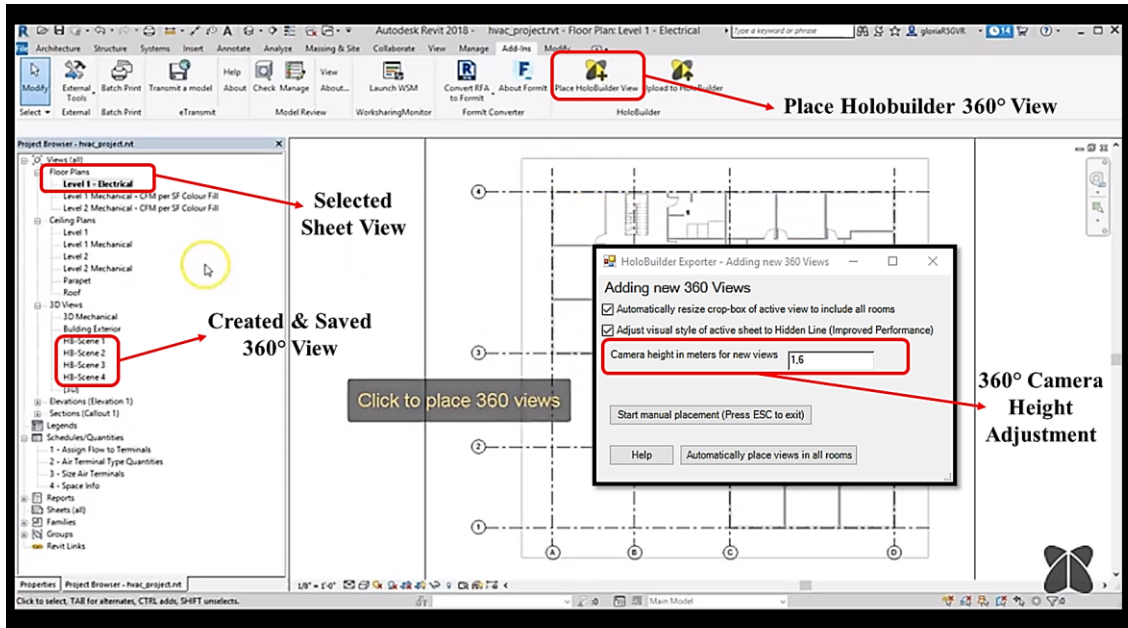


**Figure 3-25: Creating Revit 360 Rendering Views**

While using “Place HoloBuilder View” button, it is possible to adjust camera height from the selected floor in meters, so the 360° camera position in terms of (x, y) is equal to the (x, y) of predefined location in Revit and z coordinate of the 360° camera is equal to the z coordinate of the project basepoint in the selected floor plus the defined height (e.g., 1.6 m).

The second primary step is uploading all the created 360° views on the 3D model from Autodesk Revit into HoloBuilder. As illustrated in Figure 3-26, all the floor plans where 360° views have been created and saved, and also all the saved 360° views can be exported to HoloBuilder using “Upload to HoloBuilder” button on Add-In tab.

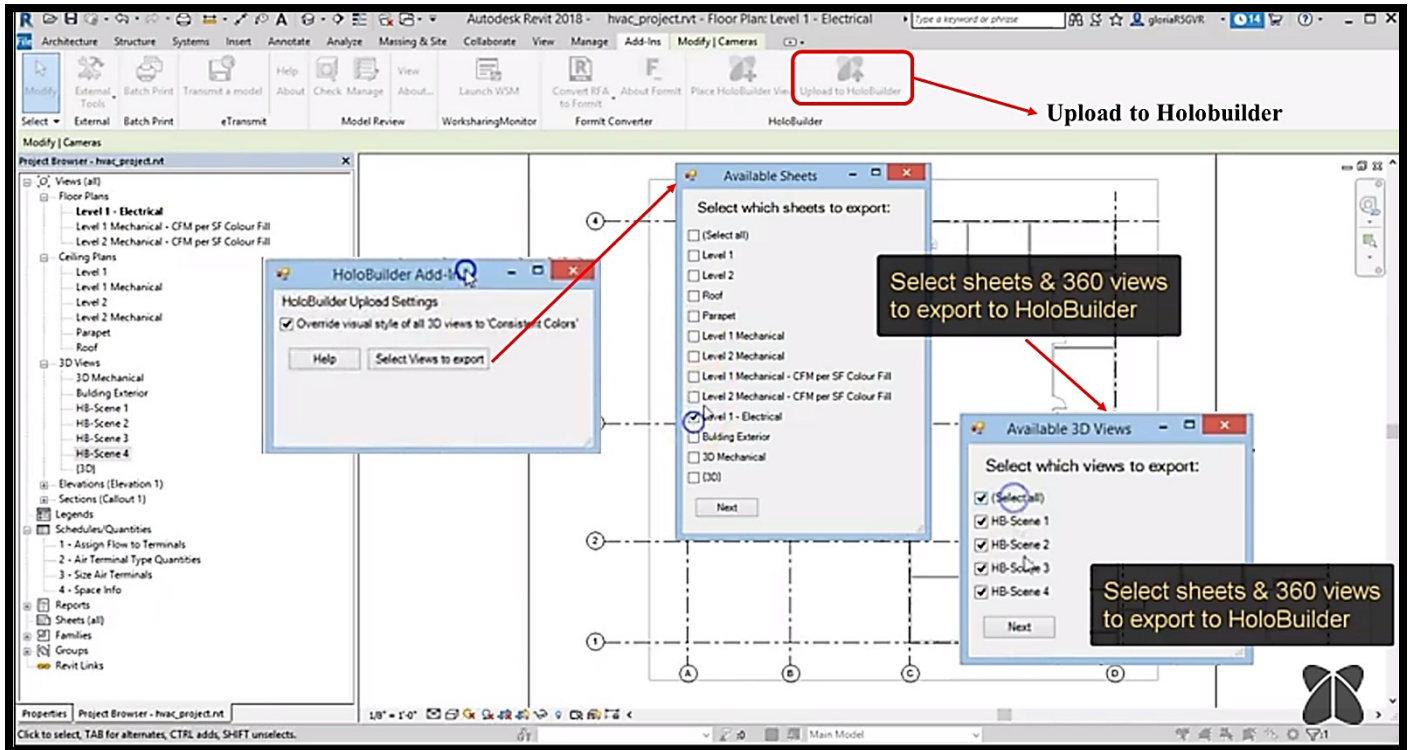


**Figure 3-26: Importing 360° Views of 3D Model from Autodesk Revit into HoloBuilder**

In the last main step and during the construction phase, 360-degree images must be captured from the actual job site using locations of 360° camera pre-defined in the previous step. In this case, 360-degree images of the 3D Revit model (as-planned) and 360-degree images of the actual job site (as-built) have been captured from the same location. They are comparable if they are imported and shown side by side in the HoloBuilder platform by enabling the Split-Screen feature (Figure 3-27). To visualize the progress, as-planned and as-built images can be extracted and used as inputs for an algorithm to be compared in the next model (Data Analysis and Reporting Model). According to the report issued by HoloBuilder (2019), “Ricoh Theta V” is recommended to capture 360-degree images at job sites (Figure 3-28).

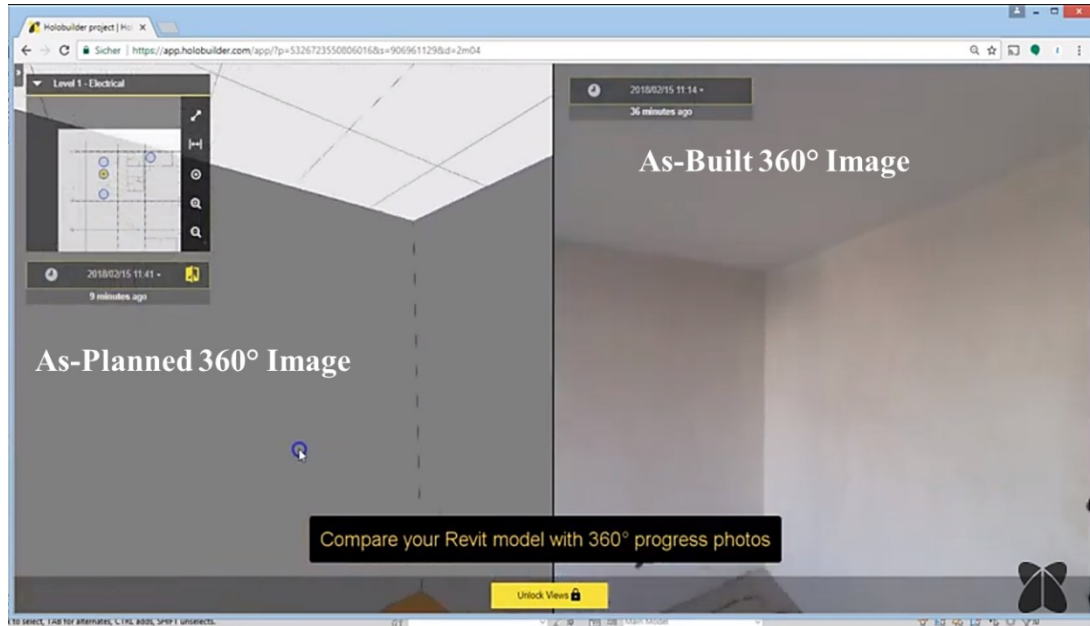


**Figure 3-27: As-Built 360° Image vs. As-Planned 360° Image in HoloBuilder Platform (©2020 HoloBuilder, Inc.)**

### Ricoh Theta V


<b>Resolution (view example)</b>	<b>6/10</b>
Low	High
<b>Speed</b>	<b>9/10</b>
Slow	Fast
<b>Battery Life</b>	<b>9/10</b>
Low	High
<b>Ease of Use</b>	<b>7/10</b>
Low	High
<b>Robustness</b>	<b>5/10</b>
Low	High
<b>Low Light Performance</b>	<b>5/10</b>
Low	High
<b>Price (latest price)</b>	\$ \$ \$ \$ \$ \$ \$ \$ \$ \$
<b>Compatibility</b>	✓

APIs supported - Works with most best-in-class apps, including 3dTrack

**Our Summary:**  
Super easy to use 360° camera and the fastest in the market. Ricoh's 5th generation model is well-tested on jobsites and is highly recommended by contractors. It has a solid plastic camera body.

**Recommended for:**  
Large construction sites that need to be captured over time. Best for fast capture with a high volume of images.

**Add-on recommendation:**  
The lenses are exposed and can be easily scratched; a lens cap is recommended to protect the lenses from scratching.



**Figure 3-28: Ricoh Theta V Specifications (HoloBuilder, 2019)**

### 3.4 Data Analysis and Reporting Model

As explained in section 3.3, as soon as the construction phase begins, there are always discrepancies between what has been planned in the planning phase and the actual project



status. Therefore actual near real-time data collected in the construction model must be analyzed and interpreted in this model entitled “Data Analysis and Reporting Model” to update the project schedule and MRP. The proposed algorithms, including CAE, SSIM, and an object detection framework are utilized in this model to visualize and detect actual progress which is needed for updating the schedule and MRP and other related steps in the preconstruction model would be repeated consequently to generate optimized material delivery and purchase schedule on a regular basis.

### 3.4.1 CAE for Project Progress Visualization

Captured real images on consecutive days during the construction phase are used as inputs to feed trained CAE in this model to visualize the changes. Figure 3-29 illustrates the developed concept and the procedure of progress visualization applying trained CAE fed with real images captured by using a non-stationary RGB camera in the construction model.

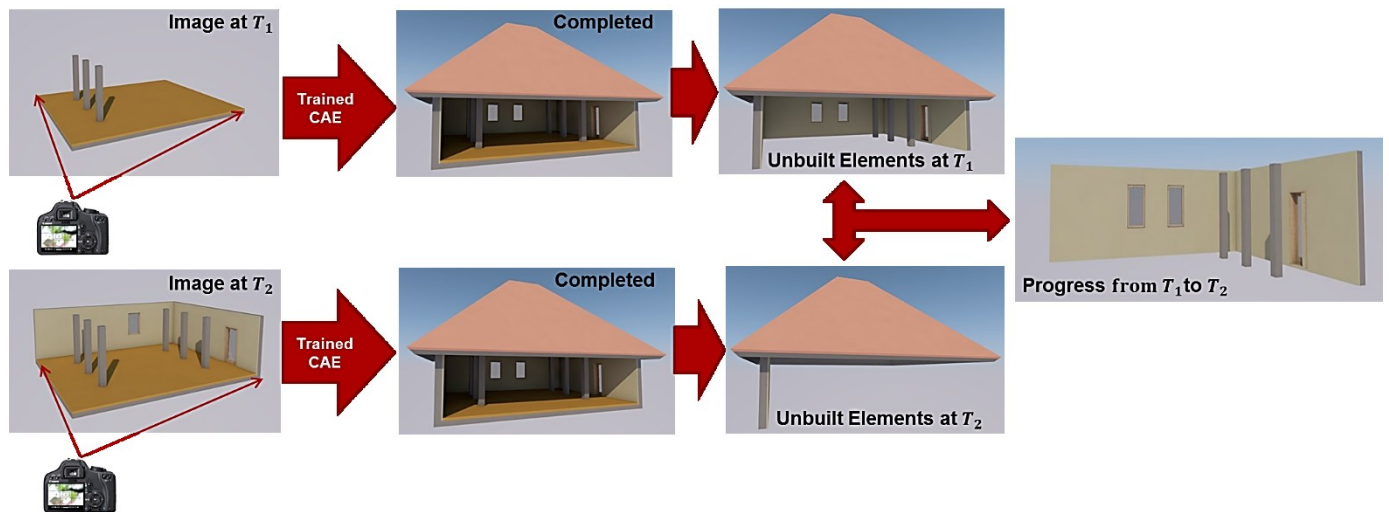


**Figure 3-29: Progress Visualization Using Trained CAE**

CAE, which was trained and tested with synthetic images in the preconstruction model, is fed with real images from the job site captured on consecutive days (obtained from the first perspective in the construction model) to make progress visually recognizable by mapping these captured images to those of planned complete building. As illustrated in Figure 3-29, and as explained in section 3.2.7, CAE has been trained to learn the mapping from a given incomplete image (image at time  $T_1$  or image at time  $T_2$ ) to another target image (image of the completed building). In other words, CAE can produce complete samples for any incomplete input samples fed to the algorithm. It is worth mentioning that in this model, CAE has already been trained and tested in the preconstruction model. It is ready to receive an incomplete image from the job site (which is captured in the construction model) to visualize the progress made between two consecutive points of time when the images have been captured (Figure 3-30).

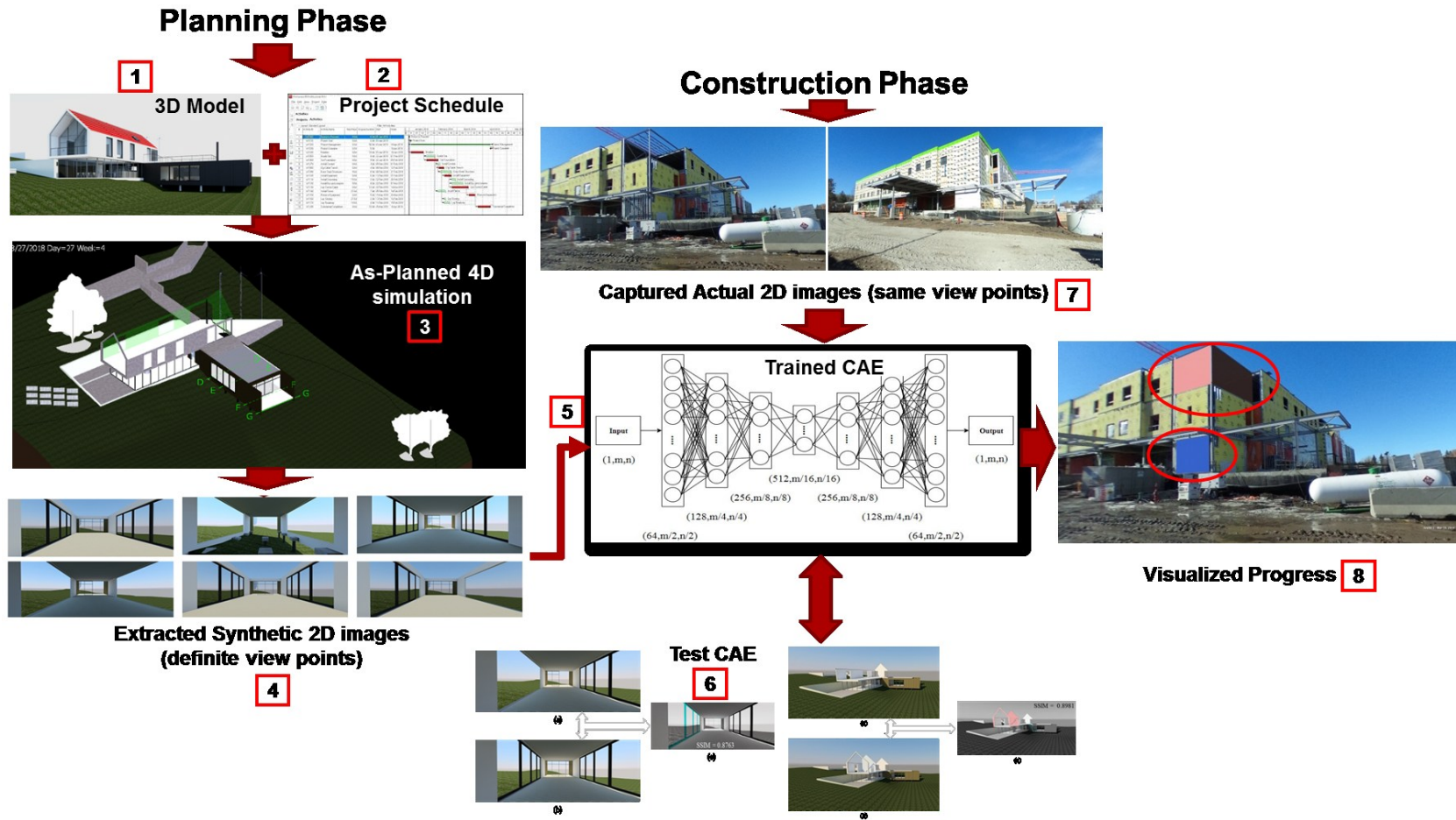


Figure 3-30: Trained CAE Fed with Job Site 2D Images for Progress Visualization

### 3.4.2 Structural Similarity Index (SSIM) to Compare Images

On top of applying CAE for progress visualization, as mentioned in the construction model, as-built (360-degree images of job site) and as-planned images (360-degree images of 3D Revit model), which are extracted from HoloBuilder platform can be compared to make the progress visualization possible in this model. Structural Similarity Index (SSIM) is proposed to visualize the differences between as-built and as-planned images.

SSIM was developed by Wang et al. in 2004 for quality assessment by measuring the similarity between two images. As Wang et al. (2004) have stated, the integration of illumination and reflectance of a surface is called luminance of that surface, and the structures of the objects in the images are independent of illumination being observed. SSIM is based on the fact that the human visual system extracts structural information from the images, so SSIM has been defined without considering the influence of luminance and contrast. Similarity measurement  $S(X, Y)$  of two images consists of three comparisons: luminance ( $l(X, Y)$ ), contrast ( $c(X, Y)$ ) and structure ( $s(X, Y)$ ) of corresponding pixels and their neighborhoods in two images ( $X$  &  $Y$ ) (Wang et al., 2004):

$$S(X, Y) = l(X, Y)^\alpha c(X, Y)^\beta s(X, Y)^\gamma \quad \text{Equation 3-23}$$

Where  $\alpha > 0$ ,  $\beta > 0$ , and  $\gamma > 0$  are the weights used to control the relative importance of the three components.

Similarity measurement should satisfy the following conditions as well (Wang et al., 2004):

- Symmetry:  $S(X, Y) = S(Y, X)$ ,
- Boundedness:  $S(X, Y) \leq 1$ ,
- Unique maximum:  $S(X, Y) = 1$  if and only if  $X = Y$

SSIM consists of the following comparison functions to compare corresponding pixels and their neighborhoods in two images ( $X$  &  $Y$ ) (Wang et al., 2004):

$$l(X, Y) = \frac{2\mu_x\mu_y + C_1}{\mu_x^2 + \mu_y^2 + C_1} \quad c(X, Y) = \frac{2\sigma_x\sigma_y + C_2}{\sigma_x^2 + \sigma_y^2 + C_2} \quad s(X, Y) = \frac{\sigma_{xy} + C_3}{\sigma_x\sigma_y + C_3} \quad \text{Equation 3-24}$$

“Where  $\mu_x$ ,  $\mu_y$ ,  $\sigma_x$  and  $\sigma_y$  denote mean pixel intensity and the standard deviations of pixel intensity in a local image patch centered at either image  $X$  or  $Y$ .  $\sigma_{xy}$  denotes the sample correlation coefficient between corresponding pixels in the patches centered at  $X$  and  $Y$  and for the numerical stability small values are added and shown by  $C_1$ ,  $C_2$  and  $C_3$ ” (Snell et al., 2017). SSIM can identify and visualize the perceptual differences between as-built and as-planned images, as shown in Figure 3-31.

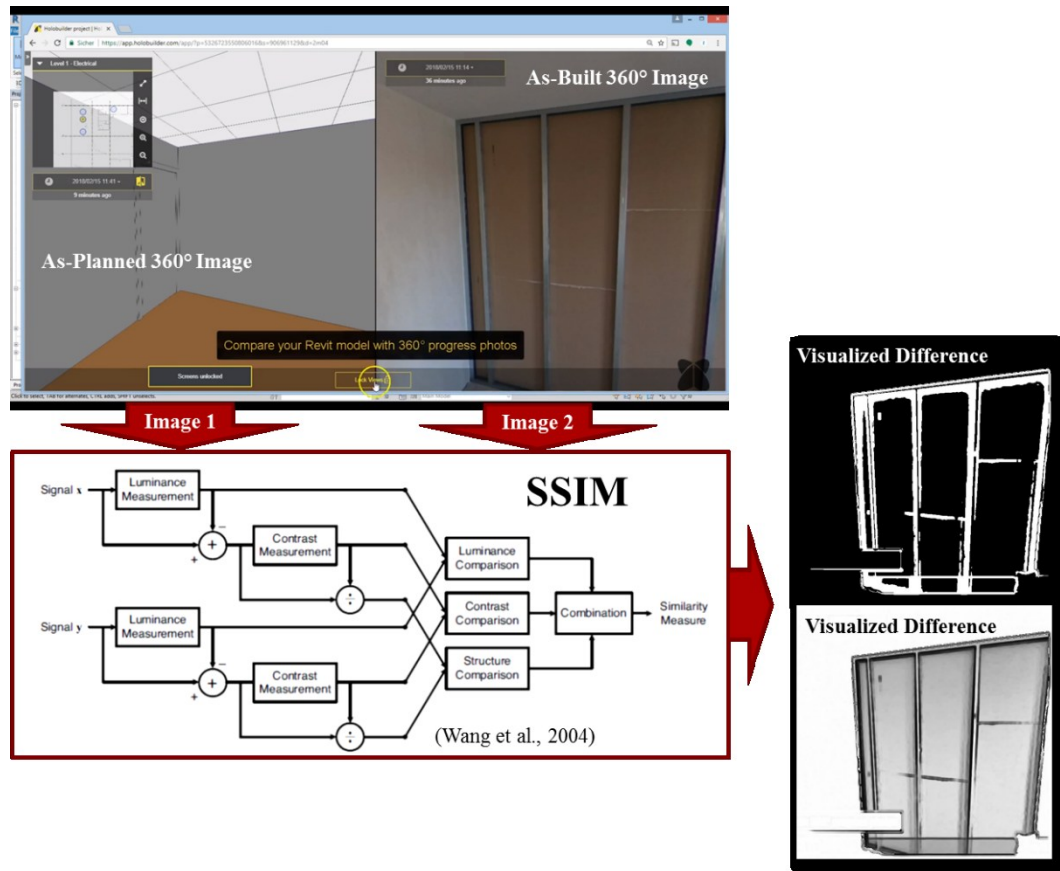


**Figure 3-31: Progress Visualization using SSIM**

It is worth mentioning that the index of structural similarity and its closeness to 1 is not crucial in this method, because the purpose of using this algorithm is visualizing the differences between as-built and as-planned status of the building. In this case, the closeness of SSIM to 1 indicates that the project is neither behind nor ahead of schedule; it is roughly on schedule.

### 3.4.3 Automated Detection of Building Components (Using Deep-Learning and Synthetic Images)

After progress visualization, which is the output of CAE or SSIM, there is a need for an effective method for extracting the information and identifying various building components included in the images. As illustrated in Figure 3-32, a generalized object detection framework for automated identification of building components can provide a suitable replacement for the time-consuming manual information retrieval. It is shown that after progress visualization, applying the developed object detection framework results in detecting various building elements and consequently updating the project schedule based on the perceived progress.

The literature reveals that automated detection of these components using images is still in its infancy stage. This is attributed to the dynamic execution environment of construction operation and for the fact that automated object detection methods require large training

datasets of images, which may prove challenging to have. So a newly developed framework is presented for automated detection of building components using a mix of real and synthetic-images for training Mask Region-based CNN (Mask R-CNN). The novelty of the developed framework lies in its efficient utilization of generated synthetic-images and the selection and use of a well-suited object detection algorithm.

As explained in section 2.8, deep learning-based object detection algorithms require large training datasets of images, and there is no available open image dataset of building components. According to the studies (Movshovitz-Attias et al. 2016; Rajpura et al. 2017; Tremblay et al. 2018), it is believed that synthetically generated datasets of images with high variation have the potential in facilitating the detection of building components in the construction industry. We envision the framework developed in this study, which consists of Mask R-CNN and a suitable mix of real and synthetically generated datasets of images, to offer a promising method for the detection of building components.

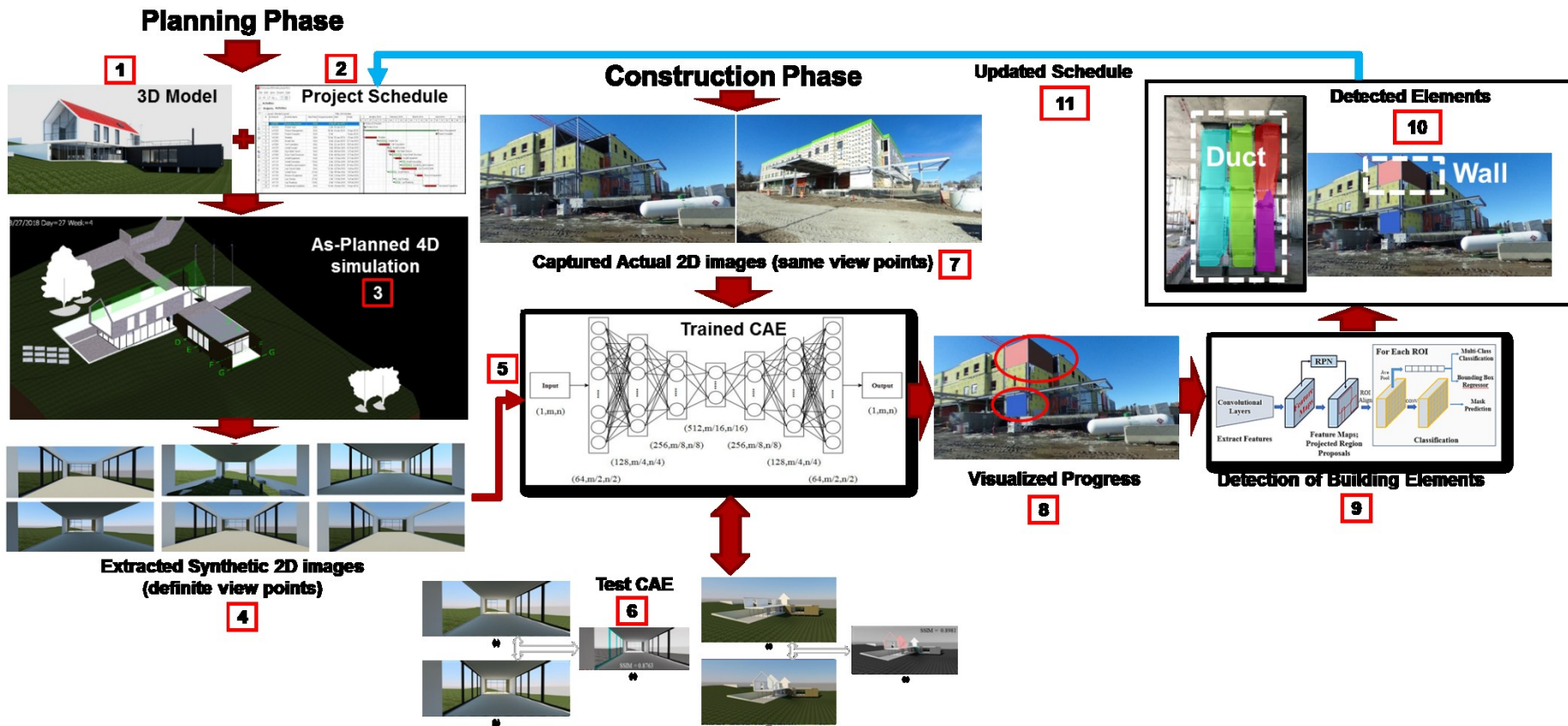
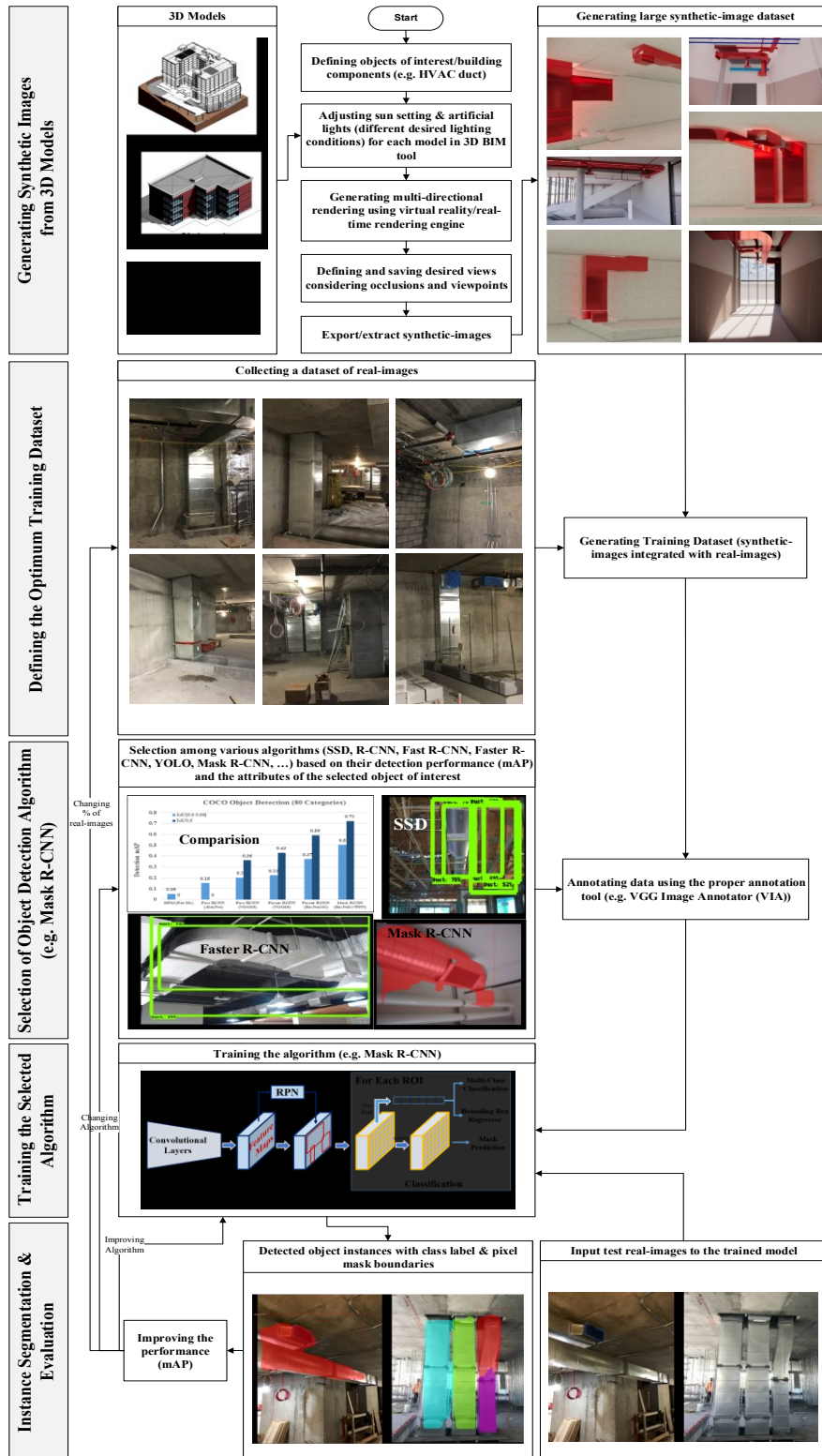


Figure 3-32: Automated Detection of Building Components for Updating Project Schedule

The overall schematic diagram of the developed framework is shown in Figure 3-33. The developed framework has five major processes: (1) synthetic image generation from 3D models (2) defining the optimum training dataset (3) selection of object detection algorithm (4) algorithm training and (5) object instance segmentation and evaluation. The framework enables the detection of building components benefiting from the generation of synthetic-images and mixing them with real images. Each of these processes is described subsequently.

In the first process, “synthetic image generation from 3D models”, 3D BIM models are used. Objects of interest or building components are defined in the first step of this process. All available 3D models (consisting of different components with different materials, shapes, and backgrounds) are used to deal with the variability existed in real-world data. In the following step, sun-setting and artificial lights (different desired lighting conditions) are adjusted and saved for each 3D model in the employed 3D BIM tool. Generating multi-directional rendering for each 3D model using a virtual reality/real-time rendering engine is performed next. Then, the desired views considering occlusions and viewpoints are defined and saved for each of these 3D models. Finally, synthetic-images are exported/extracted in JPG or PNG format using employed virtual reality rendering engine. So a large dataset of synthetic-images is generated illustrating the selected building components from various viewpoints, with different levels of occlusion and under diverse illumination conditions.



**Figure 3-33: Developed Framework of Automated Detection of Building Components**



In the second process, which is defining the optimum training dataset, the effect of combining real images and synthetic images in the training dataset on the performance of the detection model is investigated. The purpose here was to find whether the additional use of synthetic images to real images can be used without a negative impact on detection accuracy. And, if so, to find the most suitable mix of these two types of images. Various training data mix scenarios were tested, and achieved results (in terms of various performance metrics) were recorded in search of the most suitable mix. Five different training datasets, including only real-images, only synthetic-images, and a mix of both with different ratios (real/synthetic  $\approx 1/3$ , real/synthetic  $\approx 1/2$ , and real/synthetic  $\approx 2/3$ ), were used.

In view of the proven superiority of deep learning-based algorithms over traditional algorithms for object detection, the third process, “selection of object detection algorithm,” has focused on various deep learning-based object detection algorithms to find the most proper one for the detection of building components. Liu et al. (2019) categorized deep learning-based object detection frameworks into region-based frameworks (such as Spatial Pyramid Pooling (SPP)-Net, Region-based Convolutional Neural Networks (R-CNN) series, Mask R-CNN, and Region-based Fully Convolutional Network (RFCN) and unified frameworks (such as DetectorNet, CornerNet, OverFeat, Single Shot multi-box Detector (SSD), and You Only Look Once (YOLO)). Region-based frameworks consist of three general steps: generating category-independent region proposals from an image, extracting CNN features from generated regions, and determining the category labels of the proposals applying category-specific classifiers. In contrast, in the unified frameworks, class probabilities and bounding box offsets are predicted from images using a single feed-forward CNN. Since a single network contains all computations and does not need to optimize each component of a complex region-based pipeline, so these frameworks significantly decrease required complex and expensive computation (Liu et al., 2019). Hou et al. (2020) classified available deep learning-based object detection algorithms into two distinct groups: algorithms that are based on the region proposals (such as R-CNN family) and algorithms that are based on regression (such as YOLO and SSD). These algorithms are described in the following sections:

- **R-CNN**

Using a sliding window with pre-defined size to scan an image has been a conventional method for object detection. But it had two limitations, including high computational time and power and failure of detecting objects with different sizes. So a novel algorithm named “R-CNN” was proposed by Girshick et al. in 2014 to address the mentioned issue through introducing region proposal concept and selective search process in which adjacent pixels were grouped based on their color and texture to form different segments in the image and then segmented objects were surrounded by bounding boxes with different sizes as shown in Figure 3-34. After extracting region proposals from an input image and using CNN for computing proposals’ features, SVM and a linear regression model were used to classify the detected objects and fit the bounding boxes with the objects, respectively. Despite the superiority of R-CNN over sliding window detectors, there are still some shortcomings applying R-CNN, such as high computational time due to running CNN for each region

proposal and complexity resulted from the training process required for CNN, SVM and regression model (Panthula, 2018).

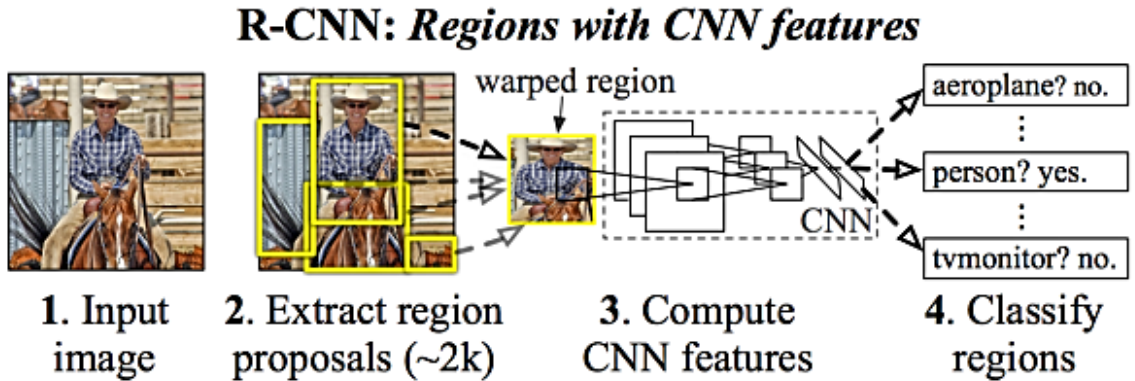


Figure 3-34: R-CNN Flow Diagram (Girshick et al., 2014)

- **Fast R-CNN**

In 2015, Girshick proposed Fast R-CNN in which training and testing speed and detection accuracy were improved compared with R-CNN. As shown in Figure 3-35, the Region of Interest Pooling (RoIPool) technique was used to run CNN once for overlapping regions instead of applying CNN on every single region. Moreover, he applied the Softmax layer (which does not need to be trained) and the linear regressor layer in parallel instead of training CNN, SVM classifier, and bounding box regressor. Despite the achieved improvement, Selective Search was still used to generate bounding boxes and resulted in a slow process (Panthula, 2018).

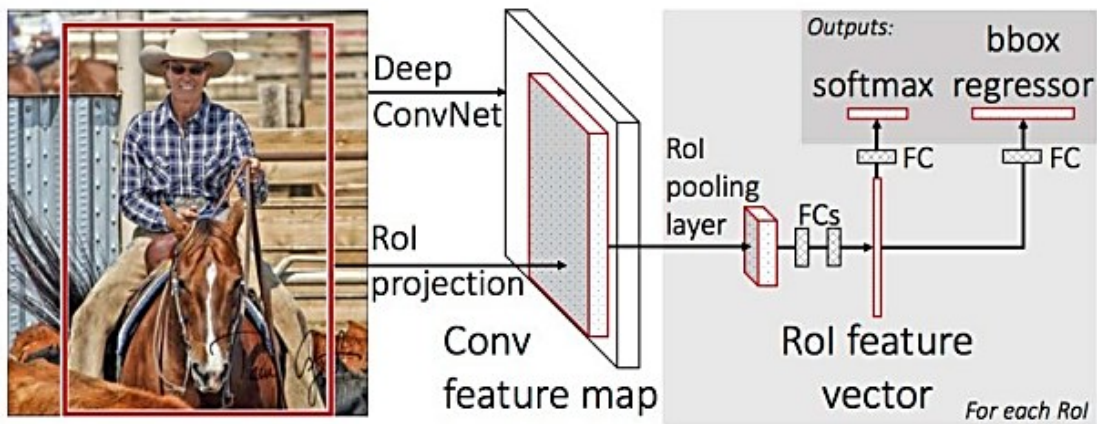
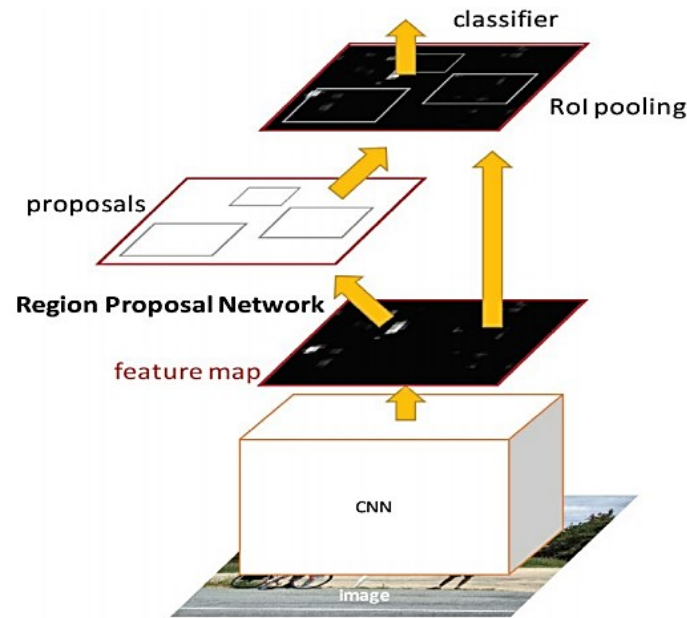


Figure 3-35: Fast R-CNN Flow Diagram (Girshick, 2015)

- **Faster R-CNN**

In another research done by Ren et al. (2017), Region Proposal Network (RPN) was introduced, and only a single CNN was applied for both region proposal and classification to improve Fast R-CNN.

As shown in Figure 3-36, Faster R-CNN included RPN in which a CNN was applied to generate detection proposals and a detector similar to Fast R-CNN. To implement RPN, many anchor boxes were used to generate region proposals using the sliding window technique. A set of anchor boxes surrounded each object while each anchor box covered a portion of that object, and Intersection Over Union (IOU) algorithm was used to calculate the accuracy (through comparing with a pre-defined threshold) of various anchor boxes to detect the object. Using anchor boxes could also make the algorithm able to detect various objects which were overlapping each other (Panthula, 2018).



**Figure 3-36: Faster R-CNN Flow Diagram (Ren et al., 2017)**

- **Mask R-CNN**

In the Mask R-CNN algorithm developed by He et al. in 2017, instead of localizing and classifying an object using bounding boxes and a classifier respectively, each pixel of each object is localized and segmented. As shown in Figure 3-37, Mask R-CNN includes the class box, which is an object detector acquired from Faster R-CNN and a fully convolutional network for objects semantic segmentation. Moreover, Mask R-CNN uses “Bilinear Interpolation” to achieve ROI alignment against other region-based algorithms (Panthula, 2018).

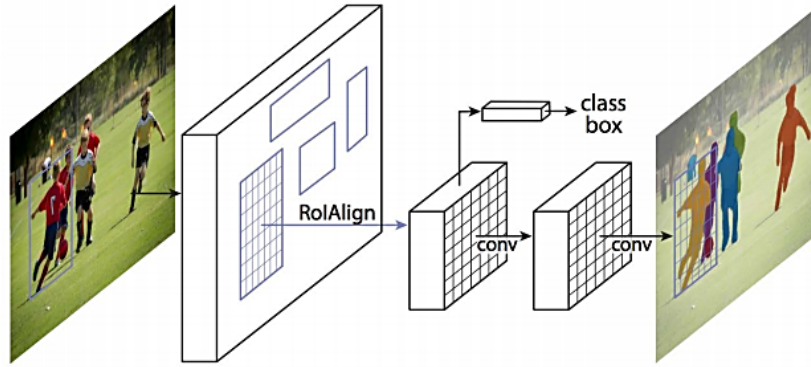


**Figure 3-37: Mask R-CNN Framework (He et al., 2017)**

- **SSD**

As mentioned before, the generation of region proposals and using a classifier to classify the detected objects from region proposals are the main processes of all the region-based algorithms, which results in a complicated and slow detection procedure. These algorithms are not proper for real-time object detection. In contrast, in regression-based algorithms like SSD, region proposals have been replaced by bounding boxes, which can imbed the whole detection procedure in a single forward pass network. Due to the high accuracy of the VGG model in object detection, transfer learning is used in SSD by adding the VGG model in the first layers as the base model. SSD is trained to generate a class prediction related to each anchor box and an offset value (using the IOU algorithm). Non-maximum suppression is used to select the anchor box with the highest confidence score among multiple boxes generated per object. Since the frame rate of processing images affects SSD in detecting objects, so SSD is not the proper algorithm for object detection using videos with a high frame rate (Panthula, 2018). Figure 3-38 illustrates the SSD framework. Figure 3-38(a) indicates the input image with ground truth boxes for all the objects, Figure 3-38(b) shows the evaluation of a small set (e.g., 4) of default boxes of various aspect ratios at each location in several feature maps (with different scales, e.g.,  $8 \times 8$  and  $4 \times 4$ ), and Figure 3-38(c) illustrates prediction of both the shape offsets of each default box and the confidences for all object categories ( $c_1, c_2, \dots, c_p$ ) (Liu et al., 2016).

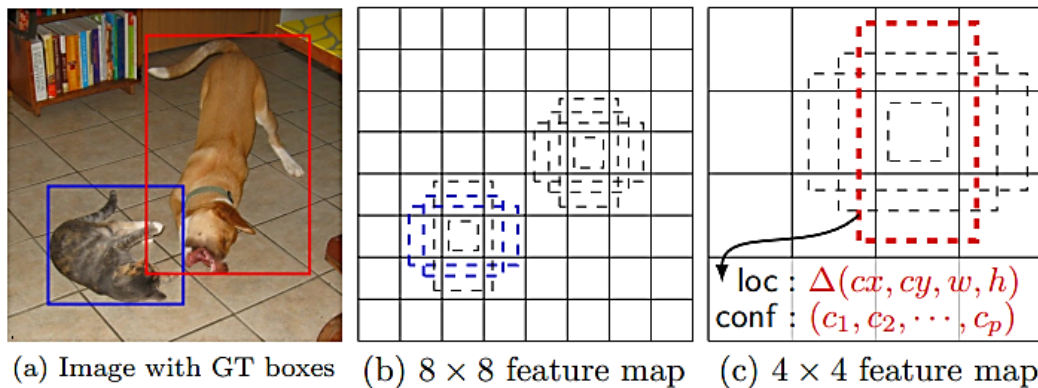


**Figure 3-38: SSD Framework (Liu et al., 2016)**

- **YOLO**

YOLO is also a regression-based object detection algorithm. YOLO was introduced by Redmon et al. in 2016, and it has been one of the fastest object detection algorithms with frame rates up to 155 FPS, which makes it capable of detecting objects in real-time. Its high speed is attributed to its end-to-end framework in which the entire image is used once for both training and testing (Figure 3-39). Dividing the input image into a grid, predicting various bounding boxes for every grid cell, a confidence score for all the bounding boxes, and also class probabilities are the main processes of the YOLO algorithm. However, YOLO is really fast and applicable using real-time videos; it has shortcomings as well, such as failing to detect more than one class of objects in a single grid cell (Panthula, 2018).

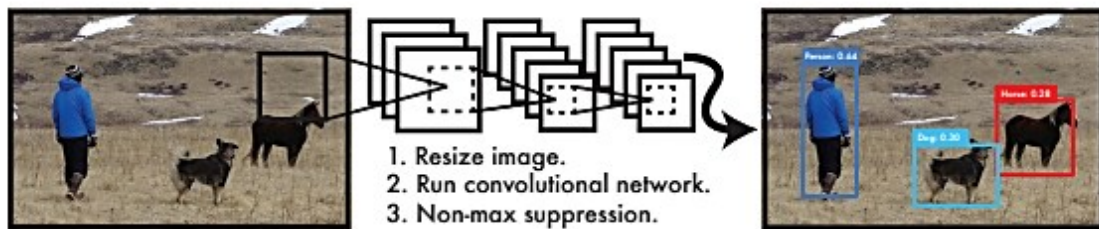


**Figure 3-39: YOLO Detection System (Redmon et al., 2016)**

Each object detection algorithm has its pros and cons. For example, “end-to-end multitask training” can be achieved by applying Faster R-CNN, but it cannot be used as a real-time object detector, or YOLO v3 is “fast and accurate in meeting real-time requirements,” but it is not a suitable detector for “medium-sized and larger objects” (Hou et al. 2020). The algorithm used in this study is selected based on the published results reported by other researchers. Figure 3-40 illustrates the performance (mean Average Precision (mAP) for two thresholds of Intersection over Union (IoU)) of various object detectors on Common Objects in Context (COCO) dataset. It indicates that Faster R-CNN and Mask R-CNN (with a backbone network of ResNet101 and ResNeXt101- Feature Pyramid Network (FPN) respectively) achieved the highest performance for object instance segmentation (Liu et al. 2019). In another research done by Huang et al. (2017), it was shown that Faster R-CNN has higher performance (overall mAP) for detecting medium and large objects compared with SSD and R-FCN (Figure 3-41).

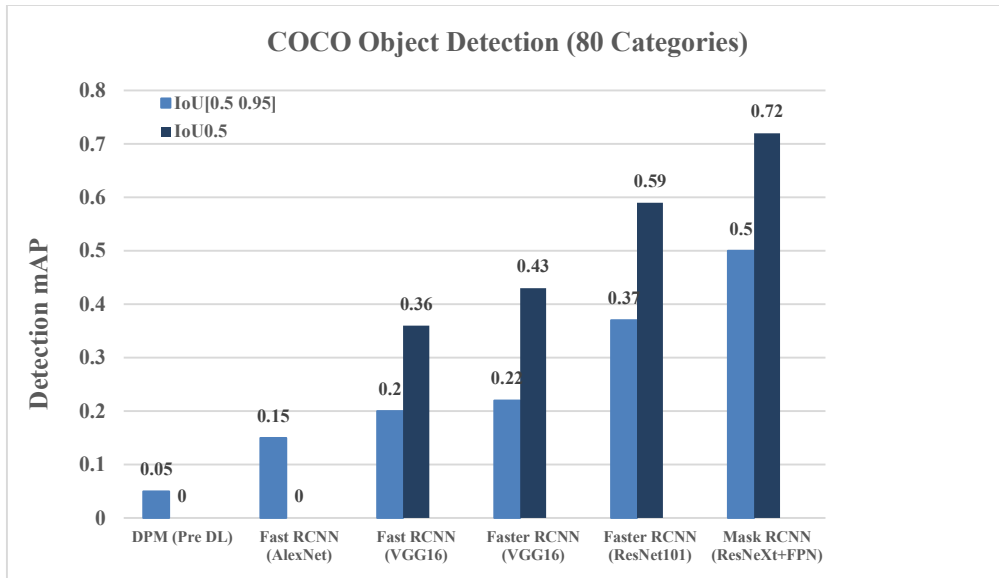


**Figure 3-40: Evolution of Object Detection Performance on COCO from Early 2015 to Late 2017 (Liu et al., 2019)**

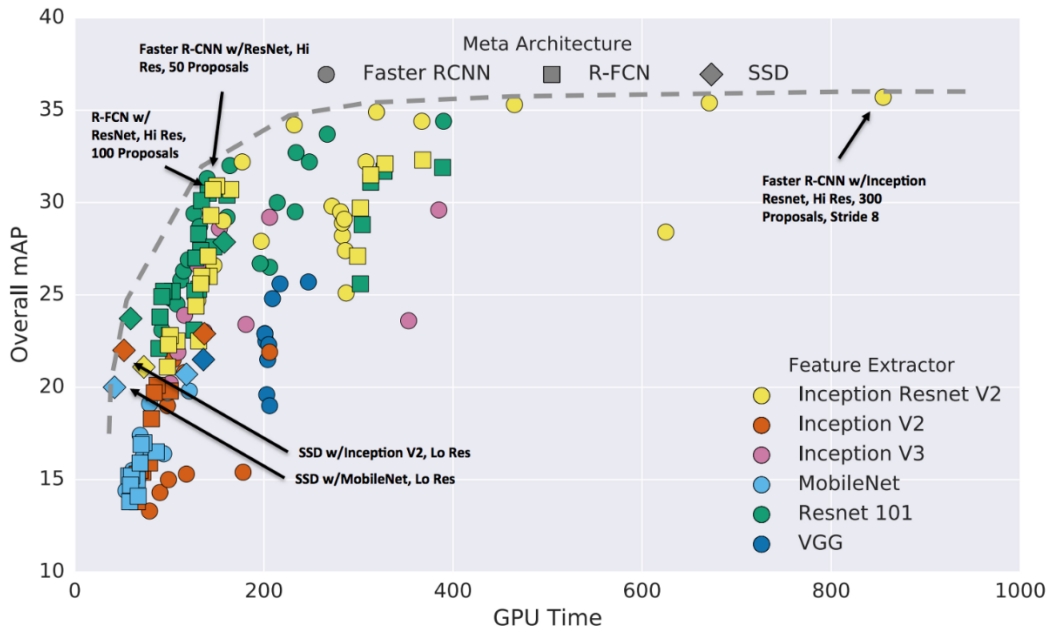


**Figure 3-41: Detection Accuracy versus Detection Time of Different Algorithms (Huang et al., 2016)**

Furthermore, SSD, R-FCN, and Faster R-CNN were evaluated based on their detection speed and accuracy. As shown in Figure 3-42, among other algorithms, Faster R-CNN possesses a logical trade-off between the accuracy (mAP) and speed (running time per image in terms of milliseconds). For instance, Faster R-CNN roughly requires 300 milliseconds for object detection with around 35% mAP, or in another case, it needs about 250 milliseconds to approximately detect objects in an image with about 33.5% mAP. So

in this process, the most suitable algorithm (SSD, Faster R-CNN, Mask R-CNN, YOLO, etc.) is selected based on its performance (mAP) and also the attributes of the building components to be detected.

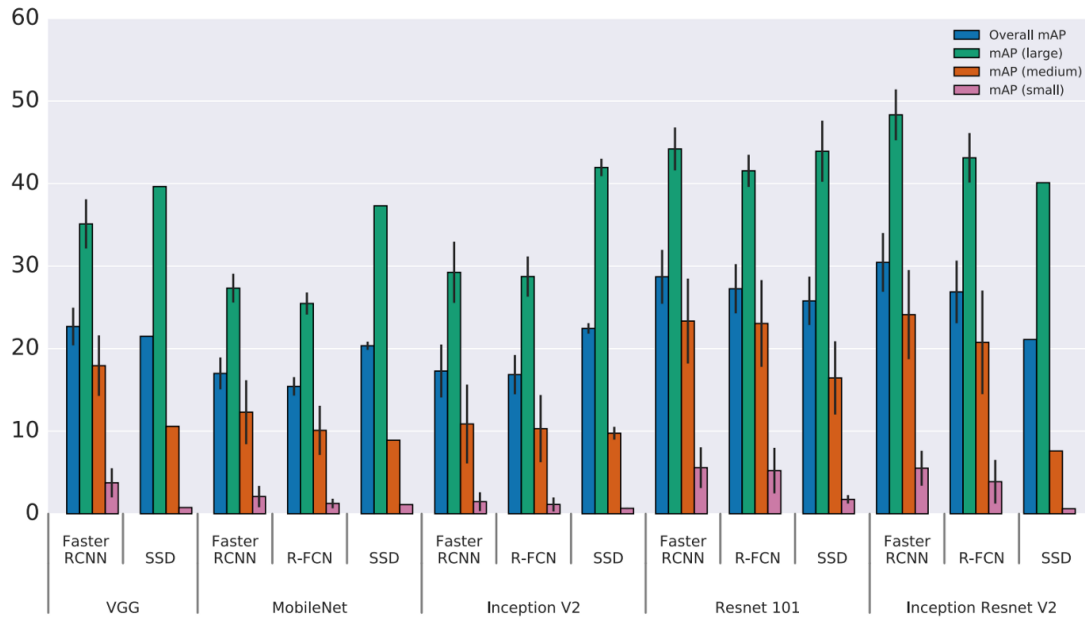


**Figure 3-42: Detection accuracy of different algorithms to detect objects with large, medium, and small sizes (Huang et al., 2016)**

After generating the training datasets, the next process is training the selected algorithm. The first step for training any selected deep learning-based algorithm is labeling the images with ground truth annotations using a proper annotation tool. The annotations include the location and class of the selected building components. To obtain the optimal weight parameters of the model, the annotation file and the generated dataset are used as the inputs to train the selected algorithm in which the input images are mapped to their corresponding annotations with the minimum loss value (sum of the classification loss, bounding-box loss, and mask loss).

After generating various training datasets and training the algorithm in the previous processes, now it is time to test the trained model, which is the last process (object instance segmentation and evaluation) of the object detection framework. Thus, a subset of real-images which were not included in the training datasets are used as inputs to the trained model and mask, bounding-box, and the class category for each object of interest are predicted in the output image as shown in Figure 3-33 (while Mask R-CNN is selected as the detection algorithm). Precision and recall are commonly used metrics for performance evaluation of the object detectors. The accurate percentage of the predicted objects is measured by precision rate, and the accuracy of the model to find positive cases is evaluated by the recall rate (Equations 3-25 & 3-26).

$$\text{Precision} = \frac{TP}{TP+FP}$$

Equation 3-25

$$\text{Recall} = \frac{TP}{TP+FN}$$

Equation 3-26

TP, FP, and FN stand for True Positive, False Positive, and False Negative, respectively. Precision and recall are always between 0 and 1, and Average Precision (AP) shows the area under the precision-recall curve. The higher precision and recall are, the more robust the model is with a compelling AP.

At the end of this process, we have a trained and tested object detection algorithm that is ready to be fed with real images to detect various building elements. The input images are the image taken from the job site during the construction model and have already been used as inputs for CAE or SSIM to visualize the progress. The objective of this developed framework is to detect and recognize the building elements included in the images visualizing the progress, which results in identifying the installed or constructed elements throughout a specific period when the progress has been visualized. The project schedule is consequently updated based on actual progress. It will be used as an input for updating MRP and optimized material delivery schedule, respectively, during the construction phase.



## CHAPTER 4: TESTING AND VALIDATION

In this chapter, the algorithms developed and customized in Chapter 3 are tested and validated using real data and laboratory experiments. So the first section of this chapter is related to the performance evaluation of the newly developed GA-MLP algorithm, and the second section includes validation of the developed progress visualization methods. Eventually, in the third section, the performance of the developed framework for automated detection of building components using a mix of real and synthetic-images for training Mask Region-based CNN (Mask R-CNN) is evaluated in the context of a real-world case example, and the results are presented.

### 4.1 GA-MLP Algorithm

This section is a marginally modified version of “Optimized material management in construction using multi-layer perceptron” published in Canadian Journal of Civil Engineering (Golkhoo and Moselhi, 2019) and has been reproduced here.

The performance of the newly developed automated method is evaluated using a numerical example of the construction of two office buildings. The outputs of the GA-MLP algorithm are compared with the outputs of the application of pure GA optimization in the same case. To simplify the comparison, the first scenario in which material shortage is prohibited during the construction phase, and only one material which is reinforcing steel (rebar with diameter  $\geq 20\text{mm}$ ) is selected. The project schedule shows that the buildings have to be constructed in 64 weeks. It is worth noting that based on the size and complexity of the project, the developed algorithm can generate an optimized material delivery schedule on a daily, weekly, or monthly basis. The required data to run GA, and the developed GA-MLP algorithm is shown in Table 4-1.

**Table 4-1: Input Data for GA and GA-MLP (Golkhoo and Moselhi, 2019)**

Cost Type	Symbol	Amount	Unit
The average administrative cost for a single order	$C_o$	10	\$/Order
The unit price for order $d$	$p_d$	710 if $Q_d < 100$ 628 if $Q_d \geq 100$	\$/Ton
Storage cost for an individual unit quantity (Ton)	$C_s$	40	\$/Week
Weekly Interest Rate	$I$	0.0003	NA
Annual Escalation Rate	$i$	0.015	NA

By having the project schedule in which materials are assigned to the activities and by following the developed algorithm shown in Figure 3-5, Material Requirement Vector is generated and illustrated in Figure 4-1 and Figure 4-2.

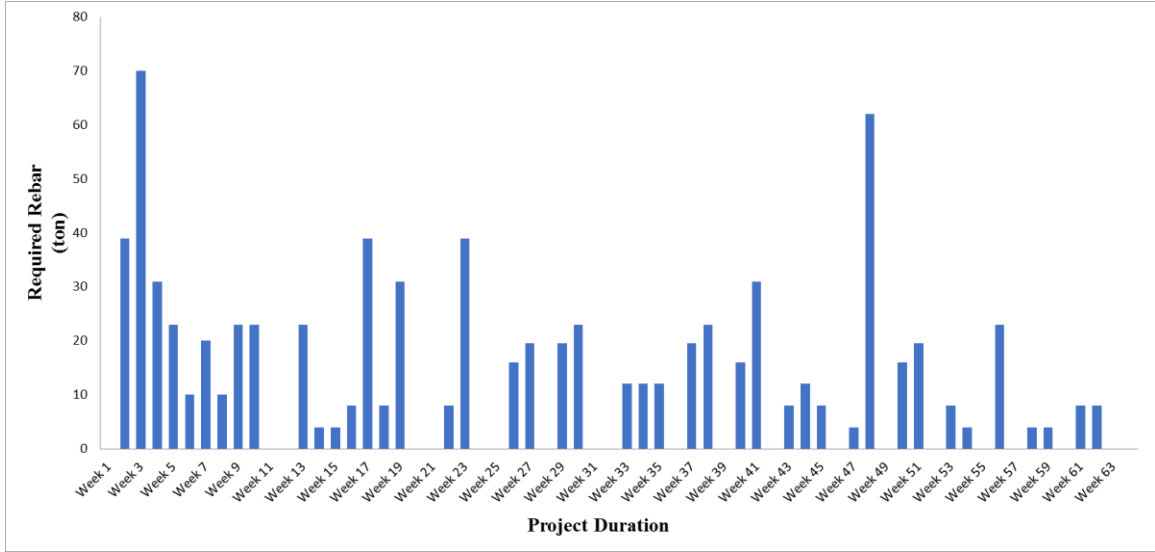


**Figure 4-1: Material Requirement Plan (Golkhoo and Moselhi, 2019)**

W1	W2	W3	W4	W5	W6	W7	W8	W9	W10	...	W60	W61	W62	W63	W64
Q1	Q2	Q3	Q4	Q5	Q6	Q7	Q8	Q9	Q10	...	Q60	Q61	Q62	Q63	Q64
0	39	70	31	23	0	0	0	23	23	...	0	8	8	0	0

**Figure 4-2: Rebar Requirement Vector (ton/day) (Golkhoo and Moselhi, 2019)**

Using the input data from Table 4-1 and the following parameters (It is worth mentioning that sensitivity analysis could be useful to define population size, mutation and crossover probabilities) and by applying Equations 3-1 to 3-7, it is possible to run GA and GA-MLP algorithm to generate Optimized Material Delivery Schedule for rebar:

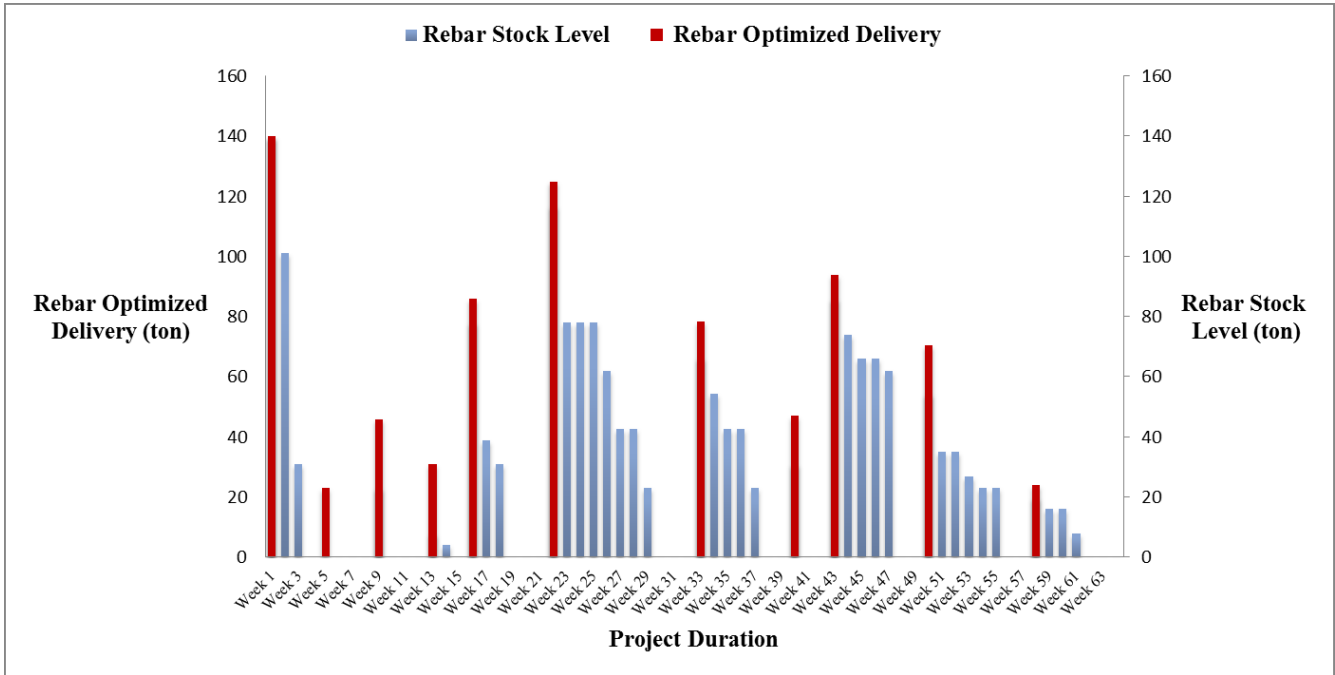
- Population size: 200
- Number of Generation: 200
- Number of epoch: 200
- Crossover probability: 0.85;
- Mutation probability: 0.06; and
- Termination condition (applied for GA): no improvement for 20 iterations

The following constraints have been taken in to account as well:

- $0 \leq SQ_{T_C}$  (Stock Quantity at time  $T_C \leq 200$  (Max Storage Capacity (ton)) which means there should not be any shortage of material during the construction phase
- $Q_{T_C}$  (Material Quantities per Order)  $\geq 10$  (Min Shipping Quantity (ton)); and
- $\sum_{T_C=1}^D Q_{T_C} - \sum_{T_C=1}^D q_{T_C} = 0$ , which shows that there should not be a surplus quantity of material at the end of the project.

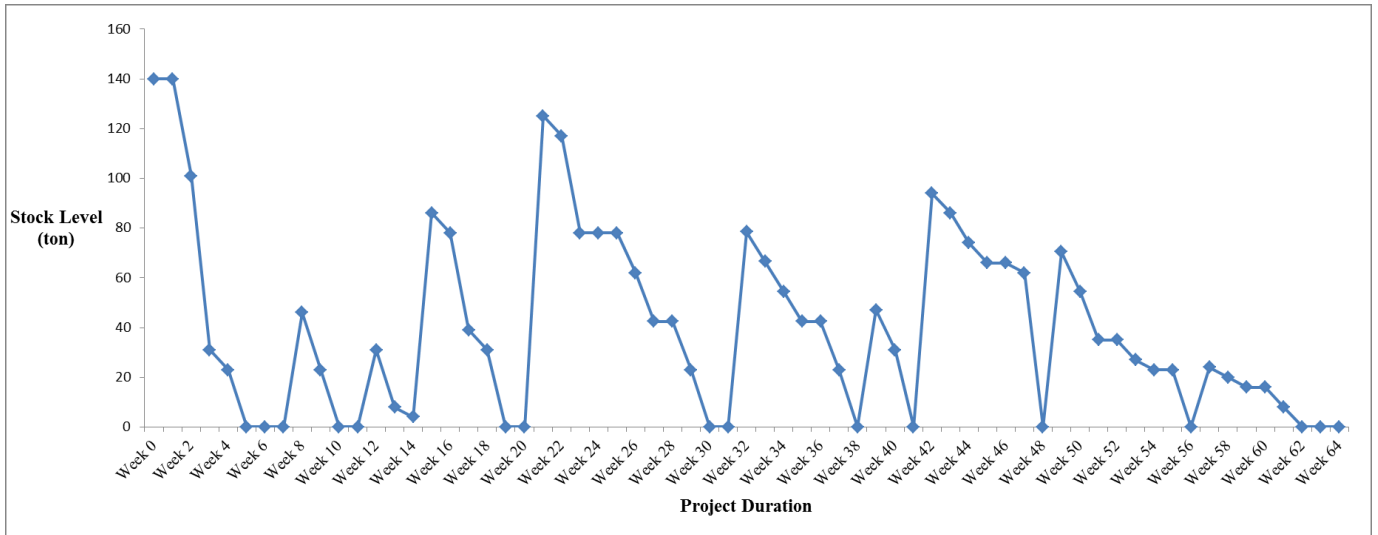
The developed GA-MLP algorithm is coded in a user-friendly computational platform using MATLAB® 2018a. It can be used as a stand-alone application or can be integrated with the other algorithms in the CMM framework. The outputs obtained from the GA-MLP algorithm run are illustrated in terms of optimized rebar delivery schedule (the near-

optimum chromosome as the final output of the algorithm) in combination with rebar stock level during the construction phase (output of Equation 3-7) in Figure 4-3.



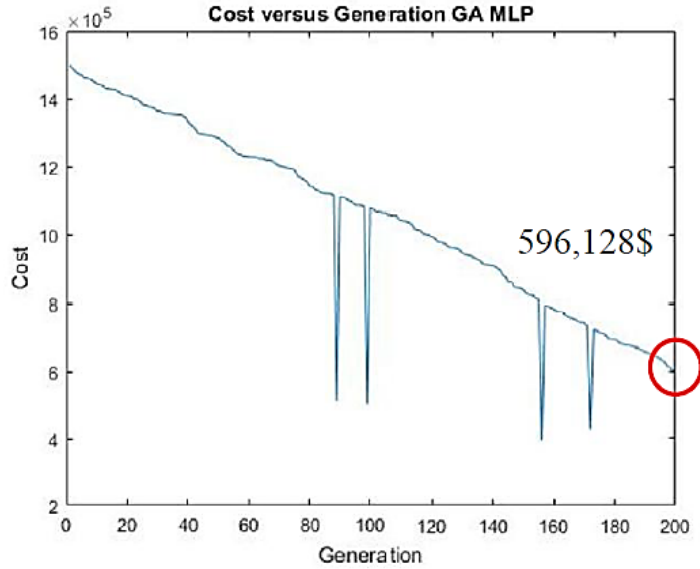
**Figure 4-3: Optimized Rebar Delivery Schedule and Rebar Stock Level (Golkhoo and Moselhi, 2019)**

Figure 4-3 indicates that in this project, if rebar is bought according to the red columns, it will result in the least cost, without leading to rebar shortage or surplus. It is worth noting that the numbers in the left vertical axis related to the optimized rebar delivery indicate that how much rebar on which week has to be bought if a contractor or a material professional tends to procure rebar with the least cost without any shortage during the construction phase or without a surplus at the end of the project. The maximum storage space and the minimum shipping size are considered in this optimal solution, which results in the minimum cost. The right vertical axis specifies rebar quantity in the storage in each week. Figure 4-4 illustrates the optimized rebar delivery schedule, including rebar delivery, consumption, and stock level. For example, it is shown that a batch of 140 tons of rebar is delivered in the first week, but there is not any rebar consumption during this week. So the rebar stock level remains constant (140 tons). In the second week, the rebar consumption is 39 tons, and because there is no rebar delivery, the rebar stock level is reduced to 101 tons.



**Figure 4-4: Rebar Delivery, Consumption and Stock Level (Golkhoo and Moselhi, 2019)**

The convergence of total rebar cost as the value of the objective function in the given generation is shown in Figure 4-5. It can be seen that the total rebar cost that has been optimized by the GA-MLP algorithm in 200 generations is 596,128\$. As indicated in Figure 4-5, some discontinuities are common in learning or heuristic process, which is not over-trained and consequently over-fitted. The only thing that matters is the fact that the general behavior of the graph should be minimized. The amount of error showing the performance of the GA-MLP algorithm is presented in Figure 4-6. To clarify the concept of error, which is measured to present the performance of the GA-MLP algorithm, it should be mentioned that, GA chromosomes are the coefficients of a polynomial that maximizes our gain in the process of optimization. In other words, it should be defined that in each step forwarding to reach the objective function, how close it has gotten through this function. This process is called minimizing error. Based on this policy, we move toward our desired function, the closer we are to the function, the better approximation has been computed by chromosomes. Chromosomes are the coefficients of a polynomial; this polynomial can lead to the answer close to zero if we substitute it into the objective function. Since GA-MLP is the biased version of the pure GA, we should apply mini-batch inside of the processing algorithm to be able to minimize the error. So it should be mentioned that in Figure 4-6, the mini-batch size instead of epoch or iteration value is shown on axis *X*, and axis *Y* shows the scaled expected error, which is the log-likelihood of the error to visualize the error in a better scale.



**Figure 4-5: Convergence of Total Material Cost (Golkhoo and Moselhi, 2019)**

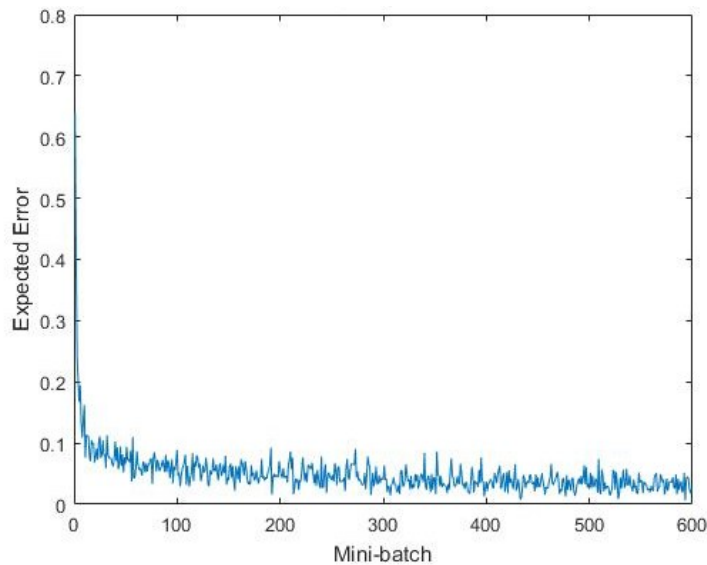


**Figure 4-6: Error in GA-MLP algorithm (Golkhoo and Moselhi, 2019)**

As mentioned before, the same required information used to run GA as well. While running GA, there was not any tangible improvements after 200 generations and termination condition was met reaching 220 iterations. To indicate the superiority of the developed GA-MLP algorithm over GA, first, the fitness value calculated by GA-MLP is compared to the fitness value calculated by GA illustrated in Figure 4-7. The total rebar cost that has been optimized by the GA algorithm in 200 generations is 688,978\$, which is more than the 596,128\$ (the minimum cost obtained from the GA-MLP algorithm considering 200 iterations).

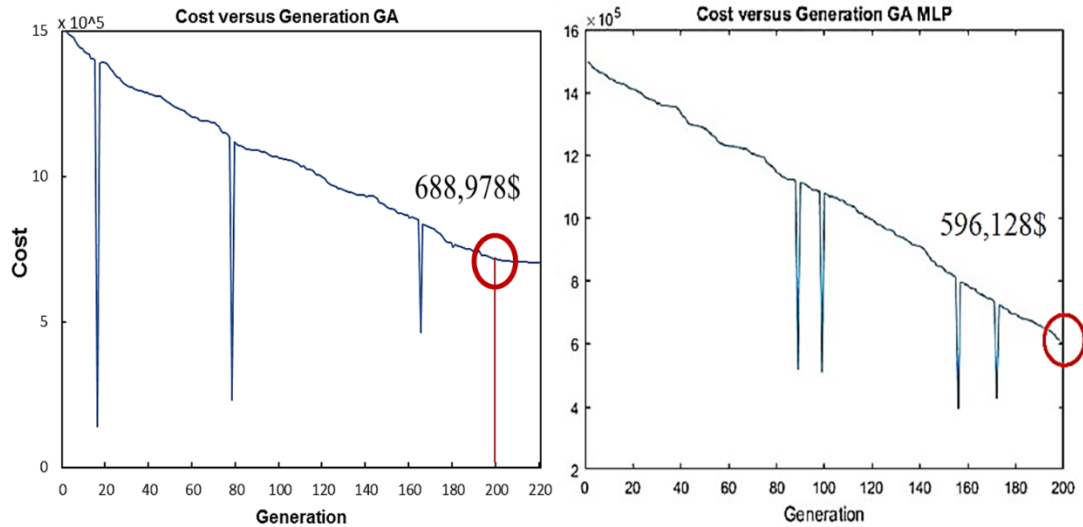


**Figure 4-7: Comparison of the Convergence of Total Material Cost Using GA (Left) and GA-MLP algorithm (Right) (Golkhoo and Moselhi, 2019)**

Second, the amount of error in both algorithms are compared and presented in Figure 4-8. Comparing the error value, it can be concluded that against the error value in GA, the error in GA-MLP algorithm converges toward zero when the mini-batch size is increasing and reaching almost to 600.

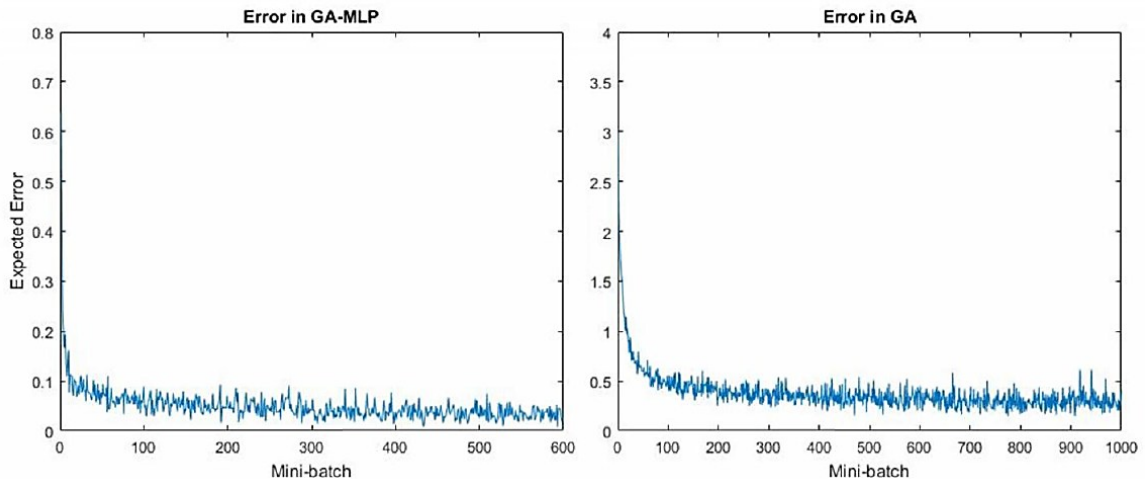


**Figure 4-8: Comparison of Error in GA-MLP (Left) and GA (Right) (Golkhoo and Moselhi, 2019)**

In addition to profiting from the capabilities of GA as a greedy optimization engine, practicality and the excellence of the presented method is due to creating a memory for GA by integrating MLP with GA to avoid getting stuck to the local minima as the main weakness of GA. MLP gives a capacity of inference to GA by regularizing the parameters using their fluctuation history to be able to jump over the local minima. In summary, the automated GA-MLP method represents a promising way forward to optimize the delivery and inventory of construction materials not only in the planning phase but also in the construction phase.

## 4.2 Progress Visualization Methods

Different laboratory and field experiments have been conducted to validate the developed progress visualization methods, including CAE and SSIM. The following subsections present the detailed descriptions of the experiments.

### 4.2.1 CAE

Validation of CAE as the first developed progress visualization method was done through three laboratory and one field experiments. The preliminary obtained results were decisive for the proof of concept.

To visualize the progress occurred in both indoor and outdoor construction sites between time “ $T_1$ ” and time “ $T_2$ ” under diverse illumination conditions, six scenarios were designed (see Table 4-2).

For example in the 2nd experiment for the outdoor environment, the first input image is taken from the southeast elevation of a building under construction at the time “ $T_1$ ”. After some progress, the second input image is taken from the southeast elevation of the same building at time “ $T_2$ ”. The input images had a small change in their viewpoints to examine CAE performance in detecting progress dealing with slight rotation in viewpoints (around 5 degrees). In these laboratory experiments, the available sample architecture project in Autodesk Revit software (i.e., a small residential building with two floors) was selected. As mentioned in the previous section, in the first step, the 3D model of the building was exported from Autodesk® Revit 2017 as an NWC file to be integrated with its corresponding schedule in Autodesk® Navisworks® Manage 2017. The generated 4D as-planned model (saved as NWD file) was used to simulate the construction process, as shown in Figure 4-9. To apply the proposed CAE algorithm for both indoor and outdoor progress monitoring, various viewpoints were created and saved in Navisworks. Two viewpoints illustrated the living room as an indoor environment and the southeast elevation of the building as an outdoor environment, respectively.

**Table 4-2: Laboratory Experiments Scenarios**

	<b>Indoor</b>	<b>Outdoor</b>
<b>1<sup>st</sup> Experiment</b>	Scenario #1	Scenario #2
	1 <sup>st</sup> Input Image (incomplete building at time “ $T_1$ ” “Living room.”	1 <sup>st</sup> Input Image (incomplete building at time “ $T_1$ ” “Southeast elevation.”
	2 <sup>nd</sup> Input Image with <u>same viewpoint and illumination</u> (incomplete building with some progress at time “ $T_2$ ” “Living room.”	2 <sup>nd</sup> Input Image with <u>same viewpoint and illumination</u> (incomplete building with some progress at time “ $T_2$ ” “Southeast elevation.”
<b>2<sup>nd</sup> Experiment</b>	Scenario #3	Scenario #4
	1st Input Image (incomplete building at time “ $T_1$ ” “Living room.”	1st Input Image (incomplete building at time “ $T_1$ ” “Southeast elevation.”
	2 <sup>nd</sup> Input Image with a <u>different viewpoint and same illumination</u> (incomplete building with some progress at time “ $T_2$ ” “Living room.”	2 <sup>nd</sup> Input Image with a <u>different viewpoint and same illumination</u> (incomplete building with some progress at time “ $T_2$ ” “Southeast elevation.”
<b>3<sup>rd</sup> Experiment</b>	Scenario #5	Scenario #6
	1 <sup>st</sup> Input Image ( <u>incomplete</u> building at time “ $T_1$ ” “Living room.”	1 <sup>st</sup> Input Image ( <u>incomplete</u> building at time “ $T_1$ ” “Southeast elevation.”
	2 <sup>nd</sup> Input Image with <u>different viewpoint and illumination</u> ( <u>incomplete</u> building with some progress at time “ $T_2$ ” “Living room.”	2 <sup>nd</sup> <u>Input</u> Image with <u>different viewpoint and illumination</u> (incomplete building with some progress at time “ $T_2$ ” “Southeast elevation.”



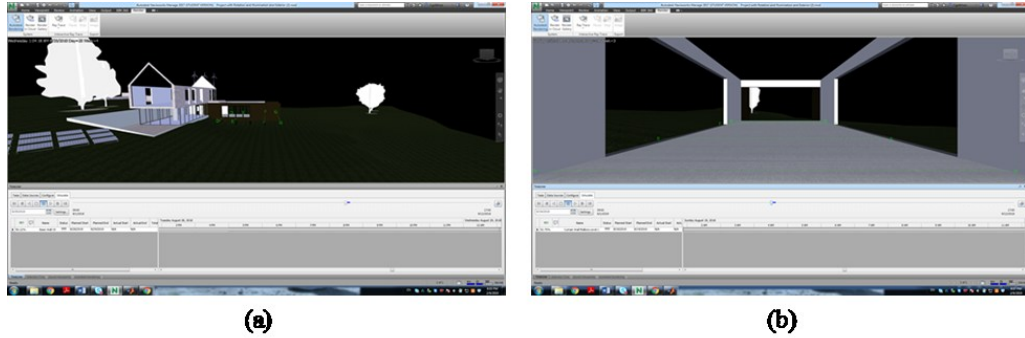


**Figure 4-9: Construction Process Simulation in Autodesk Navisworks: (a) Outdoor, and (b) Indoor Environment**

Various viewpoints can be set and saved using options to control the camera projection, position, and orientation in Autodesk Navisworks. So the world coordinates of the camera can be predefined in the project 3D model to be used in the construction phase for capturing real images from the construction job site. On the one hand, when a viewpoint is set and saved in Autodesk Navisworks, the camera position (local coordinate  $(x, y, z)$ ) and the distance between camera location and any specific points are known. On the other hand, since there is always a site survey drawing for any construction projects which has been imported into Autodesk Revit, so the world coordinate of project origin point, base point, and all other specific points of the 3D model are known. As a result, the world coordinate of the camera can be achieved and saved easily for future use knowing the world coordinate of any specific points and the distance between the camera location and that particular point.

Furthermore, as discussed in advance, to train CAE properly to make it independent of small visual changes, both indoor and outdoor viewpoints with slight rotation were saved as new viewpoints in Navisworks. In the second step, having generated as-planned simulation model with definite indoor and outdoor viewpoints (with and without rotation), frames (image) were extracted from the simulation through rendering in the cloud and were saved in datasets. Experiments were designed in such a way that the performance of the method for progress detection and visualization could be assessed in different illumination conditions. It is worth noting that, while extracting frames (images) from 4D model simulated in Autodesk Navisworks through rendering in the cloud, factors affecting illumination such as sun, exposure, time zone, latitude and longitude, north direction, date and time of image capturing can be simulated according to the real project condition as well. Images were rendered in two different time points (one in the morning and one in the evening).

In the next step, CAE was trained on generated image datasets of the indoor and outdoor environment, respectively. Training and test datasets of indoor environment images included 152 and 38 images, respectively, from both complete and incomplete buildings.

Training and test datasets of outdoor environment images also included 328 and 72 images, respectively, from both complete and incomplete buildings. The training datasets were augmented using 4-DoF affine transformation (similarity transformation) to bootstrap the

datasets to improve the performance of the algorithm. It is worth noting that 5 fold cross-validation was used while training CAE to improve its performance. So the training dataset was split into 5 folds, and CAE was trained on 4 folds (80%) of the training dataset. Then it was validated to check the performance for the 5th fold (20% of the training dataset). However, the larger size of the input images will result in better reconstruction; for memory issues, we reduced the size of the input images to 1/4 of their original dimensions. So CAE was trained, validated, and tested on images with size  $400 \times 122$  pixels using MATLAB (R2018a) on a Windows 64-bit platform with 3.40 GHz Core i7 CPU and 8 GB of memory. The CAE training procedure during 2000 epochs took about 45 minutes and 105 minutes for indoor and outdoor environment images, respectively, on four parallel CPU workers. Training time can be reduced to 1/4 if the operation is done using GPU.

Having trained CAE, progress was detected and visualized in terms of constructed building elements between two consecutive time points using test images. For the performance evaluation purpose, the output image visualizing the progress was compared with the ground truth image using the Structural Similarity (SSIM) index, which can measure the similarity between two images.

Each experiment is comprehensively elaborated in the following sections:

In the first experiment and scenario #1, Figure 4-10a shows the first test image of the outdoor environment (southeast elevation) illustrating the incomplete building at time  $T_1$ . Figure 4-10b shows the second test image of the same incomplete building at time  $T_2$  in which a Structural Insulated Panel (SIP) wall is built in place. Both input images have identical viewpoints and illumination conditions. Both test images were fed into the trained CAE sequentially. As explained before, the trained CAE mapped the first input image of an incomplete building to the complete building in the first step. So in the first output image (Figure 4-11(a)), all the elements remained to be completed from  $T_1$  to the end of the project were reconstructed and visualized in a particular color space. The same process is implemented for the second input image, and in the second output image (Figure 4-11(b)) all the elements remained to be completed from  $T_2$  to the end of the project were reconstructed and visualized in a different color space.

Then by fusing (correlating color spaces) the output images, the progress was visually recognized. As shown in Figure 4-11(c), the constructed SIP wall as the progress made between time " $T_1$ " and time " $T_2$ " was visualized. Final output (Figure 4-11(c)) was compared with the ground truth using the SSIM index, which is a decimal value between (-1) and (1), and getting closer to value (1) represents perfect structural similarity. The obtained SSIM index for the first outdoor experiment is 0.8919, being close to (1) it is deemed satisfactory. All the mentioned steps were implemented to visualize the progress of the indoor environment as well. Figure 4-12(a) shows the first test image of the indoor environment (living room) illustrating the incomplete building at time  $T_1$ . Figure 4-12(b) shows the second test image of the same unfinished building at time  $T_2$  in which four window frames in the eastern side of the living room and curtain wall mullions on the southern side of the living room are installed as simple progress. Both input images have identical viewpoints and illumination conditions. These test images were fed into the trained CAE sequentially and as shown in Figure 4-12(c), the installed window frames and

curtain wall mullions as the progress made between time “ $T_1$ ” and time “ $T_2$ ” were visualized. The obtained SSIM index for the first indoor experiment is 0.8763, which is deemed satisfactory as well.

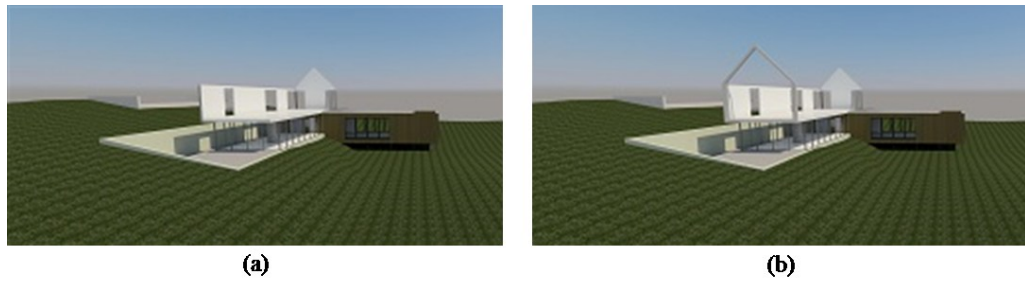


**Figure 4-10: Outdoor Test Images in Scenario #1: (a) at  $T_1$ , and (b) at  $T_2$**

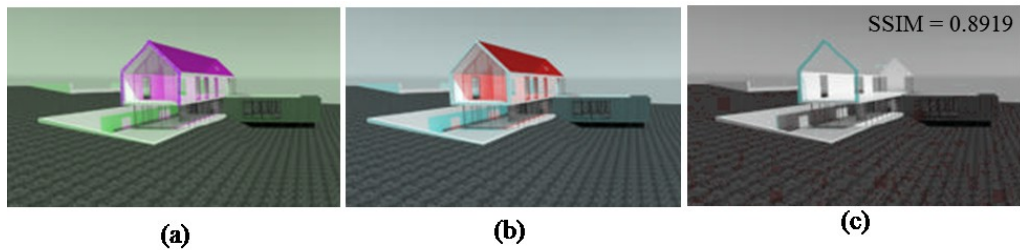


**Figure 4-11: CAE Output Images: (a) Reconstructed Image at  $T_1$ , (b) Reconstructed Image at  $T_2$ , and (c) Visualized SIP Wall**

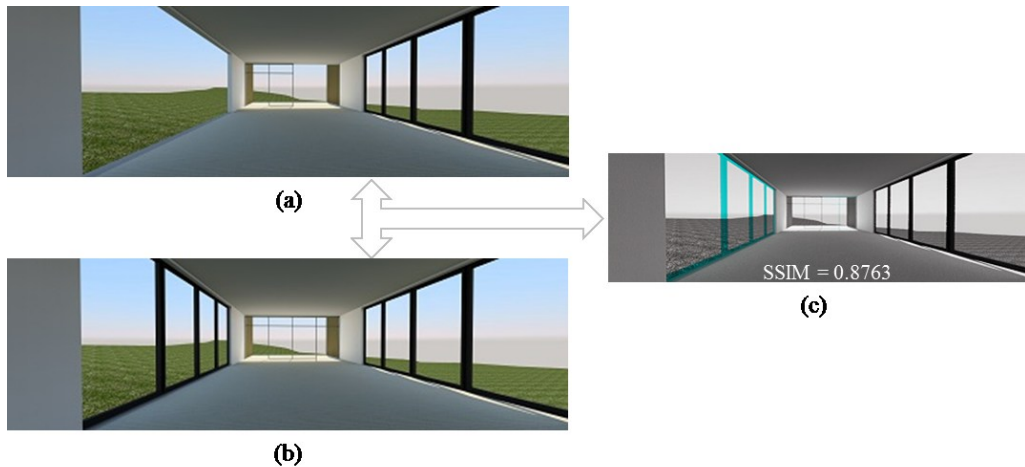
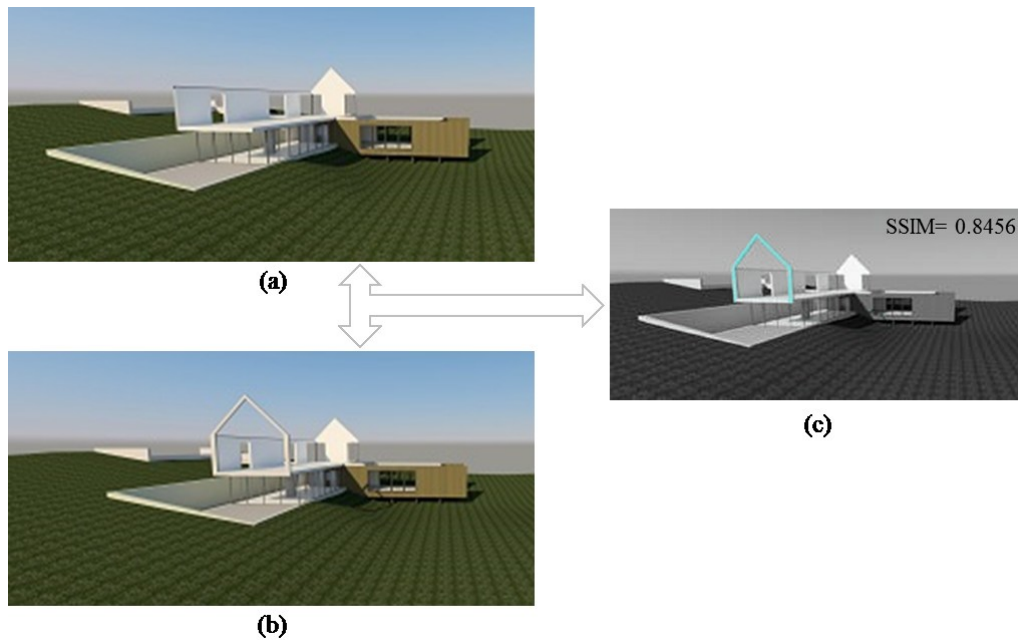


**Figure 4-12: Test Images in scenario #2: (a) at  $T_1$ , (b) at  $T_2$ , and CAE Output: (c) Visualized Window Frames and Curtain Wall Mullions**

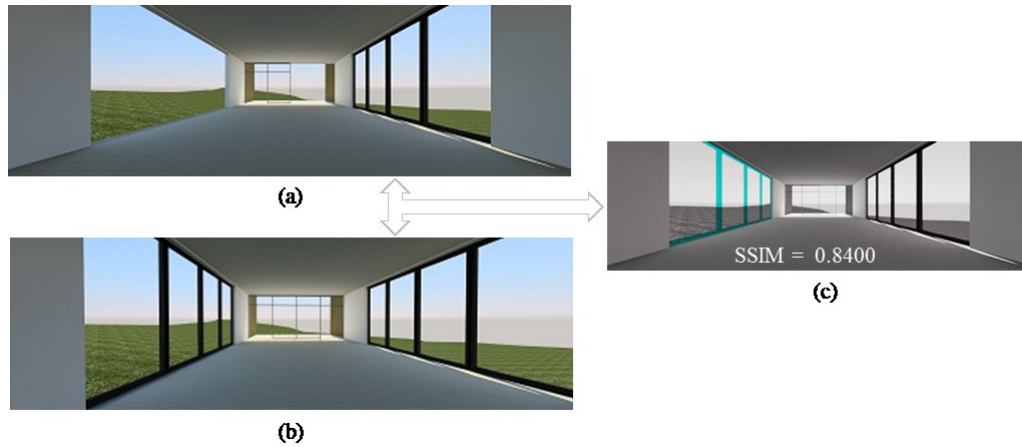
In the second experiment and scenario #3, Figure 4-13(a) shows the first test image of the outdoor environment (southeast elevation) illustrating the incomplete building at time  $T_1$ . Figure 4-13(b) shows the second test image of the same unfinished building at time  $T_2$  in which a SIP wall is built in place as simple progress. As presented in Table 4-2, the viewpoint was rotated around 5 degrees in the second test image to assess the developed

algorithm performance facing rotational deviations of the cameras capturing images. But both input images have identical illumination conditions in this experiment. Both test images were fed into the trained CAE sequentially. As shown in Figure 4-13(c), the constructed SIP wall as the progress made between time “ $T_1$ ” and time “ $T_2$ ” was visualized. The obtained SSIM index is 0.8456, and it is acceptable.

All the mentioned steps were implemented to visualize the progress of the indoor environment as well. The first test image of the indoor environment (living room) at time  $T_1$  and the second test image of the same incomplete building at time  $T_2$  are shown in Figure 4-14(a) and 4-14b, respectively. It is shown in Figure 4-14(b) that four window frames in the eastern side of the living room and curtain wall mullions on the southern side of the living room are installed as simple progress. Both input images have identical illumination conditions, but the viewpoints are different. These test images were fed into the trained CAE sequentially and as shown in Figure 4-14(c), the installed window frames and curtain wall mullions as the progress made between time “ $T_1$ ” and time “ $T_2$ ” were visualized successfully. SSIM index is 0.8400, which shows a high similarity between the output and the ground truth images. While conducting the second experiment, visualizing more complex progress was a matter of question. Therefore we added more building elements as progress in the second test images for both indoor and outdoor environments to evaluate the algorithm.



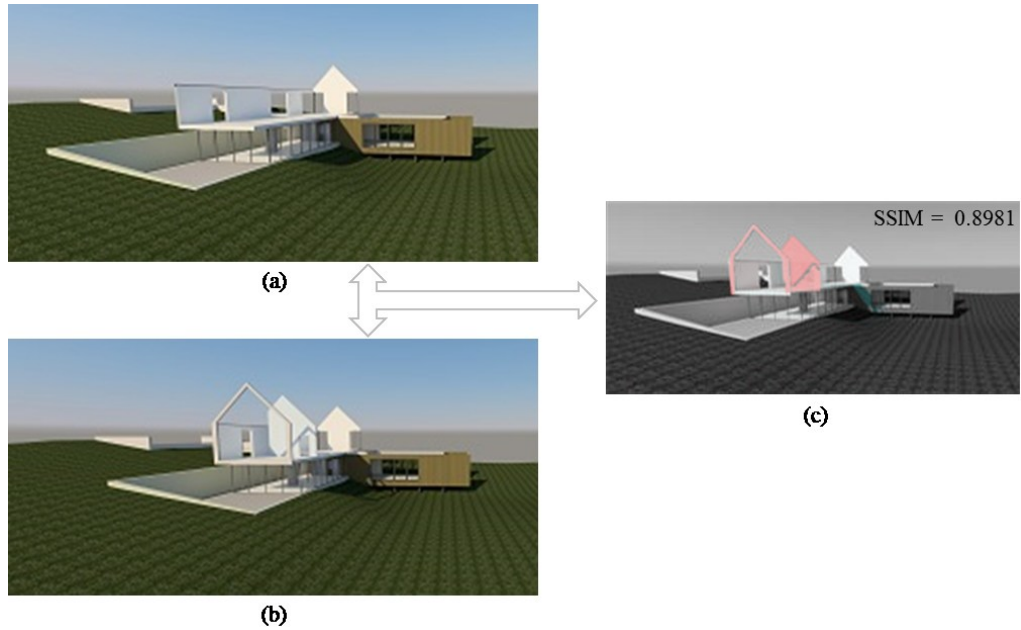
**Figure 4-13: Outdoor Test Images in Scenario #3: (a) at  $T_1$ , (b) at  $T_2$ , and CAE Output: (c) Visualized SIP Wall**



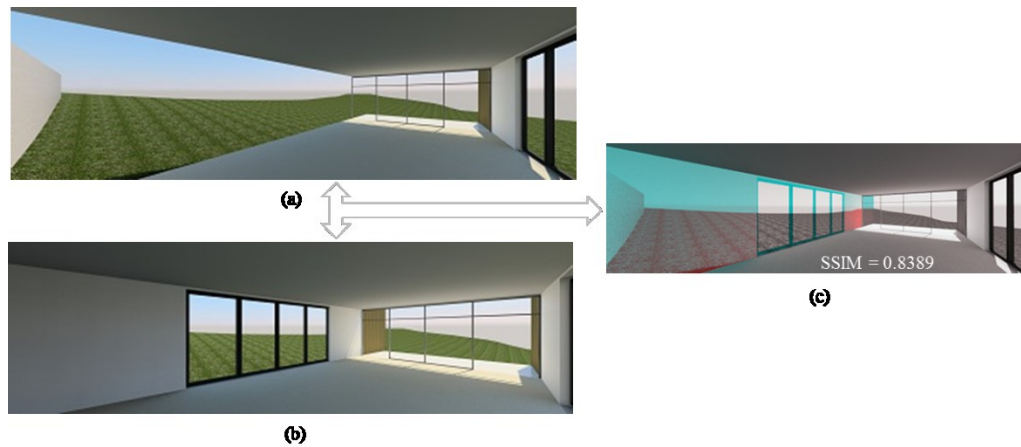
**Figure 4-14: Indoor Test Images in Scenario #4: (a) at  $T_1$ , (b) at  $T_2$ , and CAE Output: (c) Visualized Window Frames and Curtain Wall Mullions**

Figure 4-15(a) shows the first test image of the outdoor environment (southeast elevation) at time  $T_1$  while Figure 4-15(b) illustrates the second test image of the same incomplete building at time  $T_2$  in which two building elements (a SIP wall and an interior partition) are built in place as progress made between  $T_1$  and  $T_2$ .

However, the illumination condition of both input images was similar; the viewpoint was rotated around 5 degrees in the second test image. Having fed test images into the trained CAE, SIP wall, and an interior partition were recognized and visualized in Figure 4-15(c), which is the final output of the algorithm. The Achieved SSIM index is 0.8981. The same scenario (more than one building element as the progress between two different time points) was considered for the indoor environment as well. Figure 4-16(a) and 4-16(b) show test images of the living room under construction at time  $T_1$  and  $T_2$  respectively. Installed eastern wall and window frames were considered as the progress between these time points in Figure 4-16(b). As mentioned before, this experiment examined the algorithm performance using input images captured from different viewpoints but under the same illumination condition. The algorithm output (Figure 4-16(c)) was generated visualizing wall and window frames successfully as the actual progress with the SSIM index equals to 0.8389.



**Figure 4-15: Outdoor Test Images in Scenario #3: (a) at  $T_1$  (b) at  $T_2$ , and CAE Output: (c) Visualized SIP Wall and Interior Partition**



**Figure 4-16: Indoor Test Images in Scenario #4: (a) at  $T_1$ , (b) at  $T_2$ , and CAE Output: (c) Visualized Window Frames and SIP Wall**

According to Table 4-2, in the third experiment and scenario #5, test images were captured not only from different viewpoints but also under different illumination conditions. Figure 4-17(a) and 4-17(b) shows the first outdoor test image at time  $T_1$  and the second outdoor test image at time  $T_2$  respectively. As illustrated in Figure 4-17(a) and 4-17(b), the viewpoints and the illumination conditions were different, and the built SIP wall was considered as simple progress. The algorithm correctly recognized and visualized the SIP wall, as illustrated in Figure 4-17(c) with the SSIM index equals to 0.8309. The same scenario was implemented for the indoor test images indicated in Figure 4-18(a) and 4-18(b). Four window frames in the eastern side of the living room and curtain wall mullions

on the southern side of the living room were successfully visualized in Figure 4-18(c) with the SSIM index equals to 0.8477.

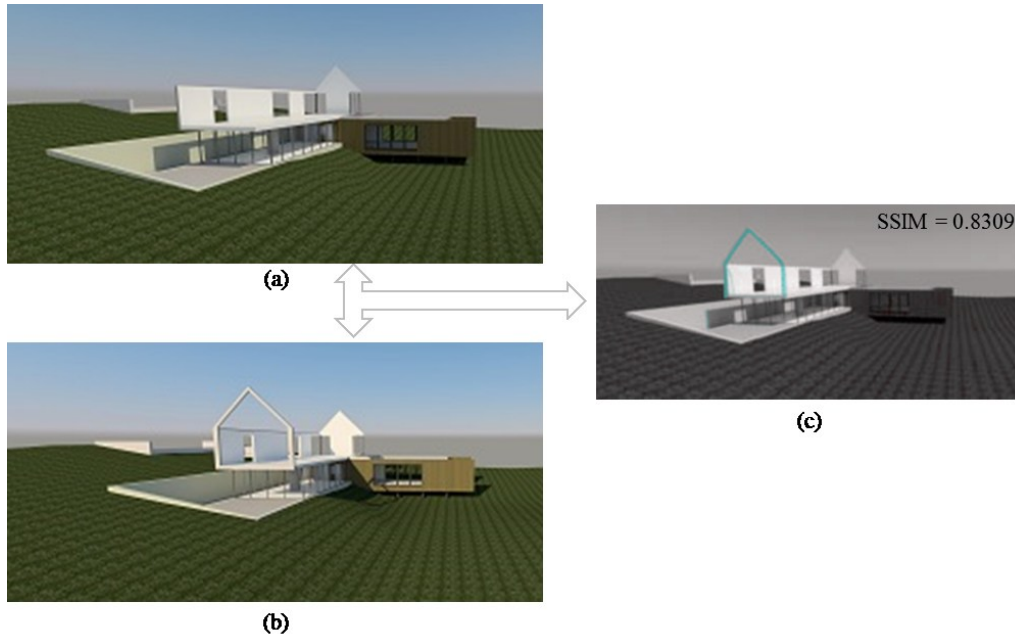


**Figure 4-17: Outdoor Test Images in Scenario #5: (a) at  $T_1$ , (b) at  $T_2$ , and CAE Output: (c) Visualized SIP Wall**

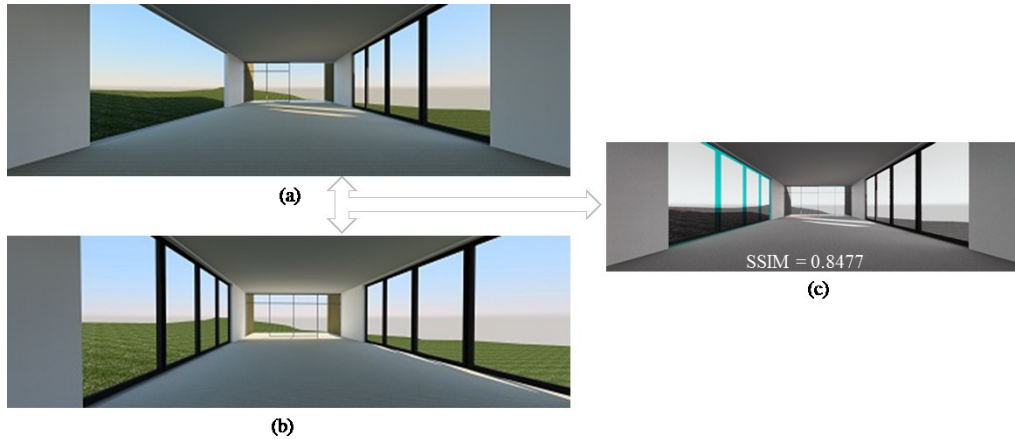


**Figure 4-18: Indoor Test Images in Scenario #6: (a) at  $T_1$ , (b) at  $T_2$ , and CAE Output: (c) Visualized Window Frames and Curtain Wall Mullions**

Considering the results of the designed laboratory experiments, it can be stated that the developed method can recognize and visualize the progress between different time points in terms of building elements. The measured SSIM indices in the laboratory experiments for the proof of concept seem to be satisfactory using the developed progress-tracking method for the first time. Table 4-3 indicates all the measured SSIM indices for all designed scenarios. By comparing the indices, it can be concluded that identical viewpoints and illumination conditions of the test images result in more accurate progress detection and

visualization. At the same time, the method is still responsive to small changes of viewpoints, diverse illumination conditions, and even various viewpoints along with varied illumination conditions.

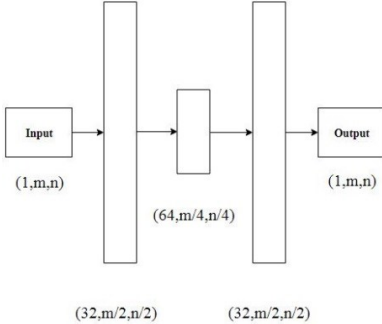
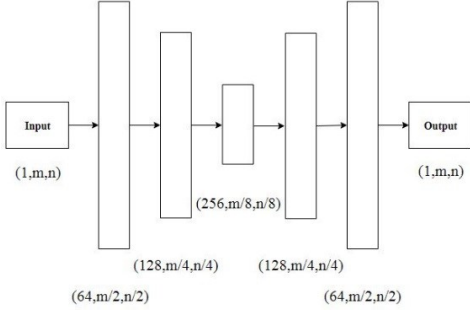
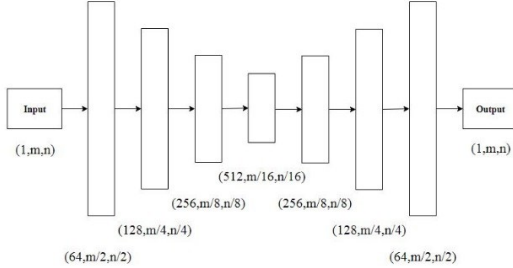
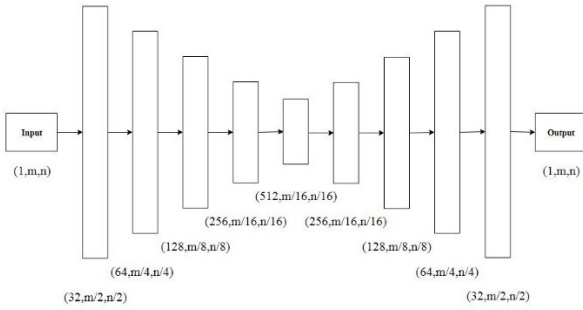
**Table 4-3: SSIM Index of Different Experiments**

<b>Experiment #</b>	<b>Environment</b>	<b>SSIM Index</b>
1 <sup>st</sup> Experiment	Outdoor	0.8919
	Indoor	0.8763
2 <sup>nd</sup> Experiment	1 <sup>st</sup> Outdoor	0.8456
	1 <sup>st</sup> Indoor	0.8400
	2 <sup>nd</sup> Outdoor	0.8981
	2 <sup>nd</sup> Indoor	0.8389
3 <sup>rd</sup> Experiment	Outdoor	0.8309
	Indoor	0.8477

Moreover, to come up with the proper CAE architecture, CAE was trained with a different number of convolution layers using datasets of outdoor environment images. However, any significant difference was not seen among different designed architectures in terms of computational time and validation errors, CAE architecture elaborated in section 3.2.7 was selected among others due to less cross-validation error (the average of 5 fold recorded errors) as shown in Table 4-4.



**Table 4-4: Cross-Validation Errors of Different Designed CAE Architecture**

Number of Convolutional Layers	Designed Architecture	5 Fold Cross Validation Error
3		0.0031969
5		0.003185
7		0.0031751
9		0.0031812

According to the recorded computational efficiency in the previous researches, such as one performed by Golparvar-fard et al. (2015), the computation time of progress monitoring using their proposed model is a few hours for any received observation. Moreover, the computational time to generate a sparse point cloud for a single column using captured images is around 7 hours, which shows that point cloud creation is a time-consuming

process (Kopsida et al., 2015). However, to compare automated monitoring models based on conventional computer vision algorithms with the developed method which is based on deep learning algorithms, specific metrics need to be set using similar construction case studies; considering the above two examples of computational time, it can be stated that the developed method outperforms their models. Different CAEs related to definite viewpoints are trained and tested in the planning phase once, and then progress in near real-time during the construction phase can be visualized.

In the field experiment, CAE was trained and tested using a real construction project of a hospital in the Montreal area. A field experiment was conducted to capture real images from the job site during the construction phase of the project, and it was used to examine the performance and the applicability of the developed method.

In this experiment, one outdoor and one indoor environment have been selected for capturing images from the job site. As explained before, the 3D Revit model of the building was used to simulate the construction process, as shown in Figure 4-19.

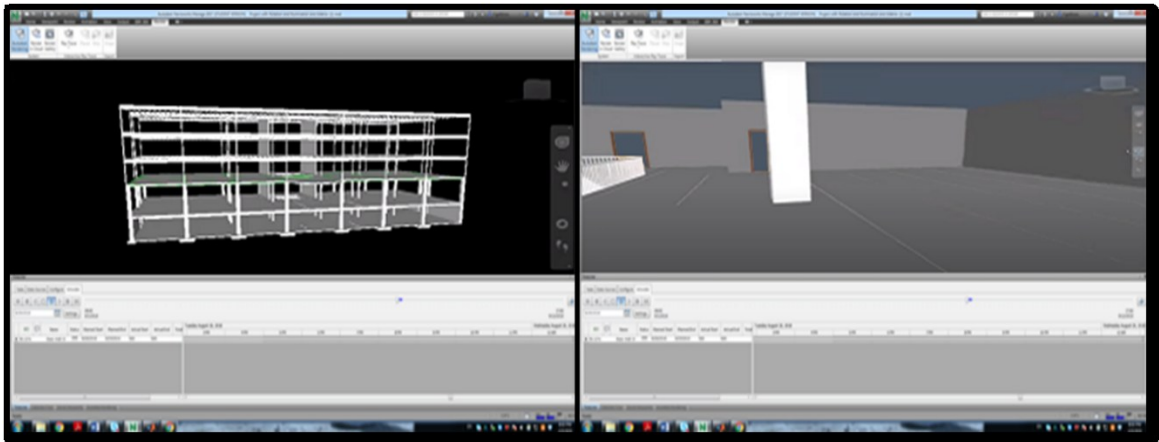


**Figure 4-19: Construction Process Simulation**

For the outdoor environment, the first real image was taken from the southeast elevation of the hospital under construction at the time “ $T_1$ ”. After some progress, the second real image was taken from the same elevation of the same building at time “ $T_2$ ”. For the indoor environment, the first real image was taken from a specific viewpoint on the seventh floor of the hospital at the time. “ $T_1$ ”, and the second real image was taken from the same scene at time “ $T_2$ ”. The input images had a small change in their viewpoints and illumination to examine the performance of CAE in visualizing progress dealing with slight rotation in viewpoints (around 5 degrees) and different illumination conditions. As discussed in the laboratory experiments, datasets of images extracted from the as-planned simulation (considering small visual changes and factors affecting illumination) for both selected indoor and outdoor viewpoints were used to train and test CAE. Training and test datasets of indoor environment included 160 and 40 images, respectively. For the outdoor environment, 340 and 80 images were included in the training and test datasets, respectively. Similar to the previous experiments, the training datasets were augmented using 4-DoF affine transformation (similarity transformation) to bootstrap the datasets to improve the performance of the algorithm, and 5 fold cross-validation was used in training

CAE. CAE being trained and tested using images extracted from the as-planned simulation was fed with real images captured at two consecutive time points to visualize the progress. The output image visualizing the progress was compared with the ground truth image using the Structural Similarity (SSIM) index, which can measure the similarity between two images. Figure 4-20(a) shows the first real input image captured from the southeast elevation illustrating the incomplete building at time  $T_1$ . Figure 4-20(b) shows the second real input image of the same incomplete building at time  $T_2$  in which the southeast facade of the last floor has been built in place. As shown in Figure 4-20(c,) the progress made between time “ $T_1$ ” and time “ $T_2$ ” of the constructed facade was visualized. The final output (Figure 4-20(c)) was compared with the ground truth using the SSIM index, which was calculated to be 0.7744, being close to (1), it is deemed satisfactory.

All the above steps were implemented to visualize the progress of the indoor environment as well. Figure 4-21(a) shows the first real input image captured from the seventh floor illustrating the incomplete building at time  $T_1$ . Figure 4-21(b) shows the second real input image of the same unfinished building at time  $T_2$  in which the HVAC duct has been installed. As shown in Figure 4-21(c), the installed HVAC duct depicts the progress made between time “ $T_1$ ” and time “ $T_2$ ”. The calculated SSIM index for this experiment was 0.7973, which is deemed satisfactory as well.

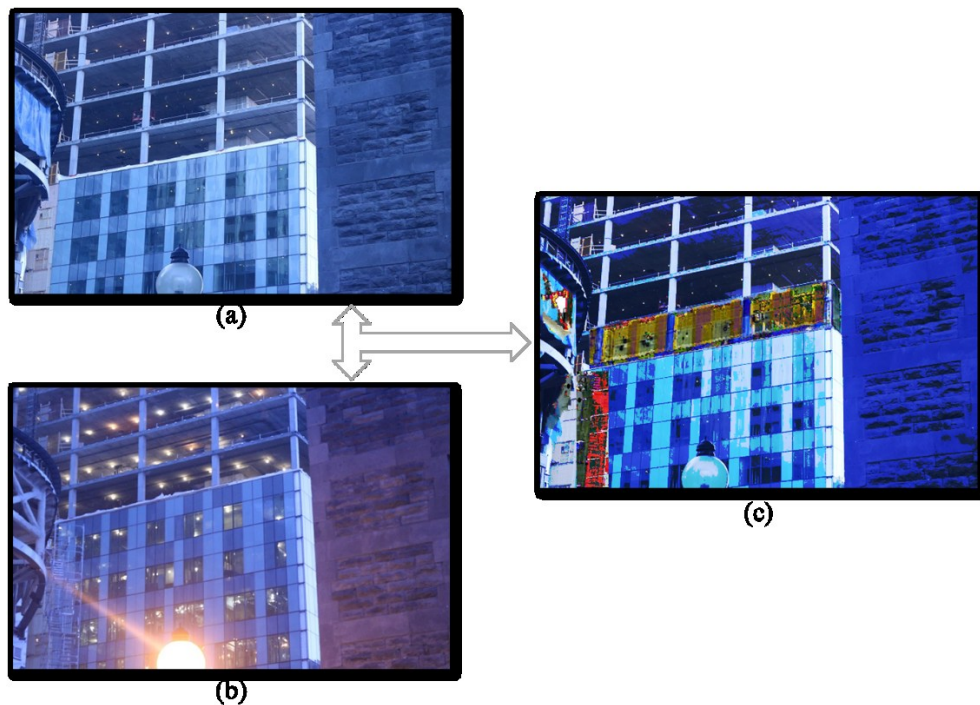


**Figure 4-20: Outdoor Real Images in Field Experiment: (a) at  $T_1$ , (b) at  $T_2$ , and CAE Output: (c) Visualized the Constructed Façade of the Last Floor**

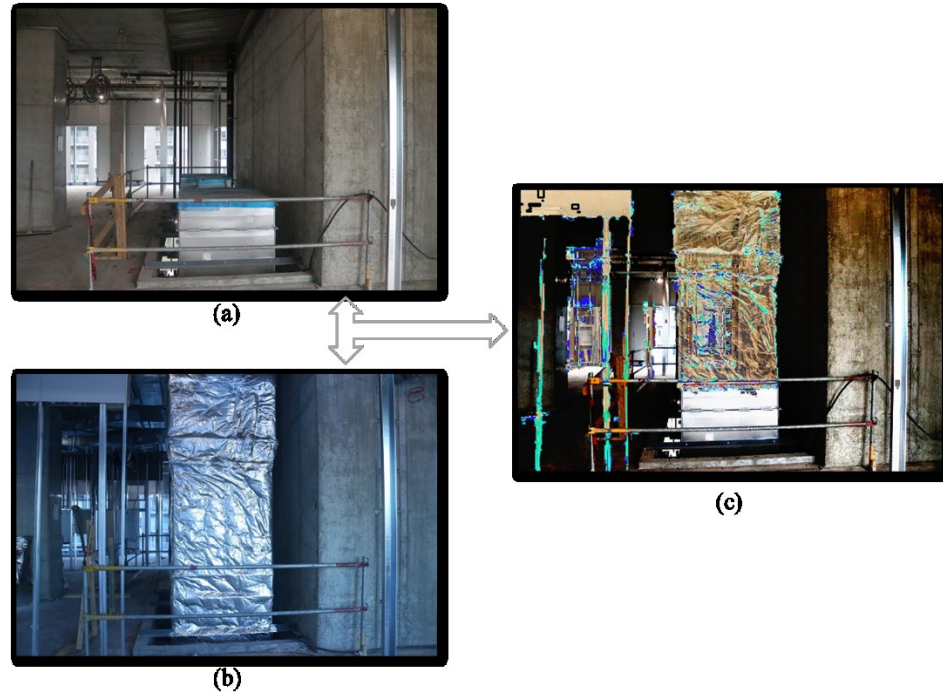


**Figure 4-21: Indoor Real Images in Field Experiment: (a) at  $T_1$ , (b) at  $T_2$ , and CAE Output: (c) Visualized the Installed HVAC Duct**

#### 4.2.2 SSIM

Validation of the proposed SSIM for progress visualization was done through an experiment in which 360-degree images and the HoloBuilder platform have been used in a real project (Airport project in Montreal area). The preliminary obtained results were decisive for the proof of concept. As-built condition of the project has been captured and visualized through spatially linking the 360-degree images to existing 2D plans in the HoloBuilder platform. Moreover, 360° rendering views of the 3D model has been imported from Autodesk Revit into HoloBuilder through keeping the same focus and point of view for both scenes (as-built status and 3D as-planned model) (see Figure 4-22).

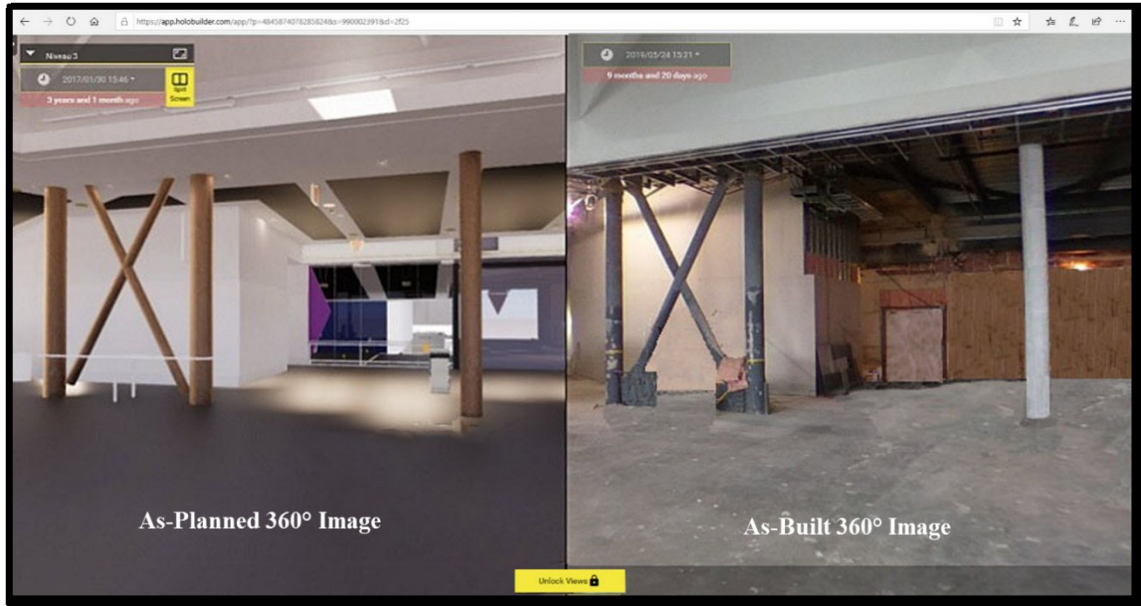


**Figure 4-22: As-Built 360° Image vs. As-Planned 360° Image in HoloBuilder Platform**

As shown in Figure 4-22, 360-degree image of 3D Revit model (as-planned) and 360-degree images of the actual job site (as-built) have been captured from the same location and are comparable, So to visualize the progress, as-planned and as-built images were extracted and used as inputs for SSIM. SSIM could successfully identify and visualize the perceptual differences between as-built and as-planned images, as shown in Figure 4-23.

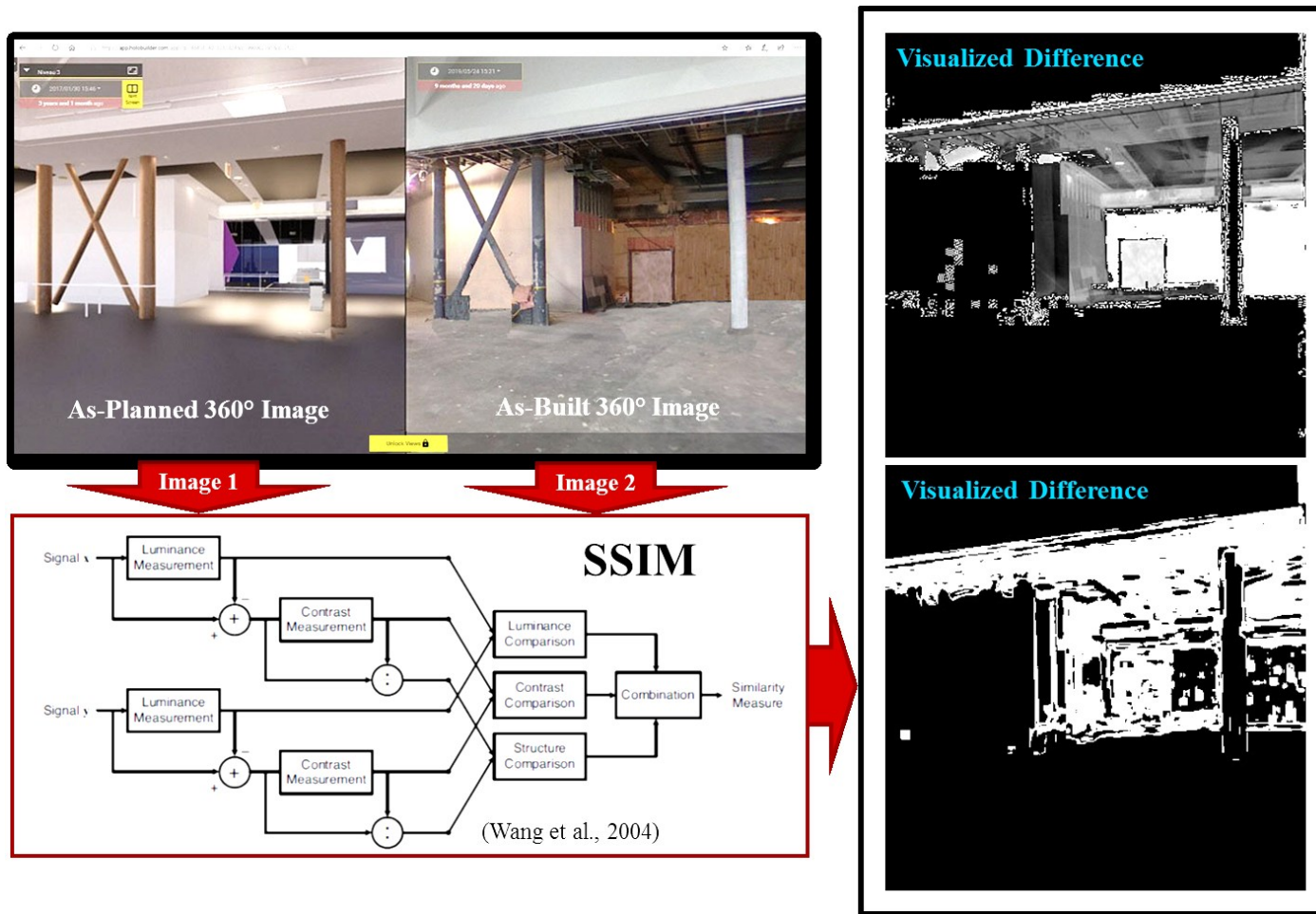


**Figure 4-23: Visualized Differences Using SSIM**

### 4.3 Automated Detection of Building Components

In this section, the performance of the developed automated detection framework is evaluated in the context of a real-world case example, and the results are presented. The experiments demonstrated that existing 3D BIM models of building projects could be used to generate large synthetic datasets for training purposes without the need for high realism and high-quality real-images. As such, the use of the developed framework alleviates the need for large sets of real-images and offer a viable alternative that circumvents that obstacle.

To illustrate how beneficial synthetically generated image datasets are, the most proper detection algorithm was selected and trained on five datasets. As described in section 3.4.3, the first step was to define the object of interest. HVAC ducts were determined to be detected in this research. As mentioned before, to ensure the generalization of the developed framework, the 3D BIM models of two real construction projects (a hospital and a university in Montreal area) were used to generate a synthetic-image dataset. Autodesk® Revit 2019 was employed as a 3D BIM tool in which sun setting and artificial lights were adjusted to simulate different lighting conditions. Multi-directional renderings for each 3D model were then generated using Enscape v2.3. Enscape is a Revit Add-ons and was employed as a real-time rendering engine. Various views considering occlusions and viewpoints were determined and saved for each 3D model in Autodesk® Revit 2019. Figure 4-24 indicates defined views from both 3D models simulating diverse illumination conditions, degree of occlusions, and viewpoints. Finally, synthetic-images were exported in JPEG format, and a dataset of 604 synthetic images was generated depicting HVAC ducts from various viewpoints, with different levels of occlusion and under diverse illumination conditions.

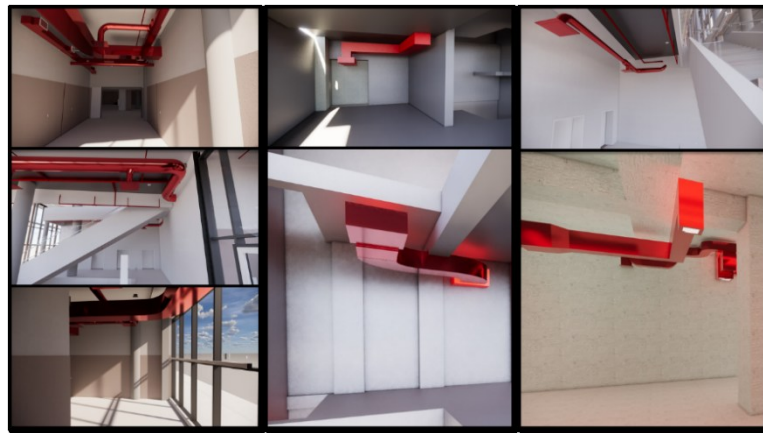


**Figure 4-24: Synthetic Image Examples Generated from 3D Models of Hospital and University Projects**

According to the second process of the developed framework (Figure 3-33), five training datasets were generated to investigate the effect of combining real images and synthetic-images on the performance of building components detection. One dataset consisted of only HVAC duct images generated synthetically, the second just included real-images of HVAC ducts which were captured from a real project (hospital) in the Montreal area, and

the remaining consisted of a mix of real and synthetic-images with different proportions (real/synthetic  $\approx 1/3$ , real/synthetic  $\approx 1/2$ , and real/synthetic  $\approx 2/3$ ). So, to carry out the designed experiments, a dataset of 622 real-images (captured from the hospital project) was created.

According to Figure 3-34, 3-35, and 3-36, Faster R-CNN was selected to detect HVAC ducts as the most suitable detector in the first step. But after implementing Fast R-CNN to detect HVAC ducts (using training dataset including only real-images), it was observed that the bounding boxes in the output images detecting and localizing HVAC ducts included other objects (such as lamps, ceiling, etc.) as well (Figure 4-25).

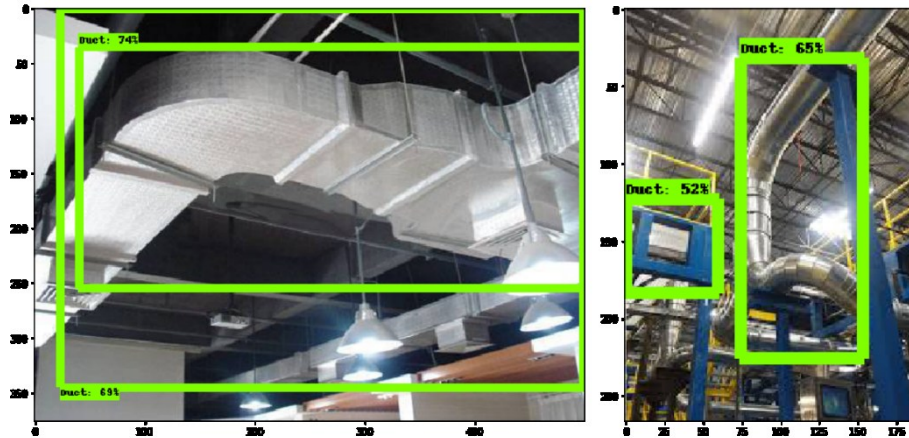


**Figure 4-25: Example Detections of HVAC Ducts Using Faster R-CNN**

Considering the shape of HVAC duct as its attribute (variant parts in different directions), and the fact that sometimes more than one bounding box is needed to localize one HVAC duct, Faster R-CNN did not seem to be the most proper algorithm for detection of HVAC ducts. As a result, pixel-wise methods like Mask-RCNN (which is a human-designed features-free algorithm) was selected instead. Mask R-CNN, as a region-based deep learning algorithm, is one of state-of-the-art object detection algorithms. Mask RCNN was proposed by He et al. (2017) to extend Faster RCNN and address pixel-wise object segmentation. Mask RCNN has the same detection framework as Faster RCNN. “The only difference is in the second stage, in which a binary mask for each Region of Interest (RoI) is generated in parallel to predicting the class and box offset. This binary mask is the output of a Fully Convolutional Network (FCN) on top of a CNN feature map” (Liu et al. 2019). Figure 4-26 indicates the network architecture of Mask R-CNN.



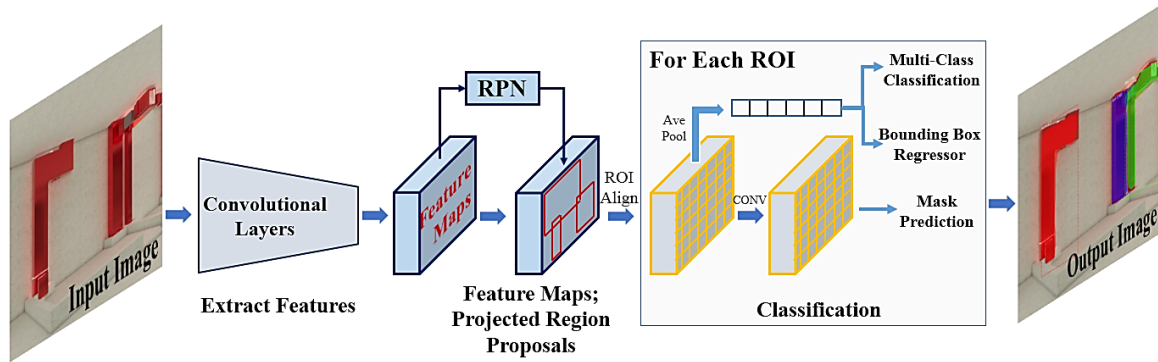


**Figure 4-26: Mask R-CNN Architecture with Input and Output Images (He et al., 2017 & Liu et al., 2019)**

The generated datasets were used to train Mask R-CNN, which is based on the Feature Pyramid Network (FPN) and a ResNet101 backbone (Abdulla, 2017). The backbone network acts as a feature extractor to generate feature maps through extracting low-level, and high-level features in the first and later layers, respectively, and FPN enables the model to detect objects in different scales via generated multi-scale feature maps. Mask R-CNN was not trained from scratch. Transfer learning (in terms of optimized pre-trained weights) was a starting point to initialize training our model. So, the feature extractor network was pre-trained on Microsoft’s Common Objects in Context (MS COCO) as a larger dataset (which contains object segmentation notation data). Then the initial weights were updated using our small dataset, which resulted in learning the relevant features of HVAC ducts. An open-source package with Tensorflow backend developed by Abdulla (2017) and modified by RomRoc (2018) was employed to detect HVAC ducts. Both datasets (real-image and synthetic-image datasets) were split into the train (90%) and test (10%) subsets. Not only datasets but also annotation files were required to start training Mask R-CNN. Thus, the images were labeled with ground truth annotations using a well-designed annotator tool. Among various available tools, the VGG Image Annotator (VIA) web tool developed by the University of Oxford (Dutta and Zisserman 2019) was selected to specify HVAC ducts boundaries and generated masks annotations in pixel level. So images were manually annotated through drawing polygonal shapes and adding HVAC duct as the class tag. The annotations were saved as JSON files to be used as input for model training. Figure 4-27 shows a sample of real and synthetic images annotated using VIA.

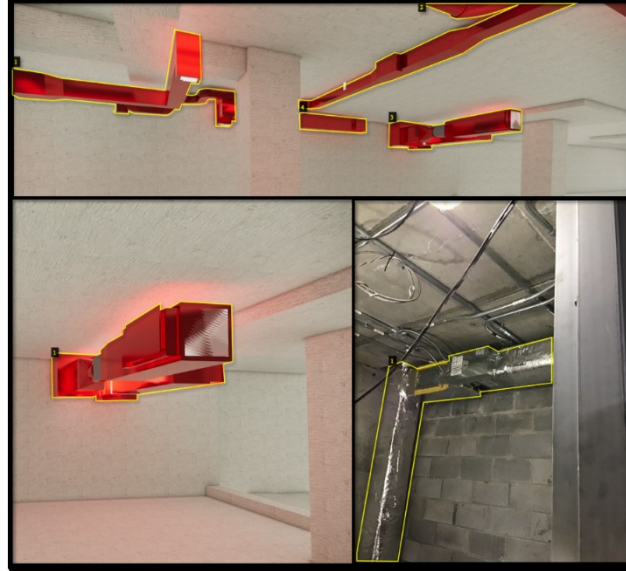


**Figure 4-27: Samples of Real and Synthetic-Images Annotated by VIA**

Google Colab notebook (Colab Runtime type: Python3, GPU enabled (Tesla K80 GPU is accessible up to 12 hours)) as a free cloud service was used to train Mask R-CNN. Mask R-CNN was trained with 50 epochs (various epochs were selected, and the best results were achieved for 50 epochs based on the size of training datasets) to map each training dataset to their corresponding annotations with the minimum loss value. Test datasets and their corresponding annotation files were used as the inputs to test the trained model. Each HVAC duct was detected by a mask boundary, a bounding box, and a class name along with a confidence score (probability showing that the bounding box contains an HVAC duct). In this research, precision and recall were used to evaluate the performance of the trained model, and Average Precision (AP) was used to compare its performance in the five designed experiments. As explained before, five experiments were designed to find the optimum training dataset for benefiting from synthetic-images to make the detection of building components applicable and reliable in the construction industry.

There are two experiments on the extreme ends of the experiment spectrum. The first (experiment #1) used only synthetic-images, and the second (experiment #5) used only real-images. In experiment #1, 604 synthetic-images generated from 3D BIM models of hospital & university projects were used for training Mask R-CNN, and 62 real-images from the hospital were used in testing it. In experiment #5, 560 real-images from the hospital were used for training Mask R-CNN, and 62 real-images were used for testing the model. Across this spectrum, three other experiments were designed. In the second experiment (experiment #2), training dataset included 604 synthetic-images combined with 200 real-images (real/synthetic  $\approx 1/3$ ), in the third experiment (experiment #3), training dataset consisted of 604 synthetic-images integrated with 300 real-images (real/synthetic  $\approx 1/2$ ), and in the fourth experiment (experiment #4), training dataset included of 604 synthetic-images integrated with 400 real-images (real/synthetic  $\approx 2/3$ ). In the fifth experiment, the test dataset included 62 real-images from the hospital. Finally, both training and validation datasets comprised only synthetic-images in the sixth experiment (experiment #6) to facilitate project progress monitoring (via comparison of as-planned

components segmentations with as-built components segmentations.) In this experiment, a dataset of 604 synthetic-images was split into a training dataset of 544 images and a test dataset of 60 images. Precision and recall were calculated for performance evaluation (IoU threshold was set to 0.5 to predict true positive or false positive and confidence threshold was set to 0.75) of the HVAC duct detection in each of the designed experiments (Table 4-5).

Figure 4-28 illustrates the output images from HVAC duct detection on real-images (achieved from experiments # 1, 2, 3, 4, and 5) using Mask R-CNN trained on different types of datasets.

**Table 4-5: Performance Comparison for Different Experiments**

#	Training Dataset	Test Dataset	TP	FP	FN	Precision	Recall
1	604 Synthetic-Images	62 Real-Images	38	45	57	46%	40%
2	200 Real-Images + 604 Synthetic Images (Real/Synthetic $\simeq 1/3$ )	62 Real-Images	73	27	22	73%	77%
3	300 Real-Images + 604 Synthetic Images (Real/Synthetic $\simeq 1/2$ )	62 Real-Images	67	34	28	66%	71%
4	400 Real-Images + 604 Synthetic Images (Real/Synthetic $\simeq 2/3$ )	62 Real-Images	65	33	30	66%	68%
5	560 Real-Images	62 Real-Images	70	30	25	70%	74%
6	544 Synthetic-Images	60 Synthetic-Images	102	34	18	75%	85%

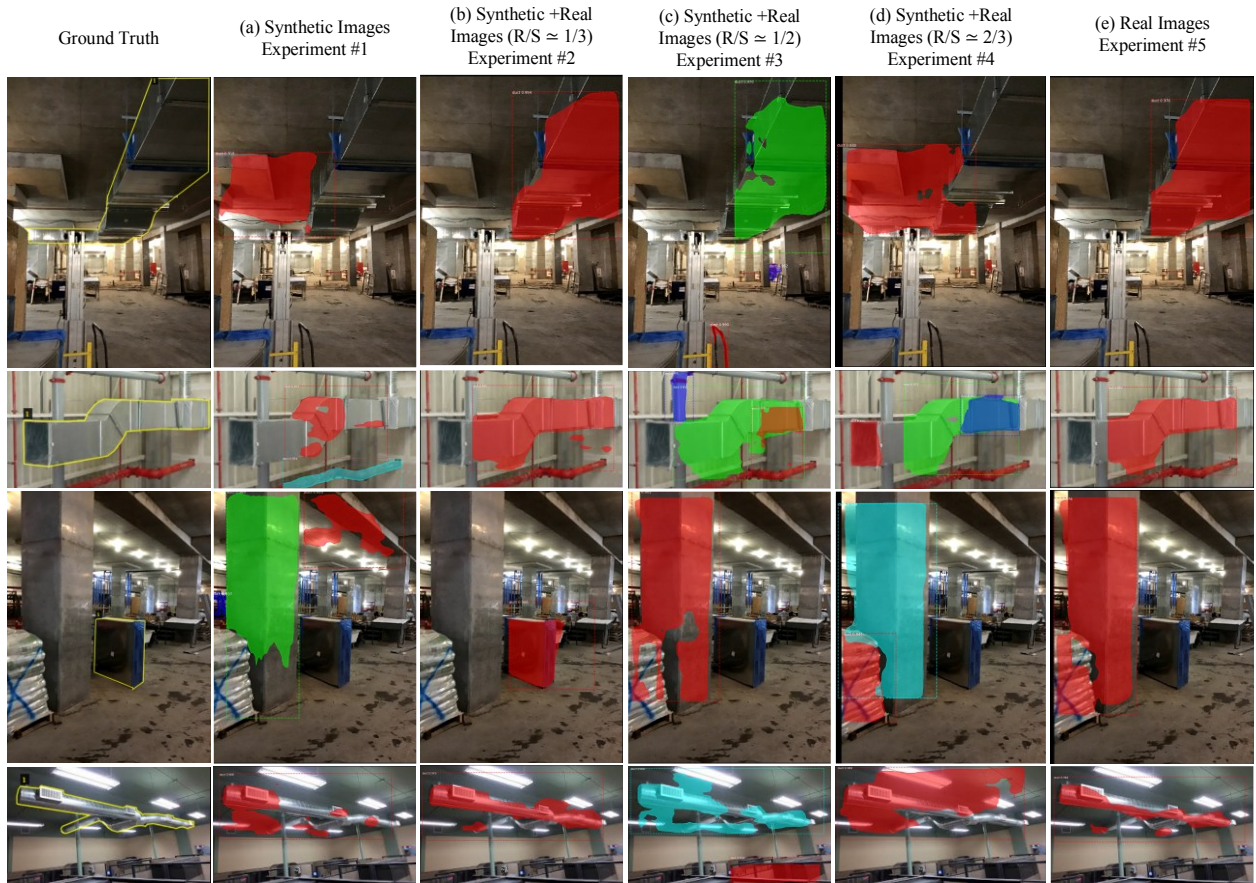


**Figure 4-28: HVAC Duct Detection on Real-Images Using Mask R-CNN (a) Experiment #1, (b) Experiment #2, (c) Experiment #3, (d) Experiment #4, and (e) Experiment #5**

Figure 4-29 illustrates the output images from HVAC duct detection on synthetic-images (achieved from the experiments # 6) using Mask R-CNN trained on a dataset including only synthetic-images.

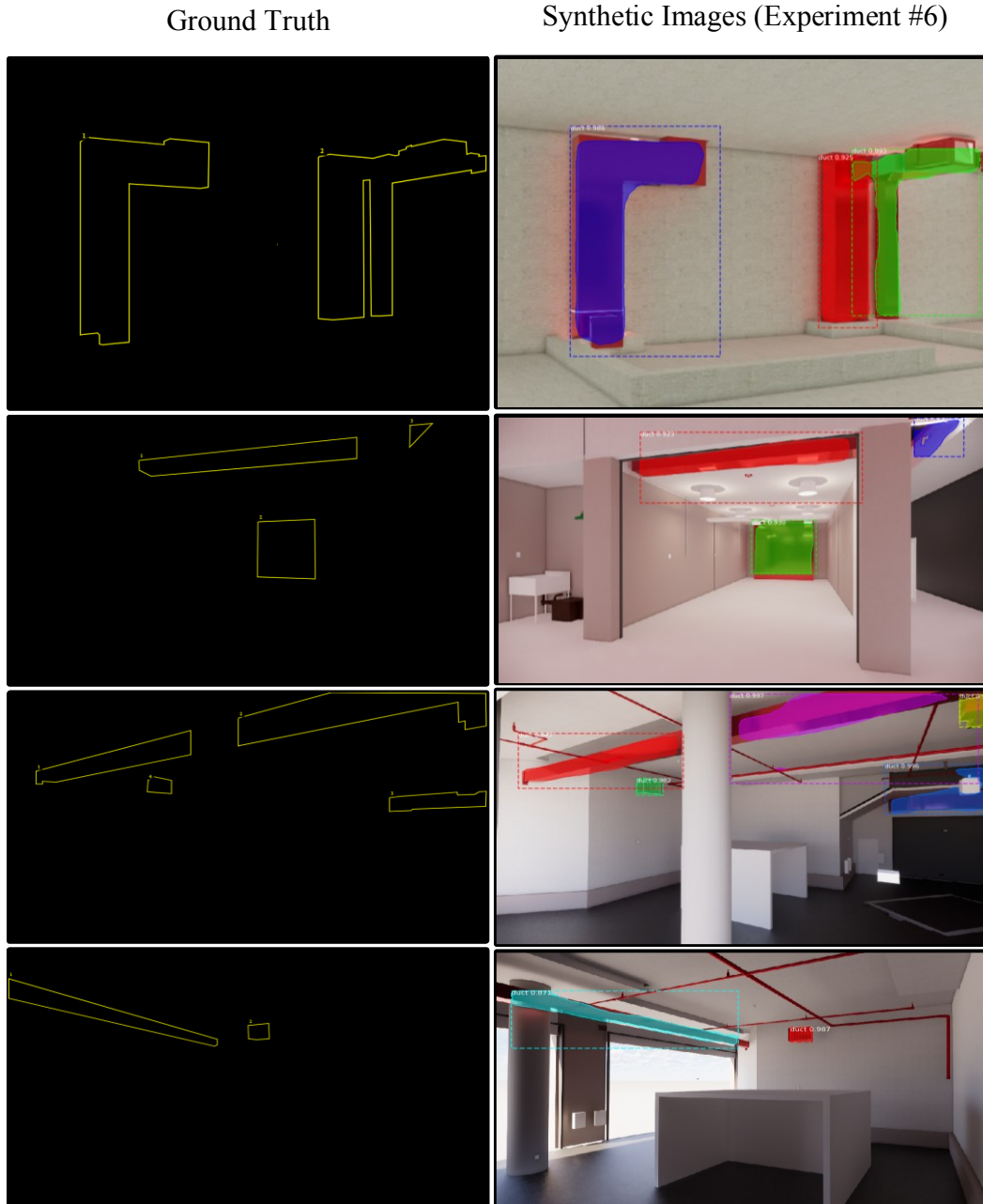


**Figure 4-29: HVAC Duct Detection on Synthetic-Images (Experiment #6)**

As shown in Table 4-5, Mask R-CNN did not achieve acceptable performance in detecting HVAC ducts when trained just on synthetic-images (experiment #1). Only 38 ducts were detected accurately, and the least precision and recall (40% and 46% respectively) were obtained across the entire spectrum of experiments. At the right of this spectrum, where Mask R-CNN was trained only on real-images (experiment #5), it was able to detect 70 HVAC ducts out of 95 HVAC ducts (in a set of 62 real images of the test dataset). There were 30 false detections as well in this experiment, which resulted in 70% and 74% precision and recall, respectively. More accurate duct detections (73 HVAC ducts) and less false detections (27) were acquired when Mask R-CNN was trained on a training dataset,

including 604 synthetic-images combined with 200 real-images (Real/Synthetic  $\approx 1/3$ ) in experiment #2. In the third experiment in which the training dataset has consisted of 604 real-images and 300 synthetic-images (Real/Synthetic  $\approx 1/2$ ), 67 HVAC ducts were detected correctly by Mask R-CNN, and 34 ducts were detected where there was none. Finally, in experiment #4, 65 HVAC ducts were detected, and there were 33 false detections when Mask R-CNN was trained on a training dataset including 604 synthetic-images mixed with 400 real-images (Real/Synthetic  $\approx 2/3$ ). Therefore, the highest precision (73%) and recall (77%) were accomplished in experiment # 2 compared with the other experiments across the entire spectrum. In addition to those five experiments, experiment #6 was performed considering synthetic-images only for testing. The results of that experiment indicated that the Mask R-CNN trained on 544 synthetic-images yielded 75% and 85% precision and recall, respectively. On top of precision and recall rates (Table 4-5), AP was used to facilitate performance evaluation of Mask R-CNN detector trained on a different mix of synthetic and real images (Figure 4-30).

Considering the test results of experiments # 2, 3, 4, and 5 shown in Table 4-5 and also the output images displayed in Figure 4-28(b), 4-28(c), 4-28(d), and 4-28(e), it can be stated that the developed framework is accurate and robust enough to recognize and segment HVAC ducts. It has been shown in Table 4-5 and also in Figure 4-28(a) that the performance of precision (40%) and recall (46%) is not acceptable when the training dataset includes only synthetic-images (experiment #1). But the achieved results (experiment # 2, 3, 4 in Table 4-5 and Figure 4-28(b), 4-28(c), and 4-28(d)) show that the combination of real and synthetic-images in the training dataset leads to a higher detection precision and recall rate. In other words, when synthetic-images form a large part of training datasets, detection accuracies are quite comparable to the accuracy of the model trained on only real-images (experiment #5).

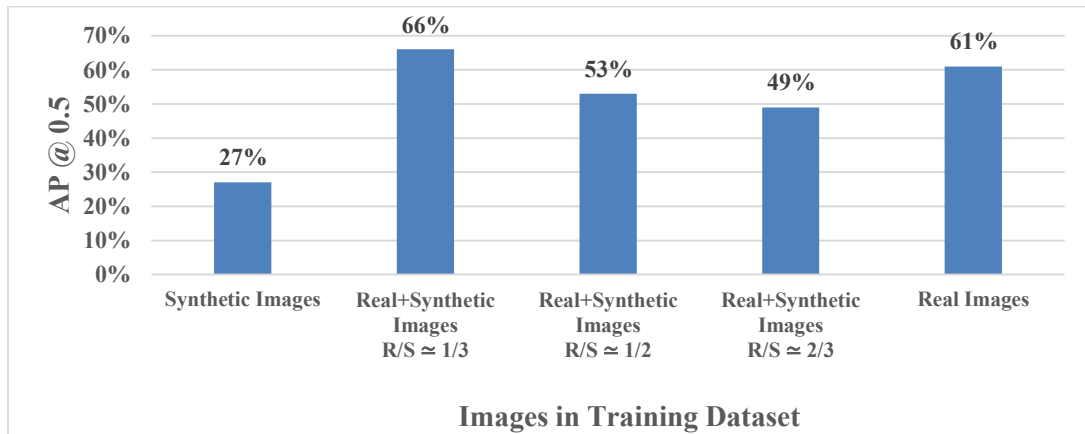


**Figure 4-30: Performance Plot Indicating the Effect of Including Synthetic-Images in the Training Dataset**

As shown in Figure 4-30, AP is 27% and 61% when Mask R-CNN was trained on synthetic-images only and real-images only, respectively. But an increase of 5% in the AP (AP=66%) was gained by adding 200 real-images to 604 images generated synthetically in the training dataset, i.e., when using a training dataset of 30% real images. The achieved higher AP can be attributed to the fact that the network was exposed to more diversified

images in terms of occlusion, viewpoint, and illumination condition during the training process. Table 4-5 demonstrates the high performance of the model in terms of precision (75%) and recall (85%) to detect ducts in synthetic-images as well.

This study reveals the successful use of less photorealistic synthetic images augmented by a small percentage of real-images in training models for object detection in construction. Accordingly, the synthetic-images generated from existing 3D models of building projects can be used in training datasets without caring about a high degree of photorealism. Thus the problem of the detection of building components can be effectively solved using the framework described in this study.

As illustrated in Figure 3-32, after progress visualization, the developed object detection framework is used to detect various building elements (visualized as progress) and consequently updating the project schedule based on the perceived progress. Since the developed automated detection framework has been applied to detect HVAC ducts in this study, so the output image of the progress visualization process related to the HVAC duct was used as an input to Mask R-CNN and the result is shown in Figure 4-31.

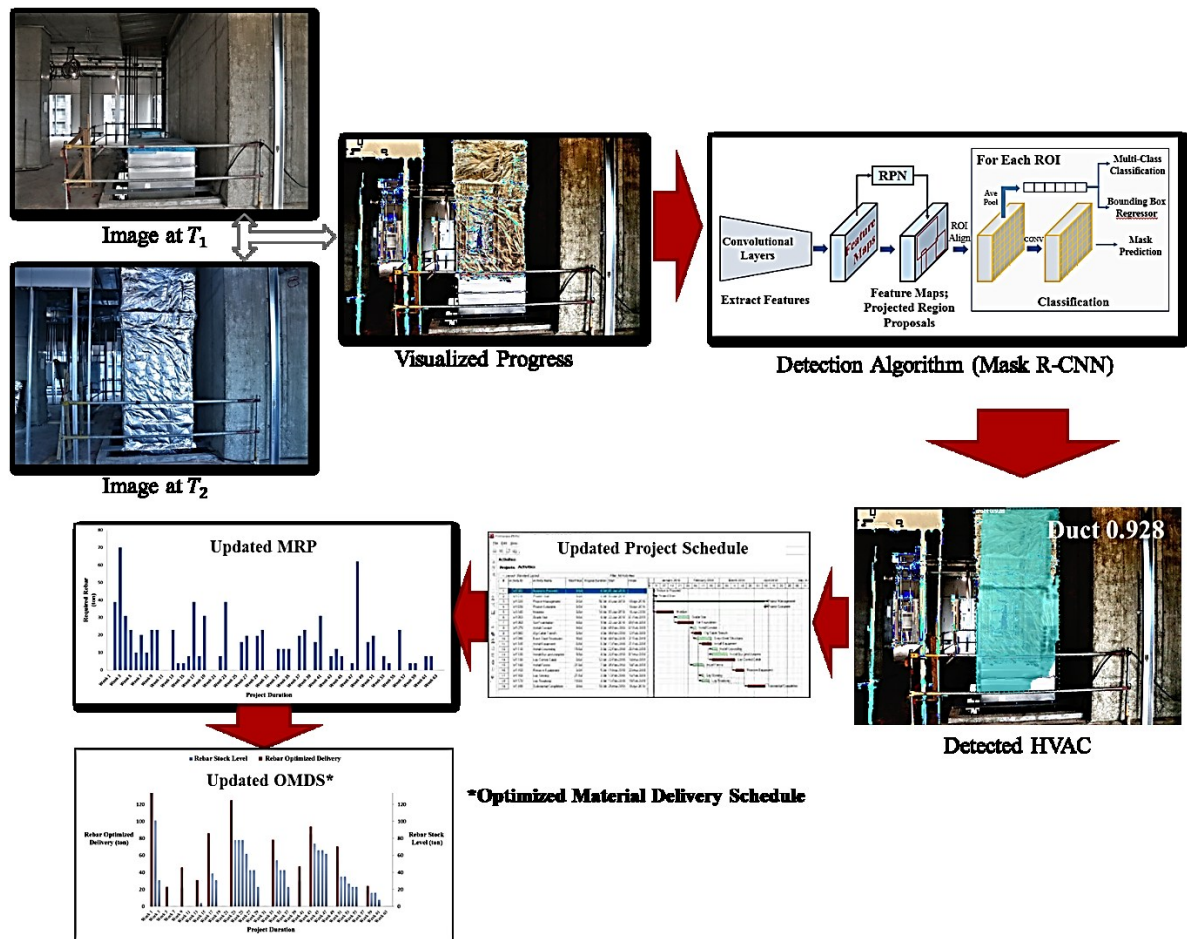


**Figure 4-31: Updating Schedule, MRP and OMDS based on the Detected Building Elements (Perceived Progress)**



## CHAPTER 5: RESEARCH CONTRIBUTION AND FUTURE WORKS

### 5.1 Summary of Research

This research covered the concepts and the background of construction materials management and literature review related to the main aspects, the current research gaps, and detailed explanation of the developed framework followed by the experiments and case studies to validate and evaluate the applicability of the developed framework and its developed models.

In the developed framework, a novel algorithm was introduced to generate an optimized material delivery schedule that can be used as a guide for contractors or material professionals in procuring material with the least cost and without early, late, excess, and insufficient purchasing. The developed algorithm can make trade-offs and optimize balance among elements of material cost. It can also consider the dynamic nature of the construction projects by realizing the progress reflected in the last up-to-date schedule. In addition to profiting from the capabilities of GA as an optimization engine, practicality and the excellence of the presented method is due to creating a memory for GA by integrating MLP with GA to avoid getting stuck to the local minima as the main weakness of GA. Another method was developed to facilitate and improve vision-based automated progress monitoring of construction operations. The method utilized a deep CAE algorithm to automate monitoring of indoor and outdoor construction progress in near real-time over the entire project duration. Having trained and tested CAE using a set of virtually captured 2D images in the planning phase, the method was able to visualize actual onsite progress using job site images captured on consecutive days. The method was observed to provide promising performance in near real-time indoor and outdoor construction progress visualization. The developed vision-based project progress monitoring method utilizes a deep learning algorithm. Unlike conventional computer vision methods applied for progress monitoring, deep learning algorithms can represent images by automatically learning the features with the superior discriminatory power rather than using hand-crafted image descriptors. Using 360-degree images, the HoloBuilder platform, and the SSIM algorithm was proposed as another approach for visualizing progress in this research.

Moreover, for extracting the information and identifying various building components included in the images, an automated object detection framework was developed in which the possible use of synthetic-images rendered from 3D BIM models was investigated to generate a training dataset large enough for detecting building components. The developed framework alleviates the need for large datasets of real images and, accordingly, overcoming a critical obstacle in the formation of needed training data sets. It addresses the lack of images captured in diverse environmental conditions (e.g., various lighting conditions, viewpoints, occlusions, and buildings with multiple usages.). The performance of Mask R-CNN trained on five different training datasets was compared using AP, precision, and recall metrics. The training datasets in the designed experiments consisted of 560 real-images, 604 images synthetically generated, and a mix of real and synthetic-images with three different ratios, respectively. Mask R-CNN trained on only 604 synthetic-images (reached 26% AP) underperformed against Mask R-CNN trained on 560

real images (reached 61% AP), but when 200 real-images were added to the dataset of synthetic-images, it boosted the detection performance by 5% (reached 66% AP). So it was concluded that training Mask R-CNN on synthetic datasets combined with an appropriate number of real images (real/Synthetic $\approx$ 1/3 in this research) is a promising approach for the detection of building components in the construction industry where there is a dearth of large enough datasets of real-images. The combination of progress visualization and detection of building elements enables project managers to monitor project progress, update project schedule, MRP, and optimized material delivery schedule respectively in near real-time.

## **5.2 Expected Research Contributions**

The main expected contributions of this research are as follows:

- 1) Considering the complex, unstructured, and dynamic nature of the construction projects through developing a dynamic Construction Materials Management (CMM) framework in which near real-time site data acquisition is used to update the project schedule. It guides materials professionals on how to procure materials with the least cost and on time, and it can result in taking more accurate and near real-time corrective actions, avoiding project schedule delays and cost overruns.
- 2) Generating an optimized material delivery schedule to prevent early, excess, or late purchasing of materials in the construction projects using a novel developed GA-MLP algorithm. This method can make trade-offs and optimize balance among elements of material cost through creating a memory for GA to avoid from getting stuck to the local minima.
- 3) Investigating and applying ADC technologies (RGB images, 360-degree images, and HoloBuilder platform) for near real-time site data acquisition.
- 4) Facilitating construction progress visualization in the indoor and outdoor environment under different illumination conditions and with a slight change in viewpoints (5 degrees) through utilizing a deep learning algorithm (CAE) algorithm instead of previously used conventional computer vision algorithms.
- 5) Automated identification of building components through developing a generalized object detection framework and deep learning algorithms as a suitable replacement for the time-consuming manual information retrieval from the images.
- 6) Exploring the benefits of synthetically generated images in training models for the detection of building components to alleviate the need for large training datasets of real-images required to make deep learning algorithms applicable and practical for robust object detection.

## **5.3 Limitations and Future Work**

Although this research has successfully achieved its objectives, some limitations have been still remained and have to be addressed in the future. The limitations and future works are as follows:

- 1) One of the practical limitations of the developed CAE method is dealing with highly cluttered scenes and occlusions on the construction job sites.

- 2) Another limitation in using CAE relates to the number of viewpoints that have to be defined and saved in BIM in the planning phase to cover the main building elements for progress monitoring and, subsequently, the number of CAEs that have to be trained and tested. Sampling strategy or Pareto Principle is recommended to make a cost-benefit tradeoff between the required efforts and the achieved results for the project progress estimation. Based on the Pareto Principle, 20% of project activities could cause 80% of project delays. So these project activities and their related building elements can subsequently be identified by members of the project team. Then the CAE is trained and applied for monitoring the selected elements.
- 3) Automated updating of the project schedule was not in the scope of this research, but developing a method to automatically identify IDs of the building elements detected and visualized as the progress is another objective of our future research.
- 4) Since CAE is trained on images with certain viewpoints defined in Autodesk Navisworks in the design and planning phase, so it is recommended to use UAV for continuously capturing images from the same viewpoints (camera position in terms of  $(x, y)$  is equal to the  $(x, y)$  of predefined location in Navisworks and  $z$  coordinate of the camera is equal to the  $z$  coordinate of the project basepoint in the same floor plus 1.7 m). These specific camera coordinates will be used to define UAV path planning during the construction phase. Then through a wireless data transfer system, captured site images are transferred and saved to the main server. Future research may consider the system developed by Freimuth and König (2015) to support progress monitoring (using CAE) as well. Their proposed system uses UAVs and 4D-BIM-data to generate UAVs' survey planning with optimal waypoints based on 4D-BIM-data. It may be helpful to use their system in planning UAVs flight missions on the job site for taking daily/weekly images from defined viewpoints.
- 5) Investigating the application of deep generative models such as Variational Autoencoder (VAE) for project progress monitoring is considered as the future objective.
- 6) Future research directions related to the automated object detection framework can investigate better ways to automatically annotate datasets using 3D CAD models.
- 7) Performing more experiments using various datasets to come up with an optimal ratio of synthetic and real images to form a training dataset, improving diversification of training images generated synthetically, and investigation of the generalization ability of the developed framework focusing on other building components is another direction of our future research.

## BIBLIOGRAPHY

Abdulla, W. (2017). "Mask R-CNN for object detection and instance segmentation on Keras and TensorFlow." Accessed: June 15, 2019. [https://github.com/matterport/Mask\\_RCNN](https://github.com/matterport/Mask_RCNN)

Abeid, J., Allouche, E., Arditi, D., and Hayman, M. (2003). "PHOTO-NET II: a computer-based monitoring system applied to project management." *Automation in Construction*, 12(5), 603-616.

Ahmadian, F.F.A., Akbarnezhad, A., Rashidi, T.H., and Waller, S.T. (2016). "Accounting for transport times in planning off-site shipment of construction materials." *Journal of Construction Engineering and Management*, 142(1).

Ahmed, S., Azher S., Castillo, M., and Kappagantula, P. (2002). "Construction Delays in Florida: An Empirical Study." Final Report, Florida International.

Ajayi, S.O., Oyedele, L.O., Akinade, O.O., Bilal, M., Alaka, H.A., and Owolabi, H.A. (2017). "Optimizing material procurement for construction waste minimization: an exploration of success factors." *Sustainable Materials and Technologies*, 11, 38–46.

Alavi, A. H., and Gandomi, A. H. (2017). "Big data in civil engineering." *Automation in Construction*, 79, 1-2.

Allahkarami E., Nuri O.S., Abdollahzadeh A., Rezai B., and Maghsoudi B. (2017). "Improving estimation accuracy of metallurgical performance of industrial flotation process by using hybrid genetic algorithm – artificial neural network (GA-ANN)." *Physicochemical Problems of Mineral Processing*, 53(1), 366–378.

Al-Momani, A.H. (2000). "Construction Delay: A Quantitative Analysis." *International Journal of Project Management*, 18, 51-59.

Alom, Md. Z. (2018). "Improved Deep Convolutional Neural Networks (DCNN) Approaches for Computer Vision and Bio-Medical Imaging." Ph.D. thesis, University of Dayton, Dayton, Ohio.

Alqahtani A., Xie, X., Deng, J., and Jones, M. W. (2018). "A deep convolutional auto-encoder with embedded clustering." In *25th IEEE International Conference on Image Processing (ICIP)*, 4058–4062.

Alshibani, A., and Moselhi, O. (2007). "Tracking and forecasting performance of earthmoving operations using GPS data." *CME 25 Conference Construction Management and Economics*, 1377-1388.

Artescan, 3d Laser Scanning History, written in May 2012, <http://artescan.net/blog/3-d-laser-scanner-history/>, Last seen December 2016.

- ASTM. ASTM E2544 09B Standard terminology for three-dimensional (3D) imaging systems. Technical report, 2009.
- Atlas RFID Store, (2016). A trusted source in the RFID hardware industry, [www.atlasrfidstore.com](http://www.atlasrfidstore.com).
- Azarm, R. (2013). "Material Status Index for Tracking and Progress Reporting of Construction Projects." MSc. Theses, Concordia University, Montreal, Canada.
- Bae, V, Golparvar-Fard, M, & White, J. (2013). "High-precision vision-based mobile augmented reality system for context-aware architectural, engineering, construction and facility management (AEC/FM) applications." *Visualization in Engineering*, 1–3.
- Bailey, P., and Farmer, D. (1982). "Materials Management Handbook." Gower Publishing Company Limited, Aldershot, Hants, England.
- Bansal, V. K., and Pal, M. (2009). "Extended GIS for construction engineering by adding direct sunlight visualizations on buildings." *Construction Innovation*, 9(4), 406 – 419.
- Barry, W., Leite, F., and O'Brien, W. (2014). "Identification of Late Deliverables and Their True Effects on Industrial Construction Projects." *Construction Research Congress*, 2296-2305.
- Behzadan, A.H., Aziz, Z., Anumba, C.J., and Kamat, V.R. (2008). "Ubiquitous location tracking for context-specific information delivery on construction sites." *Journal of Automation in Construction*, 17, 737-748.
- Behzadan, A.H., and Kamat, V.R. (2013). "Enabling discovery-based learning in construction using telepresent augmented reality." *Automation in Construction*, 33, 3–10.
- Behzadan, A.H., Dong, S., Kamat, V.R. (2015). "Augmented reality visualization: A review of civil infrastructure system applications." *Advanced Engineering Informatics*, 29 (2), 252–267.
- Bell, L. C., and Stukhart, G. (1986). "Attributes of Materials Management Systems." *Journal of Construction Engineering and Management*, 112(1), 14-21.
- Bell, L., and Stukhart, G. (1987). "Costs and Benefits of Materials Management Systems." *Journal of Construction Engineering and Management*, 113(2), 222-234.
- Bell, L.C., and McCullouch, B.G. (1988). "Barcode application in construction." *Journal of Construction Engineering and Management*, 114 (2), 263–278.
- Bennett, C. L., and Ross, G. F. (1978). "Time-domain electromagnetics and its applications." *Proceeding IEEE*, 66, 299–318.

- Bernold, L.E. (1990a). "Barcode-driven equipment and materials tracking for construction." *Journal of Computing in Civil Engineering*, 4(4), 381-395.
- Bernold, L.E. (1990b). "Testing bar-code technology in construction environment." *Journal of Construction Engineering and Management*, 116 (4), 643–655.
- Bhatla, A., Choe, S. Y., Fierro, O., and Leite, F. (2012). "Evaluation of accuracy of as-built 3D modeling from photos taken by handheld digital cameras." *Automation in Construction* 28, 116–127.
- Bognot, J. R., Candido, C. G., Blanco, A. C., and Montelibano, J. R. Y. (2018). "Building Construction Progress Monitoring Using Unmanned Aerial System (UAS), Low-Cost Photogrammetry, and Geographic Information System (GIS)." *ISPRS Annals of Photogrammetry, Remote Sensing and Spatial Information Sciences*, 41-47.
- Bosché, F., and Haas, C. T. (2008). "Automated retrieval of 3D CAD model objects in construction range images." *Automation in Construction*, 17(4), 499-512.
- Bosché, F., Haas, C. T., and Akinci, B. (2009). "Automated Recognition of 3D CAD Objects in Site Laser Scans for Project 3D Status Visualization and Performance Control." *Journal of Computing in Civil Engineering*, 23(6), 311-318.
- Bosché, F. (2010). "Automated recognition of 3D CAD model objects in laser scans and calculation of as-built dimensions for dimensional compliance control in construction." *Advanced Engineering Informatics*, 24(1), 107–118.
- Bosché, F., Guillemet A., Turkan, Y., Haas, C. T., and Haas, R. (2014). "Tracking the Built Status of MEP Works: Assessing the Value of a Scan-vs-BIM System." *Journal of Computing in Civil Engineering*, 28(4).
- Braun, A., Borrmann, A. (2019). "Combining inverse photogrammetry and BIM for automated labeling of construction site images for machine learning." *Automation in Construction*, 106.
- Breed, G. (2005). "A Summary of FCC Rules for Ultra Wideband Communications." *High Frequency Electronics*, 42–44.
- Brilakis, I. (2007). "Long distance wireless networking for site - office data communications." *Journal of Information Technology in Construction (ITCON)*, 12, 154-164.
- Brilakis, I., and Soibelman, L. (2008). "Shape-based retrieval of construction site photographs." *Journal of Computing in Civil Engineering*, 22, 14–20.

- Butcher, J. B., Day, C. R., Austin, J. C., Haycock, P. W., Verstraeten, D., and Schrauwen, B. (2014). "Defect detection in reinforced concrete using random neural architectures." *Computing Aided Civil Infrastructure Engineering*, 29, 191–207.
- Caladas, C. H, Torrent, D. G., and Haas, C. T. (2006). "Using Global Positioning System to Improve Materials-Locating Processes on Industrial Projects." *Journal of Construction Engineering and Management*, 132(7), 741-749.
- Caldas, C. H, Menches, C., Reyes, P., Navarro, L., and Vargas, D. (2015). "Materials Management Practices in the Construction Industry." *Practice Periodical on Structural Design and Construction*, 20(3).
- Carr, J. (2014). "An introduction to genetic algorithms." Senior Project, 1 – 40.
- Cha Y. J., and Choi W. (2017). "Vision-Based Concrete Crack Detection using a Convolutional Neural Network." In: Caicedo J., Pakzad S. (eds) *Dynamics of Civil Structures, Conference Proceedings of the Society for Experimental Mechanics Series*. Springer, Cham, 2, 71–3.
- Chandler, Ian E. (1978). "Materials Management on Building Sites." The Construction Press Ltd, Lancaster, England.
- Chapman, I, Olomolaiye, P., and Harris, F. (1990). "Automation problems in materials management on large construction projects." *Proceedings of the 7th ISARC, Bristol, United Kingdom*, 499-504.
- Chase, W. G., and Simon, H. A. (1973). "Perception in chess." *Cognitive Psychology*, 4(1), 55-81.
- Chen, Z., Li, H., and Wong, C. T. C. (2002). "An application of bar-code system for reducing construction wastes." *Automation in Construction*, 11(5), 521-533.
- Cheng, M-Y., and Chen, J-C. (2002). "Integrating barcode and GIS for monitoring construction progress." *Automation in Construction*, 11 (2002), 23-33.
- Cheng, T., Venugopal, M., Teizer, J., and Vela, P.A. (2011). "Performance evaluation of Ultra Wide Band technology for construction resource location tracking in harsh environments." *Automation in Construction*, 20(8), 1173–1184.
- Cheng, T., and Teizer, J. (2013). "Real-time resource location data collection and visualization technology for construction safety and activity monitoring applications." *Automation in Construction*, 34, 3–15.
- Chi, S., and Caldas, C. (2011). "Automated object identification using optical video cameras on construction sites." *Computer-Aided Civil and Infrastructure Engineering*, 26(5), 398-380.

Chin, S., and Yoon, S. (2008). "RFID+4D CAD for Progress Management of Structural Steel Works in High-Rise Buildings." *Journal of Computing in Civil Engineering*, 22(2), 74-89.

Clevert, D., Unterthiner, T., and Hochreiter, S. (2015). "Fast and accurate deep network learning by exponential linear units (ELUs)." *5th International Conference on Learning Representations*.

Construction Industry Institute (CII). (1999). "Procurement and Material Management: A Guide to Effective Project Execution." The University of Texas at Austin.

Construction Industry Institute (CII). (2011). "Global Procurement and Material Management: An eGuide to Effective Project Execution." The University of Texas at Austin.

Dakhli, Z., & Lafhaj, Z. (2018). "Considering materials management in construction: An exploratory study." *Logistics*, 2(1), 1-13.

Davidson, I., and Skibniewski, M. (1995). "Simulation of Automated Data Collection in Buildings." *Journal of Computing in Civil Engineering*, 9(1), 9-20.

Deng, Y., Gan, V. J. L., Das, M., Cheng, J. C. P., and Anumba, C. (2019). "Integrating 4D BIM and GIS for Construction Supply Chain Management." *Journal of Construction Engineering and Management*, 145(4).

Department of Defense of USA, 2008, "Global Positioning System Standard Positioning Service Signal Specification." 4th Edition.

Ding, L., Fang, W., Luo, H., Love, P. E. D., Zhong, B., and Ouyang, X. (2018). "A deep hybrid learning model to detect unsafe behavior: Integrating convolution neural networks and long short-term memory." *Automation in Construction*, 86, 118–124.

Divya, M., Janet, J., and Suguna, R. (2014). "A genetic optimized neural network for image retrieval in telemedicine." *EURASIP Journal on Image and Video Processing*, 1–9.

Dimitrov, A., and Golparvar-Fard, M. (2014). "Vision-based material recognition for automated monitoring of construction progress and generating building information modeling from unordered site image collections." *Advanced Engineering Informatics*, 28(1), 37-49.

Dong, S., Kamat, V.R. (2013). "SMART: scalable and modular augmented reality template for rapid development of engineering visualization applications." *Journal of Visualization in Engineering*, 1(1).

Dutta, A., and Zisserman, A. (2019). "The VIA Annotation Software for Images, Audio and Video." In *Proceedings of the 27th ACM International Conference on Multimedia*



(MM '19), Nice, France. Accessed: June 5, 2019.  
<http://www.robots.ox.ac.uk/~vgg/software/via/>

Eirini, K., and Ioannis, B. (2018). "Matching construction workers across views for automated 3d vision tracking on-site." *Journal of Construction Engineering and Management*, 144 (7).

El-Omari, S. (2008), "Automated data acquisition for tracking and control of construction projects." Ph.D. thesis, Concordia University, Montreal, Canada.

El-Qader Al Haddad, E. A. (2006). "A construction materials management system for Gaza strip building contractors." MSc. thesis, The Islamic University of Gaza.

Elzarka, H., and Bell, L. (1995). "Object-Oriented Methodology for Materials-Management Systems." *Journal of Construction Engineering and Management*, 121(4), 438-445.

Ergen, E., Akini, B., and Sacks S. (2007). "Tracking and locating components in a precast storage yard utilizing radio frequency identification technology and GPS." *Journal of Automation in Construction*, 16, 354-367.

Eiris Pereira R., Moud H.I., and Gheisari M. (2017). "Using 360-Degree Interactive Panoramas to Develop Virtual Representation of Construction Sites." In: *Proceeding of Lean & Computing in Construction Congress (LC3)*, Vol. 3 (CONVR), Heraklion, Greece, 775-782.

Eiris Pereira, R., and Gheisari, M. (2018). "360-Degree Panoramas as a Reality Capturing Technique in Construction Domain: Applications and Limitations." *55th ASC Annual International Conference Proceedings*, Denver, Colorado.

Fallahnejad, M. H. (2013). "Delay causes in Iran gas pipeline projects." *International Journal of Project Management*, 31(1), 136–146.

Fang, Y., and Ng, S. T. (2011). "Applying activity-based costing approach for construction logistics cost analysis." *Construction Innovation*, 11 (3), 259–281.

Fathi, H., Dai, F., and Lourakis, M. (2015). "Automated as-built 3D reconstruction of civil infrastructure using computer vision: Achievements, opportunities, and challenges." *Advanced Engineering Informatics*, 29(2), 149–161.

Formoso, C.T., and Revelob, V.H. (1999). "Improving the materials supply system in small-sized building firms." *Automation in Construction*, 8(6), 663–670.

Freimuth, H., and König, M. (2015). "Generation of waypoints for UAV-assisted progress monitoring and acceptance of construction work." In *15th International Conference on Construction Applications of Virtual Reality (CONVR)*, Alberta, Canada.

Furukawa, Y., and Ponce, J. (2006). "High-fidelity image based modeling." Technical Rep. 2006-02, Univ. of Illinois, Urbana IL.

Georgy, M., and Basily, S.Y. (2008). "Using genetic algorithms in optimizing construction material delivery schedules." *Construction Innovation*, 8(1), 23-45.

Géron, A. (2017). "Hands-on Machine Learning with Scikit-Learn and TensorFlow: Concepts, Tools, and Techniques to Build Intelligent Systems." Sebastopol, CA: O'Reilly Media.

Gheisari, M., Sehat, N., and Williams, G. (2015). "Using Augmented Panoramic Views as an Online Course Delivery Mechanism in MOOCs." 51st ASC Annual International Conference Proceedings, Washington DC.

Gheisari, M., Sabzevar, M. F., Chen, P., and Irizarry, J. (2016). "Integrating BIM and Panorama to Create a Semi-Augmented-Reality Experience of a Construction Site." *International Journal of Construction Education and Research*, 12(4).

Girshick, R., Donahue, J., Darrell, T., and Malik, J. (2014). "Rich feature hierarchies for accurate object detection and semantic segmentation." 2014 IEEE Conference on Computer Vision and Pattern Recognition, Columbus, OH, 580–587.

Girshick, R. (2015). "Fast R-CNN." 2015 IEEE International Conference on Computer Vision (ICCV), Santiago, 1440–1448.

Glorot, X., and Bengio, Y. (2010). "Understanding the difficulty of training deep feedforward neural networks." *Proceedings of the Thirteenth International Conference on Artificial Intelligence and Statistics (AISTATS)*, 9, 249–256.

Glorot, X., Bordes, A., and Bengio, Y. (2011). "Deep sparse rectifier neural networks." *Proceedings of the Fourteenth International Conference on Artificial Intelligence and Statistics (AISTATS 2011)*, 15, 315–323.

Golkhoo, F., and Moselhi, O. (2019). "Optimized material management in construction using multi-layer perceptron." *Canadian Journal of Civil Engineering*, 46(10), 909-923.

Golparvar-Fard, M. (2006). "Assessment of Collaborative Decision-Making in Design Development and Coordination Meetings." The University of British Columbia.

Golparvar-Fard, M., and Peña-Mora, F. (2007). "Application of visualization techniques for construction progress monitoring." In *Proceedings of the ASCE International Workshop on Computing in Civil Engineering*, Pittsburgh, PA, 261(27), 216-223.

Golparvar-Fard, M., Peña-Mora, F., Arboleda, C. A., and Lee, S. (2009). "Visualization of Construction Progress Monitoring with 4D Simulation Model Overlaid on Time-Lapsed Photographs." *Journal of Computing in Civil Engineering*, 23(6), 391-404.

- Golparvar-Fard, M., Peña-Mora, F., and Savarese, S. (2011). "Integrated Sequential As-Built and As-Planned Representation with D4AR Tools in Support of Decision-Making Tasks in the AEC/FM Industry." *Journal of Construction Engineering and Management*, 137(12), 1099-1116.
- Golparvar-Fard, M., Peña-Mora, F., and Savarese, S. (2015). "Automated Progress Monitoring Using Unordered Daily Construction Photographs and IFC-Based Building Information Models." *Journal of Computing in Civil Engineering*, 29(1), 147-165.
- Gong, J., and Caldas, C. (2007). "Processing of High Frequency Local Area Laser Scans for Construction Site Resource Management." *Computing in Civil Engineering*, 665-672.
- Gonzalez, R. C., Woods, R. E., and Eddins, S. L. (2009). "Digital Image processing using MATLAB®." United States: Gatesmark Publishing.
- Goodrum, P.M., McLaren, M.A., and Durfee, A. (2006). "The application of active radio frequency identification technology for tool tracking on construction job sites." *Journal of Automation in Construction*, 15(3), 292-302.
- Gordon, C., Boukamp, F., Huber, D., Latimer, E., Park, K., and Akinci, B. (2003). "Combining reality capture technologies for construction defect detection: A case study." *Proc., 9th EuropIA Int. Conf. (EIA9), Istanbul, Turkey*, 99–108.
- Gurmu, A. T. (2018). "Construction materials management practices enhancing labour productivity in multi-story building projects." *International Journal of Construction Management*, 1-10.
- Gurmu, A. T. (2019). "Tools for measuring construction materials management practices and predicting labor productivity in multistory building projects." *Journal of construction engineering and management*, 145(2), 1-13.
- Guo, W. (2008). "Automated Defect Detection and Recognition for Wastewater Infrastructure Inspection and Condition Assessment." Ph.D. thesis, Carnegie Mellon University, Pittsburgh, US.
- Halpin D.W., Escalona A.L., and Szmurlo P.M. (1987). "Work Packaging for Project Control." *Construction Industry Institute, Austin, TX*.
- Hamledari, H., McCabe, B., and Davari, S. (2017). "Automated computer vision-based detection of components of under-construction indoor partitions." *Automation in Construction*, 74, 78-94.
- Han, S., Lee, S., and Peña-Mora, F. (2012). "Vision-Based Motion Detection for Safety Behavior Analysis in Construction." *Construction Research Congress, 2012*. 1032-1041. The USA.

- Han, K. K., and Golparvar-Fard, M. (2017). "Potential of big visual data and building information modeling for construction performance analytics: An exploratory study." *Automation in Construction*, 73, 184–198.
- Hattori, H., Naresh Boddeti, V., Kitani, K.M., Kanade, T. (2015). "Learning scene-specific pedestrian detectors without real data." In *Proceedings of the IEEE Conference on Computer Vision and Pattern Recognition (CVPR)*. Boston, USA.
- He, K., Gkioxari G., Doll'ar P., Girshick R. (2017). "Mask RCNN." *The IEEE International Conference on Computer Vision (ICCV)*, Venice, Italy, 2961-2969.
- Hedgepeth, W.O. (2007). "RFID METRICS Decision Making Tools for Today's Supply Chains." CRC Press, Taylor & Francis Group, Boca Raton, FL.
- Hinterstoisser, S., Lepetit, V., Wohlhart, P., and Konolige, K. (2017). "On pre-trained image features and synthetic images for deep learning." in *European Conference on Computer Vision (ECCV) Workshops*, Munich, Germany, 682-697.
- Holland, J.H. (1975). "Adaptation in Natural and Artificial Systems." Ann Arbor: University of Michigan Press, MIT Press, Cambridge 183 pp.
- HoloBuilder, 2019, "The Ultimate 2019 Construction 360° Camera Guide." Available: [https://holobuilder.link/camera\\_guide](https://holobuilder.link/camera_guide)
- Hou, X., Zeng, Y., and Xue, J. (2020). "Detecting Structural Components of Building Engineering Based on Deep-Learning Method." *Journal of Construction Engineering and Management*, 146(2).
- Huang, J., Rathod, V., Sun, C., Zhu, M., Korattikara, A., Fathi, A., Fischer, I., Wojna, Z., Song, Y., and Guadarrama S. (2017). "Speed/accuracy trade-offs for modern convolutional object detectors." *The IEEE Conference on Computer Vision and Pattern Recognition (CVPR)*, Honolulu, Hawaii, 7310-7311.
- Huertas, A., and Nevatia, R. (2000). "Detecting changes in aerial views of man-made structures." *Image and Vision Computing*, 18(8), 583–596.
- Ibrahim, Y. M., Lukins, T.C., Zhang, X., Trucco, E., and Kaka, A.P. (2009). "Towards automated progress assessment of work package components in construction projects using computer vision." *Advanced Engineering Informatics*, 23(1), 93-103.
- Irizarry, J., Karan, E. P., and Jalaei, F. (2013). "Integrating BIM and GIS to improve the visual monitoring of construction supply chain management." *Automation in Construction*, 31, 241-254.

- Iyer, K. C., and Jha, K. N. (2005). "Factors affecting cost performance: evidence from Indian construction projects." *International Journal of Project Management*, 23(4), 283-295.
- Jalal, M., Spjut, J., Boudaoud, B., and Betke, M. (2019). "Sidod: A synthetic image dataset for 3d object pose recognition with distractors." In *Proceedings of the IEEE Conference on Computer Vision and Pattern Recognition Workshops*.
- Jalali, S. (2007). "Quantification of construction waste amount." 6th International technical conference of waste, Viseu, Portugal.
- Jang, W. S. (2007). "Embedded system for construction material tracking Using combination of radiofrequency and Ultrasound signal." Ph.D. thesis, University of Maryland, US.
- Jang, H., Lee, S., and Choi, S. (2007). "Optimization of floor-level construction material layout using Genetic Algorithms." *Automation in Construction*, 16(4), 531–545.
- Jaselskis, E., Anderson, M., Jahren, C., Rodriguez, Y., and Njos, S. (1995). "Radio-Frequency Identification Applications in Construction Industry." *Journal of Construction Engineering and Management*, 121(2), 189-196.
- Jaselskis, E., and El-Misalami, T. (2003). "Implementing Radio Frequency Identification in the Construction Process." *Journal of Construction Engineering and Management*, 129(6), 680-688.
- Jaśkowski, P., Sobotka, A., Czarnigowska, A. (2018). "Decision model for planning material supply channels in construction." *Automation in Construction*, 90, 235-242.
- Jung, M., Park, M., Lee, H.S., and Chi, S. (2018). "Multimethod Supply Chain Simulation Model for High-Rise Building Construction Projects." *Journal of Computing in Civil Engineering*, 32(3).
- Kasim, N. (2008). "Improving materials management on construction projects." Ph.D. thesis, Loughborough University, United Kingdom.
- Kasim, N. (2015). "Intelligent Materials Tracking System for Construction Projects Management." *Journal of Engineering and Technological Sciences*, 47(2), 218-230.
- Kasim, N., Sarpin, N., Mohd Noh, H., Zainal, R., Mohamed, S., Manap, N., and Yahya, M., Y. (2019). "Automatic materials tracking practices through RFID implementation in construction projects." In: *MATEC Web of Conferences (EDP Sciences)*, 1-5.
- Kerridge, A.E. (1987). "Manage material effectively (part I)." *Hydrocarbon Processing*, 63-71.

- Houry, H.M., and Kamat, V.R. (2009). "Evaluation of position tracking technologies for user localization in indoor construction environments." *Journal of Automation in Construction*, 18, 444-457.
- Kim, H., and Kano, N. (2008). "Comparison of construction photograph and VR image in construction progress." *Automation in Construction*, 17(2), 137-143.
- Kim, H., Kim, H., Hong, Y. W. and Byun, H. (2018). "Detecting Construction Equipment Using a Region-Based Fully Convolutional Network and Transfer Learning." *Journal of Computing in Civil Engineering*, 32(2).
- Kim, C., Son, H., and Kim, C. (2013a). "Automated construction progress measurement using a 4D building information model and 3D data." *Automation in Construction*, 31, 75-82.
- Kim, C., Kim, B., and Kim, H. (2013b). "4D CAD model updating using image processing-based construction progress monitoring." *Automation in Construction*, 35, 44-52.
- Kini, D. (1999). "Materials Management: The Key to Successful Project Management." *Journal of Management in Engineering*, 15(1), 30-34.
- Kirk, K. E. (2010). "Genetic Algorithms and an Exploration of the Genetic Wavelet Algorithm." Master thesis, Villanova University, Pennsylvania.
- Kivrak, S., and Arslan, G. (2019). "Using Augmented Reality to Facilitate Construction Site Activities." *Advances in Informatics and Computing in Civil and Construction Engineering*, 215-221.
- Kiziltas, S., Akinci, B., Ergen, E., and Tang, P. (2008). "Technological assessment and process implications of field data capture technologies for construction and facility/infrastructure management." *Journal of Information Technology in Construction*, 13, 134-154.
- Klein, L., Li, N., and Becerik-Gerber, B. (2012). "Imaged-based verification of as-built documentation of operational buildings." *Automation in Construction*, 21, 161-171.
- Koch, C., Paal, S., Rashidi, A., Zhu, Z., König, M., and Brilakis, L. (2014). "Achievements and challenges in machine vision-based inspection of large concrete structures." *Advances in Structural Engineering*, 17 (3), 303-318.
- Kong, C.W., Li, H. r., Love, P.E.D. (2001). "An E-commerce System for Construction Material Procurement." *Construction Innovation*, 1(1), 43-54.
- Kong X., and Li J. (2018). "Vision-based fatigue crack detection of steel structures using video feature tracking." *Computing in Civil Infrastructure Engineering*, 33(9), 783-799.

- Kopsida, M., Brilakis, I., and Vela, P. A. (2015). "A review of automated construction progress monitoring and inspection methods." in Proceedings of the 32nd CIB W78 Conference, Eindhoven, Netherlands.
- Kopsida, M., and Brilakis, I. (2020). "Real-Time Volume-to-Plane Comparison for Mixed Reality-Based Progress Monitoring." *Journal of Computing in Civil Engineering*, 2020, 34(4).
- Kropp, C., Koch, C., and König, M. (2018). "Interior construction state recognition with 4D BIM registered image sequences." *Automation in Construction*, 86, 11-32.
- Kumar, A. (2010). "Lean Construction in the Building Industry." Technical Report, University of Illinois, Urbana-Champaign.
- Le, K. T. (2017). "Material Inventory Control and Management System in Construction Using GIS Applications and a "Hybrid" Tracking System." Ph.D. thesis, Illinois Institute of Technology, Chicago, Illinois.
- Lee, W. J., Song, J. H., Kwon, S. W., Chin, S., Choi, C., and Kim, Y. S. (2008). "A gate sensor for construction logistics." *Proceeding of 25th International Symposium on Automation and Robotics in Construction*, Institute of Internet and Intelligent Technologies, Vilnius, Lithuania, 100–105.
- Lee, A. (2016). "Comparing Deep Neural Networks and Traditional Vision Algorithms in Mobile Robotics." Available: <https://pdfs.semanticscholar.org/1b6f/569b79721037425fca034c7ae47904fb9276.pdf>
- Lei, L., Zhou, Y., Luo, H., and Love, P. E. D. (2019). "A CNN-based 3D patch registration approach for integrating sequential models in support of progress monitoring." *Advanced Engineering Informatics*, 41.
- Leng, B., Guo, S., Zhang, X., Xiong Z. (2015). "3D object retrieval with stacked local convolutional autoencoder." *Signal Processing*, 112, 119-128.
- Li, H., Chen, Z., Yong, L., and Kong, S.C.W. (2005). "Application of integrated GPS and GIS technology for reducing construction waste and improving construction efficiency." *Automation in Construction*, 14(2005), 323-331.
- Lin, K., and Fang, J. (2013). "Applications of computer vision on tile alignment inspection." *Automation in Construction*, 35, 562-567.
- Lin, Y.C., Cheung, W.F., and Siao F.C. (2014). "Developing mobile 2D barcode/RFID-based maintenance management system." *Automation in Construction*, 37, 110-121.

- Liu, W., Anguelov, D., Erhan, D., Szegedy, C., Reed, S., Fu, C. Y., and Berg, A. C. (2016). "SSD: Single shot multibox detector." European Conference on Computer Vision (ECCV 2016), Amsterdam, Netherlands, 21-37.
- Liu, L., Ouyang, W., Wang, X., Fieguth, P., Chen, J., Liu, X., and Pietikainen, M. (2019). "Deep learning for generic object detection: A survey." *International Journal of Computer Vision*, 1-58.
- Lu, M., Chen, W., Shen, X., Lam, H.C., and Liu, J. (2007). "Positioning and tracking construction vehicles in highly dense urban areas and building construction sites." *Automation in Construction*, 16, 647-656.
- Lu, L., Wang, F., and Liu, R. (2011). "A Tracking Management Information System for Railway Construction Materials." 11th International Conference of Chinese Transportation Professionals (ICCTP), 3742-3748.
- Lu, H., Wang, H., Xie, Y., and Wang, X. (2018). "Study on construction material allocation policies: A simulation optimization method." *Automation in Construction*, 90, 201–212.
- Lu Q., Lee S., and Chen L. (2018). "Image-driven fuzzy based system to construct as-is IFC BIM objects." *Automation in Construction*, 92, 68-87.
- Luo, X., Li, H., Cao, D., Dai, F., Seo, J., and Lee, S. (2018). "Recognizing diverse construction activities in site images via relevance networks of construction-related objects detected by convolutional neural networks." *Journal of Computing in Civil Engineering*, 32 (3).
- Lytle, A. M. (2011). "A framework for object recognition in construction using building information modeling and high frame rate 3D imaging." Ph.D. thesis, Virginia Polytechnic Institute and State University.
- Ma, Z., Liu, Z., and Zhang, D. (2013). "An Integrated Mobile Material Management System for Construction Sites." *AEI*, 2013, 354-363.
- Maalek, R., and Sadeghpour, F. (2012). "Reliability assessment of Ultra Wide Band for indoor tracking of static resources on construction sites." in CSCE conferences, Edmonton, Alberta.
- Macoir, N., Bauwens, J., Jooris, B., Van Herbruggen, B., Rossey, J., Hoebeke, J., and De Poorter, E. (2019). "UWB Localization with Battery-Powered Wireless Backbone for Drone-Based Inventory Management." *Sensors*, 2019, 19, 467.
- MajrouhiSardroud, J. (2012). "Influence of RFID technology on automated management of construction materials and components." *Scientia Iranica*, 19 (3), 381–392.



- Mahmood Maad, M., Noori Sadeq, A. (2019). "Reducing Waste of Construction Materials in Civil Engineering Projects in Iraq." ZANCO Journal of Pure and Applied Sciences (ZJPAS), 31(s3), 257-263.
- Masci, J., Meier, U., Cireşan, D., and Schmidhuber, J. (2011). "Stacked convolutional auto-encoders for hierarchical feature extraction." in 21th International Conference on Artificial Neural Networks (ICANN), 52-59.
- Marktscheffel, A.A. (2020). "How to create a new Revit 360 rendering project with the HoloBuilder plug-in (manual view placing)." Available: <https://help.holobuilder.com/en/articles/3158292-how-to-create-a-new-revit-360-rendering-project-with-the-holobuilder-plug-in-manual-view-placing>
- Matthews, J., Love, P., Heinemann, S., Chandler, R., Rumsey, C., Olatunj, O. (2015). "Real time progress management: Re-engineering processes for cloud-based BIM in construction." Automation in Construction, 58, 38-47.
- McCulloch, W. S., and Pitts, W. (1943). "A logical calculus of the ideas immanent in nervous activity." Bulletin of Mathematical Biology, 5(4), 115–133.
- Memarzadeh, M., Golparvar-Fard, M., and Niebles, J. C. (2013). "Automated 2D detection of construction equipment and workers from site video streams using histograms of oriented gradients and colors." Automation in Construction, 32, 24–37.
- Mnemyneh, B. E., Abbas, M., and Khoury, H. (2018). "Evaluation of computer vision techniques for automated hardhat detection in indoor construction safety applications." Frontiers of Engineering Management, 5(2), 227-239.
- Montaser, A. (2013). "Automated Site Data Acquisition for Effective Project Control." Ph.D. thesis, Concordia University, Montreal, Quebec, Canada.
- Morgan, D., Scofield. P., and Christopher L. (1991). "Neural Networks and Speech Processing." In: Neural Networks and Speech Processing. The Springer International Series in Engineering and Computer Science (VLSI, Computer Architecture and Digital Signal Processing), 130. Springer, Boston, MA.
- Moselhi, O., Bardareh, H., Zhu, Z. (2020). "Automated Data Acquisition in Construction with Remote Sensing Technologies." Applied Science, 10(8).
- Movshovitz-Attias, Y., Naresh Boddeti, V., Wei, Z., Sheikh, Y. (2014). "3D pose-by-detection of vehicles via discriminatively reduced ensembles of correlation filters." In Proceedings of the British Machine Vision Conference (BMVC), Nottingham, UK.
- Movshovitz-attias, Y., Kanade, T., and Sheikh, Y. (2016). "How Useful is Photo-Realistic Rendering for Visual Learning?" In Computer Vision– ECCV 2016 Workshops, Amsterdam, Netherlands, 202-217.

- Nair, V., and Hinton, G. E. (2010). "Rectified linear units improve restricted Boltzmann machines." *Proceedings of the 27th International Conference on Machine Learning (ICML10)*, 807–814.
- Nasir, H. (2008). "A model for automated construction materials tracking." Master thesis, University of Waterloo, Waterloo, Canada.
- Nasseri, M., Asghari, K., and Abedini, M.J. (2008). "Optimized scenario for rainfall forecasting using genetic algorithm coupled with artificial neural network." *Expert Systems with Applications*, 35(3), 1415-1421.
- Nath, N. D., and Behzadan, A. H. (2019). "Deep Learning Models for Content-Based Retrieval of Construction Visual Data." *ASCE International Conference on Computing in Civil Engineering*, Atlanta, Georgia.
- Navon, R., and Goldschmidt, E. (2003). "Can Labor Inputs be Measured and Controlled Automatically?" *Journal Construction Engineering Management*, 129(4), 437-445.
- Navon, R., Goldschmidt, E., and Shpatnisky Y. (2004). "A concept proving prototype of automated earthmoving control." *Automation in Construction*, 13, 225–239.
- Navon, R., and Shpatnitsky, Y. (2005). "Field Experiments in Automated Monitoring of Road Construction." *Journal of Construction Engineering and Management*, 131(4), 487-493.
- Navon, R., and Berkovich, O. (2006). "An automated model for materials management and control." *Construction Management and Economics*, 24(6), 635-646.
- Navon, R. (2007). "Research in automated measurement of project performance indicators." *Automation in Construction*, 16(2), 176-188.
- Nialidjoubi, L and Yang, J. L. (2001). "An Intelligent Materials Routing System on Complex Construction Sites. *Logistics Information Management*." 14(516), 337-343.
- Oliveira Filho, J., Su, Y., Song, H., Liu, L., and Hashash, Y. (2005). "Field Tests of 3D Laser Scanning in Urban Excavation." *Computing in Civil Engineering*, 1-10.
- Olsen, M., Kuester, F., Chang, B., and Hutchinson, T. (2010). "Terrestrial Laser Scanning-Based Structural Damage Assessment." *Journal of Computing in Civil Engineering*, 24(3), 264-272.
- Oloufa, A.A., Ikeda, M., Oda, H. (2003). "Situational awareness of construction equipment using GPS wireless and web technologies." *Automation in Construction*, 12 (6), 737-748.
- Omar, T., and Nehdi, M. L. (2016). "Data acquisition technologies for construction progress tracking." *Automation in Construction*, 70, 143–155.

- Paine, T. L. (2017). "Practical Considerations for Deep Learning." Ph.D. thesis, the University of Illinois at Urbana-Champaign, Urbana, Illinois.
- Panthula, G. A. (2018). "Object Detection Techniques Using Convolutional Neural Networks." Master thesis, Florida State University, Tallahassee, Florida.
- Papon, J., and Schoeler, M. (2015). "Semantic pose using deep networks trained on synthetic RGB-D." in IEEE International Conference on Computer Vision (ICCV), 774-782.
- Park, M.W., and Brilakis, I. (2016). "Continuous localization of construction workers via integration of detection and tracking." *Automation in Construction*, 72, 129–142.
- Perdomo, J., and Thabet, W. (2002). "Material Management Practices for the Electrical Contractor." *Computing in Civil Engineering*, 232-243.
- Peyret, F., and Tasky, R. (2002). "Asphalt quality parameters traceability using electronic tags and GPS." *Proceedings of International Symposium on Automation and Robotics in Construction, 19th (ISARC), NIST, Gaithersburg, Maryland*, 155-160.
- Pham, H.C., Dao, N., Pedro, A., Le, Q.T., Hussain, R., Cho, S., and Park, C. (2018). "Virtual Field Trip for Mobile Construction Safety Education Using 360-Degree Panoramic Virtual reality." *International Journal of Engineering Education*, 34(4), 1174-1191.
- Plemmons, J., and Bell, L. (1995). "Measuring Effectiveness of Materials Management Process." *Journal of Management in Engineering*, 11(6), 26-32.
- Polat, G., Arditi, D., and Mungen, U. (2007). "Simulation-Based Decision Support System for Economical Supply Chain Management of Rebar." *Journal of Construction Engineering and Management*, 133(1), 29-39.
- Poon, C. S., Yu, A. T. W., Wong, S. W., and Cheung, E. (2004). "Management of construction waste in public housing projects in Hong Kong." *Construction management and economics*, 22 (7), 675-689.
- Poon, C. S., Yu, A. T. W., and Ng, L. H. (2001). "On-site sorting of construction and demolition waste in Hong Kong." *Resources, conservation and recycling*, 32 (2), 157-172.
- Poulton, M. (2001). "Computational neural networks and neural networks for geophysical data processing." Pergamon, Amsterdam, Netherlands.
- Pour Rahimiana, F., Seyedzadeh, S., Oliver, S., Rodriguez, S., and Dawood, N. (2020). "On-demand monitoring of construction projects through a game-like hybrid application of BIM and machine learning." *Automation in Construction*, 110.

Pučko, Z., Šuman, N., and Rebolj, D. (2018). "Automated continuous construction progress monitoring using multiple workplace real-time 3D scans." *Advanced Engineering Informatics*, 38, 27-40.

Rad, M., Oberweger, M., and Lepetit, V. (2018). "Feature Mapping for Learning Fast and Accurate 3D Pose Inference from Synthetic Images." *IEEE Conference on Computer Vision and Pattern Recognition (CVPR)*, Salt Lake City, Utah, 4663-4672.

Rahman, I., Memom, A., and Karim, A. (2013). "Relationship between Factors of Construction Resources Affecting Project Cost." *Modern Applied Science*, 7(1), 67-75.

Rajpura, P. S., Hegde, R. S., and Bojinov, H. (2017). "Object detection using deep CNNs trained on synthetic images." Ithaca, NY: Cornell University.

Rankohi, S., and Waugh, L. (2013). "Review and analysis of augmented reality literature for construction industry." *Journal of Visualization in Engineering*, 1-9.

Rankohi, S., and Waugh, L. (2014). "Image-based modeling approaches for projects status comparison." in *CSCE 2014 General Conference*, Halifax, Nova Scotia.

Rebolj, D., Čuš Babič, N., Magdič, A., Podbreznik, P., Pšunder, M. (2008). "Automated construction activity monitoring system." *Advanced Engineering Informatics*, 22(4), 493-503.

Redmon, J., Divvala, S., Girshick, R., and Farhadi, A. (2016). "You Only Look Once: Unified, Real-Time Object Detection." *IEEE Conference on Computer Vision and Pattern Recognition (CVPR)*, Las Vegas, Nevada, 779-788.

Ren, Z., Anumba, C.J., and Tah, J. (2011). "RFID-facilitated construction materials management (RFID-CMM) – A case study of water-supply project." *Advanced Engineering Informatics*, 25(2), 198-207.

Ren, S., He, K., Girshick, R., and Sun, J. (2017). "Faster R-CNN: Towards Real-Time Object Detection with Region Proposal Networks." in *IEEE Transactions on Pattern Analysis and Machine Intelligence*, 39(6), 1137-1149.

Ren, X., Zhu, Z., Germain, C., Belair, R., and Chen, Z. (2017). "Automated monitoring of the utilization rate of onsite construction equipment." In *Proceeding of Computing in Civil Engineering*, Reston, VA, 74-81.

RFID Journal (2016). RFID frequently asked questions, General RFID Information <http://www.rfidjournal.com>

RomRoc. (2018). Mask R-CNN instance segmentation with custom dataset in Google Colab, GitHub repository, Accessed: June 15, 2019. [https://github.com/RomRoc/maskrcnn\\_train\\_tensorflow\\_colab](https://github.com/RomRoc/maskrcnn_train_tensorflow_colab)

- Ros, G., Sellart, L., Materzynska, J., Vazquez, D., and Lopez, A. M. (2016). "The SYNTHIA Dataset: A large collection of synthetic images for semantic segmentation of urban scenes." in IEEE Conference on Computer Vision and Pattern Recognition (CVPR), 3234-3243.
- Rumelhart, D.E., Hinton, G.E., and Williams, R.J. (1986). "Learning internal representations by error propagation." In Parallel Distributed Processing.0 1: Foundations. MIT Press, Cambridge, MA.
- Sacks, R., Treckmann, M., and Rozenfeld, O. (2009). "Visualization of Work Flow to Support Lean Construction." *Journal of Construction Engineering and Management*, 135(12), 1307-1315.
- Sacks, R., Navon, R., and Goldschmidt, E. (2003). "Building Project Model Support for Automated Labor Monitoring." *Journal of Computing in Civil Engineering*, 17(1), 19-27.
- Said, H., and El-Rayes, K. (2011). "Optimizing Material Procurement and Storage on Construction Sites." *Journal of Construction Engineering and Management*, 421-431.
- Said, H., and El-Rayes, K. (2013). "Optimal utilization of interior building spaces for material procurement and storage in congested construction sites." *Automation in Construction*, 31, 292–306.
- Said, H., and El-Rayes, K. (2014). "Automated Multi-objective Construction Logistics Optimization System." *Automation in Construction*, 43, 110-122.
- Saidi, K.S., Lytle, A.M., and Stone, W.C. (2003). "Report of the NIST Workshop on Data Exchange Standards at the Construction Job Site." in proceedings, ISARC 2003, The Future Site, Eindhoven Technical University, Eindhoven, 617-622.
- Sakurada, K. (2015). "Four-dimensional City Modeling using Vehicular Imagery." Ph.D. thesis, Tohoku University, Sendai, Japan.
- Salimans, T., and Kingma, D. P. (2016). "Weight normalization: A simple reparameterization to accelerate training of deep neural networks." In *Advances in Neural Information Processing Systems*, 901-909.
- Seiffert, U. (2001). "Multiple Layer Perceptron Training Using Genetic Algorithms." *ESANN-proceedings - European Symposium on Artificial Neural Networks*, Bruges (Belgium), April, 159-164.
- Siddula, M., Dai, F., Ye, Y., and Fan, J. (2016). "Unsupervised feature learning for objects of interest detection in cluttered construction roof site images." *Procedia Engineering*, 145, 428–435.

- Simon, D. (2013). "Evolutionary Optimization Algorithms." John Wiley & Sons, Inc., Hoboken, New Jersey.
- Shehab-Eldeen, T. (2001). "An automated system for detection, classification and rehabilitation of defects in sewer pipes." Ph.D. thesis, Concordia University, Quebec, Canada.
- Shirvany, Y., Hayatia, M., and Moradian, R. (2009). "Multilayer perceptron neural networks with novel unsupervised training method for numerical solution of the partial differential equations." *Applied Soft Computing*, 9(1), 20-29.
- Snell, J., Ridgeway, K., Liao, R., Roads, B. D., Mozer, M. C., and Zemel, R. S. (2017). "Learning to generate images with perceptual similarity metrics." in *IEEE International Conference on Image Processing (ICIP)*.
- Soleimanifar, M. (2011). "IntelliSensorNet: A Positioning Technique Integrating Wireless Sensor Networks and Artificial Neural Networks for Critical Construction Resource Tracking." M.Sc. thesis, University of Alberta.
- Soleimanifar, M., Shen, X., Lu, M., and Nikolaidis, I. (2014). "Applying received signal strength based methods for indoor positioning and tracking in construction applications." *Canadian Journal of Civil Engineering*, 41(8): 703-716.
- Son, H., and Kim, C. (2010). "3D structural component recognition and modeling method using color and 3D data for construction progress monitoring." *Automation in Construction*, 19(7), 844-854.
- Song, J., Haas, C.T., and Caldas, C.H. (2006a). "Tracking the location of materials on construction job sites." *Journal of Construction Engineering and Management*, 132 (9), 911-918.
- Song, J., Ergen, E., Haas, C.T., Akinci, B., and Caldas, C. (2006b). "Automating the task of tracking the delivery and receipt of fabricated pipe spools in industrial projects." *Journal of Automation in Construction*, 15(2), 166-177.
- Soudarissanane, S.S. (2016). "The geometry of terrestrial laser scanning; identification of errors, modeling and mitigation of scanning geometry." Ph.D. thesis, Faculty Civil Engineering and Geosciences, Delft University of Technology, Netherlands.
- Specht, C., Dąbrowski, P., Dumalski, A., and Hejbudzka, K. (2016). "Modeling 3D Objects for Navigation Purposes Using Laser Scanning." *International Journal on Marine Navigation and Safety of Sea Transportation*, 10(2), 301-306.
- Stukhart, G. (1995). "Construction Materials Management." Marcel Dekker Inc. New York.

- Su, Y., and Liu, L. (2007). "Real-Time Construction Operation Tracking from Resource Positions." *Computing in Civil Engineering*, 200-207.
- Su, H., Qi, C. R., Li, Y., and Guibas, L. (2015). "Render for CNN: Viewpoint Estimation in Images Using CNNs Trained with Rendered 3D Model Views." in *IEEE International Conference on Computer Vision (ICCV)*, Santiago, Chile, 2686-2694.
- Subsomboon, K., Christodoulou, S., and Griffis, F. (2003). "Procurement of Services and Materials Using a FIAPP-Based System—New York City Case Studies." *Construction Research Congress*, 1-9.
- Sun, B., Saenko, K. (2014). "From virtual to reality: Fast adaptation of virtual object detectors to real domains." In *Proceedings of the British Machine Vision Conference (BMVC)*. Nottingham, United Kingdom.
- Tahmasebi, P., and Hezarkhani, A. (2012). "A hybrid neural networks-fuzzy logic-genetic algorithm for grade estimation." *Computers & Geo sciences* 42, 18–27.
- Tang, P., Huber, D., Akinci, B., Lipman, R., and Lytle, A. (2010). "Automatic reconstruction of as-built building information models from laser-scanned point clouds: A review of related techniques." *Automation in Construction*, 19(7), 829-843.
- Teizer, J., Lao, D., and Sofer, M. (2007). "Rapid Automated Monitoring Of Construction Site Activities Using Ultra-Wideband." *24th International Symposium on Automation & Robotics in Construction (ISARC 2007)*.
- Teizer, J., Venugopal M., and Walia, A. (2008). "Ultrawideband for Automated Real-Time Three-Dimensional Location Sensing for Workforce, Equipment, and Material Positioning and Tracking." *Transportation Research Record: Journal of the Transportation Research Board*, 2081.
- The Business Roundtable. (1982). "Modern Management Systems." *Construction Industry Cost Effectiveness Report A-6*, New York.
- Thomas, H., Sanvido, V., and Sanders, S. (1989). "Impact of Material Management on Productivity—a Case Study." *Journal of Construction Engineering and Management*, 115(3), 370-384.
- Thomas, H. R., Riley, D. R., and Sanvido, V. E. (1999). "Loss of Labor Productivity due to Delivery Methods and Weather." *Journal of Construction Engineering and Management*, 125(1), 39-46.
- Thomas, H. R., and Sandivo, V. E. (2000). "Role of the fabricator in labor productivity." *Journal of Construction Engineering and Management*, 126 (5), 358-365.

- Thomas, H.R., Riley, D.R., and Messner, J.I. (2005). "Fundamental principles of site material management." *Journal of Construction Engineering and Management*, ASCE, 131(7), 808–15.
- Tian, G., Zhang, X., and Hu, F. (2012). "The Design of Electric Materials Management System Based on QR-Code." *ICLEM*, 1345-1351.
- Tremblay, J., Prakash, A., Acuna, D., Brophy, M., Jampani, V., Anil, C., To, T., Cameracci, E., Boochoon S., and Birchfield, S. (2018). "Training Deep Networks with Synthetic Data: Bridging the Reality Gap by Domain Randomization." *IEEE Conference on Computer Vision and Pattern Recognition (CVPR) Workshops*, Salt Lake City, Utah, 969-977.
- Turchenko, V., Chalmers, E., Luczak, A. (2017). "A Deep Convolutional Auto-Encoder with Pooling - Unpooling Layers in Caffe." *Computing Research Repository (CoRR)*, Available: <https://arxiv.org/abs/1701.04949>.
- Turkan, Y., Bosché, F., Haas, C. T., and Haas, R. (2012). "Automated progress tracking using 4D schedule and 3D sensing technologies." *Automation in Construction*, 22, 414-421.
- Turkan, Y., Bosché, F., Haas, C. T., and Haas, R. (2013). "Toward Automated Earned Value Tracking Using 3D Imaging Tools." *Journal of Construction Engineering and Management*, 139(4), 423-433.
- Vartiainen, J., Kallonen, T. and Ikonen, J. (2008), "Barcodes and mobile phones as part of logistic chain in construction industry." *16th International Conference on Software, Telecommunications and Computer Networks*, Split, 305-308.
- Vazquez, D., Lopez, A.M., Marin, J., Ponsa, D., Geronimo, D. (2014). "Virtual and real world adaptation for pedestrian detection." *IEEE transactions on pattern analysis and machine intelligence*, 36(4), 797 - 809.
- Vrat, P. (2014). "Materials Management: An Integrated Systems Approach." Springer India, New Delhi, India.
- Voulodimos, A., Doulamis, N., Doulamis, A., and Protopapadakis, E. (2018). "Deep learning for computer vision: A brief review." *Computational Intelligence and Neuroscience*, vol. 2018, 13 pages.
- Wang, Z., Bovik, A. C., Sheikh, H. R., and Simoncelli, E. P. (2004). "Image quality assessment: From error visibility to structural similarity." *IEEE Transactions on Image Processing*, 13(4), 600–612.



- Wang, C., Wu, H., and Tzeng, N. F. (2007). "RFID-Based 3-D Positioning Schemes, INFOCOM 2007." 26th IEEE International Conference on Computer Communications. IEEE, 1235-1243.
- Wang, L.C. (2008). "Enhancing construction quality inspection and management using RFID technology." *Automation in Construction*, 17, 467-479.
- Wang, X., Truijens, M., Hou, L., Wang, Y., and Zhou, Y. (2014). "Integrating Augmented Reality with Building Information Modeling: Onsite construction process controlling for liquefied natural gas industry." *Automation in Construction*, 40, 96–105.
- Wang, Z., Hu, H., and Zhou, W. (2017). "RFID enabled knowledge-based precast construction supply chain." *computer-aided civil and infrastructure, Engineering*, 1–16.
- Wickramatillake, C. D., Lenny Koh, S. C., Gunasekaran, A., and Arunachalam, S. (2007). "Measuring performance within the supply chain of a large scale project." *Supply Chain Management: An International Journal*, 12(1), 52 – 59.
- Won, D., Park M.-W., and Chi, S. (2018). "Construction Resource Localization Based on UAV-RFID Platform Using Machine Learning Algorithm." *IEEE International Conference on Industrial Engineering and Engineering Management (IEEM)*, Bangkok, 2018, 1086-1090.
- Wong, E. T. T., and Norman, G. (1997). "Economic Evaluation of Materials Planning Systems for Construction. *Construction Management and Economics*." 15(1), 39-47.
- Wu, Y., and Kim, H. (2004). "Digital imaging in assessment of construction project progress." *Proceedings of the 21st ISARC*, Jeju, South Korea.
- Wu, Y., Kim, H., Kim, C., and Han, S. H. (2010). "Object Recognition in Construction-Site Images Using 3D CAD-Based Filtering." *Journal of Computing in Civil Engineering*, 24(1), 56-64.
- Wu, W., Yang, H., Chew, A.S., Yang, S.H., Gibb, G.F., and Li, Q. (2010). "Towards an autonomous real-time tracking system of near-miss accidents on construction sites." *Journal of Automation in Construction*, 19, 134-141.
- Yang, J., Arif, O., Vela, P. A., Teizer, J., and Shi, Z. (2010). "Tracking multiple workers on construction sites using video cameras." *Advanced Engineering Informatics*, 24(4), 428–434.
- Yang, J., Park, M. W., Vela, P. A., and Golparvar-Fard, M. (2015). "Construction performance monitoring via still images, time-lapse photos, and video streams: Now, tomorrow, and the future." *Advanced Engineering Informatics*, 29(2), 211-224.

- Yang, J., Shi, Z.K., and Wu, Z.Y. (2016), "Towards automatic generation of as-built BIM: 3D building facade modeling and material recognition from images." *International Journal of Automation and Computing*, 13(4), 338-349.
- Yeo, K. T., and Ning, J. H. (2002). "Integrating supply chain and critical chain concepts in engineer–procure–construct (EPC) projects." *Int. Journal of Project Management* 20(4), 253–262.
- Ying, H. Q., and Lee, S. (2019). "A Mask R-CNN Based Approach to Automatically Construct As-is IFC BIM Objects from Digital Images." In *Proceedings of the 36th ISARC*, Banff, Alberta, Canada, 764-771.
- Young, D., Haas, C., Goodrum, P., and Caldas, C. (2011). "Improving Construction Supply Network Visibility by Using Automated Materials Locating and Tracking Technology." *Journal of Construction Engineering and Management*, 137(11), 976-984.
- Zdziarski, Z. (2018). "The reasons behind the recent growth of computer vision." Retrieved February/10, 2019, Available: <http://zbigatron.com/the-reasons-behind-the-recent-growth-of-computer-vision/>.
- Zaher, M., D. Greenwood, and Marzouk, M. (2018). "Mobile augmented reality applications for construction projects." *Construction Innovation*, 18(2), 152–166.
- Zhang, J., Shan, S., Kan, M., Chen, X. (2014). "Coarse-to-fine auto-encoder networks (CFAN) for real-time face alignment." *European Conference on Computer Vision (ECCV)*, Zurich, Switzerland, 1-16.
- Zhang, S., Bogus, S. M., Lippitt, C. D., and Sprague, J. E. (2018). "Geospatial Technologies for Collecting Construction Material Information." *Construction Research Congress*, 2018, 660-669.
- Zhang, X., Bakis, N., Lukins, T. C., Ibrahim, Y. M., Wu, S., Kagioglou, M., Aouad, G., Kaka, A. P., and Trucco, E. (2009). "Automating progress measurement of construction projects." *Automation in Construction*, 18(3), 294-301.
- Zhu, Z., and Brilakis, I. (2010). "Concrete column recognition in images and videos." *Journal of Computing in Civil Engineering*, 24 (6).
- Zollmann, S., Hoppe, C., Kluckner, S., Poglitsch, C., Bischof, H., and Reitmayr, G. (2014). "Augmented reality for construction site monitoring and documentation." *Proceedings of the IEEE* 102 (2), 137–154.
- Zou, J., and Kim, H. (2007). "Using hue, saturation, and value color space for hydraulic excavator idle time analysis." *Journal of Computing in Civil Engineering*, 21, 238–246.